UCSF

UC San Francisco Electronic Theses and Dissertations

Title

The Role of Transporters in the Absorption, Distribution, Metabolism and Excretion (ADME) of Orally Administered Drugs

Permalink

https://escholarship.org/uc/item/6vp711dt

Author

Shugarts, Sarah

Publication Date

2010

Peer reviewed|Thesis/dissertation

The Role of Transporters in the Absorption, Distribution, Metabolism, and Excretion (ADME) of Orally Administered Drugs

by

Sarah B. Shugarts

DISSERTATION

Submitted in partial satisfaction of the requirements for the degree of

DOCTOR OF PHILOSOPHY

in

PHARMACEUTICAL SCIENCES AND PHARMACOGENOMICS

in the

GRADUATE DIVISION

of the

UNIVERSITY OF CALIFORNIA, SAN FRANCISCO

This dissertation is dedicated to:

My family, Bill, Amy, Angela, and Walt

Acknowledgments

we've formed over the years. Along with my class I want to thank Debbie Acoba, the PSPG program coordinator, for being a wonderful friend and an invaluable source of help and encouragement over the years.

I'd also like to show my thanks and respect for both my orals and my thesis committees: Dr. Kathleen Giacomini, Dr. Betty-Ann Hoener, Dr. Laura Bull, and Dr. Yong Huang, for their excellent input, advice, and suggestions on my projects and thesis.

I also need to thank Dr. Paul Pearson, a great friend, former running partner, and perhaps future cycling partner, whose advice and support have been invaluable to me for nearly a decade now. I sincerely appreciate it, along with some good laughs and the excellent meals at Slanted Door that kept a poor grad student from starving.

To move on to my family and friends from home, I have to thank them all for being supportive when I decided to leave a decent job, move across the country, and spend 5+ years in school to get a degree in something they couldn't even pronounce. I want to acknowledge my Grandmother and Grandfather Carr, who loved me so much and whom I still miss every single day since they've been gone. I want to thank my Aunt Nancy and Uncle Lou for being so giving and generous all of my life, I love them dearly. I want to thank my cats too, Combs and Basil, for not complaining too much about the 5 hour airplane ride to move out here or the much smaller apartment. They've been a source of love, calm and amusement all the years I've had them with me.

I want to thank Walt Kline, my best friend, who has been there for me through so much I can't hope to thank him enough. I can only hope to be as positive and comforting a force in his life as he has been in mine. Forever plus twelve years, my dear.

I must thank my sister, who was reticent about her younger sister gallivanting off to California when U. of Penn was so close by, but who was always sure to let me know how proud of me she was. I am looking forward to showing her all the wonders the West Coast has to offer. I want to thank my dad for always having a fun story to tell me when I called, for keeping me updated on the football and NASCAR standings, and for never forgetting to tell me he loved me before we hung up. Finally, I want to thank my mom. This degree is dedicated to her, for all of the hardship she's gone through in her life. I thank her for deciding before I was born that I would be educated, for taking an active part in my education and instilling in me a love and passion for learning, for making sure I followed a different path in life than the one that was dictated for her, for sheltering me from the condescension of those who didn't believe I could be as smart as I was, for always telling me I was smart and pretty instead of pretty and smart, for being a role model of perseverance, determination, creativity, and strength. She is my hero and there is no way I could have gotten to where I am today without her. Thanks, Mom!

Abstract

EXAMINING THE ROLE OF TRANSPORTERS IN THE ABSORPTION, DISTRIBUTION, METABOLISM, AND EXCRETION (ADME) PROPERTIES OF DRUGS

Sarah B. Shugarts

Over the last two decades drug tranporter proteins have been the focus of increased study to determine their roles in drug pharmacokinetics and pharmacodynamics. Their importance is increasingly recognized by regulatory agencies, the drug development industry, and the medical community. Although a great deal of progress has been made in the field, the finer nuances and full range of transporter influence and function is still an important area of investigation.

My dissertation research investigated the role of transporters on drug ADME properties in a variety of systems, including stably transfected cells, isolated rat and human hepatocytes, the isolated perfused rat liver (IPRL) system, isolated rat jejunal segments, and a human clinical study. Transfected cells and the IPRL system were used to examine the ability of the Organic Anion Transporting Polypeptides (OATP/Oatp) to efflux drugs out of cells with inconclusive results. Transfected cells and isolated rat jejunal segments were used to study the interplay of the Breast Cancer Resistance Protein (BCRP/Bcrp) with intestinal drug metabolizing enzymes, again with inconclusive results. Transfected cells and isolated rat and human hepatocytes were used to determine whether or not warfarin or phenytoin are substrates for hepatic uptake transporters. Significant inhibition of warfarin uptake by the OATP/Oatp inhibitor rifampin was seen, but further

studies with OATP1B1 and OATP2B1-expressing cells indicated that neither of these isoforms are responsible for warfarin uptake. No inhibitable uptake of phenytoin was seen in hepatocytes or in transfected cells. A human clinical study was conducted to determine the effect of hepatic OATP inhibition on warfarin pharmacokinetics with the result that OATP inhibition did not increase warfarin plasma levels as would be expected if hepatic OATP uptake was an important factor in warfarin disposition. Transfected cells were used to explore possible transporter-based mechanisms for the drug-drug interactions seen between raltegravir and immunosuppressants. The experiments indicated that while this was an unlikely mechanism for the specific interactions seen, raltegravir did interact significantly with hepatic uptake and efflux transporters.

TABLE OF CONTENTS

CHAPTER 3

INVESTIGATION OF TRANSPORTER-ENZYME INTERPLAY BETWEEN BREAST CANCER RESISTANCE PROTEIN AND INTESTINAL DRUG METABOLIZING ENZYMES

CHAPTER 4

EXAMINING HEPATIC UPTAKE OF WARFARIN AND PHENYTOIN IN VITRO

LIST OF TABLES

LIST OF FIGURES

CHAPTER 1

CHAPTER 2

CHAPTER 3

OVERALL PROJECT GOALS

The purpose of this thesis project was to investigate the influence hepatic and intestinal transporters have in drug absorption, distribution, metabolism, and excretion using *in vitro*, *ex situ*, and *in vivo* studies:

1. To investigate the ability of the organic anion transporting polypeptides (OATPs) to mediate passage of drug out of cells using transporter-expressing cell systems and the isolated perfused rat liver system.

2. To demonstrate that the Breast Cancer Resistance Protein (BCRP) and drug metabolizing enzymes in the gut cooperate in a manner similar to P-glycoprotein (Pgp) and Cytochrome P450 3A4 (CYP3A4) to increase drug exposure to enzymes and decrease bioavailability by using cells and isolated rat jejunum sections.

3. To determine whether warfarin or phenytoin are substrates for hepatic uptake transporters using transporter expressing cells in addition to rat and human hepatocytes.

4. Examine the effect of inhibition of hepatic uptake on the pharmacokinetics of warfarin in a human clinical study.

5. To investigate transporter-based mechanisms to explain observed drug-drug interactions between raltegravir and cyclosporine and between raltegravir and tacrolimus and to investigate the ability of raltegravir to inhibit uptake and efflux transporters using transporter expressing cell systems along with rat and human hepatocytes.

CHAPTER 1

Introduction: The Role of Intestinal and Hepatic Transporters in Oral Drug Absorption, Distribution, Metabolism and Excretion (ADME)

1.1 Intestinal and Hepatic Drug Transporters

Since the discovery of Pgp in 1976 (Juliano and Ling, 1976), the importance of drug transporters in influencing the pharmacokinetics of orally dosed drugs has become increasingly evident (Fromm, 2000, Mizuno and Sugiyama, 2002, Landowski et al., 2003). Drug transporters in both the gut and the liver can help control access of drugs to systemic circulation by dictating the amount of drug that enters the body from the gut lumen and influencing how much drug escapes first pass metabolism in both gut and liver. Both uptake and efflux transporters are important in determining oral drug disposition by controlling absorption and bioavailability. See Figures 1 and 2 for transporter localization in enterocytes and hepatocytes.
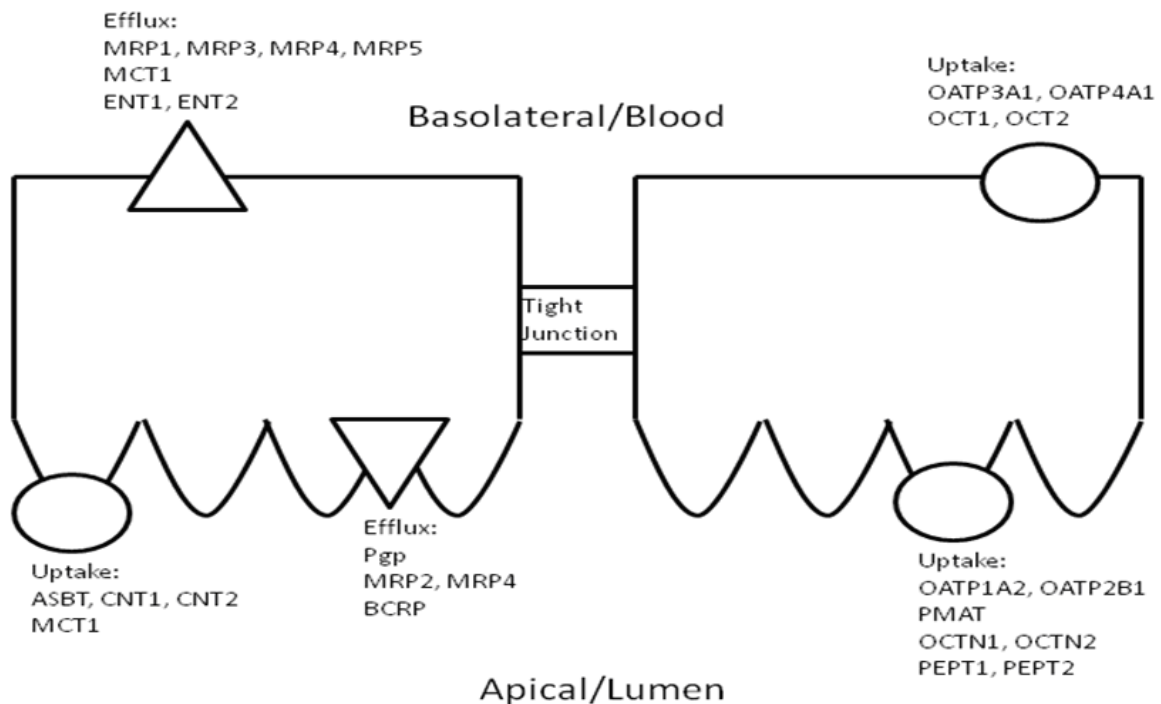
Figure 1-1 Uptake and efflux transporters in enterocytes
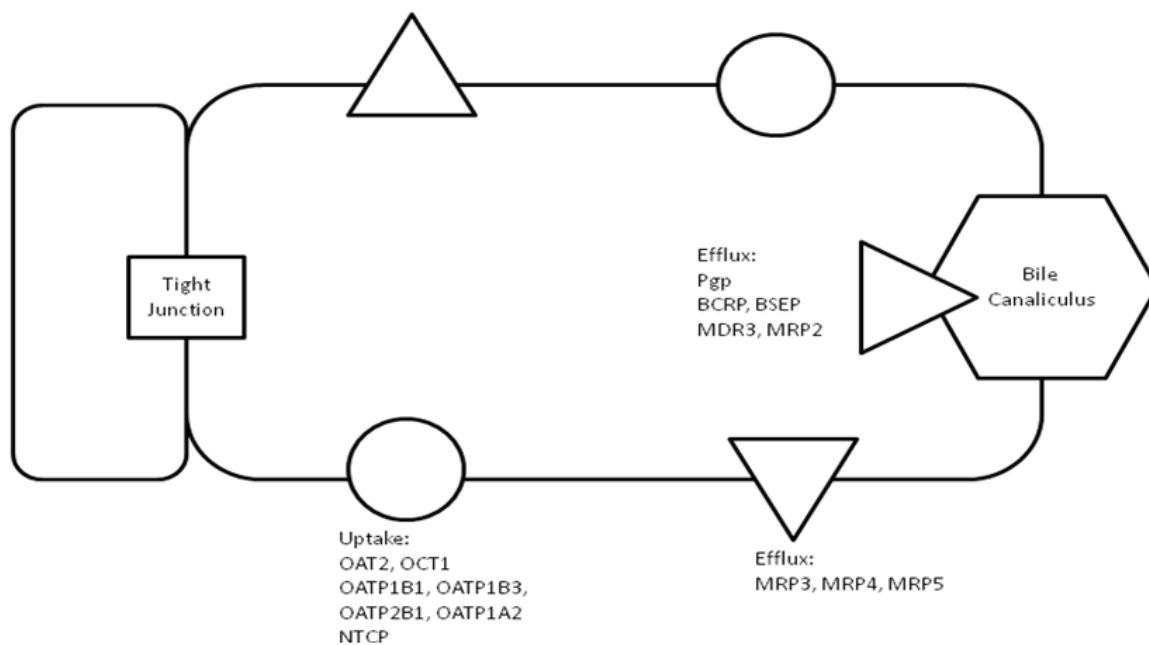
Figure 1-2 Uptake and efflux transporters in hepatocytes

The major uptake transporters responsible for xenobiotic transport belong to the

solute carrier (SLC) superfamily and an "evolutionary cluster" making up the SLCO

family (He et al., 2009). The SLC superfamily members typically transport small organic

anions (van Montfoort et al., 2001), cations, and zwitterions (Okabe et al., 2008) while

the SLCO family transport bulkier organic anions (van Montfoort et al., 2001). Members

of the SLC and SLCO families use a variety of porter mechanisms (ie. uniporter,

antiporter, symporter), not all of which have been fully elucidated for each specific

transporter. In general, these transporters do not utilize an energy source other than a

chemiosmotic gradient created by translocation of ions across the membrane (Satlin et al.,

1997, Li et al., 2000, Mahagita et al., 2007, Ciarimboli et al., 2008, Srimaroeng et al.,

2008). The SLC superfamily encompasses a variety of transporters including the organic

anion transporters (OAT, SLC22A), the organic cation transporters (OCT, SLC22A), the

novel organic cation transporters (OCTN, SLC22A), the equilibrative nucleoside

transporters (ENT, SLC29), the concentrative nucleoside transporters (CNT, SLC28), the

apical Na^+-dependent bile salt transporter (ASBT, SLC10), the monocarboxylate

transporters (MCT, SLC16), and the peptide transporters (PEPT, SLC15). The SLCO

gene family is made up of the OATPs, including the hepatically expressed isoforms

OATP1B1 (SLCO1B1), OATP1B3 (SLCO1B3), OATP1A2 (SLCO1A2), and OATP2B1

(SLCO2B1). OATP1B1 and OATP1B3 expression are liver specific, while OATP1A2

and OATP2B1 are expressed in liver and in other tissues, such as the intestines, lungs,

brain, and kidneys. OATPs are integral membrane proteins with 12 trans-membrane

spanning domains. They bear multiple N-glycosylation sites in the large extracellular

loop 5 and in extracellular loop 2, both of which are believed to be involved in substrate

recognition and transport (Konig et al., 2006). They mediate the ATP- and Na^+-

independent transport of Type II organic anions in addition to some cationic and neutral

compounds. Their wide variety of substrates include endogenous substrates such as 17β-

estradiol-D-17β-glucuronide and estrone sulfate (Miyagawa et al., 2009), taurocholate

(Bi et al., 2006), the thyroid hormones thyroxine (T_4) and triiodothyronine (T_3)

(Hagenbuch, 2007), as well as xenobiotics such as atorvastatin (Lau et al., 2007),

pravastatin (Maeda et al., 2006), digoxin (Bi et al., 2006), and temocaprilat (Maeda et al.,

2006). A complicating factor in studying substrate profiles of the Oatps/OATPs is that

there are no species orthologs between humans and rodents.

Efflux transporters expressed in the intestine and liver include P-glycoprotein

(Pgp, ABCB1), the bile salt export pump (BSEP, ABCB11), the multidrug resistance

proteins (MRP1- 6, ABCC1-6), and breast cancer resistance protein (BCRP, ABCG2), all

members of the ATP-Binding Cassette superfamily (Choudhuri et al., 2006, Kosters and

Karpen, 2008). Members of this superfamily hydrolyze ATP for an energy source,

allowing them to pump substrates against a concentration gradient. The structure for

ATP-binding consists of three highly conserved motifs, Walker A, Walker B, and

Signature C, shared between different family members. All of the family members are

made up of two transmembrane domains (TMDs) and two nucleotide-binding domains

(NBDs) (Kos et al., 2009). The organization of these domains differs between specific

proteins. For example, Pgp is a continuous polypeptide made up of two homologous

halves, each consisting of six TM segments (Sharom, 2006). In contrast, BCRP is a

"half-transporter", made up of two separate six-segment TMDs that homodimerize via

disulfide bonds between cysteines in the extracellular loops (Koshiba et al., 2008).

While the interplay between Pgp and intestinal drug metabolizing enzymes such

as CYP3A4 has been widely studied, the same is not true of BCRP. These transporters'

expression in the intestine and/or liver, the two major sites affecting how much drug will

get into the body after an oral dose, makes factors affecting their function important

determinants of oral drug pharmacokinetics.

1.2 The Biopharmaceutics Drug Disposition Classification System (BDDCS):

The Biopharmaceutics Drug Distribution Classification System (BDDCS) can be

a helpful tool in predicting the effects that drug transporters in the gut and liver will have

on a drug's pharmacokinetic profile (Wu et al., 2005). The BDDCS is a modification of

the BCS (Amidon et al., 1995), in which compounds are categorized in four classes

according to their permeability and solubility, characteristics that will greatly influence

oral absorption. The BCS (See Figure 1-3) was developed to aid in predicting *in vivo*

pharmacokinetic behavior from *in vitro* solubility and *in vitro* or *in vivo* permeability

measurements. The recognition that BCS Class 1 and 2 compounds are mainly

eliminated by metabolism while Class 3 and 4 compounds are mainly eliminated by

biliary or renal excretion of unchanged drug led to the development of the BDDCS (See

Figure 1-4 and Table 1-1) by Wu and Benet (2005), in which the permeability

characteristic was replaced by route of elimination.

Figure 1-3 Biopharmaceutics Classification System

Figure 1-4 Biopharmaceutics Drug Disposition Classification System

Class 1: High Solubility/Extensive Metabolism		Class 2: Low Solubility/Extensive Metabolism	
Abacavir	Ketoprofen	Albendazole	Ketoconazole
Acebutelol	Ketorolac	Amiodarone	Lansoprazole
Acetaminophen	Labetolol	Atorvastatin	Lopinavir
Albuterol	Levamisole	Azathioprine	Lovastatin
Allopurinol	Levodopa	Azithromycin	Medendazole
Amitryptiline	Lidocaine	Carbamazepine	Mefloquin
Antipyrine	Meperidine	Carvediol	Nalidixic acid
Buspirone	Metoprolol	Chlorpromazine	Naproxen
Caffeine	Metronidazole	Cisapride	Nelfinavir
Chloramphenicol	Midazolam	Clofazamine	Nevirapine
Chlorpheniramine	Minocycline	Cyclosporine	Nifedipine
Codeine	Misoprostol	Danazol	Oxaprozin
Colchicine	Morphine	Dapsone	Phenytoin
Cyclophosphamide	Phenobarbital	Diclofenac	Piroxicam
Desipramine	Phenylalanine	Diflunisol	Praziquantel
Dexamethasone	Prednisolone	Efavirenz	Raloxifene
Diazepam	Primaquine	Felodipine	Rifampin
Diltiazem	Promazine	Flurbiprofen	Ritonavir
Diphenhydramine	Promethazine	Glipizide	Saquinavir
Disopyramide	Propranolol	Glyburide	Sirolimus
Doxepin	Pyranzinamide	Griseofulvin	Spironolactone
Enalapril	Quinidine	Haloperidol	Sulfamethoxazole
Ergonovine	Quinine	Ibuprofen	Tacrolimus
Ergotamine	Rosiglitizone	Indinavir	Tamoxifen
Ethinyl estradiol	Salicyclic acid	Indomethacin	Terfenadine
Fluoxetine	Sotolol	Itrazonazole	Warfarin
Glucose	Theophylline	Ivermectin	
Hydralazine	Valproic acid		
Imipramine	Verapamil		
Isoniazid	Zidovudine		
Isosorbid dinitrate			

Class 3: High Solubility/Poor Metabolism		Class 4: Low Solubility/Poor Metabolism
Acyclovir	Ganciclovir	Acetazolamide
Amiloride	Hydrochlorothiazide	Aluminum hydroxide
Amoxicillin	Lamivudine	Amphotericin
Atenolol	Levofloxacin	Chlorothiazide
Atropine	Lisinopril	Chlorothalidone
Bidisomide	Lithium	Ciprofloxacin
Bisphosphonates	Lomefloxacin	Colistin
Captopril	Merformin	Digoxin
Cefazolin	Methotrexate	Furosemide
Cetirizine	Metoclopramide	Neomycin
Chloroquine	Nadolol	Nystatin
Cimetidine	Neostigmine	Ofloxacin
Cloxacilin	Penicillins	Phenazopyridine
Dicloxacilin	Pitavastatin	Talinolol
Doxycycline	Pravastatin	
Ephedrine	Pyridostigmine	
Erythromycin	Ranitidine	
Ethambutol	Riboflavin	
Famotidine	Tetracycline	
Fexofenadine	Trimethoprim	
Fluconazole	Valsartan	
Folinic acid	Zalcitabine	

Table 1-1 Classification of 172 Drugs by BDDCS adapted from Wu and Benet (2005)

It is believed that extent of metabolism (by oxidative Phase 1 and conjugative Phase 2 enzymes) is an appropriate surrogate for permeability since for a drug to get metabolized, it must get absorbed (Benet et al., 2008). Generally, a drug's elimination route is much easier to determine than its extent of absorption or its permeability in humans. Currently, there are several methods for determining drug permeability detailed in the FDA CDER guidance (FDA, 2000). Human pharmacokinetic studies to determine mass balance or absolute bioavailability can be used, but can be affected by high inter-subject variability and such studies are expensive and time-consuming. Human *in vivo*

intestinal perfusion studies, extensively reviewed by Lennernas (2007), are useful and several methods are available to conduct these experiments, but they have the same drawbacks as pharmacokinetic studies. Intestinal perfusion studies with representative animal models either *in vivo* or *in situ*, or excised tissue studies with human or animal intestinal tissue are other options, as are *in vitro* cell studies in an epithelial cell line, such as Caco2 monolayers (FDA, 2000). While the use of animal models is less expensive and time-consuming than human studies, there are species differences in expression and substrate profiles for transporters and metabolic enzymes that can lead to misclassification of compounds (Li et al., 2009, Katoh et al., 2006, Cao et al., 2006). Indeed, the CDER guidance recommends that non-human systems be used only for compounds transported by passive processes (FDA, 2000). When using human cell lines in permeability studies, care must be taken to ensure that expression levels of transporters are representative of those seen *in vivo* (Hayeshi et al., 2008, Arthur, 2000, Sun et al., 2002) or discrepancies could arise between *in vitro* and *in vivo* results.

The use of human liver microsomes, microsomes generated from Sf9 insect cells expressing recombinant metabolic enzymes, and isolated human and animal hepatocytes are widely employed to help determine if a drug will be eliminated by metabolism. Simple incubation experiments will determine if a compound is a substrate for metabolizing enzymes and can be followed by *in vivo* animal and human studies to determine the importance of metabolism as a route of elimination. Information on the elimination route is obtained by measuring parent drug and metabolite levels in plasma and urine collected during Phase 1 human pharmacokinetic studies.

In the BDDCS framework, if a drug is ≥90% metabolized (a conservative estimate that matches the 90% absorbed criteria currently used in BCS), based on solubility the drug can be designated as Class 1 or 2. Wu and Benet (2005) recommend for transporter predictions utilizing ≥70% metabolism for Class 1 and 2 drugs and <70% metabolism for Class 3 and 4 drugs. They point out, that in fact very few marketed drugs fall into the 30 to 70% metabolism category and that most drugs are either extensively metabolized (≥70%) or markedly poorly metabolized (<30%).

The BDDCS allows for some general predictions regarding the role of transporters in oral drug disposition based upon the drug's classification (Figure 1-5).

	High Solubility	Low Solubility
Extensive Metabolism	Class 1: High Solubility Extensive Metabolism	Class 2: Low Solubility Extensive Metabolism
Poor Metabolism	Class 3: High Solubility Poor Metabolism	Class 4: Low Solubility Poor Metabolism

Figure 1-5 Oral dosing: Transporter effects by BDDCS class

The relevant transporters in terms of BDDCS class in Fig. 1-5 reflect what Wu and Benet observed for the great majority of drugs in each class. Of course, such a simple categorization in only four classes for all drugs cannot be expected to be

universally true with no exceptions, as stated by Wu and Benet (2005). It is even more difficult to hypothesize universal scientific explanations for these findings. However, those proposed by Wu and Benet (2005) as possible explanations are as follows: Class 1 drugs are highly permeable and highly soluble, allowing them to pass through the gut lumen unaided by transporters. This will occur even if a Class 1 compound is a substrate *in vitro* for an uptake or efflux transporter expressed in the gut. This is hypothesized to occur because the gut is sufficiently leaky that the high permeability of these drugs does not give the transporter sufficient access to the drug or alternatively, the drugs' physicochemical properties allow it to achieve a high enough concentration in the lumen and within enterocytes that it will saturate any such transporter and be independent of transporter effects (Wu and Benet, 2005). Class 2 drugs are also highly permeable, so they will generally be able to enter enterocytes by passive diffusion, unaided by uptake transporters. However, due to low solubility limiting lumenal concentration, they are unlikely to saturate efflux transporters. Consequently, Class 2 compounds can be effluxed out of enterocytes and subject to efflux transporter effects that can influence bioavailability and absorption rate.

When considering the liver, only the first of the two explanations above for high permeability, i.e., that the hepatocyte is sufficiently leaky that the high permeability of these drugs does not give the transporter sufficient access to the drug, seems reasonable for Class 1 drugs. At this time, we have no good explanation for why certain (but not all) Class 2 drugs are substrates for hepatic uptake and efflux transporters. Perhaps the explanation of Fagerholm (2007) that difference in the degrees of "high" permeability

dictate whether the compound will be a substrate for transporters is correct, but this requires further investigation.

Class 3 compounds have high solubility but low permeability while Class 4 compounds have both low solubility and low permeability. For both of these classes, drug is unable to get into enterocytes or hepatocytes unless aided by an uptake transporter. Even for highly soluble Class 3 drugs, the need for uptake transport will limit the intra-enterocyte drug concentration, making saturation of efflux transporters unlikely. Therefore, both Class 3 and Class 4 drugs may be subject to uptake and efflux transporter effects.

1.3 Oral Bioavailability (F) and Exposure (Area Under the Concentration-Time Curve):

Oral bioavailability is defined as the fraction of a dose administered that is absorbed into the systemic circulation intact (Wu et al., 1995). It is a function of the fraction of the dose that is absorbed in the enterocytes (F_A), the fraction of the absorbed dose that passes through the gut membranes intact (F_G) and the fraction passing through the liver intact (F_H) before reaching the systemic blood supply (Eq.1). Transporters will help modulate F of drugs by playing a role in how much drug gets across the gut membranes and how much drug is taken up into hepatocytes.

$$F = F_A \text{ x } F_G \text{ x } F_H \hspace{4cm} (\text{Eq. 1})$$

Bioavailability is proportional to the area under the concentration-time curve (AUC), which is a measure of drug exposure (Eq. 2). Consequently, transporter effects on F will result in a corresponding effect on AUC. Changes in AUC are easier to determine than

those on F, since both *in vivo* oral and IV studies are needed to quantitate absolute

bioavailability. Many drugs are only available in either oral or IV formulations, but not

both.

F = (CL·AUC)/Dose   (Eq. 2)

The concept of bioavailability relates to Eq. 2. For an IV dose, bioavailability is assumed

to be complete, i.e. F = 1. Thus assuming clearance (CL) to be constant between the IV

and oral dosings, oral F may be determined by comparing exposure for oral and IV doses,

while correcting for any differences in dose between the two studies. *In situ* and *ex situ*

experiments with individual organs, such as the intestine or liver, using perfusion

techniques are very useful for studying transporter effects on F and coupling results from

these organ experiments with whole animal and human AUC data can help elucidate the

mechanisms involved in altering both bioavailability and drug exposure.

In the gut, Class 1 and 2 compounds have favorable permeability characteristics,

allowing them to enter enterocytes unaided by apical uptake transporters. As explained

above, due to their high solubility and rapid permeability, Class 1 compounds also readily

bypass efflux transporters or, alternatively, the high concentrations likely saturate apical

efflux transporters and therefore Class 1 drug AUC and F will not be influenced by efflux

transporters even if they are substrates *in vitro*. Cao et al. (2005) demonstrated this *in

situ* with an intestinal rat perfusion model in which they determined verapamil and

propranolol permeabilities and showed that they were independent of Pgp expression

level, which increased 6-fold along the intestinal tract from the duodenum to the ileum.

While the status of propranolol as a Pgp substrate is unclear, it is well recognized that

verapamil is a good Pgp substrate. Although AUC and F of Class 1 compounds are independent of apical efflux transporters, such efflux transporters will influence AUC and F of Class 2 compounds. Due to their low solubility, the low concentration of Class 2 compounds should not saturate apical efflux transporters as Class 1 compounds can. Therefore, apical efflux transporters will be able to pump drug back out into the lumen where it may re-enter enterocytes, thus allowing repeated exposure to drug metabolizing enzymes within the enterocytes. This interplay between apical gut efflux transporters and metabolizing enzymes within enterocytes has been well-characterized using *in vitro* and *in vivo* systems (Cummins et al., 2002, Cummins et al., 2003). Cummins and coworkers used both a Caco2 cell line overexpressing CYP3A4 (Cummins et al., 2002) and a rat intestinal perfusion model (Cummins et al., 2003) to demonstrate the importance of Pgp in influencing metabolism of K77, a cysteine protease inhibitor and dual substrate of Pgp and CYP3A4. In brief, both the cell line studies and the intestinal perfusion studies showed that Pgp inhibition increased intracellular K77 concentrations or appearance in mesenteric blood while decreasing efflux transport. No corresponding changes were seen for the CYP3A4 substrates felodipine (Cummins et al., 2002), a Class 2 compound that is not a substrate of Pgp, or midazolam (Cummins et al., 2003), a Class 1 compound not influenced by Pgp in the gut. The effects of inducing Pgp have been shown to yield opposite effects to that for Pgp inhibition *in vivo* with the Class 2 (BCS)/Class 4 (BDDCS) compound talinolol. Schwarz et al. (2007) induced gut Pgp by pretreatment with St. John's Wort and saw a significant reduction (25%) in F compared to the water control. Likewise, Westphal et al. (2000) saw a significant (~20%) reduction in F for talinolol when Pgp was induced with rifampin. While the interplay between Pgp and

CYP3A4 has been extensively studied, this phenomenon may also occur with other enterocytic drug metabolizing enzymes [CYP2C9, CYP2C19, CYP2C8, CYP2D6, esterases, epoxide hydrolases, UGT1A1, UGT1A7-10, SULT1E1, SULT2A1, SULT1A3, N-acetyltransferases, and glutathione-S-transferases (Lee et al., 2003)] and other apical efflux transporters (ie. BCRP, MRP2). One such example is provided by Sesink et al. (2005). Using Mrp2 knockout mice and the specific Bcrp1 inhibitor FTC, they showed in an *in situ* intestinal perfusion model that inhibiting apical efflux of quercetin glucuronides by Bcrp1 increased plasma quercetin levels more than 2-fold after enzymatic hydrolysis of the plasma samples. Another example is provided by Su et al. (2007) in which rat ileal perfusions were performed with topotecan in the presence and absence of novobiocin, a Bcrp1 inhibitor. With novobiocin, a ~50% decrease in intestinal secretion was seen with a corresponding increase in permeability, indicating that Bcrp1 inhibition influences topotecan absorption and bioavailability. Currently it is difficult to study BCRP and MRP2 interactions in human clinical studies due to the lack of specific inhibitors that can be dosed to people. Also, many drugs are substrates for multiple efflux transporters. Pgp and BCRP have extensive substrate overlap and therefore one transporter may compensate when the other is inhibited. In preclinical studies, the use of knockout animals can circumvent this problem, but an effective strategy for human studies remains to be found. More studies with these other gut enzymes and efflux transporters is needed to fully characterize the importance of their potential interplay in influencing AUC and F of substrate drugs.

BDDCS Class 3 and 4 drugs, which have low permeability, require apical uptake transporters to help them cross the luminal barrier since their low permeability limits

diffusion into enterocytes. Clinical studies have shown that inhibition of apical gut

uptake transporters can also influence plasma levels of substrate drugs. Glaeser et al.

(2007) showed that administration of grapefruit juice concomitantly or 2 hours prior to

dosing the Class 3 compound fexofenadine, an OATP1A2 substrate, decreased

fexofenadine plasma levels compared to water control, as well as dosing of grapefruit

juice 4 hours prior to fexofenadine dosing. Since fexofenadine, like all BDDCS Class 3

drugs, is not extensively metabolized, the authors concluded that the effect was due to

inhibition of OATP1A2 uptake of fexofenadine. Kato et al. (2009) demonstrated in

mouse pharmacokinetic and Ussing chamber studies that celiprolol absorption was

significantly decreased by bromosulfophthalein (BSP), a broad organic anion transport

inhibitor. They used mdr1a/1b knockout mice to avoid any confounding effects of Pgp

and demonstrated decreased plasma levels of celiprolol upon BSP coadministration in the

pharmacokinetic studies. They confirmed that the effect was due to decreased absorption

in Ussing chamber studies by showing that BSP significantly reduced apical to

basolateral permeability.

Induction of intestinal uptake transporters conversely should increase the AUC

and F of their substrates. In a rat pharmacokinetic study, Koitabashi et al. (2006)

demonstrated that administration of orange juice significantly increased the AUC of

orally dosed pravastatin while having no effect on IV pravastatin, indicating a change in

F. They further investigated mRNA and protein levels of rat Oatp1a1 and Oatp1a4 and

saw significant increases in both for each transporter. In addition to the rat studies,

Koitabashi et al. (2006) ran a human study to examine the effect of orange juice on oral

pravastatin. As with the rats, a significant increase in AUC was seen, although a

corresponding IV study was not possible to provide evidence that the change was due to increased F.

Class 3 and 4 drugs also have the potential to be influenced by efflux transporters since they are unlikely to attain intracellular concentrations high enough to saturate efflux transporters. Dahan et al. (2009) examined the effect of intestinal Pgp on two Class 3 compounds, famotidine and cimetidine. They determined in rat *in situ* intestinal perfusion studies that differential Pgp expression in the proximal jejunum versus the distal ileum led to different famotidine and cimetidine permeabilities in these segments with significantly decreased permeability seen in the distal segment compared to the proximal segment, corresponding to the higher Pgp expression observed in the distal segment. Upon Pgp inhibition by verapamil, a significant increase in permeability for both compounds was seen in the distal ileum segment, while no significant difference was seen in the proximal jejunum. The distal ileum permeability approached the permeability seen in the proximal jejunum segment, effectively making permeability constant along the small intestine in the presence of verapamil. Evidence supporting the effect of apical gut efflux on BDDCS Class 4 drug absorption also exists for digoxin, a Pgp substrate. A human clinical study by Greiner et al. (2002) showed that induction of Pgp by rifampin decreased the absorption of orally dosed digoxin, even though digoxin is not metabolized by CYPs in humans. Subjects received either IV or oral digoxin before and after Pgp induction. Pgp induction was examined by immunohistochemistry and Western blot analysis of duodenal samples, which were shown to increase 3.5-fold after ~2 weeks of rifampin dosing. F was significantly decreased (19%) after Pgp induction.

Further work is required to fully characterize the effect of gut apical transporters on Class 3 and 4 drugs.

The influence of intestinal basolateral uptake and efflux transporters has not yet been examined in depth to determine their influence on AUC and F, however we can predict what effects they may have based on what we predict for the effects of apical transporters. A summary of the effects of intestinal drug transporters on AUC by BDDCS class is given in Table 1-2.

BDDCS Class	1	2	3	4
Inhibition				
Apical Uptake	⟺	⟺	⇩	⇩
Apical Efflux	⟺	⇧	⇧	⇧
Basolateral Uptake	⟺	?	⇧	⇧
Basolateral Efflux	⟺	?	⇩	⇩
Induction				
Apical Uptake	⟺	⟺	⇧	⇧
Apical Efflux	⟺	⇩	⇩	⇩
Basolateral Uptake	⟺	?	⇩	⇩
Basolateral Efflux	⟺	?	⇧	⇧

Table 1-2 Predicted effects of inhibition and induction of intestinal drug transporters on exposure (AUC) by BDDCS class

The BDDCS is also useful for making predictions regarding food effects on orally dosed drugs. The AUC and F of many compounds are greatly affected by concomitant food intake and the FDA recommends that high fat meals (800-1000 cal: 50-65% from

fat, 25-30% from carbohydrates, 15-20% from protein) be used in food-effect studies in the guidance "Food Effect Bioavailability and Fed Bioequivalence Studies" (FDA, 2002). Many factors are believed to contribute to these food effects, including changes in gastric emptying time, bile flow, pH of the intestine, splanchnic blood flow, and gut wall metabolism. A variety of evidence exists supporting food effects on transporters as well and is described in detail in a review by Custodio et al. (2008). The BDDCS is able to predict what is seen clinically in food effect studies. These predictions are explained if it holds that high-fat meal components inhibit apical gut uptake and efflux transporters. Figure 1-6 summarizes the effects of high fat meals on F and t_{max} by BDDCS Class (Wu and Benet, 2005, Custodio et al., 2008).
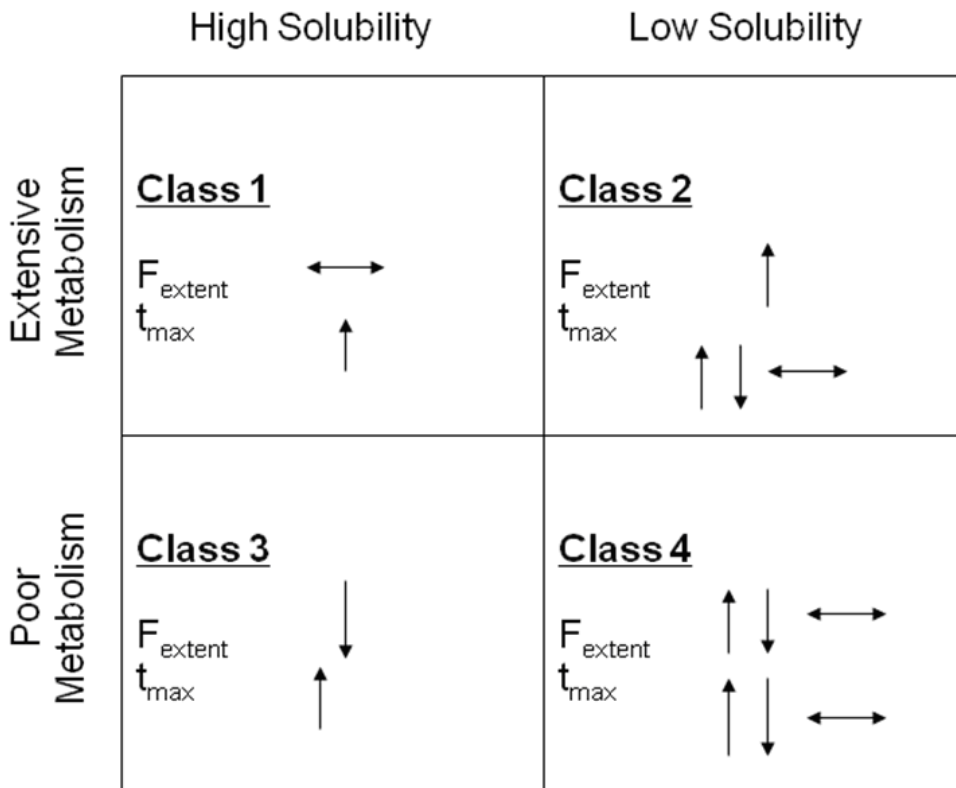
Figure 1-6 Food effects of high fat meals predicted by BDDCS class

Drug that crosses the intestinal barrier passes into the hepatic portal vein and travels tothe liver, the final major site for first-pass effects, before reaching the systemic circulation. Drug transporters will play a role in determining how much drug enters hepatocytes and is exposed to hepatic drug metabolizing enzymes and biliary excretion. In hepatocytes, basolateral uptake transporters function to take drug up from the sinusoidal blood into hepatocytes while basolateral efflux transporters pump drug back out into the sinusoidal blood. Apical transporters face the bile ducts, therefore apical efflux transporters will pump drug into the bile.

The major predictive difference for the BDDCS system between the gut and the liver relates to the importance of uptake transporters for BDDCS Class 2 drugs. It is possible that the intestinal membrane may be "leakier" than the hepatic membrane, allowing more drug to diffuse across the intestinal barrier than the hepatic barrier. For example, while BDDCS Class 2 compounds do not require uptake transporters to get into enterocytes, it has been shown that hepatic uptake transporters can be an important determinant of drug entry into hepatocytes and could thereby affect F through the first pass effect and AUC through the combination of the first pass effect and subsequent passages through the liver. Tirona et al. (2003) demonstrated that the Class 2 compound rifampin could be transported by OATP1B1 and, to a lesser extent, OATP1B3 expressed in HeLa cells. Su et al. (2004) determined that OATP1A2 is able to transport saquinavir, also a Class 2 compound, in oocytes and in HepG2 cells, a human hepatocellular liver carcinoma cell line. The AUC and F of Class 3 and 4 drugs, due to their low permeability, will also be influenced by hepatic uptake transporters. Watanabe et al. (2009) investigated the importance of hepatic uptake transporters on the plasma levels of

the Class 3 compound pravastatin. They developed a physiologic based pharmacokinetic (PBPK) model that incorporated hepatic sinusoidal uptake and demonstrated the sensitivity of plasma levels to a change in uptake. Decreasing uptake transporter activity to 1/3 of control led to simulated pravastatin plasma levels 271% of the control, while increasing uptake transporter activity to 3x that of the control led to simulated plasma levels 14% of control. Hepatic basolateral efflux transporters (i.e. MRP3, 4, 5, 6) may influence AUC and F since they provide an avenue of exit from hepatocytes. As in the intestine, it is possible that these membrane bound transporters can interact with drug before it interacts with metabolizing enzymes associated with the endoplasmic reticulum. Altering these transporters' function could affect the AUC and F of their substrates by altering first pass hepatic metabolism or biliary excretion. Theoretically, the apical efflux transporters could also affect AUC and F by helping to control intra-hepatocyte drug levels, although this effect would be dependent on the drug's ability to get back out of the hepatocyte into sinusoidal blood either by diffusion or by basolateral efflux. A summary of the effects of hepatic drug transporters on AUC is given in Table VI and explicated in the next section.

BDDCS Class	1	2	3	4
Inhibition				
Apical Efflux	⟺	⇩	⇧	⇧
Basolateral Uptake	⟺	⇧	⇧	⇧
Basolateral Efflux	⟺	⇩	⇩	⇩
Induction				
Apical Efflux	⟺	⇧	⇩	⇩
Basolateral Uptake	⟺	⇩	⇩	⇩
Basolateral Efflux	⟺	⇧	⇧	⇧

Table 1-3 Predicted effects of inhibition and induction of hepatic drug transporters on exposure (AUC) by BDDCS class

1.4 Clearance (CL):

Clearance is technically defined as a proportionality factor that relates the rate of elimination of drug to the systemic drug concentration (Wu et al., 1995). It must be kept in mind that metabolism that occurs in the gut and first pass in the liver does not contribute to CL since that drug is lost before it reaches systemic circulation. For orally dosed drugs, CL and F are intimately associated and cannot be separated unless corresponding IV studies have been done. Since this review deals with orally dosed drugs, we will discuss transporter effects on CL/F in addition to the intrinsic clearance by the liver.

$$CL = F \cdot Dose/AUC \qquad\qquad\qquad Eq.\ 2a$$

$$CL/F = Dose/AUC \qquad\qquad\qquad Eq.\ 2b$$

Gut transporters will exclusively affect F, thus CL will not change in response to induction or inhibition of gut transporters, only F will. For orally dosed drugs the liver and the kidneys are the major eliminating organs and their clearances are additive.

Total CL = CL_H + CL_R Eq.3

CL_H can further be divided into uptake and elimination processes, with the latter divided into biliary excretory clearance and hepatic metabolic clearance (Watanabe et al., 2009). Both mechanisms can be affected by transporters.

Transporters in the liver and kidney can affect the CL of the portion of an orally administered drug that escapes the first-pass effect. Hepatic uptake transporters are expressed on the basolateral surface of hepatocytes facing the sinusoidal blood supply. Inhibiting these transporters prevents drug from being exposed to metabolizing enzymes within hepatocytes, decreasing the CL_H of drugs that are substrates for these enzymes. For drugs that are not metabolized but are eliminated by biliary excretion, CL_H may also decrease since drug is prevented from getting into the bile through the hepatocytes. Conversely, induction of hepatic uptake transporters will increase the amount of drug able to get into hepatocytes and thus gain exposure to metabolizing enzymes or get pumped into the bile, thereby increasing CL_H. CL/F will change in the same direction as CL_H for each case, but the CL value is not separable from F based on oral data alone. In addition to basolateral uptake transporters, hepatocytes also express basolateral efflux transporters that pump drug back out into the sinusoidal blood. The effects of inhibiting or inducing these transporters will be opposite those for the basolateral uptake transporters. Inhibiting basolateral efflux will cause more drug to remain inside

hepatocytes and will lead to increased CL_H either by increased exposure to metabolizing enzymes or to efflux into the bile, while inducing them will lead to more drug being pumped out of hepatocytes and decreased CL_H. Again, CL/F will change in the same direction as CL_H.

Class 1 compounds, due to their high permeability appear not to be influenced by basolateral hepatic uptake transporters. In the gut, Class 2 compounds are not strongly influenced by apical uptake transporters due to their high permeability, however it has been shown that, at least, some of these compounds are influenced by basolateral hepatic uptake transporters. In a human pharmacokinetic study Lau et al. (2007) showed that a single IV dose of the OATP inhibitor rifampin significantly decreased CL/F of atorvastatin, presumably by decreasing basolateral uptake by OATP1B1 leading to decreased hepatic metabolism by CYP3A4. *In vitro* studies showed that 50μM rifampin did not inhibit CYP3A4 metabolism of atorvastatin and rifampin plasma levels in the human study were ~15μM, indicating that inhibition of hepatic metabolism was not a causal factor in reducing CL/F. Similar results were seen by Zheng et al. (2009) in a human study examining the effect of IV rifampin on orally dosed glyburide, an OATP2B1 substrate. Upon multiple dosing of rifampin, but when rifampin was no longer present in the systemic circulation, glyburide CL/F was significantly increased compared to the control, due to induction of metabolic enzymes and transporters. As stated earlier, we have no good explanation for why some BDDCS class 2 compounds are substrates for hepatic uptake transporters but this is not seen for BDDCS class 1 compounds. It is difficult to imagine a scientific explanation based on a solubility effect in the liver. This is an area requiring further investigation.

As expected due to their low permeability potential, the CL/F of Class 3 and 4 drugs also can be influenced by basolateral hepatic uptake transporter effects. Studies with the Class 3 drugs, pravastatin and pitavastatin, have shown the effects of decreased function of OATP1B1 on CL/F. Deng et al. (2008) performed human clinical studies looking at the effect of genotype of OATP1B1 (OATP1B1*1a homozygotes versus OATP1B1*15 homozygotes) on pitavastatin and pravastatin pharmacokinetics. They saw that CL/F for both compounds was significantly decreased in subjects with OATP1B1*15/*15 genotype compared to wildtype (2.07-fold and 2.88-fold for pravastatin and pitavastatin, respectively). Transporter influence on pharmacokinetic parameters for metformin, another Class 3 compound and a substrate for OCT1, has also been shown. Shu et al. (2008) performed a clinical study to determine the effect of OCT1 genetic variation on metformin pharmacokinetics. Metformin was orally dosed in two subject groups, one group with wildtype OCT1 and the other composed of subjects carrying at least one reduced function allele. They found that CL/F was significantly reduced in the variant allele group.

Hepatic apical efflux transporters responsible for pumping drug into the bile may also affect both hepatic metabolic clearance and biliary excretory clearance of their substrate drugs. Inhibiting apical efflux causes drug to remain trapped within hepatocytes. If the compound is a substrate for metabolizing enzymes (BDDCS Class 1 and 2 compounds), its metabolism will increase due to increased exposure to enzymes and CL_H will increase. If the drug is not subject to metabolic transformation but rather is eliminated by biliary excretion (Class 3 and 4 compounds), its CL_H may decrease due to decreased excretion into bile. An alternative route of elimination is possible though,

which may cause a situation to arise in which there is no net change in CL/F, but rather a change in the clearance profile seen as decreased biliary excretion and increased renal excretion if the drug is sufficiently hydrophilic to be eliminated in the urine. Induction of hepatic apical efflux transport could lead to increased biliary excretion but decreased metabolic transformation, making the effect on CL_H dependent upon a drug's substrate status for metabolizing enzymes. Studies remain to be done to elucidate the effect of hepatic apical efflux transporters on CL/F separate from that of apical gut efflux transporters.

While work has been done on determining effects of hepatic basolateral efflux in *in situ* isolated perfused rat liver studies (Tian et al., 2008) and *in vivo* with intraperitoneal dosing (Zelcer et al., 2005), the effect of hepatic basolateral efflux transporters on oral drug pharmacokinetics has not been extensively studied. However we can hypothesize what effects inhibition or induction will have. Inhibition of hepatic basolateral efflux will cause drug to be trapped within hepatocytes, similar to hepatic apical efflux inhibition, and will lead to increased exposure to drug metabolizing enzymes or to apical efflux. This may lead to an increase in hepatic metabolic or biliary excretory clearance. Induction of hepatic basolateral efflux will cause more drug to be pumped back into the sinusoidal blood, decreasing the hepatic contribution to CL/F, but depending on the drug's hydrophilicity may be compensated for by increased renal CL.

1.5 Half-life ($t_{1/2}$):

The elmination half-life is dependent upon CL and V (Eq. 4).

$$t_{1/2} \approx 0.693 \text{x} V/CL \qquad\qquad\qquad\qquad \text{Eq. 4}$$

Whatever effects transporters exert on V and CL will influence the $t_{1/2}$, either causing it to increase if the increase in V predominates, decrease if the increase in CL is more pronounced, or have no net effect if changes in V and CL cancel out each other. However, transporters in the gut may affect the absorption half-life, $t_{1/2,abs}$ (Eq. 5).

$$t_{1/2,abs} = .693/k_a \qquad\qquad\qquad\qquad \text{Eq. 5}$$

The rate constant of absorption, k_a, may be influenced by gut transporters and the BDDCS can be useful in predicting which drugs are likely to be affected. As stated before, Class 3 and 4 drugs are dependent on gut uptake transporters to get across the luminal membrane. If their uptake is inhibited, this is likely to decrease their absorption rate, driving down k_a and increasing $t_{1/2,abs}$. The opposite will hold true when uptake transporters are induced. The k_a will increase and $t_{1/2,abs}$ will decrease as more drug is pumped into enterocytes. Parker et al. (2003) ran a human study in which a single oral dose of digoxin was administered after 5 days pretreatment with grapefruit juice and saw a significant decrease in the digoxin k_a compared to the water control arm (3.0 ± 2.4 to 1.2 ± 1.0 hr^{-1}, $p<0.05$). The plasma concentration vs. time profile also showed a later t_{max}. No other pharmacokinetic parameters were significantly different between the treatment groups. The k_a and t_{max} results were not what would be expected if the interaction were due to Pgp inhibition (Parker et al., 2003, Benet et al., 1999), but rather what would be expected from inhibition of an intestinal uptake transporter. Although the

specific OATP isoform responsible for intestinal uptake of digoxin has not been

identified, the drug is known to be an OATP1B3 (Kullak-Ublick et al., 2001) substrate.

The BDDCS predicts the clinical results seen by Parker et al. (2003) since digoxin is a

Class 4 compound in humans and uptake transporter effects will be important for these

compounds. Intestinal efflux transporters may also affect k_a and $t_{1/2,abs}$, especially for

Class 2 compounds. If apical efflux transporters are inhibited, this will decrease the

"cycling" effect that is seen when a drug is repeatedly pumped out and gains reentry into

enterocytes, allowing the drug to exit basolaterally more quickly. In a study on the

effects of ABCB1 genotype, Solas et al. (2007) found that subjects carrying one

decreased function allele, C3435CT, dosed with indinavir (Class 2 compound) had a

significantly higher k_a (2-fold) compared to controls and carriers of two mutant alleles

(they explain the lack of significant difference in the C3435TT group as possible due to

lack of statistical power with the small number of subjects). The $t_{1/2,abs}$ of Class 3 and 4

compounds may also be subject to apical efflux transporter effects. For the Class 3

compound fexofenadine, a Pgp substrate (Zhou et al., 2004, Peng et al., 2006).

Tannergren et al. (2003) determined in human intestinal perfusion studies with the LOC-

I-GUT system that co-perfusion of fexofenadine with the Pgp inhibitor verapamil caused

a significant increase in k_a compared to the control [0.0030 ± 0.0012 min^{-1} to $0.0255 \pm$

0.0103 min^{-1} ($P < .001$)], which changes $t_{1/2,abs}$. Decreasing the absorption rate often

changes the appearance of the plasma concentration vs. time profile, even if no change in

the extent of absorption as measured by area under the curve (AUC) is seen. The t_{max} can

shift later and C_{max} can decrease, causing the profile to appear flatter. Increasing the

absorption rate constant may cause t_{max} to shift earlier and C_{max} to increase, sharpening

the plasma concentration vs. time profile. Class 1 drugs, for which transporter effects are minimal, should not show a significant change in the absorption rate constant or $t_{1/2,abs}$.

Transporter effects on k_a may also have implications for oral multiple dosing regimens. In a recent analysis Sahin and Benet (2008) defined a new half-life parameter, the operational multiple dosing half-life ($t_{1/2,op}$), as "the half-life equal to the dosing interval at steady-state where the maximum concentration at steady-state is twice the maximum concentration found for the first dose and where the fall off to the trough concentration from the maximum concentration is consistent with this half-life." They found that this $t_{1/2,op}$ parameter for some drugs may be quite sensitive to changes in k_a. In simulations with diazepam, decreasing the k_a from 2.77 h^{-1} to 0.347 h^{-1} led to a drastic increase in the $t_{1/2,op}$, increasing it from about 13 h to 35 h. Diazepam is a Class 1 drug, therefore we would not expect to see transporter effects on k_a, however further study is warranted to determine what effect varying k_a has on the $t_{1/2,op}$ for Class 2, 3, and 4 compounds through transporter interactions.

1.6 Volume of Distribution (V):

Volume of distribution is defined as the "volume into which a drug distributes in the body at equilibrium (Rowland et al., 1995)" and is a "direct measure of the extent of distribution" (Rowland and Tozer, 1995). Transporters in the gut will not affect V as it relates the concentration of drug in the systemic concentration to amount of drug in the body. Like CL, V for orally adminstered drugs cannot be separated from F and V is reported as V/F. Very few drugs remain within physiologically realistic volumes (Rowland and Tozer, 1995), such as the plasma (3L), extracellular water (16L), or total

29

body water (42L). Instead they distribute into organs and tissues, greatly increasing their apparent V. Transporters may influence V by mediating their transport into and out of a variety of tissues and organs. The most widely studied sites thus far in relation to transporter influence on distribution are the liver and the brain, but the principles determined for these organs should hold for other organs and tissues expressing drug transporters. Several drugs whose site of action is the liver, including some statins, are concentrated in the liver by hepatic uptake transporters. If their hepatic uptake is inhibited, more drug remains in the plasma and less drug gets into the liver, decreasing V/F. For example, Lau et al. (2007) saw a significant reduction in V_{ss}/F in response to a single IV dose of rifampin inhibiting the hepatic uptake of atorvastatin.   Zheng et al. (2009) showed a similar effect of rifampin on the V_{ss}/F for glyburide. Induction may increase the amount of drug getting into the liver, decrease the amount in plasma, and may increase V/F. While the effects of altering function of hepatic apical efflux transporters may influence V/F, this effect isn't always predictable. Decreasing hepatic basolateral efflux may keep drug within hepatocytes, possibly decreasing plasma levels and increasing V/F while inducing basolateral efflux may lead to decreased V/F by causing there to be more drug in the plasma.

From the discussed examples, it's clear that transporters exert substantial and clinically relevant influence on many drugs' pharmacokinetic behavior. Experiments described in this thesis seek to help further clarify when one must consider transporter effects when investigating or predicting pharmacokinetics.

1.7 References

Amidon, G.L., Lennernäs, H., Shah, V.P. and Crison, J.R. (1995). "A theoretical basis for a biopharmaceutic drug classification: the correlation of in vitro drug product dissolution and in vivo bioavailability." Pharm. Res. **12**(3): 413-420.

Arthur, J. M. (2000). "The MDCK cell line is made up of populations of cells with diverse resistive and transport properties." Tissue Cell. **32**(5): 446-450.

Benet, L.Z., Izumi, T., Zhang, Y., Silverman, J.A. and Wacher, V.J. (1999). "Intestinal MDR transport proteins and P-450 enzymes as barriers to oral drug delivery." J. Control. Rel. **62**(1-2): 25-31.

Benet, L.Z., Amidon, G.L., Barends, D.M., Lennernäs, H., Polli, J.E., Shah, V.P., Stavchansky, S.A. and Yu, L.X. (2008). "The use of BDDCS in classifying the permeability of marketed drugs." Pharm. Res. **25**(3): 483-488.

Bi, Y., Kazolias, D. and Duignan, D.B. (2006). "Use of cryopreserved human hepatocytes in sandwich culture to measure hepatobiliary transport." Drug Metab. Dispos. **34**(9): 1658-1665.

Cao, X., Yu, L. X., Barbaciru, C., Landowski, C. P., Shin, H.C., Gibbs, S., Miller, H.A., Amidon, G.L. and Sun, D. (2005). "Permeability dominates in vivo intestinal absorption of P-gp substrate with high solubility and high permeability." Mol. Pharmaceut. **2**(4): 329-340.

Cao, X., Gibbs, S.T., Fang, L., Miller, H.A., Landowski, C.P., Shin, H.C., Lennernas, H., Zhong, Y., Amidon, G.L., Yu, L.X. and Sun, D. (2006). "Why is it challenging to predict intestinal drug absorption and oral bioavailability in human using rat model." Pharm. Res. **23**(8): 1675-1686.

Choudhuri, S. and Klaassen, C.D. (2006). "Structure, function, expression, genomic organization, and single nucleotide polymorphisms of human ABCB1 (MDR1), ABCC (MRP), and ABCG2 (BCRP) efflux transporters." Int. J. Toxicol. **25**(4): 231-259.

Ciarimboli, G. (2008). "Organic cation transporters." Xenobiotica. **38**(7-8): 936-971.

Cummins, C.L., Jacobsen, W. and Benet, L.Z. (2002). "Unmasking the dynamic interplay between intestinal P-glycoprotein and CYP3A4." J. Pharmacol. Exp. Ther. **300**(3): 1036-1045.

Cummins, C.L., Salphati, L., Reid, M.J. and Benet, L.Z. (2003). "In vivo modulation of intestinal CYP3A metabolism by P-glycoprotein: studies using the rat single-pass intestinal perfusion model." J. Pharmacol. Exp. Ther. **305**(1): 306-314.

Custodio, J.M., Wu, C.Y. and Benet, L.Z.. (2008). "Predicting drug disposition, absorption/elimination/transporter interplay and the role of food on drug absorption." Adv. Drug Deliv. Rev. **60**(6): 717-733.

Dahan, A. and Amidon, G.L. (2009). "Segmental Dependent Transport of Low Permeability Compounds along the Small Intestine Due to P-Glycoprotein: The Role of Efflux Transport in the Oral Absorption of BCS Class III Drugs." Mol. Pharmaceut. **6**(1): 19-28.

Deng, J.W., Song, I.S., Shin, H.J., Yeo, C.W., Cho, D.Y., Shon, J.H. and Shin, J.G. (2008). "The effect of SLCO1B1*15 on the disposition of pravastatin and pitavastatin is substrate dependent: the contribution of transporting activity changes by SLCO1B1*15." Pharmacogenet. Genomics. **18**(5): 424-433.

Fagerholm, U. (2007). "The role of permeability in drug ADME/PK, interactions and toxicity-presentation of a permeability-based classification system (PCS) for prediction of ADME/PK in humans." Pharm. Res. **25**(3):625-638.

FDA (2000). "Guidance for Industry: Waiver of In Vivo Bioavailability and Bioequivalence Studies for Immediate Release Solid Oral Dosage Forms Based on a Biopharmaceutics Classification System." FDA Guidance

FDA (2002). "Guidance for Industry: Food- Effect Bioavailability and Fed Bioequivalence Studies." FDA Guidance.

Fromm, M.F. (2000). "P-glycoprotein: a defense mechanism limiting oral bioavailability and CNS accumulation of drugs." Int. J. Clin. Pharmacol. Ther. **38**(2): 69-74.

Glaeser, H., Bailey, D..G, Dresser, G.K., Gregor, J.C., Schwarz, U.I., McGrath, J.S., Jolicoeur, E., Lee, W., Leake, B.F., Tirona, R.G. and Kim, R.B. (2007). "Intestinal drug transporter expression and the impact of grapefruit juice in humans." Clin. Pharmacol.Ther. **81**(3): 362-370.

Greiner, B., Eichelbaum, E., Fritz, P., Kreichgauer, H.P., von Richter, O., Zundler, J. and Kroemer, H.K. (2002). "The role of intestinal P-glycoprotein in the interaction of digoxin and rifampin." J. Clin. Invest. **104**(2): 147-53 (1999). Erratum in: J. Clin. Invest. **110**(4):571.

Hagenbuch, B. (2007). "Cellular entry of thyroid hormones by organic anion transporting polypeptides." Best Practice and Research Clinical Endocrinology and Metabolism. **21**(2): 209-221.

Hayeshi, R., Hilgendorf, C., Artursson, P., Augustijns, P., Brodin, B., Dehertogh, P., Fisher, K., Fossati, L., Hovenkamp, E., Korjamo, T., Masungi, C., Maubon, N., Mols, R., Müllertz, A., Mönkkönen, J., O'Driscoll, C., Oppers-Tiemissen, H. M., Ragnarsson, E. G., Rooseboom, M. and Ungell. A. L. (2008). "Comparison of drug transporter gene expression and functionality in Caco-2 cells from 10 different laboratories." Eur. J. Pharm. Sci. **35**(5): 383-396.

He, L., Konstandinos, V., and Nebert, D.W. (2009). "Analysis and update of the human solute carrier (SLC) gene superfamily." Hum. Genomics. **3**(2): 195-206.

Juliano, R.L. and Ling, V. (1976). "A surface glycoprotein modulating drug permeability in Chinese hamster ovary cell mutants." Biochim. Biophys. Acta. **455**: 152-162.

Kato, Y., Miyazaki, T., Kano, T., Sugiura, T., Kubo, Y. and Tsuji, A. (2008). 'Involvement of influx and efflux transport systems in gastrointestinal absorption of celiprolol.' J. Pharm. Sci. **98**(7):2529-2539.

Katoh, M., Suzuyama, N., Takeuchi, T., Yoshitomi, S., Asahi, S. and Yokoi, T. (2006). "Kinetic analyses for species differences in P-glycoprotein-mediated drug transport." J. Pharm. Sci. **95**(12): 2673-2683.

Koitabashi, Y., Kumai, T., Matsumoto, N., Watanabe, M., Sekine, S., Yanagida, Y. and Kobayashi, S. (2006). "Orange juice increased the bioavailability of pravastatin, 3-hydroxy-3-methylglutaryl CoA reductase inhibitor, in rats and healthy human subjects." Life Sci. **78**(24):2852-2859.

Konig J., Seithel A., Gradhand U. and Fromm M.F. (2006). "Pharmacogenomics of human OATP transporters." Naunyn-Schmiedeberg's Arch. Pharmacol. **372**: 432-443.

Kos, V. and Ford, R.C. (2009). "The ATP-binding cassette family: a structural perspective." Cell. Mol. Life Sci. **66**(19): 3111-3126.

Koshiba, S., An, R., Saito, H., Wakabayashi, K., Tamura, A. and Ishikawa, T. (2008). "Human ABC transporters ABCG2 (BCRP) and ABCG4." Xenobiotica. **38**(7-8):863-888.

Kosters, A. and Karpen, S.J. (2008). "Bile acid transporters in health and disease." Xenobiotica. **38**(7-8): 1043-1071.

Kullak-Ublick, G.A., Ismair, M.G., Stieger, B., Landmann, L., Huber, R., Pizzagalli, F., Fattinger, K., Meier, P.J. and Hagenbuch, B. (2001). "Organic anion-transporting polypeptide B (OATP-B) and its functional comparison with three other OATPs of human liver." Gasotroenterology. **120**: 525-533.

Landowski, C.P., Sun, D., Foster, D.R., Menon, S.S., Barnett, J.L., Welage, L.S., Ramachandran, C. and Amidon, G.L. (2003). "Gene expression in the human intestine and correlation with oral valacyclovir pharmacokinetic parameters." J. Pharmacol. Exp. Ther. **306**(2): 778-786.

Lau, Y.Y., Huang, Y., Frassetto, L. and Benet, L.Z. (2007). "Effect of OATP1B transporter inhibition on the pharmacokinetics of atorvastatin in healthy volunteers." Clin. Pharmacol. Ther. **81**(2): 194-204.

Lee, J.S., Obach, R.S. and Fisher, M.B. (2003). "Drug Metabolizing Enzymes: Cytochrome P450 and Other Enzymes in Drug Discovery and Development." Marcel Dekker, New York.

Lennernäs, H. (2007). "Intestinal permeability and its relevance for absorption and elimination." Xenobiotica. **37**(10-11): 1015-1051.

Li, L., Meier, P.J. and Ballatori, N. (2000). "Oatp2 mediates bidirectional organic solute transport: a role for intracellular glutathione." Mol. Pharmacol. **58**(2): 335-340.

Li, N., Zhang, Y., Hua, F. and Lai, Y. (2009). "Absolute difference of hepatobiliary transporter MRP2/Mrp2 in liver tissues and isolated hepatocytes from rat, dog, monkey and human." Drug Metab. Dispos. **37**(1): 66-73.

Maeda, K., Ieiri, I., Yasuda, K., Fujino, A., Fujiwara, H., Otsubo, K., Hirano, M., Watanabe, T., Kitamura, Y., Kusuhara, H. and Sugiyama, Y. (2006). "Effects of organic anion transporting polypeptide 1B1 haplotype on pharmacokinetics of pravastatin, valsartan, and temocapril." Clin. Pharmacol. Ther. **79**(5):427-439.

Mahagita, C., Grassl, S.M., Piyachaturawat, P. and Ballatori, N. (2007). "Human organic anion transporter 1B1 and 1B3 function as bidirectional carriers and do not mediate GSH-bile acid cotransport." Am. J. Physiol. Gastrointest. Liver Physiol. **293**(1): G271-278.

Miyagawa, M., Maeda, K., Aoyama, A. and Sugiyama, Y. (2009). "The eighth and ninth transmembrane domains in Organic Anion Transporting Polypeptide 1B1 affect the transport kinetics of estrone-3-sulfate and estradiol-17β-D-glucuronide. J. Pharmacol. Exp. Ther. **329**(2): 551-557.

Mizuno, N. and Sugiyama, Y. (2002). "Drug transporters: their role and importance in the selection and development of new drugs." Drug Metab. Pharmacokinet. **17**(2): 93-108.

van Montfoort, J.E., Müller, M., Groothuis, G.M., Meijer, D.K., Koepsell, H. and Meier, P.J. (2001). "Comparison of "type I" and "type II" organic cation transport by organic cation transporters and organic anion-transporting polypeptides." J. Pharmacol. Exp. Ther. **298**(1): 110-115.

Okabe, M., Szakács, G., Reimers, M.A., Suzuki, T., Hall, M.D., Abe, T., Weinstein, J.N. and Gottesman, M.M. (2008). "Profiling SLCO and SLC22 genes in the NCI-60 cancer cell lines to identify drug uptake transporters." Mol. Cancer Ther. **7**(9): 3081-3091.

Parker, R.B., Yates, C.R., Soberman, J.E. and Laizure, S.C. (2003). "Effects of grapefruit juice on intestinal P-glycoprotein: evaluation using digoxin in humans." Pharmacotherapy. **23**(8): 979-987.

Peng, S.X., Ritchie, D.M., Cousineau, M., Danser, E., Dewire, R. and Floden, J (2006). "Altered oral bioavailability and pharmacokinetics of P-glycoprotein substrates by coadministration of biochanin A." J. Pharm. Sci. **95**(9): 1984-1993.

Rowland, M. and Tozer, TN.. (1995). Clinical Pharmacokinetics: Concepts and Applications 3rd ed., Lippincott Williams & Wilkins, Philadelphia, PA.

Sahin, S. and Benet, L.Z. (2008). "The operational multiple dosing half-life: a key to defining drug accumulation in patients and to designing extended release dosage forms." Pharm. Res. **25**(12): 2869-2877.

Satlin, L.M., Amin, V. and Wolkoff, A.W. (1997). "Organic anion transporting polypeptide mediates organic anion/HCO$_3^{3-}$ exchange." J. Biol. Chem. **272**(42): 26340-26345.

Schwarz, U.I., Hanso, H., Oertel, R., Miehlke, S., Kuhlisch, E., Glaeser, H., Hitzl, M., Dresser, G.K., Kim, R.B. and Kirch, W. (2007). "Induction of intestinal P-glycoprotein by St John's wort reduces the oral bioavailability of talinolol." Clin. Pharmacol. Ther. **81**(5): 669-678.

Sesink, A.L., Arts, I.C., de Boer, V.C., Breedveld, P., Schellens, J.H., Hollman, P.C. and Russel, F.G. (2005). "Breast cancer resistance protein (Bcrp1/Abcg2) limits net intestinal uptake of quercetin in rats by facilitating apical efflux of glucuronides." Mol. Pharmacol. **67**(6): 1999-2006.

Sharom, F.J. (2006). "Shedding light on drug transport: structure and function of the P-glycoprotein multidrug transporter (ABCB1)." Biochem. Cell Biol. **84**:979-992.

Shu, Y., Brown, C., Castro, R.A., Shi, R.J., Lin, E.T., Owen, R.P., Sheardown, S.A., Yue, L., Burchard, E.G., Brett, C.M. and Giacomini, K.M. (2008). "Effect of genetic variation in the organic cation transporter 1, OCT1, on metformin pharmacokinetics." Clin. Pharmacol. Ther. **83**(2): 273-280.

Solas, C., Simon, N., Drogoul, M.P., Quaranta, S., Frixon-Marin, V., Bourgarel-Rey, V., Brunet, C., Gastaut, J.A., Durand, A., Lacarelle, B. and Poizot-Martin, I. (2007). "Minimal effect of MDR1 and CYP3A5 genetic polymorphisms on the pharmacokinetics of indinavir in HIV-infected patients." Br. J. Clin. Pharmacol. **64**(3): 353-362.

Srimaroeng, C., Perry, J.L. and Pritchard, J.B. (2008). "Physiology, structure, and regulation of the cloned organic anion transporters." Xenobiotica. **38**(7-8): 889-935.

Su, Y., Zhang, X. and Sinko, P.J. (2004). "Human organic anion-transporting polypeptide OATP-A (SLC21A3) acts in concert with P-glycoprotein and multidrug resistance protein 2 in the vectorial transport of Saquinavir in Hep G2 cells." Mol. Pharmaceut. **1**(1): 49-56.

Su, Y., Hu, P., Lee, S.H. and Sinko, P.J. (2007). "Using novobiocin as a specific inhibitor of breast cancer resistant protein to assess the role of transporter in the absorption and disposition of topotecan." J. Pharm. Sci. **10**(4): 519-536.

Sun, D., Lennernas, H., Welage, L. S., Barnett, J. L., Landowski, C. P.,Foster, D., Fleisher, D., Lee, K-D. and Amidon, G. L. (2002). "Comparison of human duodenum and Caco-2 gene expression profiles for 12,000 gene sequences tags and correlation with permeability of 26 drugs." Pharm. Res. **19**(10): 1400-1416.

Tannergren, C., Knutson, T., Knutson, L. and Lennernäs, H. (2003). "The effect of ketoconazole on the in vivo intestinal permeability of fexofenadine using a regional perfusion technique." Br. J. Clin. Pharmacol. **55**(2): 182-190.

Tian, X., Swift, B., Zamek-Gliszczynski, M.J., Belinsky, M.G., Kruh, G.D. and Brouwer, K.L. (2008). "Impact of basolateral multidrug resistance-associated protein (Mrp) 3 and Mrp4 on the hepatobiliary disposition of fexofenadine in perfused mouse livers." Drug Metab. Dispos. **36**(5): 911-915.

Tirona, R.G., Leake, B.F., Wolkoff, A.W. and Kim, R.B. (2003). "Human organic anion transporting polypeptide-C (SLC21A6) is a major determinant of rifampin-mediated pregnane X receptor activation." J. Pharmacol. Exp. Ther. **304**(1): 223-228.

Watanabe, T., Kusuhara, H., Maeda, K., Shitara, Y. and Sugiyama, Y. (2009). "Physiologically based pharmacokinetic modeling to predict transporter-mediated clearance and distribution of pravastatin in humans." J. Pharmacol. Exp. Ther. **328**(2): 652-662.

Westphal, K., Weinbrenner, A., Zschiesche, M., Franke, G., Knoke, M., Oertel, R., Fritz, P., von Richter, O., Warzok, R., Hachenberg, T., Kauffmann, H.M., Schrenk, D., Terhaag, B., Kroemer, H.K. and Siegmund, W. (2000). "Induction of P-glycoprotein by rifampin increases intestinal secretion of talinolol in human beings: a new type of drug/drug interaction." Clin. Pharmacol. Ther. **68**(4): 345-355.

Wu, C. Y., Benet, L. Z., Hebert, M. F., Gupta, S. K., Rowland, M., Gomez, D. Y. and Wacher, V. J. (1995). "Differentiation of absorption and first-pass gut and hepatic metabolism in humans: studies with cyclosporin." Clin. Pharmacol. Ther. **58** (5): 492-497.

Wu, C.Y. and Benet, L.Z. (2005). "Predicting drug disposition via application of BCS: transport/absorption/ elimination interplay and development of a biopharmaceutics drug disposition classification system." Pharm. Res. **22**(1): 11-23.

Zelcer, N., van de Wetering, K., Hillebrand, M., Sarton, E., Kuil, A., Wielinga, P.R., Tephly, T., Dahan, A., Beijnen, J.H. and Borst, P. (2005). "Mice lacking multidrug resistance protein 3 show altered morphine pharmacokinetics and morphine-6-glucuronide antinociception." Proc. Natl. Acad. Sci. U S A. **102**(20): 7274-7279.

Zheng, H.X., Huang, Y., Frassetto, L. and Benet, L.Z. (2009). "Elucidating rifampin's inducing and inhibiting effects on glyburide pharmacokinetics and blood glucose in healthy volunteers: unmasking the differential effects of enzyme induction and transporter inhibition for a drug and its primary metabolite." Clin. Pharmacol. Ther. **85**(1): 78-85.

Zhou, S., Chan, E., Pan, S.Q., Huang, M. and Lee, E.J. (2004). "Pharmacokinetic interactions of drugs with St John's wort." J. Psychopharmacol. **18**(2): 262-276.

CHAPTER 2

Investigating Bidirectional Transport Mediated by the Organic Anion Transporting Polypeptides

2.1 Introduction

It is accepted that for the great majority of drugs, absorption into the blood/plasma and systemic availability are required to exert a therapeutic or toxic effect. Some drugs, such as Biopharmaceutics Drug Disposition Classification System (BDDCS) Class 1 compounds, can often passively diffuse into and out of cells to gain intracellular access or blood/plasma access. However, many drugs, such as BDDCS Class 2, 3 and 4 compounds, often utilize transporter proteins to cross cell membranes. It is well recognized that hepatic uptake transporters influence metabolism and disposition of their substrate drugs by controlling the amount of drug that enters hepatocytes and is available to enzymes for metabolism, as well as to canalicular transporters for efflux into bile. However, hepatic basolateral efflux transporters are also important because they too can control the amount of drug available to metabolizing enzymes and canalicular transporters, in addition to being an avenue by which drugs can regain access to the systemic circulation. Factors that allow a drug to get back into the sinusoidal blood are an important determinant of drug efficacy and toxicity. For example, pravastatin, an HMG-CoA reductase inhibitor and BDDCS Class 3 compound, exerts its pharmacological effect in the liver. It is known to be an OATP1B1 substrate and impaired hepatic uptake has been shown to potentially decrease its cholesterol lowering effect in humans (Niemi et al., 2005). If OATP1B1 is also able to efflux pravastatin out of the liver and into the sinusoidal blood, it could be an important factor in determining pravastatin efficacy by virtue of both uptake and efflux functions.

The Oatp/OATPs are members of the solute carrier gene superfamily (SLCO) and include the hepatically expressed human isoforms OATP1B1, OATP1B3, OATP1A2, and OATP2B1. OATP1B1 and OATP1B3 expression are liver-specific, while OATP1A2 and OATP2B1 are expressed in liver and in other tissues, such as the intestines, lungs, brain, and kidneys (Meier-Abt et al., 2005). Rat hepatic Oatps include Oatp1a1, Oatp1a4, and Oatp1b2. OATPs/Oatps are integral membrane proteins with 12 trans-membrane spanning domains. They bear multiple N-glycosylation sites in the large extracellular loop 5 and in extracellular loop 2, both of which are believed to be involved in substrate recognition and transport (Konig et al., 2006). They mediate the ATP- and Na^+-independent transport of amphipathic organic anions in addition to some cationic and neutral compounds. Their wide variety of substrates include endogenous substrates such as estradiol-17β-glucuronide, estrone sulfate, taurocholate, and the thyroid hormones thyroxine (T_4) and triiodothyronine (T_3), as well as xenobiotics such as atorvastatin, pravastatin, digoxin, and rifampin (Hagenbuch and Gui, 2008). See Figure 2-1 for proposed OATP1B1 topology.
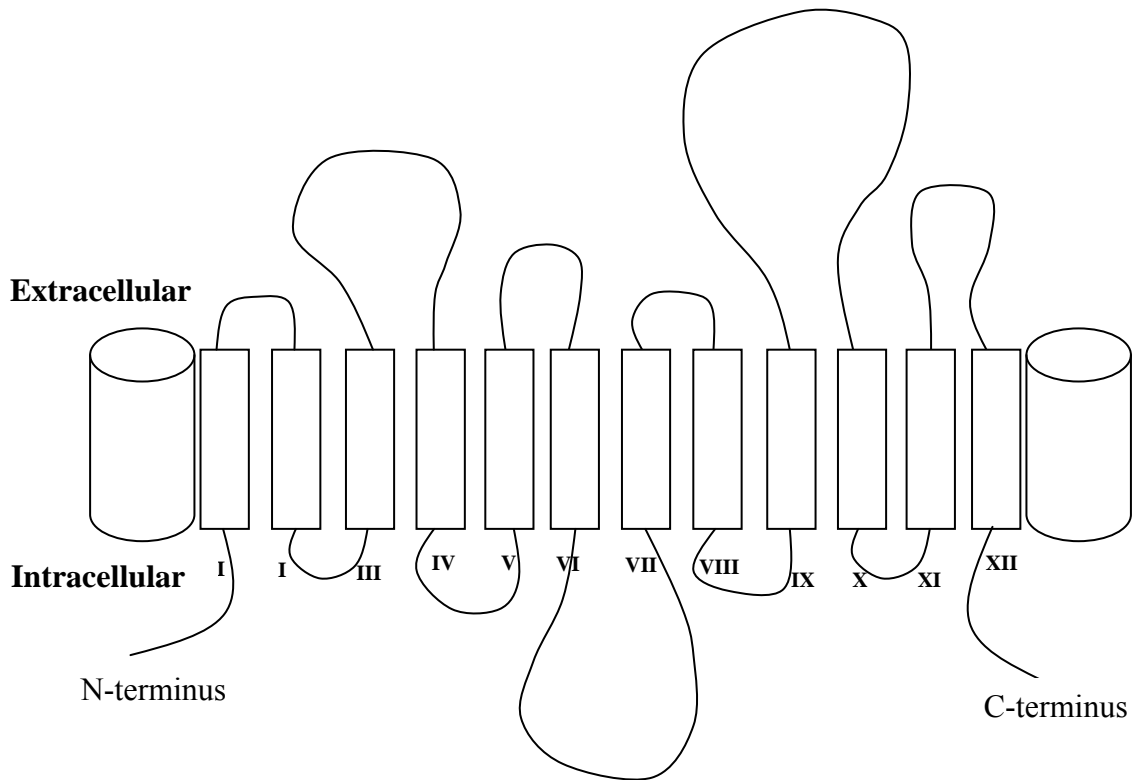
Figure 2-1 Proposed OATP1B1 topology (adapted from Hagenbuch and Gui, 2008).

Transporters of the Oatp/OATP family have been well-characterized as hepatic

uptake transporters. Previous work has shown that these transporters are a major

determinant of drug metabolism due to their ability to control how much drug enters

hepatocytes (Lau et al., 2006a; Lau et al., 2006b). However, limited evidence currently

exists in the literature describing Oatp/OATP mediated efflux of drugs, as opposed to

drug metabolites or endogenous substrates, into sinusoidal blood. The current evidence

focuses on investigating bidirectional transport as it pertains to providing a driving force

for uptake by Oatp/OATPs. This evidence includes a study in which it was indicated that

Oatps mediate bidirectional transport that is dependent on HCO_3^-. Satlin et al. (1997)

investigated the effect of an "outwardly directed pH gradient" on taurocholate transport

in HeLa cells expressing Oatp. They determined that HCO_3^- efflux from alkali-loaded HeLa cells with induced Oatp expression was stimulated by the presence of extracellular taurocholate. In a more recent paper, Leuthold et al. (2009) also examined HCO_3^- efflux in response to substrate uptake of various rat and human Oatps/OATPs. By measuring the change in intracellular pH in cells or oocytes expressing Oatp/OATP that were preloaded with HCO_3^-, they determined that for all of the Oatp/OATP isoforms studied substrate uptake was accompanied by HCO_3^- efflux. Another study postulated that intracellular glutathione participates in bidirectional transport by Oatp1a4.
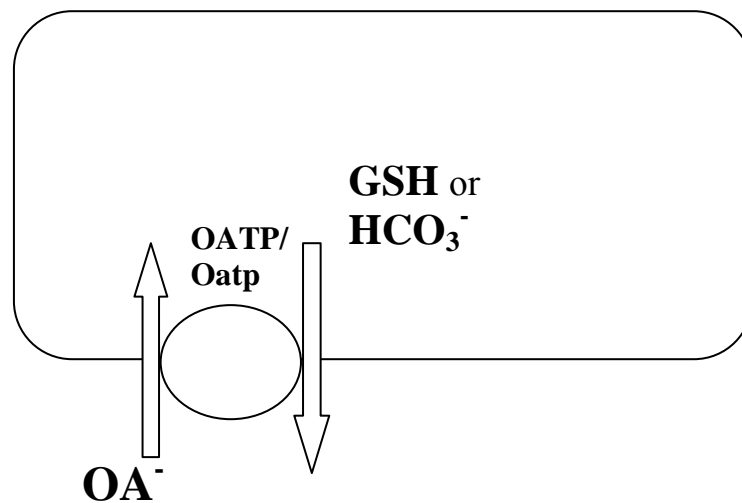
Figure 2-2 Uptake of organic anions (OA^-) coupled to extrusion of glutathione (GSH) or bicarbonate (HCO_3^-).

Using oocytes expressing Oatp1a4, Li et al. (2000) showed a trans-stimulatory effect on ^{3}H-digoxin and ^{3}H-taurocholate uptake by intracellular glutathione, suggesting that bidirectional transport was taking place with substrate uptake being sensitive to extrusion of glutathione. Finally, there is some evidence for efflux of metabolites by hepatic uptake transporters. Nishida and coworkers (2004) investigated the efflux of the

sulfate and glucuronide metabolites of 4-methylumbelliferone in IPRL studies. They found that sinusoidal efflux of the sulfate metabolite was ATP-independent but influenced by glutathione and Cl⁻. They concluded that the sinusoidal efflux of the sulfate conjugate may be mediated by Oatp1a1, Oatp1a4, or Npt1.

The purpose of this research is to investigate the role of drug efflux mediated by hepatic transporters of the organic anion transporting polypeptide family in drug disposition. Extensive work has been done to characterize the uptake function of these transporters and how it affects drug metabolism and disposition, but little work has focused on investigating the ability of Oatp/OATPs to efflux drug substrates into the sinusoidal blood and consequently affect drug disposition. This study seeks to examine whether and to what extent Oatp/OATP family members can efflux drugs into the sinusoidal blood and how this affects drug disposition.

2.2 Materials and Methods

2.2.1 Chemicals and Materials

^{3}H-estrone sulfate (^{3}H-ES) and ^{3}H-dehydroepiandrosterone (^{3}H-DHEAS) were purchase from Perkin Elmer (Waltham, MA) and ^{3}H-saquinavir was purchased from Moravek Biochemicals and Radiochemicals (Brea, CA). Pravastatin, fexofenadine, rifampin, rifamycin-SV, and bromosulfophthalein (BSP) were purchased from Sigma-Aldrich (St. Louis, MO). Human embryonic kidney cells (HEK293) overexpressing OATP1B1, OATP2B1, or Oatp1b2 along with the empty vector HEK293-pCI-neo cell line were kind gifts from Dr. Hideaki Okochi (University of California at San Francisco). All cell culture media were obtained from the UCSF Cell Culture Facility (San Francisco,

CA). Poly-D-lysine coated six-well cell culture plates were purchased from BD

Bioscience (Bedford, MA).

2.2.2 Cellular Efflux Studies

HEK293-OATP1B1, HEK293-OATP2B1, HEK293-Oatp1b2, and HEK293-pCI-

NEO were cultured in Dulbelcco's Modified Eagle Medium with 100 U/mL

penicillin/streptomycin, and 0.5 mg/mL geneticin at 37˚C in a 5% CO_2 atmosphere with

95% humidity, while HEK293 wildtype cells were cultured in the same manner with the

exception that the media contained no geneticin. Cells were cultured in T-75 flasks and

when ~90% confluent were trypsinized and plated in 6-well poly-D-lysine coated plates.

Cells were allowed to grow to confluence for ~48-72 hours. Prior to efflux studies, cells

were washed for 5 min at 37˚C with Hanks Buffered Salt Solution (HBSS) at pH 7.4.

After washing, cells were incubated for 30 min with HBSS containing substrate plus

inhibitor to load the cells with substrate and inhibitor. After the 30 min loading phase,

the incubation solution was removed and the cells washed 3 times with ice cold

phosphate buffered saline (PBS) to remove residual drug. After washing, cells were

incubated with HBSS containing inhibitor or vehicle control at 37˚C to examine efflux

mediated by transporters and at 4˚C, which served as the diffusion control. After adding

efflux buffer, 200μL buffer aliquots were removed at selected times over a 30 min or 60

min timecourse for drug level measurement and replaced with fresh buffer containing

inhibitor or vehicle control. After the last sample was removed, cells were washed 3

times with ice cold PBS, were allowed to dry, then were collected by manually scraping

the cells from the plate and suspending in 400μL of H_2O. For ^{3}H-ES, ^{3}H-DHEAS, and

[3]H-saquinavir, 200μL cell aliquots and 200μL buffer aliquots were transferred to scintillation vials for analysis by scintillation counting.

2.2.3 Isolated Perfused Rat Liver (IPRL): Single-Pass Perfusion

Male Wistar rats (250-300g, Charles River Laboratories, Wilmington, MA) were anesthetized via peritoneal injection of 1mL/kg ketamine:xylazine (80mg/mL:12mg/mL) prior to portal vein cannulation. Livers were isolated for *ex situ* perfusion as described previously in our laboratory (Prueksaritanont et al., 1992). The liver was washed in a recirculatory fashion with a 100mL aliquot of the oxygenated liver perfusion buffer (Krebs-Henesleit buffer containing 10mM D-glucose, 2mM L-glutamine, and 1% bovine serum albumin) containing no substrate, inhibitor, or control vehicle for 10 min at a rate of 15mL/min. After this 10 min wash, the liver was loaded with substrate and inhibitor for 20 min in a single-pass perfusion at a rate of 15mL/min. The loading phase was followed by an efflux phase initiated by switching to a single-pass perfusion with buffer containing vehicle blank or inhibitor for 20 min.   During the loading and efflux phases, perfusion buffer was collected every 30 seconds using a fraction collector. The backpressure from the liver was measured and considered acceptable as long as it was below 20psi and liver viability was assessed by appearance (uniform pink to brown color). The entire chamber was maintained at 37°C for the duration of the experiment. After the completion of the efflux phase, the liver was removed from the chamber and washed by pushing two 12mL aliquots of cold normal saline through the cannula. The liver was weighed and stored at -80°C until analysis of intrahepatic drug levels by LC-MS/MS.

2.2.4 Sample Preparation

The calibration curve and samples were prepared for HPLC-MS/MS analysis by liquid-liquid extraction. The curve range for pravastatin was 25-1000nM and for fexofenadine was 10-1000nM. A 500μL aliquot of methyl-t-butyl ether containing either 1μM atorvastatin (pravastatin internal standard) or 1μM fexofenadine (d_6-fexofenadine internal standard) was added to each sample (buffer, lysed cells, or homogenized liver). Samples were vortexed for 1 min then centrifuged at 13,000g for 10 min to separate the aqueous and organic layers. After centrifuging, the lower aqueous layer was frozen in a methanol-dry ice bath and the top organic layer was transferred to a clean Eppendorf tube. The organic layer was dried down under N_2 and drugs were reconstituted in 200μL of the appropriate mobile phase.

2.2.5 Measurement of Pravastatin

Samples were analyzed on an HPLC-MS/MS system consisting of a Shimadzu (Shimadzu Scientific Instruments, Columbia, MD) CBM-20A BUS module, two Shimadzu LC-20AD Prominence liquid chromatography pumps, a Shimadzu SIL-20AC HT Prominence autosampler, and an Applied Biosystems (Foster City, CA) MDS Sciex API4000 triple quadrupole mass spectrometer. All system components were controlled by Applied Biosystems Analyst software version 1.4.2. An Agilent (Agilent Technologies, Inc., Santa Clara, CA) Eclipse XDB-C8 analytical column with dimensions 150 x 4.6mm and 5μm particle size was used at ambient temperature. The isocratic mobile phase consisted of 5mM ammonium acetate pH 4.5:acetonitrile (20:80; v:v) pumped at a flow rate of 0.7mL/min. The injection volume was 100μL and the run

time was 10.0 min. The mass spectrometer conditions were as follows: collision gas (CAD) 7 units, ionspray voltage (IS) 5500 volts, temperature (TEM) 300˚C, ion source gas 1 (GS1) 30 psi, ion source gas 2 (GS2) 0 psi, curtain gas (CUR) 10 psi, declustering potential (DP) 76 volts, entrance potential (EP) 10 volts, collision energy (CE) 21 electron volts, and exit potential (CXP) 4 volts.   The mass transitions of 447.2→327.3 for pravastatin and 559.3→440.4 for atorvastatin were monitored.

2.2.6 Measurement of Fexofenadine

The same HPLC-MS/MS system described above was used for the fexofenadine analysis. A Waters (Waters Corp., Milford, MA) Symmetry C18 analytical column with dimensions 50 x 2.1mm and 5μm particle size was used at ambient temperature with an isocratic mobile phase consisting of 10mM ammonium acetate:acetonitrile:formic acid (30:70:0.1; v:v:v) pumped at a flow rate of 0.3mL/min. The injection volume was 25μL and the run time was 3.5 min. The mass spectrometer conditions were as follows: collision gas (CAD) 7 units, ionspray voltage (IS) 5500 volts, temperature (TEM) 300˚C, ion source gas 1 (GS1) 60 psi, ion source gas 2 (GS2) 30 psi, curtain gas (CUR) 10 psi, declustering potential (DP) 76 volts, entrance potential (EP) 10 volts, collision energy (CE) 43 electron volts, and exit potential (CXP) 20 volts. The mass transitions of 502.5→466.5 for fexofenadine and 508.5→472.5 for d_6-fexofenadine were monitored.

2.2.7 Measurement of ^{3}H-Estrone Sulfate (^{3}H-ES), ^{3}H-Dehydroepiandrosterone (^{3}H-DHEAS), and ^{3}H-Saquinavir

Once cell and buffer samples were transferred to scintillation vials, 5mL of Econo-Safe counting cocktail (Research Products International Corp., Mount Prospect,

IL) were added and each sample was vortexed briefly before being analyzed in a

Beckman LS6000 liquid scintillation counter (Beckman Coulter, Inc. Fullerton, CA).

Tritium DPM were measured.

2.2.8 Data Analysis

The DPM or the concentration of drug was measured and for intracellular samples

was corrected for mg of protein. Area under the curve (AUC) was calculated by the

linear trapezoidal method. Student's two-tailed t-test or one-way ANOVA followed by

Bonferroni's t-test for multiple comparisons were used to assess statistical significance

with a p-value <0.05 considered significant.

2.3 Results

2.3.1 Efflux by HEK293-OATP1B1

Figures 2-3 through 2-5 show the efflux time profiles of ^{3}H-saquinavir

(incubation 2.5nM) in HEK293-OATP1B1 cells, the AUC over the 30 min efflux

timecourse, and the intracellular levels of ^{3}H-saquinavir after the 30 min efflux phase.

The inhibitor used was 100μM rifampin. The 37˚C control treatment group AUC was not

significantly higher than the 37˚C rifampin treated group AUC and the intracellular levels

after the completion of the efflux phase were not significantly different for these

treatments. There was no difference in the 4˚C AUC values due to rifampin treatment,

but the 37˚C groups had higher (p<0.001) AUC values than the corresponding 4˚C

groups. Intracellular differences arose only from temperature (p<0.001) and not from

rifampin treatment.
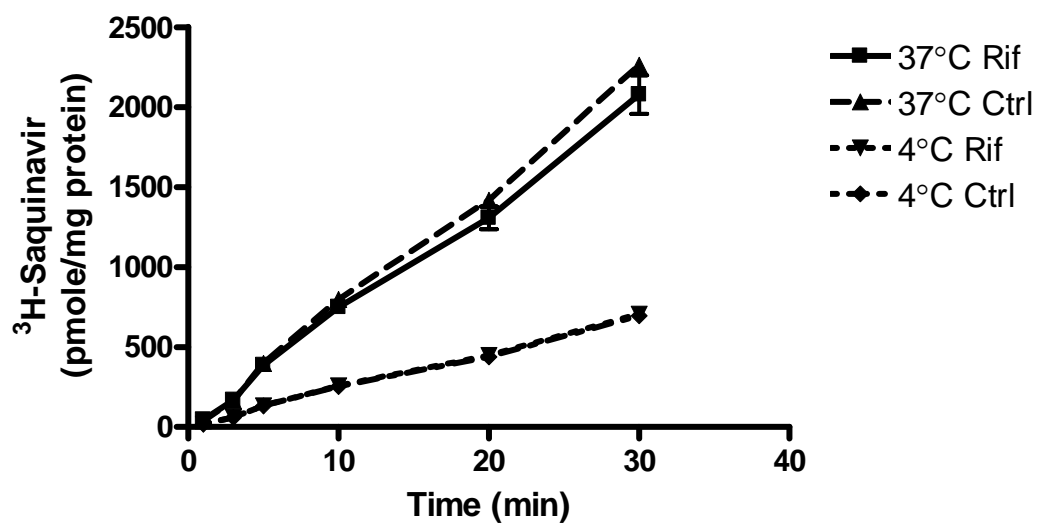
Figure 2-3 Efflux time profiles of ^{3}H-saquinavir (incubation 2.5nM) from HEK293-

OATP1B1 cells over 30 min at 37˚C and 4˚C into buffer containing 100μM rifampin or

0.1% DMSO as vehicle control. Values are mean ± SD, n=3 per group.
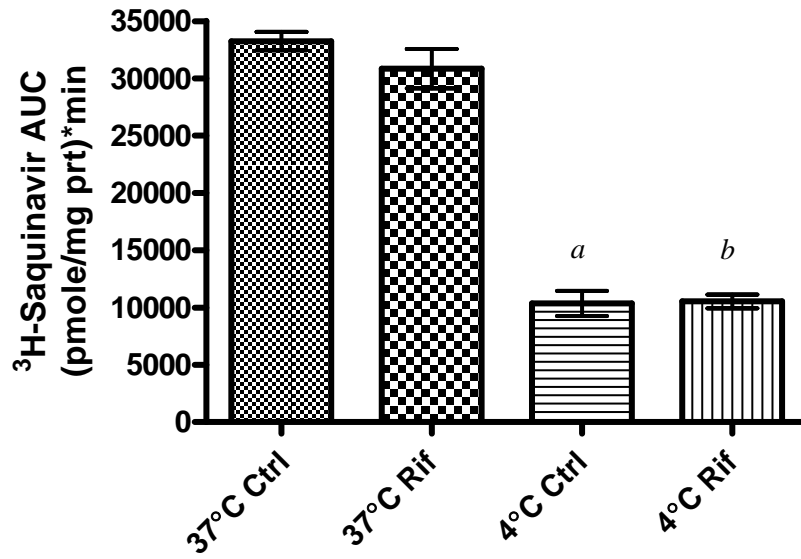
Figure 2-4 AUC values over 30 min ^{3}H-saquinavir (incubation 2.5nM) efflux timecourse

from HEK293-OATP1B1 at 37˚C and 4˚C into buffer containing 100μM rifampin or

0.1% DMSO as vehicle control. Values are mean ± SD, n=3 per group, ^{a} p<0.001 versus

37˚C control, ^{b} p<0.001 versus 37˚C rifampin.
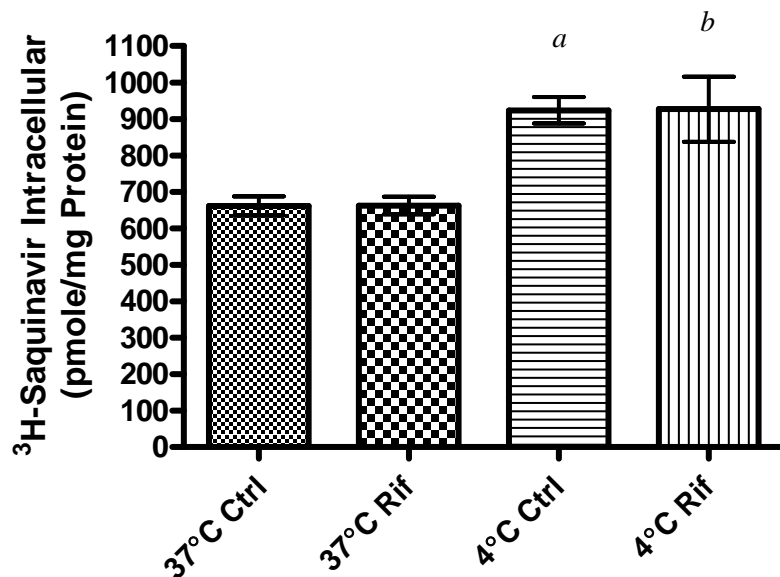
Figure 2-5 HEK293-OATP1B1 intracellular ^{3}H-saquinavir (incubation 2.5nM) levels after 30 min timecourse at 37°C and 4°C into buffer containing 100μM rifampin or 0.1% DMSO as vehicle control. Values are mean ± SD, n=3 per group, ^{a} p<0.001 versus 37°C control, ^{b} p<0.001 versus 37°C rifampin.

Figure 2-6 shows the uptake of 2.5nM ^{3}H-saquinavir into HEK293-OATP1B1 cells and empty vector HEK293-pCI-NEO cells. There was significantly higher uptake in the HEK293-OATP1B1 cells compared to empty vector cells.
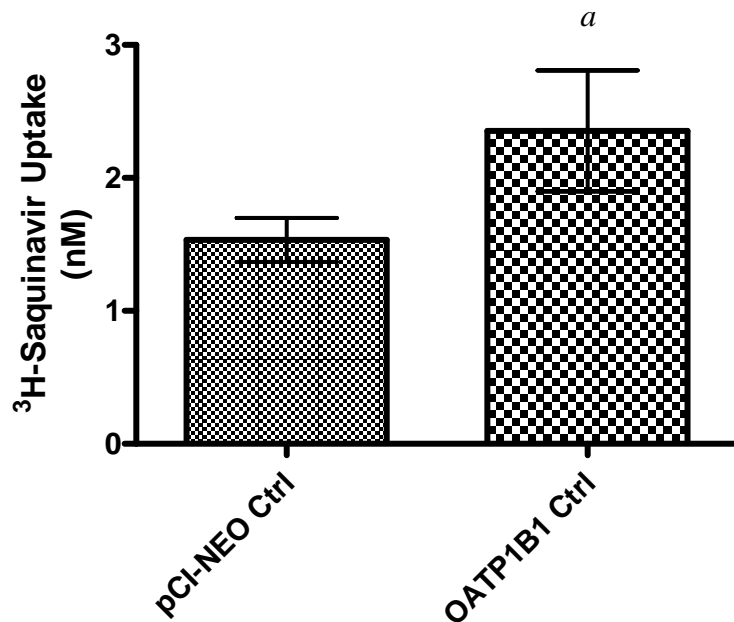
Figure 2-6 Uptake of 2.5nM ^{3}H-saquinavir in HEK293-pCI-NEO cells and HEK293-OATP1B1 cells. Values are mean±SD, n=3 per group. ^{a} p<0.05 versus HEK293-pCI-NEO control.

Figures 2-7 through 2-9 show the efflux time profiles of ^{3}H-ES (incubation 4.3nM) from HEK293-OATP1B1 cells, the AUC over the 30 min efflux period for each treatment group, and the intracellular ^{3}H-ES levels at the end of the efflux period. The inhibitor was 100μM rifampin. No differences were seen due to rifampin inhibition. The 4˚C control AUC was significantly lower (p<0.01) than the 37˚C control AUC. The intracellular ^{3}H-ES levels for the 4˚C control and the 4˚C rifampin levels were significantly higher (p<0.001) than the corresponding 37˚C treatment group intracellular levels.

Figure 2-7 Efflux time profiles of ^{3}H-ES (incubation 4.3nM) from HEK293-OATP1B1

cells over 30 min at 37˚C and 4˚C into buffer containing 100μM rifampin or 0.1%

DMSO as vehicle control. Values are mean ± SD, n=3 per group.
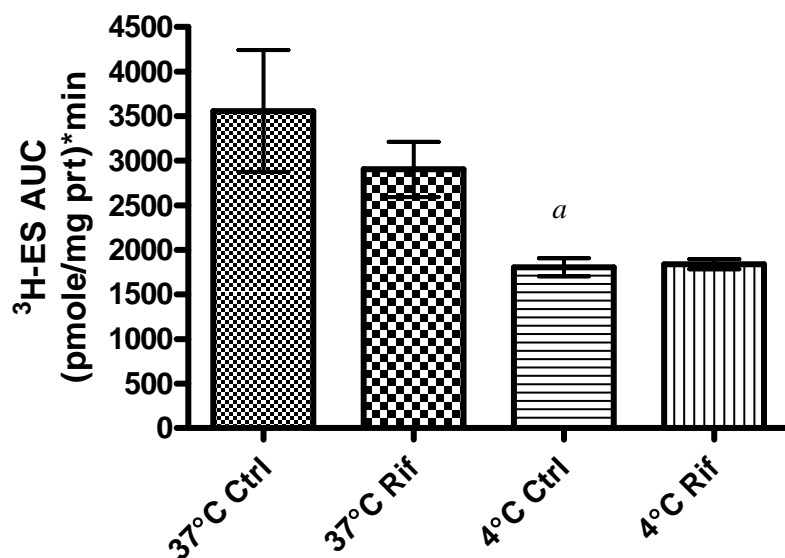
Figure 2-8 AUC values over 30 min ^{3}H-ES (incubation 4.3nM) efflux timecourse from

HEK293-OATP1B1 cells at 37˚C and 4˚C into buffer containing 100μM rifampin or

0.1% DMSO as vehicle control. Values are mean ± SD, n=3 per group, ^{a}p< 0.01 versus 37˚C control.
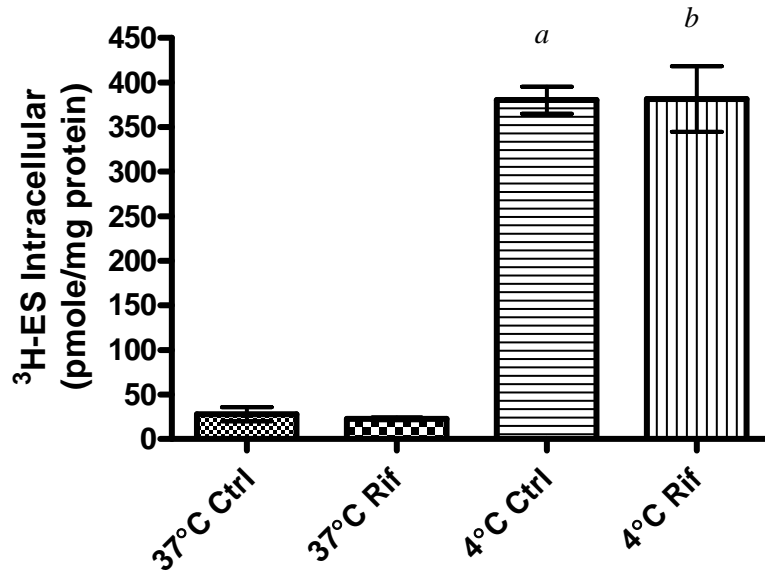
Figure 2-9 HEK293-OATP1B1 intracellular ^{3}H-ES (incubation 4.3nM) levels after 30 min timecourse at 37˚C and 4˚C into buffer containing 100μM rifampin or 0.1% DMSO as vehicle control. Values are mean ± SD, n=3 per group, ^{a} p<0.001 versus 37˚C control, ^{b} p<0.001 versus 37˚C rifampin.

Figure 2-10 shows the uptake of 4.3nM ^{3}H-ES into HEK293-OATP1B1 cells and empty vector HEK293-pCI-NEO cells with 100μM rifamycin-SV or 0.1% DMSO vehicle control. HEK293-OATP1B1 cells had significantly higher uptake of ^{3}H-ES than HEK293-pCI-NEO cells both with 0.1% DMSO (p<0.001) and with 100μM rifamycin-SV (p<0.01) treatment. There was no significant inhibition of uptake in HEK293-pCI-NEO cells by rifamycin-SV while there was in the HEK293-OATP1B1 cells (p<0.001).

Figure 2-10 Uptake of 4.3nM ^{3}H-ES in HEK293-pCI-NEO cells and HEK293-

OATP1B1 cells in the presence of 100μM rifamycin-SV or 0.1% DMSO control. Values

are mean±SD, n=3 per group. ^{a} p<0.001 compared to pCI-NEO control,

^{b} p<0.001 compared to OATP1B1 control, ^{c} p<0.01 compared to pCI-NEO R-SV.

Figures 2-11 through 2-13 show the efflux time profiles of ^{3}H-DHEAS

(incubation 4.2nM) over a 30 min timecourse, the AUC for each treatment group over the

30 min efflux period, and the ^{3}H-DHEAS intracellular levels after the 30 min efflux

period. The inhibitor was 100μM rifamycin-SV. The efflux profiles for all groups were

similar and there were no significant differences in the AUCs between any of the

treatment groups. The intracellular groups showed differences due only to temperature,

with the 37˚C control and the 37˚C rifamycin-SV ^{3}H-DHEAS levels significantly lower

(p<0.001) than the corresponding 4˚C treatment groups.
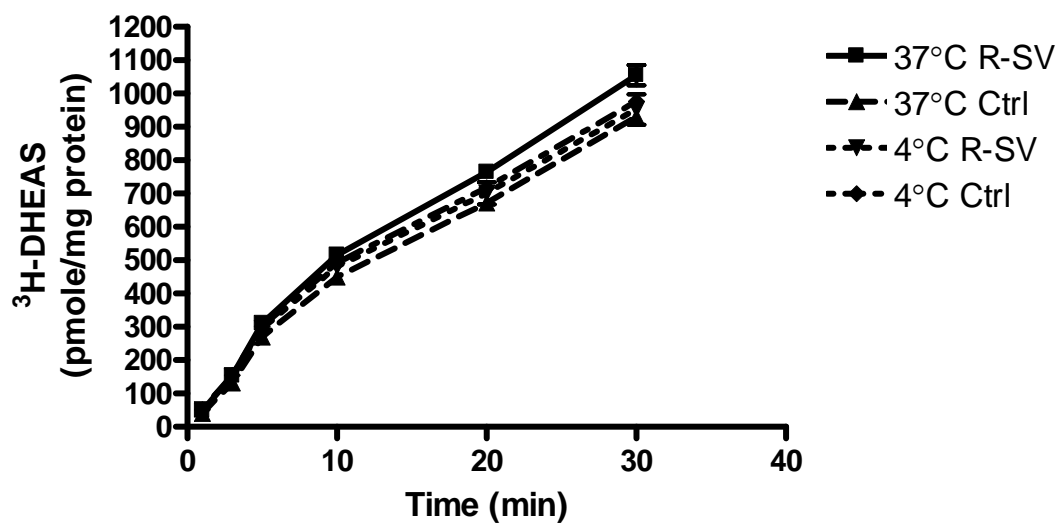
Figure 2-11 Efflux time profiles of ^{3}H-DHEAS (incubation 4.2nM) from HEK293-

OATP1B1 cells over 30 min at 37˚C and 4˚C into buffer containing 100μM rifamycin-

SV or 0.1% DMSO as vehicle control. Values are mean ± SD, n=3 per group.
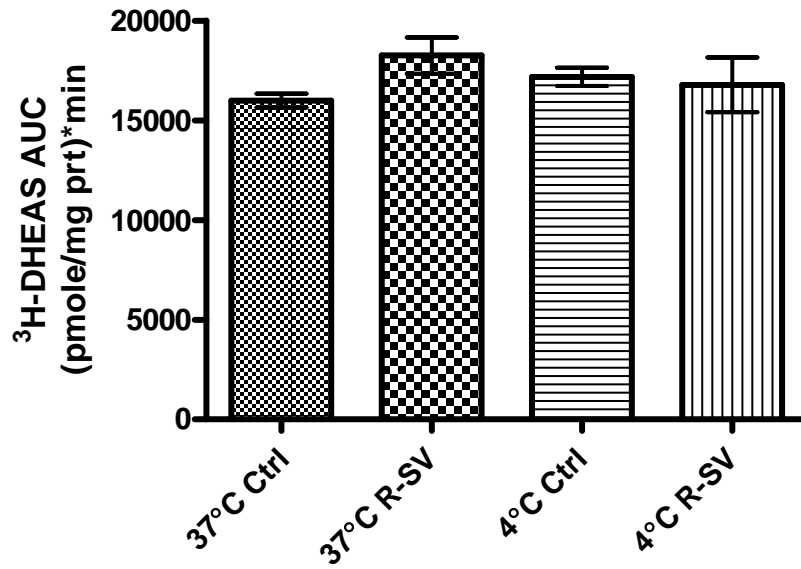
Figure 2-12 AUC values over 30 min ³H-DHEAS (incubation 4.2nM) efflux timecourse

from HEK293-OATP1B1 cells at 37˚C and 4˚C into buffer containing 100μM rifamycin-

SV or 0.1% DMSO as vehicle control. Values are mean ± SD, n=3 per group.
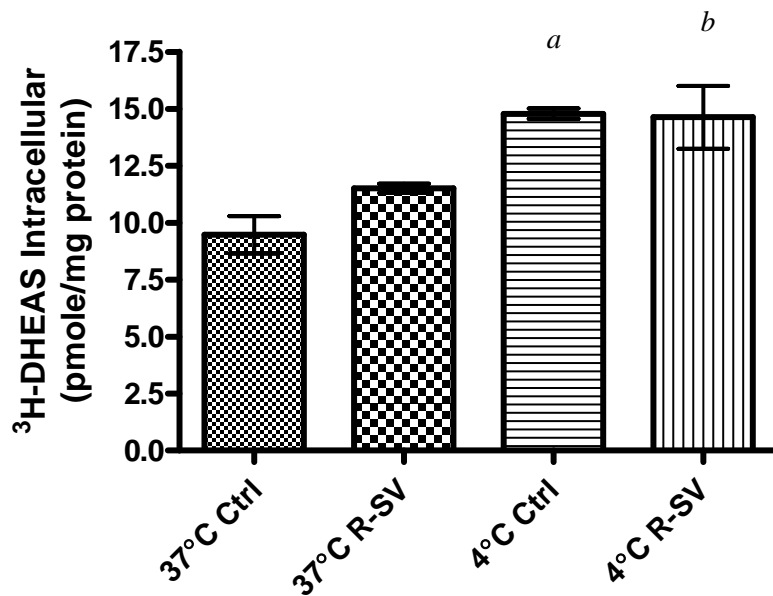
Figure 2-13 HEK293-OATP1B1 intracellular ^{3}H-DHEAS (incubation 4.2nM) levels

after 30 min timecourse at 37°C and 4°C into buffer containing 100μM rifamycin-SV or

0.1% DMSO as vehicle control. Values are mean ± SD, n=3 per group, [a] p<0.001 versus

37°C control, [b] p<0.01 versus 37°C rifamycin-SV.

2.3.2 Efflux by HEK293-OATP2B1

Figures 2-14 through 2-16 show the efflux time profiles of ^{3}H-ES (incubation

4.3nM) from HEK293-OATP2B1 cells over 30 min, the AUC for each treatment group,

and the intracellular ^{3}H-ES levels at the end of the efflux period. The inhibitor was

100μM rifampin. The AUC for 37°C control was significantly higher (p<0.05) than that

for the 4°C control, but no other differences were seen in the AUC values. The

intracellular ^{3}H-ES levels were significantly higher (p<0.001) in the 4°C rifampin group

than in the 37°C rifampin and the 4°C control group, but no other differences were

evident.
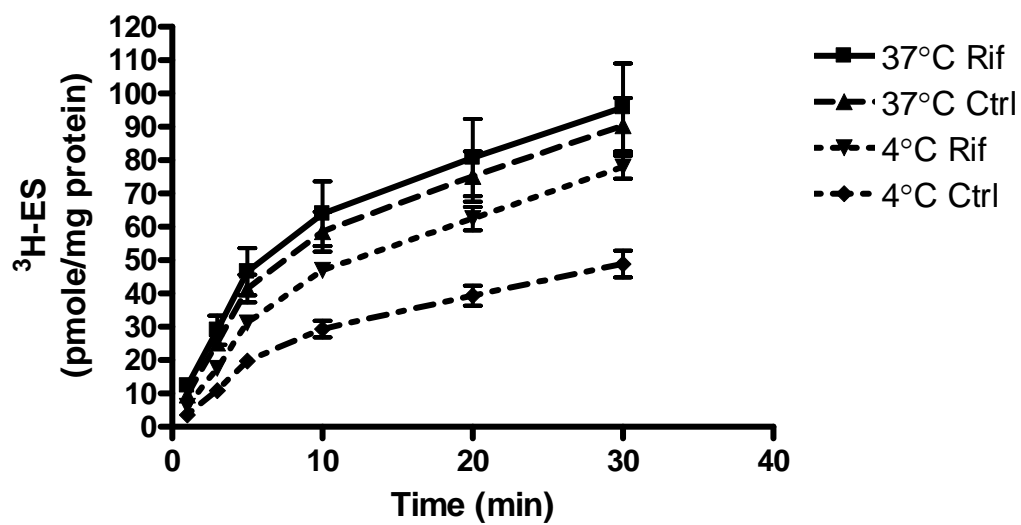
Figure 2-14 Efflux time profiles of ^{3}H-ES (incubation 4.3nM) from HEK293-OATP2B1

cells over 30 min at 37°C and 4°C into buffer containing 100μM rifampin or 0.1%

DMSO as vehicle control. Values are mean ± SD, n=3 per group.
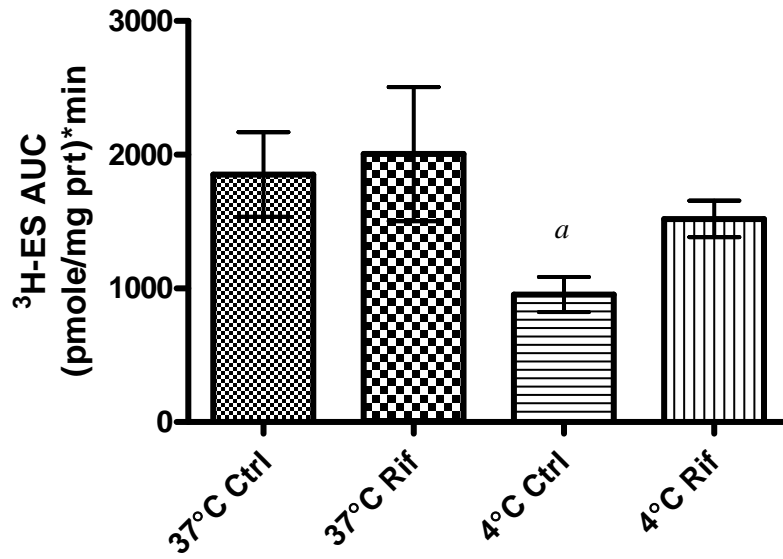
Figure 2-15 AUC values over 30 min ^{3}H-ES (incubation 4.3nM) efflux timecourse from

HEK293-OATP2B1 cells at 37°C and 4°C into buffer containing 100μM rifampin or

0.1% DMSO as vehicle control. Values are mean ± SD, n=3 per group, ^{a} p< 0.05 versus

37°C control.
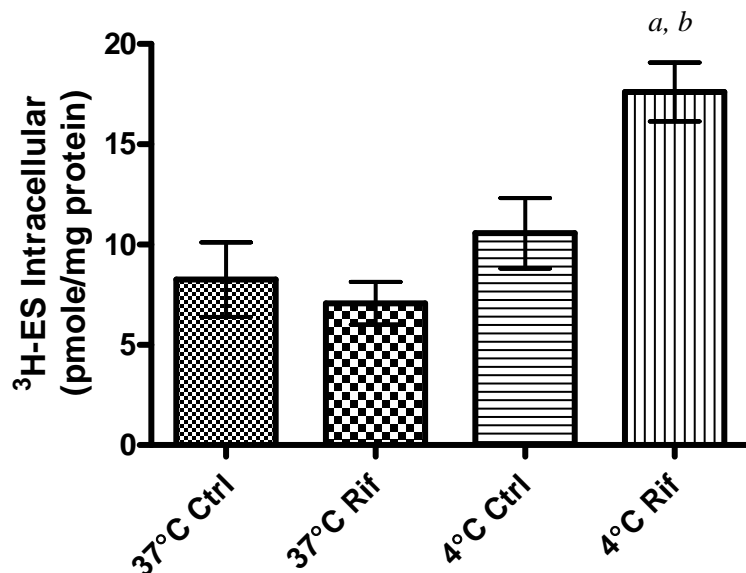
Figure 2-16 HEK293-OATP2B1 intracellular ^{3}H-ES (incubation 4.3nM) levels after 30 min timecourse at 37˚C and 4˚C into buffer containing 100µM rifampin or 0.1% DMSO as vehicle control. Values are mean ± SD, n=3 per group, ^{a} p<0.001 versus 37˚C rifampin, ^{b} p<0.01 versus 4˚C control.

Figure 2-17 shows uptake of 4.3nM ^{3}H-ES into HEK293-OATP2B1 and HEK293-pCI-NEO empty vector cells in the presence of 100µM rifamycin-SV or 0.1% DMSO vehicle control. Significantly higher uptake is seen in the HEK293-OATP2B1 cells than in the empty vector cell line (p<0.001). Significant inhibition of ^{3}H-ES uptake by rifamycin-SV is seen in the HEK293-OATP2B1 cells (p<0.001), but not in the empty vector cells.
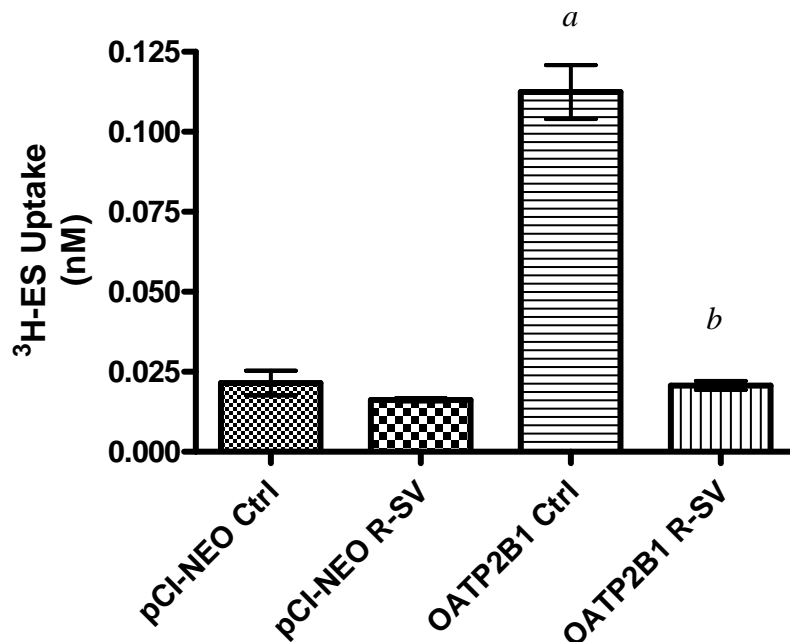
Figure 2-17 Uptake of 4.3nM ^{3}H-ES in HEK293-pCI-NEO cells and HEK293-OATP2B1 cells in the presence and absence of 100μM rifamycin-SV or 0.1% DMSO control. Values are mean±SD, n=3 per group. ^{a} p<0.001 compared to pCI-NEO control, ^{b} p<0.001 compared to OATP2B1 control.

Figures 2-18 through 2-20 show the efflux time profiles of ^{3}H-DHEAS (incubation 4.2nM) from HEK293-OATP2B1 cells, the AUC for each treatment group over the 60 min efflux period, and the intracellular ^{3}H-DHEAS levels after the end of the timecourse. The inhibitor was 100μM rifampin. The AUCs showed no significant differences between any of the treatment groups. The intracellular ^{3}H-DHEAS level for the 37°C rifampin group was significantly higher (27%, p<0.01) than the 37°C control group while the 4°C control group showed a slightly lower (10%, p<0.05) ^{3}H-DHEAS level than the 4°C rifampin group. The 37°C intracellular levels for control and rifampin were significantly less (p<0.001) than the corresponding 4°C groups.
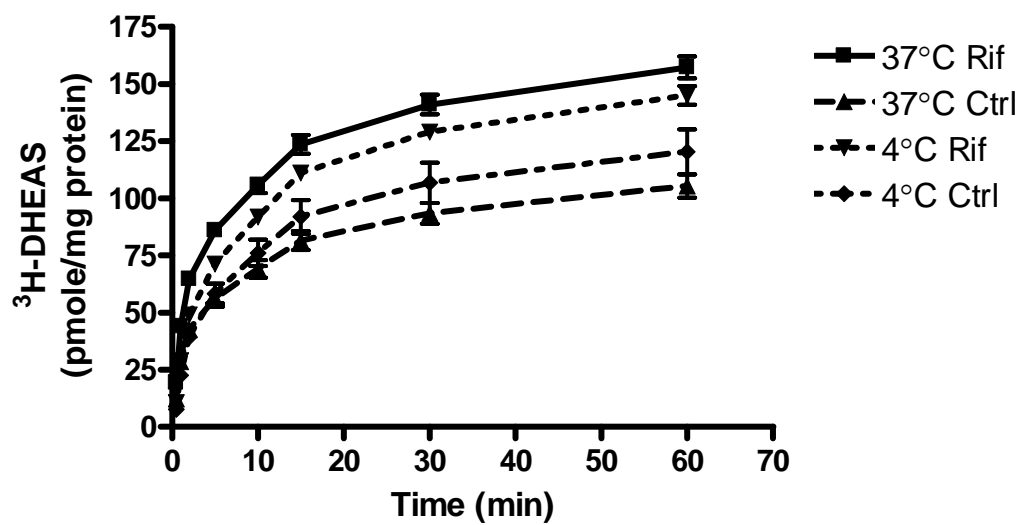
Figure 2-18 Efflux time profiles of ^{3}H-DHEAS (incubation 4.2nM) from HEK293-

OATP2B1 cells over 60 min at 37˚C and 4˚C into buffer containing 100μM rifampin or

0.1% DMSO as vehicle control. Values are mean ± SD, n=3 per group.
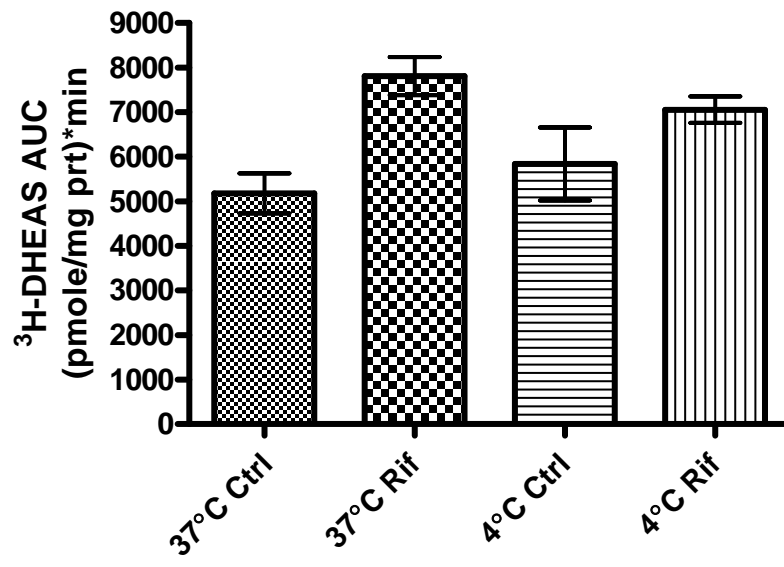
Figure 2-19 AUC values over 60 min ^{3}H-DHEAS (incubation 4.2nM) efflux timecourse

from HEK293-OATP2B1 cells at 37°C and 4°C into buffer containing 100μM rifampin

or 0.1% DMSO as vehicle control. Values are mean ± SD, n=3 per group.
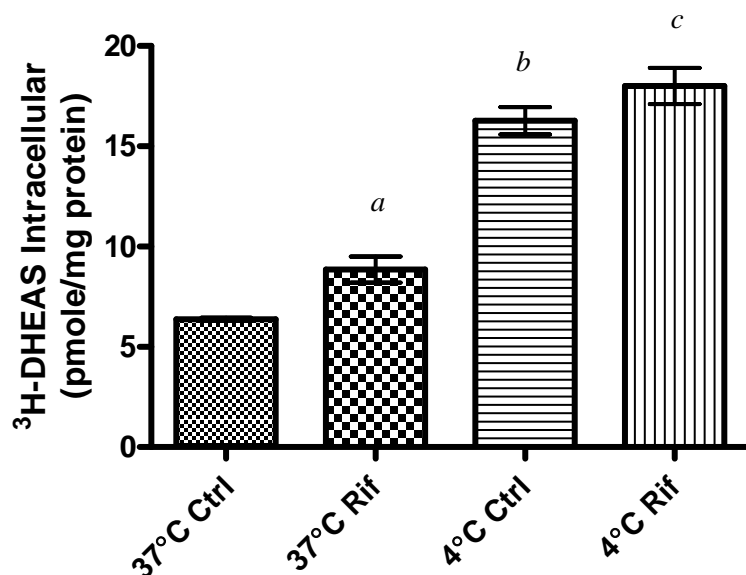
Figure 2-20 HEK293-OATP2B1 intracellular ^{3}H-DHEAS (incubation 4.2nM) levels after 60 min timecourse at 37˚C and 4˚C into buffer containing 100μM rifampin or 0.1% DMSO as vehicle control. Values are mean ± SD, n=3 per group, ^{a} $p<0.05$ versus 37˚C control, ^{b} $p<0.001$ versus 37˚C control, ^{c} $p<0.001$ versus 37˚C rifampin.

2.3.3 Efflux by HEK293-Oatp1b2

Figures 2-21 through 2-23 show the 30 min efflux time profiles for ^{3}H-ES (incubation 4.3nM) from HEK293-Oatp1b2, the AUCs of ^{3}H-ES for each treatment group over the efflux period, and the intracellular ^{3}H-ES levels at the end of the timecourse. The inhibitor was 100μM rifamycin-SV. AUC differences were due to temperature only with 37˚C control AUC higher ($p<0.05$) than the 4˚C control AUC and the 37˚C rifamycin-SV AUC higher ($p<0.01$) than the 4˚C rifamycin-SV AUC. Intracellular levels of ^{3}H-ES differed between 37˚C control and 4˚C control only with 4˚C control level being significantly higher ($p<0.05$).
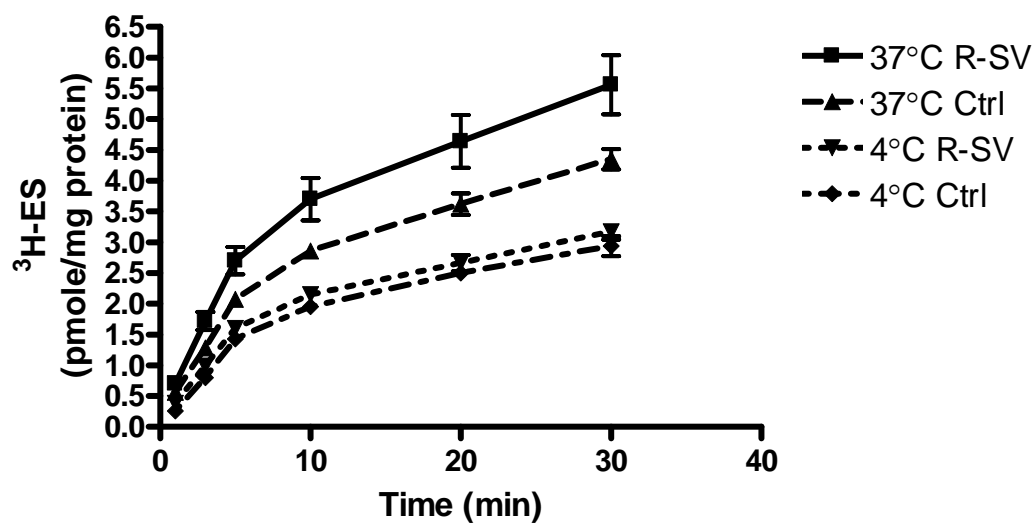
Figure 2-21 Efflux time profiles of ^{3}H-ES (incubation 4.3nM) from HEK293-Oatp1b2 cells over 30 min at 37°C and 4°C into buffer containing 100μM rifamycin-SV or 0.1% DMSO as vehicle control. Values are mean ± SD, n=3 per group.
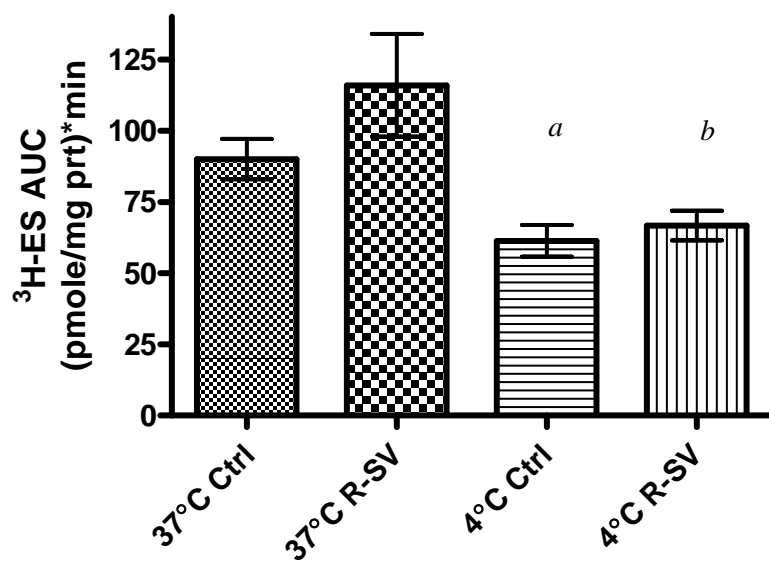
Figure 2-22 AUC values over 30 min ^{3}H-ES (incubation 4.3nM) efflux timecourse from HEK293-Oatp1b2 cells at 37°C and 4°C into buffer containing 100μM rifamycin-SV or

0.1% DMSO as vehicle control. Values are mean ± SD, n=3 per group, [a] p<0.05 versus 37˚C control, [b] p<0.01 versus 37˚C rifamycin-SV.
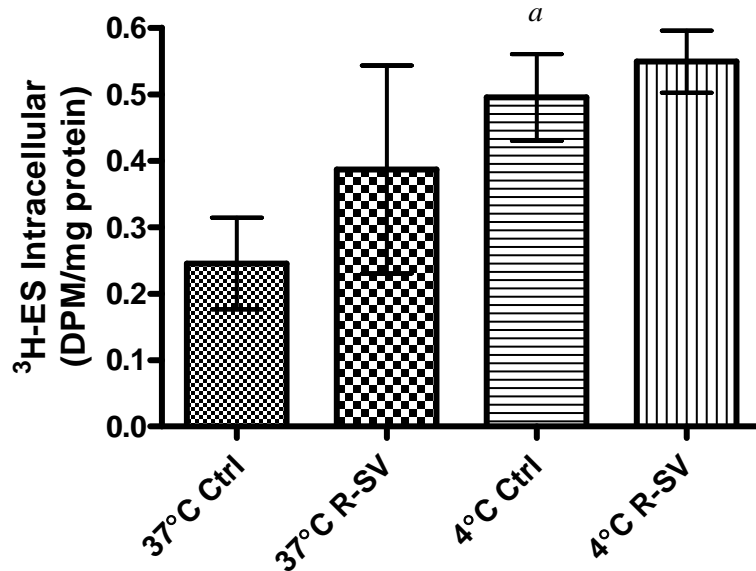
Figure 2-23 HEK293-Oatp1b2 intracellular ^{3}H-ES (incubation 4.3nM) levels after 30 min timecourse at 37˚C and 4˚C into buffer containing 100μM rifamycin-SV or 0.1% DMSO as vehicle control. Values are mean ± SD, n=3 per group, [a] p<0.05 versus 37˚C control.

Figure 2-24 shows uptake of 4.3nM ^{3}H-ES into HEK293-Oatp1b2 cells and HEK293-pCI-NEO cells in the presence of 100μM rifampin or 0.1% DMSO vehicle control. Significant inhibition was seen in the HEK293-Oatp1b2 cells in the presence of rifampin (p<0.05) but not in the empty vector cells. However, similar levels of uptake of ^{3}H-ES are seen in the two cell lines and the variability in the HEK293-pCI-NEO control group is high.
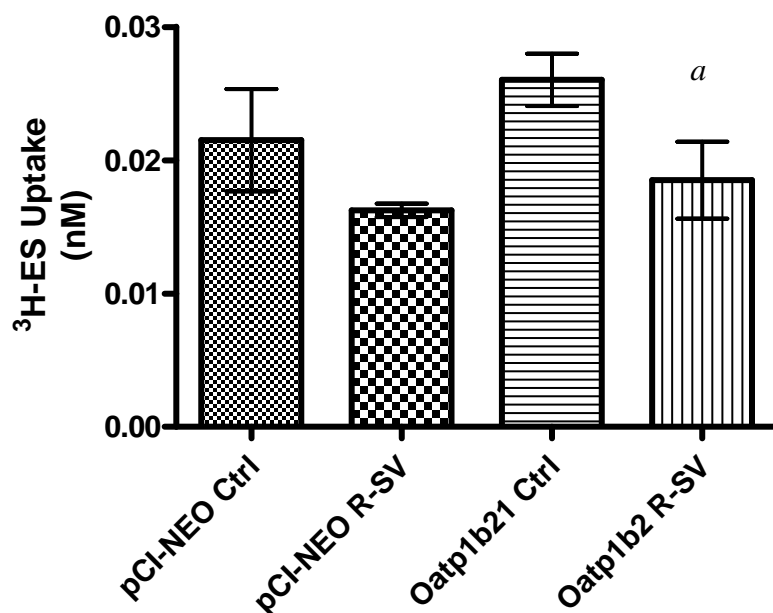
Figure 2-24 Uptake of 4.3nM ^{3}H-ES in HEK293-pCI-NEO cells and HEK293-Oatp1b2 cells in the presence of 100μM rifamycin-SV or 0.1% DMSO control. Values are mean±SD, n=3 per group. ^{a} p<0.05 compared to Oatp1b2 control.

Figures 2-25 through 2-27 show the efflux time profiles of ^{3}H-DHEAS (incubation 4.2nM) over a 60 min timcourse from HEK293-Oatp1b2, the AUC for each treatment group, and intracellular levels of ^{3}H-DHEAS after the 60 min efflux period. The inhibitor was 100μM rifampin. The presence of rifampin inhibition caused a significant decrease in the AUC value for the 37°C rifampin (p<0.001) treated group compared to the 37°C control. The 37°C control AUC was also significantly higher (p<0.001) than the 4°C control AUC and the 37°C rifampin AUC was higher (p<0.001) than the 4°C rifampin AUC. The intracellular levels differed significantly in response to temperature only, with the 4°C control and the 4°C rifampin intracellular ^{3}H-DHEAS

levels significantly higher (p<0.001) than the intracellular levels in the corresponding

37˚C treatment groups.
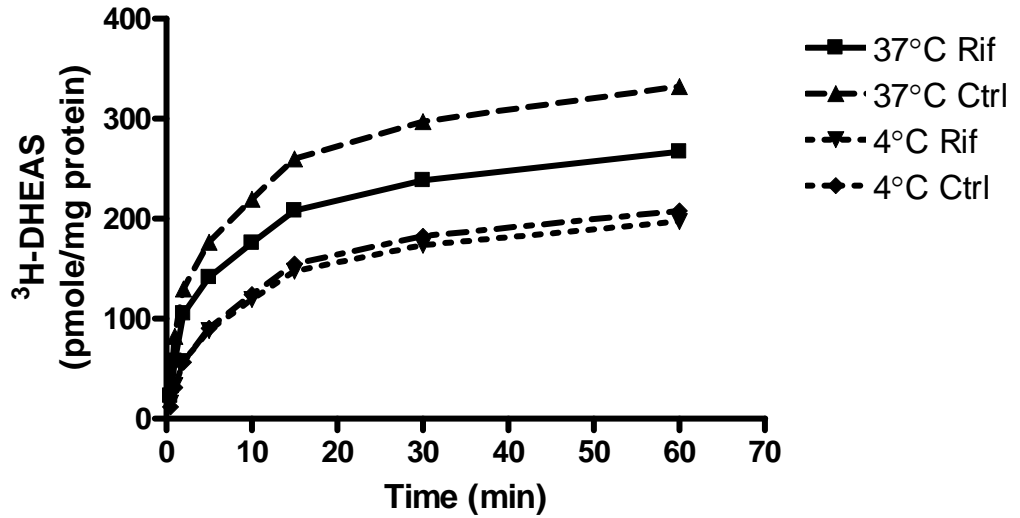
Figure 2-25 Efflux time profiles of ^{3}H-DHEAS (incubation 4.2nM) from HEK293-

Oatp1b2 cells over 60 min at 37˚C and 4˚C into buffer containing 100μM rifampin or

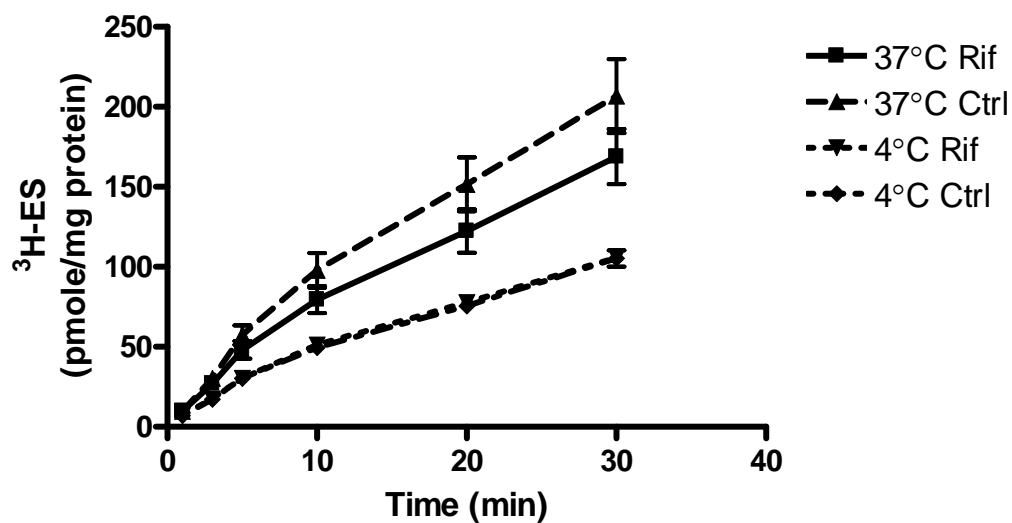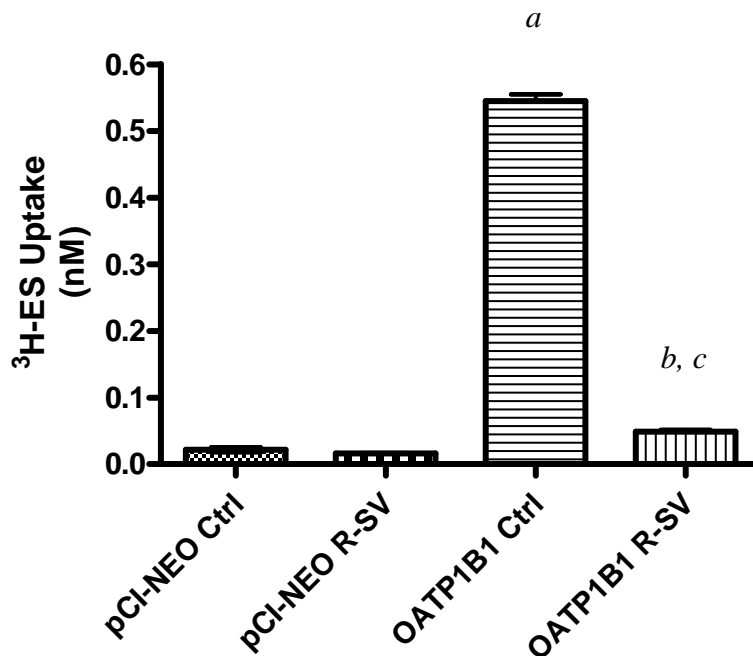0.1% DMSO as vehicle control. Values are mean ± SD, n=3 per group.
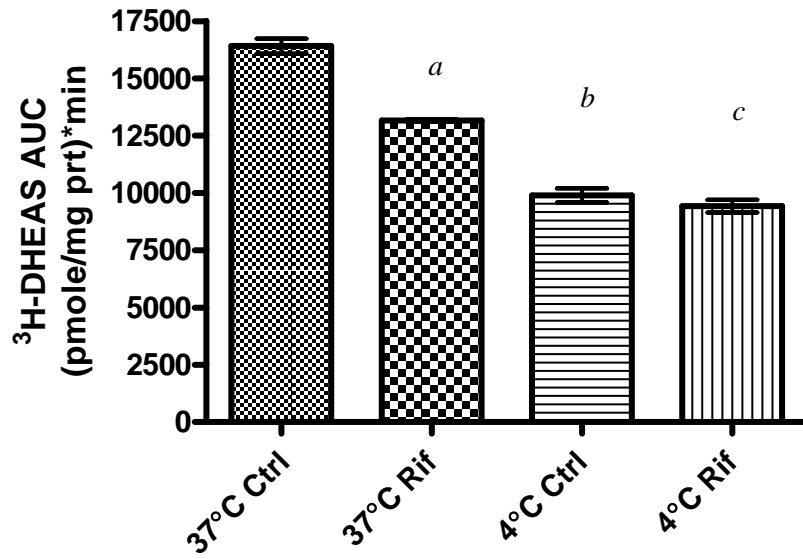
Figure 2-26 AUC values over 60 min ^{3}H-DHEAS (incubation 4.2nM) efflux timecourse from HEK293-Oatp1b2 cells at 37°C and 4°C into buffer containing 100μM rifampin or 0.1% DMSO as vehicle control. Values are mean ± SD, n=3 per group, [a] $p<0.001$ versus 37°C control, [b] $p<0.001$ versus 37°C control, [c] $p<0.001$ versus 37°C rifampin.
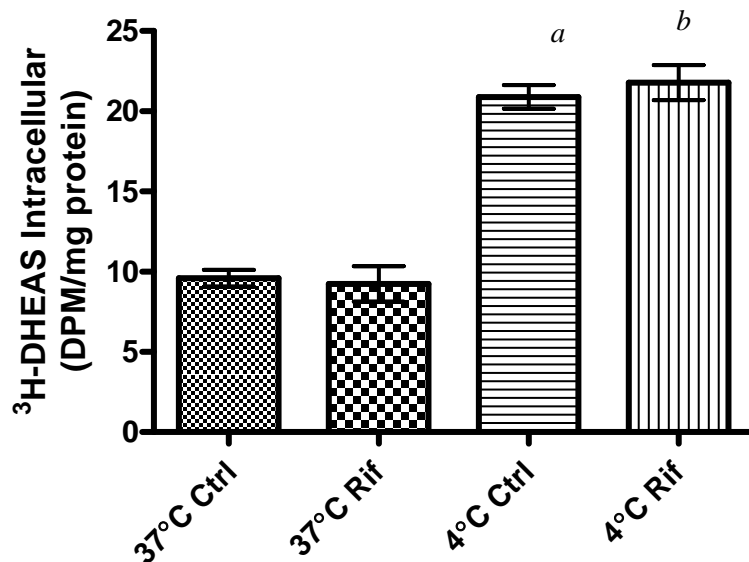
Figure 2-27 HEK293-Oatp1b2 intracellular ^{3}H-DHEAS (incubation 4.2nM) levels after 60 min timecourse at 37˚C and 4˚C into buffer containing 100μM rifampin or 0.1% DMSO as vehicle control. Values are mean ± SD, n=3 per group, ^{a} p<0.001 versus 37˚C control, ^{b} p<0.001 versus 37˚C rifampin.

2.3.4 Effect of Bicarbonate (BC) on ^{3}H-DHEAS Uptake and Efflux by HEK293-Oatp1b2

Figure 2-28 shows the uptake of 4.2nM ^{3}H-DHEAS by HEK293-Oatp1b2 cells in the presence and absence of bicarbonate (HCO_3^-) in the buffer. 100μM BSP was used as an inhibitor to assess whether cells functioned as expected in the presence of 27mM HCO_3^- (a physiologically relevant concentration) and to determine if there was any difference in inhibitory effect of BSP when HCO_3^- was absent. The intracellular levels of ^{3}H-DHEAS in the presence of 27mM HCO_3^- and absence of HCO_3^- were significantly different for both the inhibitor-treated and the non-treated groups with the presence of

HCO_3^- leading to higher intracellular levels. Table 2-1 summarizes the effect of HCO_3^- on intracellular levels.
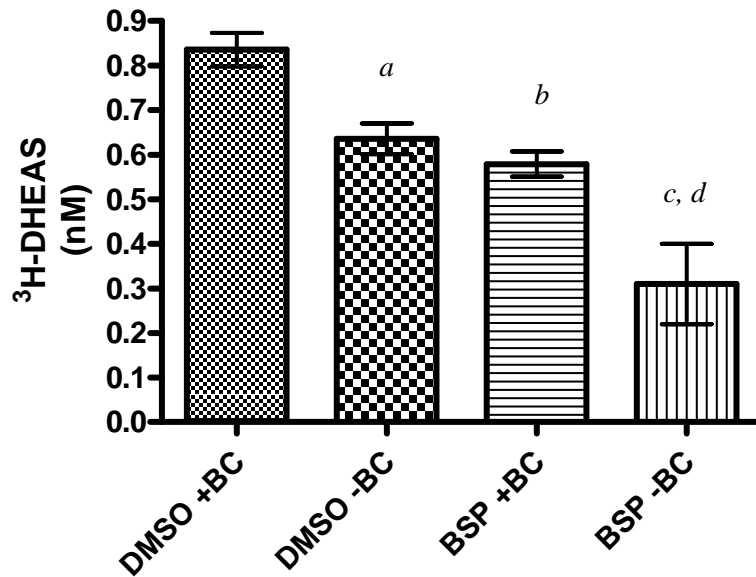
Figure 2-28 Intracellular ^{3}H-DHEAS (incubation 4.2nM) levels after 2 min uptake in HEK293-Oatp1b2 cells in the presence of 27mM HCO_3^- (+BC) and the absence of HCO_3^- (-BC), and in the presence of 100μM BSP or 0.1% DMSO vehicle control. Values are mean± SD, n=3 per group, ^{a} p<0.01 versus DMSO+BC, ^{b} p<0.01 versus DMSO+BC, ^{c} p<0.001 versus DMSO-BC, ^{d} p<0.01 versus BSP+BC.

Treatment	Uptake (nM)	Comparison	Uptake Ratio
DMSO +BC	0.836 ± 0.038	DMSO -BC/DMSO +BC	0.76
DMSO -BC	0.636 ± 0.034	BSP +BC/DMSO +BC	0.69
BSP +BC	0.579 ± 0.028	BSP-BC/DMSO -BC	0.49
BSP -BC	0.310 ± 0.090	BSP-BC/BSP +BC	0.54

Table 2-1 Summary of HCO_3^- influence on uptake of 4.2nM ^{3}H-DHEAS by HEK293-Oatp1b2. +BC denotes 27mM HCO_3^- and –BC denotes absence of HCO_3^-. Values are mean±SD, n=3 per group.

Figures 2-29 and 2-30 show the 30 min efflux timecourse of ^{3}H-DHEAS (incubation 4.2nM) from HEK293-Oatp1b2 and the AUC values for each treatment group, respectively. There were no significant differences in the AUC values due to the presence versus absence of bicarbonate in the buffer, but the 37˚C +BC AUC was significantly higher ($p<0.05$) than the 4˚C +BC AUC.
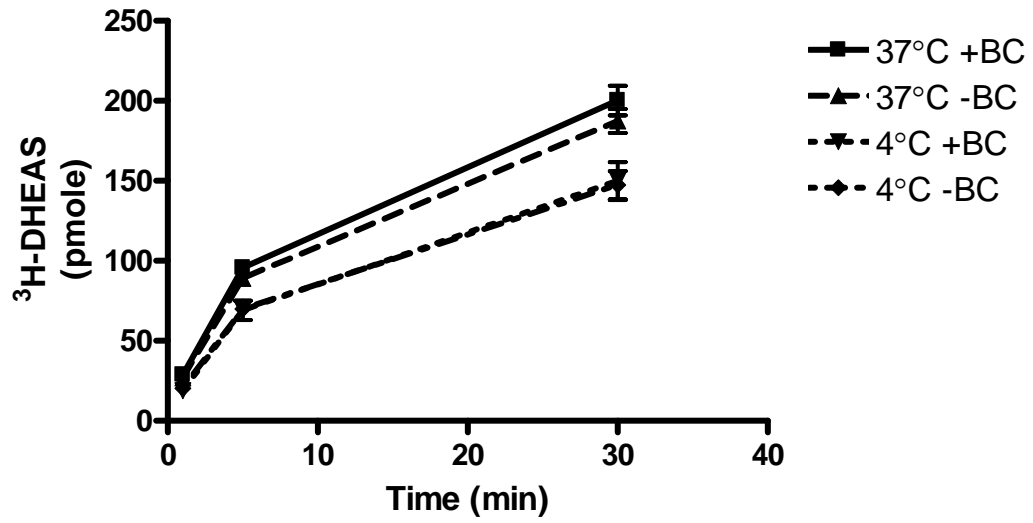
Figure 2-29 Profiles of ^{3}H-DHEAS (incubation 4.2nM) efflux over 30 min from

HEK293-Oatp1b2 cells at 37°C and 4°C into buffer containing either 27mM HCO_3^-

(+BC) or no HCO_3^- (-BC). Values are mean± SD, n=3 per group.

.
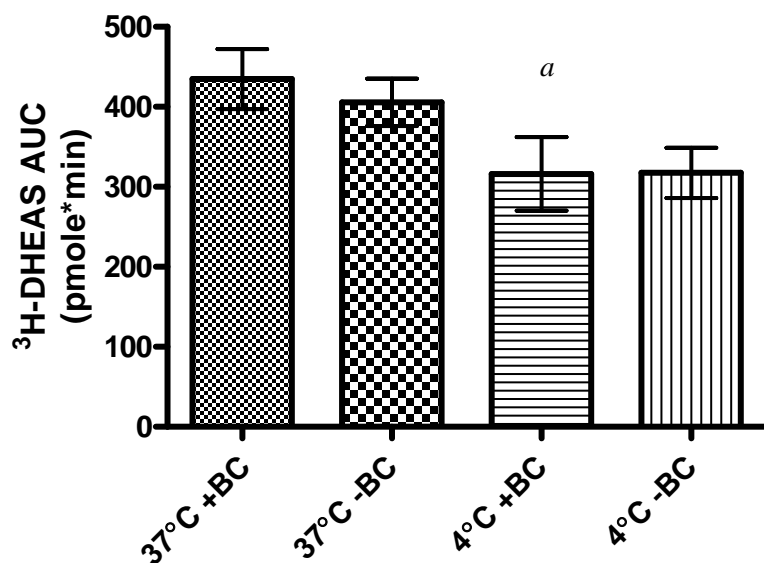
Figure 2-30 AUC values over 30 min ^{3}H-DHEAS (incubation 4.2nM) HEK293-Oatp1b2 efflux timecourse at 37°C and 4°C into buffer containing either 27mM HCO_3^- (+BC) or no HCO_3^- (-BC). Values are mean±SD, n=3 per group, [a] $p<0.05$ versus 37°C +BC.

2.3.5 Efflux of Pravastatin (PVS) and Fexofenadine (FEX) from Isolated Perfused Rat Liver

Figure 2-31 shows the concentration-time profile of pravastatin (incubation 10μM) encompassing the loading phase, steady-state, and the efflux phase from isolated perfused rat liver experiments. The inhibitor used was 100μM rifampin. Steady-state pravastatin levels were reached by 5 min and dropped rapidly once drug perfusion was discontinued. Figure 2-32 is an expanded view of the efflux time profile for pravastatin from 20 min, when the loading of drug was stopped and the efflux phase began, until 25 min, when drug levels were not detectable. Figure 2-33 shows that there were no

significant differences between the pravastatin AUC_{20-25} values between the control and

inhibitor treated groups.
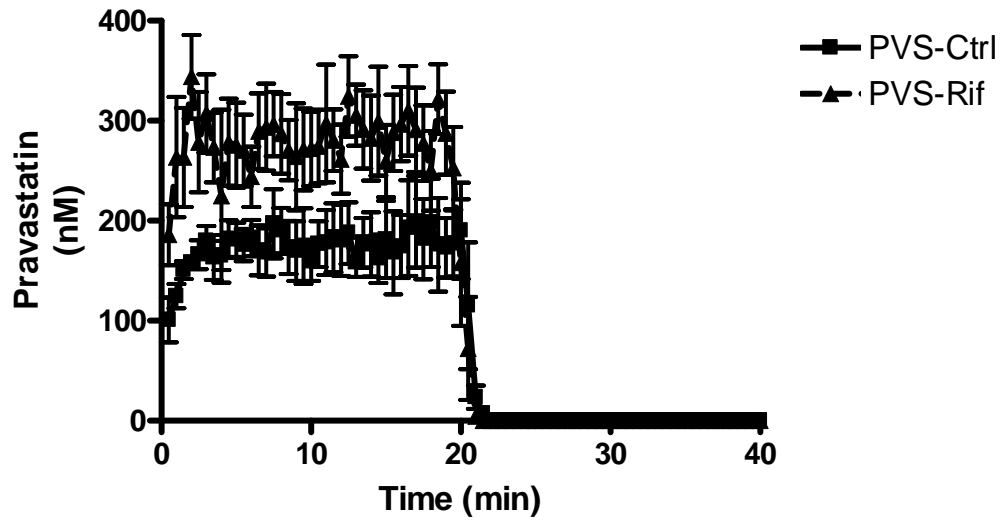
Figure 2-31 Time profiles of pravastatin (incubation 10μM) loading (~0-5 min), steady-

state (~5-20 min), and efflux (20-40 min) periods in isolated rat livers. Efflux was into

buffer containing 100μM rifampin or 0.1% DMSO vehicle control. Values reported are

mean± SD, n=3 for each group.
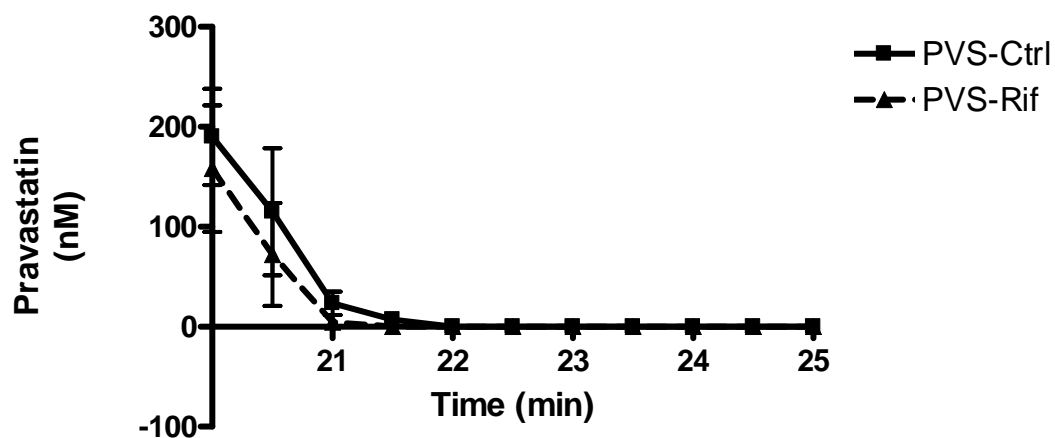
Figure 2-32 Efflux phase from 20 min-25 min for pravastatin into control and rifampin-treated buffer from isolated rat livers. Efflux was into buffer containing 100μM rifampin or 0.1% DMSO vehicle control. Values are mean±SD, n=3 per group.
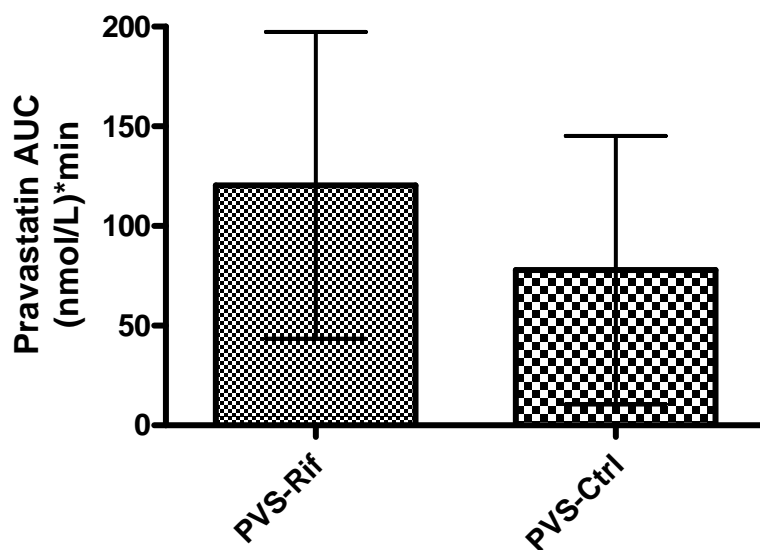
Figure 2-33 Pravastatin $AUC_{20-25min}$ for efflux into 100μM rifampin buffer or 0.1% DMSO vehicle control buffer from isolated rat livers. Values are mean ± SD, n=3 per group.

Figure 2-34 shows the concentration-time profiles of fexofenadine (incubation 10μM) including the loading phase, steady-state, and the efflux phase from isolated perfused rat liver experiments. The inhibitor used was 100μM rifampin. Steady-state fexofenadine levels were reached by 5 min and dropped rapidly once drug perfusion was discontinued. Figure 2-35 is an expanded view of the efflux time profile for fexofenadine from 20 min, when the loading of drug was stopped and the efflux phase began, until 25 min, when drug levels were not detectable. Figure 2-36 shows that there were no significant differences between the fexofenadine AUC_{20-25} values between the control and inhibitor treated groups.
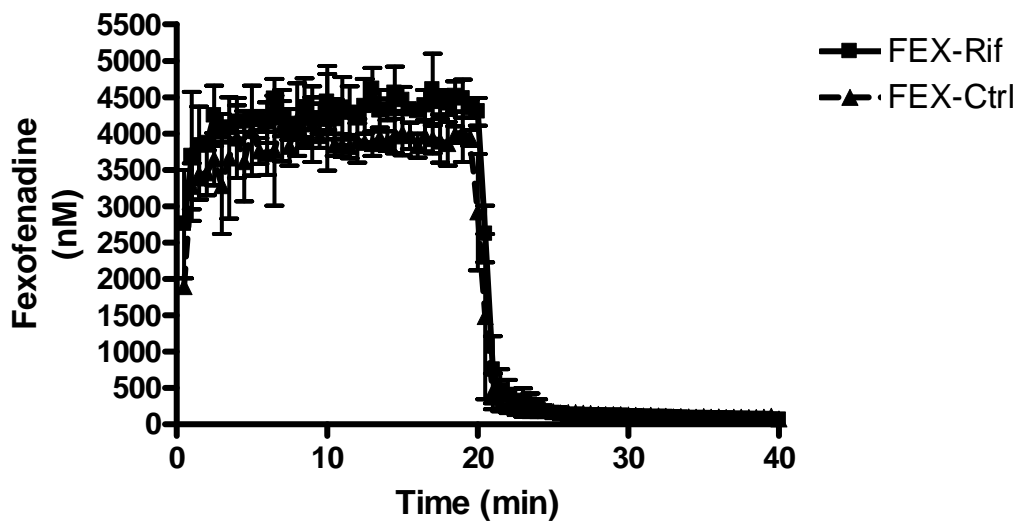
Figure 2-34 Time profiles of fexofenadine (incubation 10μM) loading (~0-5 min), steady-state (~5-20 min), and efflux (20-40 min) periods in isolated rat livers. Efflux was into buffer containing 100μM rifampin or 0.1% DMSO vehicle control. Values reported are mean± SD, n=3 for each group.
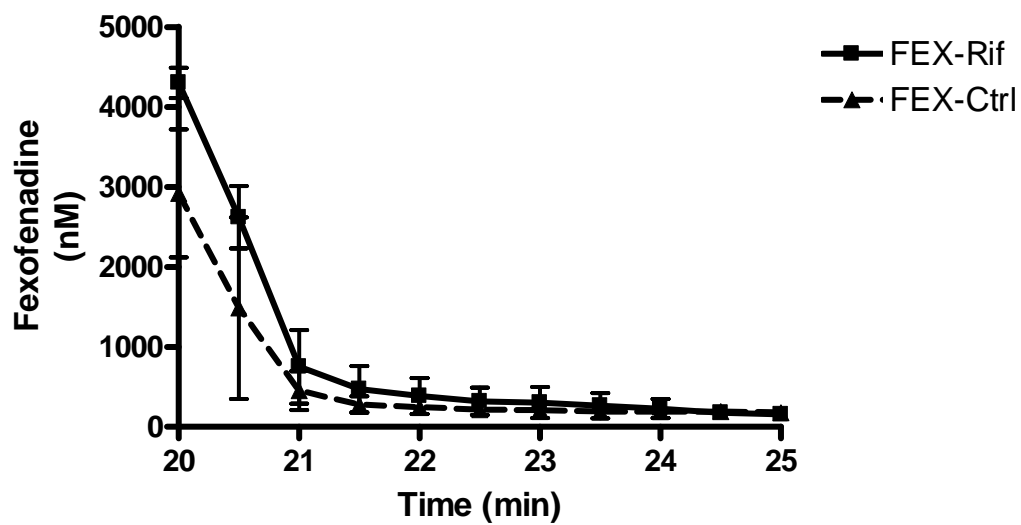
Figure 2-35 Efflux phase from 20 min-25 min for fexofenadine into control and rifampin-treated buffer from isolated rat livers. Efflux was into buffer containing 100μM rifampin or 0.1% DMSO vehicle control. Values are mean±SD, n=3 per group.
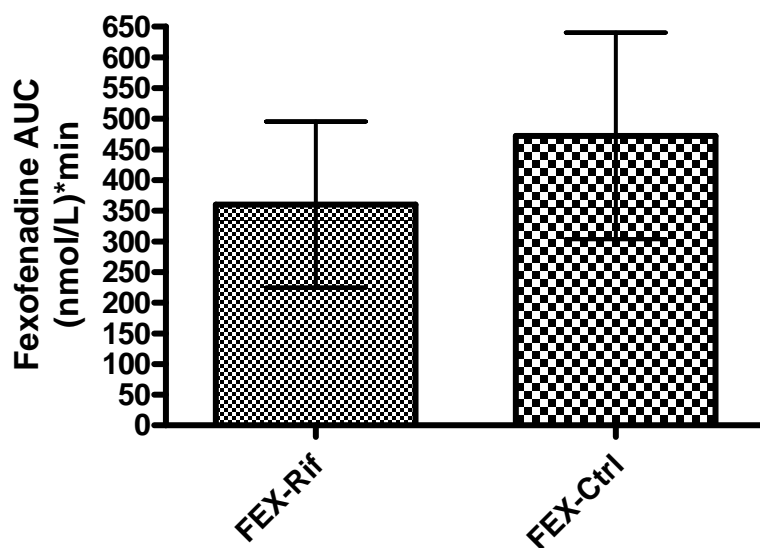
Figure 2-36 Fexofenadine $AUC_{20\text{-}25min}$ for efflux into 100μM rifampin buffer or 0.1% DMSO vehicle control buffer from isolated rat livers. Values are mean ± SD, n=3 per group.

2.4 Discussion

In the present series of studies, we attempted to examine the ability of hepatic OATP/Oatp to mediate efflux of drug out of cells using transfected cell systems and the isolated perfused rat liver system. A variety of OATP/Oatp inhibitors were used as well as 4°C control conditions to try to isolate the component of efflux due to active transport. Different OATP/Oatp inhibitors were used because different OATP isoforms have been shown to have variable sensitivities to inhibitors (Vavricka et al., 2002). Experiments done at 4°C were used as control instead of mock-transfected cells because we believed the transporter needed to be present in order to load cells with the test substrates. Uptake studies with substrates in mock-transfected and in transporter-expressing cells showed markedly higher uptake that was inhibited by OATP/Oatp inhibitors in the transporter-

expressing cells compared to the mock-transfected cells, indicating that the over-expressed transporters were taking up substrate. Inhibition by OATP/Oatp inhibitors was not seen in mock-transfected cells and substrate levels seen for those cells may be due to diffusion or adsorption of substrate. In both the cell and IPRL studies, inhibitor was loaded along with substrate drug. While this may seem counterintuitive, we did these because of certain assumptions we made regarding what may be happening with the transporter. We thought that as bidirectional facilitative transporters, there may be binding sites for the substrate both intracellular and extracellular. To inhibit uptake, the extracellular binding site would need to interact with inhibitor while to inhibit efflux, the intracellular site would need to interact with inhibitor. Therefore, to examine inhibition of efflux we felt that we needed to have inhibitor present inside the cells to interfere with substrate binding to the intracellular binding site. We wanted to insure that if inhibition of efflux was caused by inhibitor binding to an intracellular site that we would be able to inhibit at the immediate start of the efflux period. The argument could be made that by loading both the control and the inhibitor groups with inhibitor during the loading phase, then inhibition may still be playing a role and masking differences between the control and inhibitor groups until such time that the inhibitor could dissociate in the control group and no long prevent drug efflux. However, we worried that if we waited until after the cells were loaded with drug to load the inhibitor that appreciable amounts of drug may be effluxed from the cells before the inhibitor could get inside the cells, interact with the intracellular binding site and inhibit efflux, masking the effects of inhibiting efflux. We made the assumption that by carrying out the efflux experiments for 20 to 60 minutes, that the inhibitor had time to dissociate and differences in efflux would be

evident at later timepoints. This is why we used AUC and intracellular levels at the end of the efflux phase as measures of amount of efflux. Since inhibitor was present in all of the cell groups at the beginning of the efflux phase, calculation of initial rates would be confounded. Intracellular and efflux data clearly demonstrated that appreciable amounts of substrate could be loaded into the cells or liver even in the presence of OATP/Oatp inhibitors. Uptake experiments with model substrates showed higher levels of uptake in the transfected cell lines than in the empty vector HEK293-pCI-NEO cell line. Of note is that for ^{3}H-ES in the HEK293-Oatp1b2 cell line, the uptake levels between the transfected cells and the control cells were similar, although significant inhibition was seen in the HEK293-Oatp1b2 cells but not the HEK293-pCI-NEO cells. Literature reports that ^{3}H-DHEAS is an Oatp1b2 substrate (Halwachs et al., 2005; Wood et al., 2005), so the decision was made to try this compound in efflux experiments. Since significant differences were seen in the measures of efflux for Oatp1b2 and ^{3}H-DHEAS, this compound was used to study the effect of bicarbonate influence on efflux.

In the case of OATP1B1, nearly all of the compounds tested in the cellular systems, with the exception of ^{3}H-DHEAS, showed higher levels of efflux at 37˚C than at 4˚C in the concentration-time efflux profiles, indicating that there was some degree of active efflux occurring since transporter proteins are believed to have markedly lower activity at 4˚C. The same levels of efflux at 37˚C as at 4˚C for ^{3}H-DHEAS would point to passive diffusion being the predominant mechanism by which this compound exits the cells.

The ^{3}H-saquinavir efflux concenetration-time profiles showed a marked difference between the 37˚C groups and the 4˚C groups, strongly indicating an active

efflux process. Further support was provided by the AUC values for the 37°C control and the 37°C rifampin groups being significantly higher (p<0.001) than the corresponding treatment groups at 4°C and by the intracellular ^{3}H-saquinavir levels at the end of the timcourse being significantly higher (p<0.001) in the 37°C treatment groups than in the corresponding 4°C groups. Evidence supporting OATP1B1 as the active efflux mediator was lacking though in that the 37°C control AUC was not significantly higher than the 37°C rifampin AUC. Uptake in HEK293-OATP1B1 cells was significantly higher than in HEK293-pCI-NEO indicating that OATP1B1 may transport ^{3}H-saquinvair to some degree.

The efflux timecourse for ^{3}H-ES was similar to that for ^{3}H-saquinavir in that the 37°C groups showed higher efflux levels than the 4°C groups. The AUC for the 37°C control group was significantly higher (p<0.01) than for the 4°C control, but the 37°C rifampin treated group was not significantly different from the 4°C rifampin treated group. Also, there was no difference between the 37°C control and 37°C rifampin groups, indicating no inhibition of active efflux by rifampin. In contrast to the AUC data, the 37°C intracellular levels were markedly lower than the 4°C intracellular levels (p<0.001). Since the incubation solutions for all four groups were made from a single dilution of ^{3}H-ES, which was subsequently divided and spiked with control vehicle or inhibitor, it is unlikely that differing concentrations of ^{3}H-ES in the incubation solution led to such a discrepancy between the AUC and the intracellular data.

As mentioned previously, the ^{3}H-DHEAS data indicated that active efflux was not the major route of exit for this compound from the cells. The 37°C and 4°C efflux profiles were very similar and there were no significant differences in the AUC values

between any of the groups. The 37˚C intracellular levels were significantly lower than the 4˚C groups with the 37˚C control intracellular levels 55% lower ($p < 0.001$) than the 4˚C control intracellular levels and the 37˚C rifamycin-SV levels 26% lower ($p < 0.01$) than the 4˚C rifamycin-SV intracellular levels.

For OATP2B1, ^{3}H-ES and ^{3}H-DHEAS efflux were examined. ^{3}H-DHEAS was not so clearly reliant on diffusion in the HEK293-OATP2B1 cells as it appeared to be in the HEK293-OATP1B1 cells. The efflux timecourse showed higher levels of efflux for the 37˚C groups compared to the 4˚C groups, but similar to OATP1B1 there were no differences in the AUC values for any of the groups. The intracellular levels followed the trend of the efflux profile in that the 37˚C intracellular levels were significantly lower than those for the 4˚C groups ($p < 0.001$). In contrast to the OATP1B1 ^{3}H-DHEAS data that showed no significant differences upon inhibitor treatment, for OATP2B1 the 37˚C rifampin treated group had 37% higher ($p < 0.01$) ^{3}H-DHEAS level than the 37˚C control group while the 4˚C groups showed no statistically significant difference in the presence of inhibitor.

The ^{3}H-ES data does not clearly show active efflux in the timecourse profile. There were no statistically significant differences between the AUC values for any of the groups except between the 37˚C control and the 4˚C control groups, with the 4˚C control displaying 42% lower AUC than the 37˚C control. The intracellular values did not support active efflux of ^{3}H-ES by OATP2B1 in that there was no difference between the 37˚C control and the 37˚C rifampin treatment groups. Surprisingly, the 4˚C control intracellular level was significantly lower ($p < 0.01$) than the 4˚C rifampin treated group,

although this did agree with the efflux timecourse profile that showed the lowest degree of efflux for the 4°C rifampin group.

Rat Oatp1b2 was also examined for efflux function using ^{3}H-ES and ^{3}H-DHEAS. In the HEK293-Oatp1b2 cells, ^{3}H-ES showed moderately higher levels of efflux at 37°C than at 4°C. The 37°C control and 4°C control AUC values were significantly different ($p < 0.05$) as were the 37°C rifamycin-SV and the 4°C rifamycin-SV AUCs ($p < 0.01$). The intracellular ^{3}H-ES level for the 4°C control was significantly higher than the 37°C control ($p < 0.05$), but the 4°C rifamycin-SV intracellular level was not different from the 37°C rifamycin-SV. ^{3}H-DHEAS results also showed higher efflux levels at 37°C than at 4°C accompanied by significantly higher AUC values for the 37°C groups versus the 4°C groups ($p < 0.001$) and significantly higher ($p < 0.001$) intracellular ^{3}H-DHEAS levels in the 4°C treatment groups than in the 37°C treatment groups. The presence of inhibitor led to a significantly lower AUC in the 37°C rifampin group versus the 37°C control (18%, $p < 0.001$), however, the percent decrease in AUC is slight and unlikely to be clinically relevant.

The effect of bicarbonate (HCO_3^-) in the buffer on uptake and efflux in HEK293-Oatp1b2 cells was also studied. Since it is conjectured that HCO_3^- efflux from cells is coupled to substrate uptake, we wished to examine whether substrate efflux could be coupled to HCO_3^- uptake. First, an uptake study was run with ^{3}H-DHEAS in HEK293-Oatp1b2 cells and showed that after incubating cells in buffer containing HCO_3^- prior to initiation of transport by addition of substrate, uptake of ^{3}H-DHEAS was significantly higher (24%, $p < 0.01$) than when cells were not pre-incubated with HCO_3^-. In the presence of HCO_3^-, 100μM BSP inhibited ^{3}H-DHEAS uptake by 31% ($p < 0.01$). In the

absence of HCO_3^-, BSP inhibited uptake of ^3H-DHEAS by 51% (p<0.001) compared to

vehicle control with no HCO_3^- present. When cells were treated with BSP in the presence

and absence of HCO_3^-, the uptake in the absence of HCO_3^- was 46% lower (p<0.01) than

in the presence of HCO_3^-, providing further support for decreased uptake in the absence

of HCO_3^-. These results agree with those from Satlin et al. (1997) and Leuthold et al.

(2009) in that the presence of HCO_3^- does appear to facilitate substrate uptake.

The results from the study of the efflux of ^3H-DHEAS from HEK293-Oatp1b2

cells in the presence of HCO_3^- versus the absence of HCO_3^- did not show any substantial

effect of HCO_3^-. The timecourse profile of ^3H-DHEAS efflux at 37°C in the presence of

HCO_3^- was very similar to that at 37°C in the absence of HCO_3^-. No significant

differences were seen between the AUC values in the presence versus absence of HCO_3^-.

In healthy people, blood levels of HCO_3^- are ~25 mmol/L (Frassetto et al., 2007) so the

difference between the effect of HCO_3^- on uptake versus efflux could be explained by the

absence of a binding site for HCO_3^- on the extracellular surface. Also, if HCO_3^- is

concentrated within hepatocytes so that intrahepatocyte levels are higher than those found

in blood, the HCO_3^- gradient would not support uptake of HCO_3^- coupled with efflux of

substrate.

To further examine Oatp-mediated efflux in a more physiologically relevant

system, the isolated perfused rat liver system was used to study efflux of pravastatin and

fexofenadine. Another researcher in the lab had performed these IPRL experiments with

pravastatin and shown significant differences in amount of drug appearing in the efflux

buffer when rifampin was present versus when it was absent (unpublished data). We

wanted to see if these results were reproducible. Fexofenadine has been shown to be a rat

Oatp substrate (Cvetkovic et al., 1999), and since it undergoes little metabolism was chosen as a second probe substrate. As with the cellular studies, the isolated liver was loaded with substrate and inhibitor then efflux was initiated by switching to perfusate containing only vehicle control or the Oatp inhibitor rifampin. The amount of pravastatin or fexofenadine appearing in the efflux buffer over a 20 min efflux phase was measured. After initiation of the efflux phase, levels of substrate quickly fell below the limits of quantitation so AUC_{20-25} values were calculated to determine if there were any differences in substrate perfusate levels due to the presence versus absence of inhibitor. Neither pravastatin nor fexofenadine AUC_{20-25} values differed significantly between control and rifampin-treated groups. The liver and bile concentration data were inconclusive. For pravastatin, liver levels were less than the lower limit of quantitation for all rats. It is possible that pravastatin, which is an Mrp2 substrate, was transported into bile so efficiently that appreciable basolateral efflux could not occur. Bile was available for only one control rat (434ng), while the rats treated with rifampin yielded bile results for 3 rats and levels were 32 ± 18ng (mean $\pm$ SD). Since there was bile for only one control rat, no conclusions can be drawn.

In the fexofenadine treated rats, no bile was available for control or rifampin-treated rats, however fexofenadine was detected in the livers of all of the rats with control rats having an average fexofenadine level of 40 ± 11 nM/g liver and rifampin-treated rats having an average fexofenadine level 45 ± 19 nM/g liver. Values are mean $\pm$ SD and the difference between fexofenadine in control livers versus inhibitor-treated livers was not significant.

We certainly recognize the drawbacks to the systems used to try to study this phenomenon in the described experiments, namely the loading of inhibitor along with substrate, which confounded our ability to calculate initial rates of efflux. However, initial optimization experiments performed with inhibitor addition occurring at the initiation of the efflux phase yielded no differences in efflux between inhibitor treated cells and control cells. It was thought that substrate efflux may occur to a substantial degree before inhibitor has time to enter cells and bind to the active site, masking any differences in efflux that Oatp/OATP inhibition may cause. It is conceivable that the efflux periods in the cellular and the IPRL studies were not long enough to allow inhibitor to dissociate from its binding site, also masking any differences that may have arisen from efflux inhibition.

A better proof of concept system may be to use inside-out membrane vesicles made from cells (such as insect Sf9 cells) expressing OATPs/Oatps or to use *xenopus laevis* oocytes expressing OATPs/Oatps. The loading step could be eliminated with inside-out vesicles, since the opposite orientation would cause the OATP/Oatp to pump drug into the vesicle and intracellular levels could be measured as an indicator of OATP/Oatp efflux ability. Oocytes could be injected to load a known amount of drug. With both systems, the problem of loading with inhibitor could be avoided since again, the potential intracellular binding site would either be expressed on the outside of the inside-out vesicles or inhibitor could be directly injected into oocytes. Moving from these systems to a more physiologically relevant system however still presents interesting technical challenges.

2.5 Conclusions

All of the evidence from cellular and IPRL studies taken together indicate that OATP/Oatp mediated efflux may not be a major mechanism whereby drugs exit hepatocytes and re-enter systemic circulation. Even in cases where there are significant differences seen between efflux levels in the control and the inhibitor treated groups, such as for ^{3}H-DHEAS in Oatp1b2, the differences are small, <20%, indicating that they are unlikely to be physiologically relevant. In light of the experimental difficulties described though, the importance of the data should not be over stated. Although our data did not support a major role for OATP/Oatp mediated hepatic basolateral efflux, the phenomenon may warrant further investigation with the alternatives described above. While hepatic Oatp/OATP transporters are very important in determining substrates' pharmacokinetic behavior through their uptake function, their importance as an avenue of drug re-entry into systemic circulation is still unclear.

2.6 References

Cvetkovic, M., Leake, B., Fromm, M.F., Wilkinson, G.R., and Kim, R.B. (1999). "Oatp and P-glycoprotein transporters mediate the cellular uptake andex cretion of fexofenadine." Drug Metab. Dispos. **27**(8): 866-871.

Frassetto, L.A., Morris, R.C. Jr., and Sebastian, A. (2007). "Dietary sodium chloride intake independently predicts the degree of hyperchloremic metabolic acidosis in healthy humans consuming a net acid-producing diet." Am. J. Physiol. Renal Physiol. **293**: F521–F525.

Hagenbuch, B. and Gui, C. (2008). "Xenobiotic transporters of the human organic anion transporting polypeptides (OATP) family." Xenobiotica. **38**(7-8): 778-801.

Konig, J., Seithel, A., Gradhand, U., and Fromm, M.F. (2006) "Pharmacogenomics of human OATP transporters." Naunyn Schmiedebergs Arch. Pharmacol. **372**: 432–443.

Lau[a], Y.Y., Okochi, H., Huang, Y., and Benet, L.Z. (2006). "Multiple transporters affect the disposition of atorvastatin and its two active hydroxyl metabolites: application of in vitro and ex situ systems." J. Pharmacol. Exp. Ther. **316**:762–771.

Lau[b], Y.Y., Okochi, H., Huang, Y., and Benet, L.Z. (2006). "Pharmacokinetics of atorvastatin and its hydroxy metabolites in rats and the effects of concomitant rifampicin single doses: relevance of first-pass effect from hepatic uptake transporters, and intestinal and hepatic metabolism." Drug Metab. Dispos. **34**:1175–1181.

Leuthold, S., Hagenbuch, B., Mohebbi, N., Wagner, C.A., Meier, P.J., and Stieger, B. (2009). "Mechanisms of pH-gradient driven transport mediated by organic anion polypeptide transporters." Am. J. Physiol., Cell Physiol. **296**: 570-582.

Li, L., Meier, P.J., and Ballatori, N. (2000). "Oatp2 mediates bidirectional organic solute transport: a role for intracellular glutathione." Mol. Pharmacol. **58**: 335-340.

Meier-Abt, F., Mokrab, Y., and Mizuguchi, K. (2005). "Organic anion transporting polypeptides of the OATP/SLCO superfamily: identification of new members in nonmammalian species comparative modeling and a potential transport mode." J. Membrane Biol. **208**: 213-227.

Niemi, M., Neuvonen, P.J., Hofmann, U., Backman, J.T., Schwab, M., Luetjohann, D., von Bergmann, K., Eichelbaum, M., and Kivisto, K.T. (2005). "Acute effects of pravastatin on cholesterol synthesis are associated with SLCO1B1 (encoding OATP1B1) haplotype*17." Pharmacogenet. Genomics. **15**: 303-309.

Nishida, C., Ogawara, K.I., Kimura, T., and Higaki, K. (2004). "Pharmacokinetic analysis of factors determining elimination pathways for sulfate and glucuronide metabolites of xenobiotics. III: mechanisms for sinusoidal efflux of 4-methylembelliferone sulfate." Xenobiotica. **34**: 439–448.

Prueksaritanont, T., Hoener, B.A., and Benet, L.Z. (1992). "Effects of low-density lipoprotein and ethinyl estradiol on cyclosporine metabolism in isolated rat liver perfusions." Drug Metab. Dispos. **20**(4): 547-552.

Satlin, L.M., Amin, V., and Wolkoff, A.W. (1997). "Organic anion transporting polypeptide mediates organic anion/HCO3- exchange." J. Biol. Chem. **272(42)**: 26340-26345.

Vavricka, S.R., van Montfoort, J., Ha, H.R., Meier, P.J., and Fattinger, K. (2002). "Interactions of rifamycin-SV and rifampicin with organic anion uptake systems of human liver." Hepatology. **36**(1): 164-172.

CHAPTER 3

Investigation of Transporter-Enzyme Interplay between Breast Cancer Resistance Protein and Intestinal Drug Metabolizing Enzymes

3.1 Introduction

The Breast Cancer Resistance Protein (BCRP), encoded by ABCG2, is an ATP-binding cassette efflux transporter that co-localizes with P-glycoprotein (Pgp) on the apical enterocytic membrane, the apical bile canalicular membrane, and in the blood-brain barrier. Pgp in the intestine has been shown to cooperate with intestinal drug metabolizing enzymes (e.g. CYP3A4) to minimize absorption of dual substrates, decreasing their bioavailability. As drug gets into the enterocyte, it can be effluxed back out by Pgp before it is metabolized, whereupon it can re-enter the cell and have another change at being metabolized or of being effluxed into the lumen again. As this cycling repeats, it effectively increases exposure of the drug to the metabolizing enzyme (see Figure 3-1).
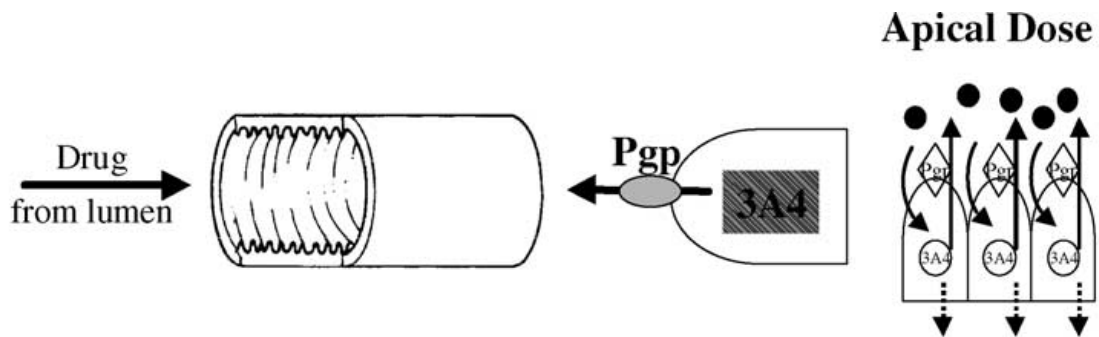
Figure 3-1 Interplay between intestinal Pgp and CYP3A4 (Cummins et al., 2004)

Due to its localization, BCRP may participate in a similar cycling phenomenon with intestinal drug metabolizing enzymes as seen for Pgp and CYP3A4 to limit drug absorption.

There is substantial substrate overlap between Pgp and BCRP, meaning that Pgp and BCRP may be able to ameliorate each others' effects on drug disposition. For example, in a study by Polli et al. (2004), the effects of Pgp and Bcrp on the exposure of orally dosed GV196771, an *N*-methyl-D-aspartate receptor antagonist, were examined in wildtype and in mdr1a/1b$^{-/-}$ mice treated with a dual Pgp/Bcrp inhibitor. The area under the concentration-time curve (AUC) of GV196771 increased 6.2-fold in mdr1a/1b$^{-/-}$ mice, 10.3-fold in inhibitor-treated wildtype mice, and 16.4-fold in inhibitor-treated mdr1a/1b$^{-/-}$ mice, suggesting a role for both Pgp and for Bcrp in determining the bioavailability.

The effect of BCRP on drug disposition will be more evident with drugs that are substrates of BCRP but not of Pgp or for dual substrates when Pgp is inhibited or has decreased function compared to BCRP. For example, after oral dosing of nitrofurantoin, a BCRP specific substrate (Feinshtein et al., 2009), the AUC was nearly 4-fold higher in Bcrp$^{-/-}$ mice compared to wildtype, while after intravenous dosing the increase in AUC was only 2-fold, indicating that intestinal Bcrp limits nitrofurantoin bioavailability (Merino et al., 2005).

The primary goal of this project was to examine the effect of BCRP/Bcrp inhibition on drug absorption. A secondary goal was to examine the inhibitory potential of anti-retroviral medications (ARV) used in HIV treatment against BCRP/Bcrp to determine if inhibition of BCRP/Bcrp by these drugs could lead to decreased bioavailability of concomitantly administered BCRP/Bcrp substrates. It has already been determined that protease inhibitors interact with Pgp, both as substrates and inhibitors (Weiss et al., 2007, Aungst, 1999). A study by Storch et al. (2007) tested the inhibitory potential of a variety of anti-HIV drugs against Pgp and showed inhibition by atazanavir,

delavirdine, lopinavir, and saquinavir. Investigation of ARV interactions through

BCRP/Bcrp remains an area where more work is needed to determine if clinically

relevant drug-drug interactions will occur when ARV therapies are coadministered with

BCRP substrates. In one report, Weiss and colleagues (2007) systematically tested the

inhibitory potential of commonly used anti-HIV therapies and determined that several

had potent inhibitory action against BCRP (see Table 3-1).

Compound	IC_{50} (μM)	Compound	IC_{50} (μM)
Fumitremorgin C	0.47	Nelfinavir	13.5
Ko143	0.01	Saquinavir	27.4
Amprenavir	181	Delavirdine	18.7
Atazanavir	69.1	Efavirenz	20.6
Lopinavir	7.66	Abacavir	385

Table 3-1 Estimated IC_{50} values for BCRP inhibition in MDCKII-BCRP cells (reported

in μM). Adapted from Weiss et al., 2007.

Information on drug-drug interactions between these ARV drugs and BCRP

substrates is lacking. One study by Busti and colleagues (2008) found a significant

interaction between rosuvastatin and atazanavir/ritonavir (ATZ/RTV). Upon

concomitant oral dosing of ATZ/RTV and rosuvastatin, AUC of rosuvastatin increased

213%, C_{max} increased 600%, and t_{max} decreased 40%. Since rosuvastatin is not a Pgp or

MRP substrate, the authors conjectured that inhibition of BCRP was causing the

pharmacokinetic changes.

This project was carried out in order to more fully examine the effect of BCRP/Bcrp on oral drug absorption and potential drug-drug interactions between BCRP substrates and anti-HIV medications.

3.2 Materials and Methods

3.2.1 Chemicals and Materials

^{14}C-Mannitol and ^{3}H-estrone sulfate were purchased from Perkin Elmer (Waltham, MA); ^{3}H-mitoxantrone, efavirenz, and lopinavir were purchased from Moravek Biochemicals and Radiochemicals (Brea, CA); fumitremorgen C (FTC) was purchased from Enzo Life Sciences (Plymouth Meeting, PA); and dantrolene, omeprazole, and pantoprazole were purchased from Sigma Aldrich (St. Louis, MO). Monoclonal anti-BCRP antibody BXP-21 was purchased from Santa Cruz Biotechnology (Santa Cruz, CA) and AlexaFluor488 antibody was purchased from Molecular Probes (Eugene, OR). Ko143 and the MDCKII-BCRP cell line were generous gifts from Dr. Alfred Schinkel at the Netherlands Cancer Institute (Amsterdam, Netherlands). The MDCKII wildtype cell line was a generous gift from Professor Piet Borst and Dr. Raymond Evers (The Netherland Cancer Institute, Netherlands). All cell culture media and the Caco2 cell line were obtained from the UCSF Cell Culture Facility (San Francisco, CA). Non-coated 6-well cell culture plates were purchased from Corning Life Sciences (Acton, MA) and 0.4µm low density polyethylene terephthalate (PET) transwell inserts and 4-chamber glass slides were purchased from BD Bioscience (Bedford, MA).

3.2.2 Confocal Microscopy

MDCKII and MDCKII-BCRP cells were grown to confluence on 4-chamber glass slides by adding 0.8mL of cell suspension to each chamber. Media was changed every other day until day 6 post-plating. Media was aspirated off and the cells were washed twice with 1mL PBS at room temperature. After washing, 200μL of 3% formaldehyde in PBS was added to each chamber to fix the cells. The cells were placed in 4˚C for 1 hr, then cells were washed 3× with 950μL of PBS at room temperature. Cells were stored at 4˚C until antibody incubation.

Cells were blocked with 0.5mL of 2% gelatin in PBS for 30 min at 37˚C then were washed 3× for 5 min with 0.1% bovine serum albumin in PBS (wash solution) at room temperature. The cells were incubated with 200μL of a 1:100 dilution of the 1˚ antibody, BXP-21 mouse, for 30 min at 37˚C. Cells were washed 3× for 5 min with wash solution at room temperature then incubated with 200μL of a 1:500 dilution of the 2˚ antibody, AlexaFluor488 antimouse, for 30 min at 37˚C. Cells were again washed 3× for 5 min with wash solution at room temperature then were sealed with 50μL of Vectashield fluorescent mounting media (Vector Laboratories, Burlingame, CA), covered with a glass coverslip (being careful to avoid bubbles under the coverslip) and sealed at the edges with clear nail polish. Cells were visualized on a Biorad LaserSharp MRC1024 confocal microscope (Hercules, CA).

3.2.3 MDCKII, MDCKII-BCRP, and Caco2 Cell Culture and Bidirectional Transport Assays

MDCKII and MDCKII-BCRP cells were cultured in Dulbelcco's Modified Eagle Medium with 100 U/mL penicillin/streptomycin at 37°C in 5% CO_2 atmosphere with 95% humidity. Caco2 cells were cultured in MEM Modified Eagle with Earle's BSS Medium with 100U/mL penicillin/streptomycin at 37°C in 5% CO_2 atmosphere with 95% humidity. All cells were cultured in T-75 flasks and when ~90% confluent were trypsinized and plated on PET inserts in Corning 6-well cell culture plates. Cells were allowed to grow to confluence for 6 days (MDCKII and MDCKII-BCRP) or 21 days (Caco2). Prior to bidirectional studies, cells were washed for 5 min at 37°C with Hanks Buffered Salt Solution (HBSS) at pH 7.4. Transepithelial electrical resistance (TEER) values were measured for all cells. For MDCKII and MDCKII-BCRP cells, TEER values of approximately 130-180 $\Omega \cdot cm^2$ were considered to indicate intact monolayers while for Caco2 cells TEER values of about 400-500 $\Omega \cdot cm^2$ were considered acceptable. The experiment was initiated by replacing wash buffer with HBSS containing test substrate in either the apical (A) chamber or in the basal (B) chamber with BCRP inhibitor (1:1000 or 1:100 dilution) or vehicle control (1:100 or 1:1000 to match inhibitor vehicle percentage) in both A and B chambers. The incubation was performed at 37°C and at selected timepoints, 200µL aliquots of buffer were removed from the receiver chamber and replaced with fresh buffer. At the end of the timecourse, buffer was removed, inserts were washed 3× in ice-cold phosphate buffered saline (PBS) and allowed to dry at room temperature before cells were scraped manually with 200µL of

H₂O and stored in Eppendorf tubes. Both buffer and cell samples were stored at -80˚C

until analysis.

3.2.4 Isolation of Rat Jejunum Segments and Use in Ussing Chamber

Male Sprague-Dawley rats weighing 200-350g (Charles River, Wilmington, MA)

were anesthetized via peritoneal injection of 1mL/kg ketamine:xylazine (80mg/mL:

12mg/mL) prior to small intestine removal. The jejunum was considered to start

approximately 10cm from the stomach and continue for at least 90cm, therefore the

segments for the Ussing chamber studies were taken from this section of the intestine.

Once the jejunum was isolated, it was washed with ice-cold Krebs-Ringer (KR) buffer

(108mM NaCl, 4.7mM KCl, 1.8mM Na₂HPO₄, 0.4mM NaH₂PO₄, 15mM NaHCO₃,

1.2mM MgSO₄, 1.25mM CaCl₂, 11.5mM D-glucose, pH 7.4) by using a 10mL syringe to

push through the buffer and push out waste matter. Once clean, the muscosa was gently

scraped off with a clean glass slide and the intestine was cut open along the mesenteric

border. Avoiding Peyer's patches, nine 3cm segments were cut from the proximal

jejunum and placed in ice-cold oxygenated KR buffer until they were mounted in the

Ussing chamber. Once the segments were mounted, 37˚C KR buffer at pH 6.5 containing

inhibitor (1:100 or 1:1000 dilution of stock) was added to the apical chambers while 37˚C

KR buffer at pH 7.4 containing inhibitor (1:100 or 1:1000 dilution of stock) was added to

the basal chambers. Tissue segments were allowed to equilibrate for 30 min in the

warmed and oxygenated buffer before addition of substrate (1:1000 dilution of stock) into

3 of the apical chambers and the 3 remaining basal chambers, so that substrate was

present in only one chamber and its appearance could be measured in the opposite

chamber. Carbogen was gently bubbled through the chambers to keep the segments

oxygenated and to agitate the buffer (see Figure 3-2).
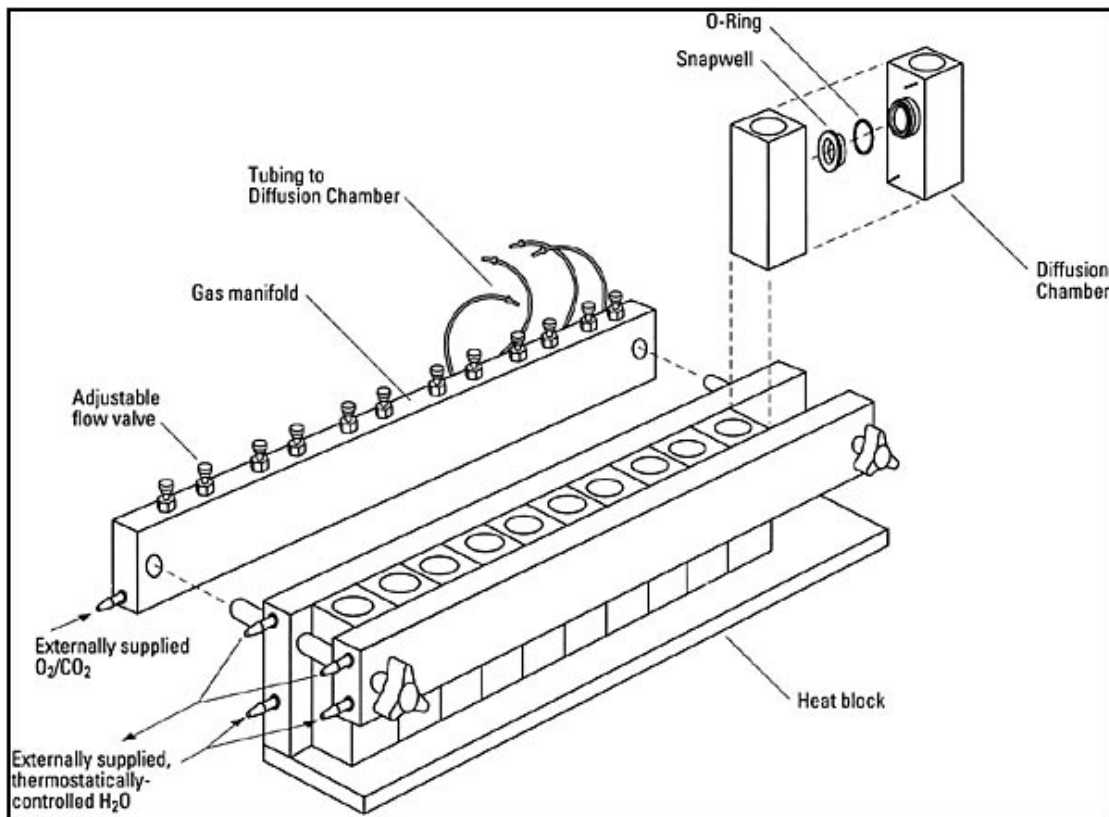
Figure 3-2 Navicyte Ussing chamber apparatus (Warner Instruments website,

www.warneronline.com).

Buffer samples (200μL) were removed from the receiver chambers at selected

timepoints and replaced with fresh buffer. At the end of the experiment, buffer was

removed from the chambers, the intestinal segments blotted dry with a paper towel and

weighed. For cold compound, intestinal segments and buffer aliquots were stored at

-80°C until analysis by LC-MS/MS. For radiolabeled compounds, the intestinal segments

were homogenized with 300μL phosphate buffered saline per 1mg of tissue and 200μL

aliquots of tissue homogenate and of buffer were placed in scintillation vials.

3.2.5 Sample Preparation

The calibration curves and samples for all drugs were prepared for HPLC-MS/MS

analysis by liquid-liquid extraction. The curve range for efavirenz was 5nM-500nM. A

2mL aliquot of methyl-t-butyl ether (MTBE) containing 1μM fluvastatin as internal

standard (IS) was added to each sample. The curve range for omeprazole was 5nM-

5000nM. A 1mL aliquot of 70:30 diethyl ether:dicholoromethane containing 1μM

lansoprazole as IS was added to each sample. The curve range for dantrolene was 25nM-

5000nM. A 2mL aliquot of MTBE containing 1μM efavirenz as IS was added to each

sample. For all drugs, samples were vortexed for 1 min then centrifuged at 3500 rpm for

10 min to separate the aqueous and organic layers. After centrifuging, the lower aqueous

layer was frozen in a methanol-dry ice bath and the top organic layer was transferred to a

clean tube. The organic layer was dried down under N_2 and drugs were reconstituted in

200μL of the appropriate mobile phase.

3.2.6 Measurement of Efavirenz

Samples were analyzed on an HPLC-MS/MS system consisting of a Shimadzu

(Shimadzu Scientific Instruments, Columbia, MD) CBM-20A BUS module, two

Shimadzu LC-20AD Prominence liquid chromatography pumps, a Shimadzu SIL-20AC

HT Prominence autosampler, and an Applied Biosystems (Foster City, CA) MDS Sciex

API4000 triple quadrupole mass spectrometer. All system components were controlled

by Applied Biosystems Analyst software version 1.4.2. An Agilent Zorbax Eclipse XDB

C18 (Agilent Technologies, Santa Clara, CA) analytical column with dimensions 150 x

4.6 mm and 5μm particle size was used at ambient temperature with an isocratic mobile

phase consisting of 0.1% formic acid in H_2O:acetonitrile (10:90; v:v) at a flow rate of 0.7mL/min. The injection volume was 100μL and the run time was 4 min. The mass spectrometer was run in multiple reaction monitoring mode with the turbospray ion source in negative ionization mode. Conditions were as follows: collision gas 7 units, ionspray voltage -4500 volts, temperature 350˚C, ion source gas 1 70 psi, ion source gas 2 30 psi, curtain gas 10 psi, declustering potential -70 volts, entrance potential -10 volts, collision energy -22 electron volts, and exit potential -13 volts. The mass transitions of 314→244.1 for efavirenz and 410.1→348.2 for fluvastatin were monitored.

3.2.7 Measurement of Omeprazole

The same HPLC-MS/MS system described above was used for the omeprazole analysis. An Agilent Zorbax Eclipse XDB C8 analytical column (Agilent Technologies, Santa Clara, CA) with dimensions 50x4.6mm and 5μM particle size was used at ambient temperature. The isocratic mobile phase consisted of 10mM acetic acid and 20mM ammonium acetate:acetonitrile:methanol (25:57:18; v:v:v) pumped at a flow rate of 0.7mL/min. The injection volume was 100μL and the run time was 5.0 min. The mass spectrometer was run in multiple reaction monitoring mode with the turbospray ion source in positive ionization mode. The mass spectrometer conditions were as follows: collision gas 7 units, ionspray voltage 5500 volts, temperature 450˚C, ion source gas 1 40 psi, ion source gas 2 40 psi, curtain gas 10 psi, declustering potential 45 volts, entrance potential 10 volts, collision energy 19 electron volts, and exit potential 48 volts. The mass transitions of 370→252 for omeprazole and 346.2→198 for lansoprazole were monitored.

3.2.8 Measurement of Dantrolene

The same HPLC-MS/MS system described above was used for the dantrolene analysis. A Waters Symmetry C18 analytical column (Waters Corp., Milford, MA) Symmetry C18 analytical column with dimensions 50 x 2.1 mm and 5μm particle size) was used at ambient temperature. The isocratic mobile phase consisted of 10mM acetic acid and 20mM ammonium acetate:acetonitrile:methanol H_2O:acetonitrile (20:80; v:v) pumped at a flow rate of 0.3mL/min. The injection volume was 25μL and the run time was 3.0 min. The mass spectrometer was run in multiple reaction monitoring mode with the turbospray ion source in negative ionization mode. The mass spectrometer conditions were as follows: collision gas 7 units, ionspray voltage -4500 volts, temperature 500˚C, ion source gas 1 50 psi, ion source gas 2 40 psi, curtain gas 10 psi, declustering potential -180 volts, entrance potential -10 volts, collision energy -20 electron volts, and exit potential -3 volts. The mass transitions of 313.2→228.1 for dantrolene and 314→244.1 for efavirenz were monitored.

3.2.9 Measurement of ^{3}H-Mitoxantrone (^{3}H-MXR)

After homogenization, 200μL of tissue homogenate and 200μL of buffer samples were transferred to scintillation vials. 5mL of Econo-Safe counting cocktail (Research Products International Corp., Mount Prospect, IL) were added and each sample was vortexed briefly before being analyzed in a Beckman LS6000 liquid scintillation counter (Beckman Coulter, Inc. Fullerton, CA). Tritium DPM were measured.

3.2.10 Data Analysis

The DPM or concentrations of drug in buffer were measured and converted to amounts. One-way ANOVA followed by Bonferroni's test for multiple comparisons or the student's t-test were used to assess statistical significance with a p-value <0.05 considered significant.

3.3 Results

3.3.1 MDCKII and MDCKII-BCRP Cell Line Confocal Microscopy

Figure 3-3 shows the expression of BCRP in the MDCKII-BCRP cell line compared to an MDCKII cell line as determined by confocal microscopy after incubating cells with the anti-BCRP antibody, BXP-21, and the fluorescent antibody, AlexaFluor488. The figure shows that the MDCKII-BCRP cell line does have appreciable BCRP expression, as evidenced by the bright areas inside the cells and on the cell borders, while the MDCKII cell line does not show as extensive fluorescence.
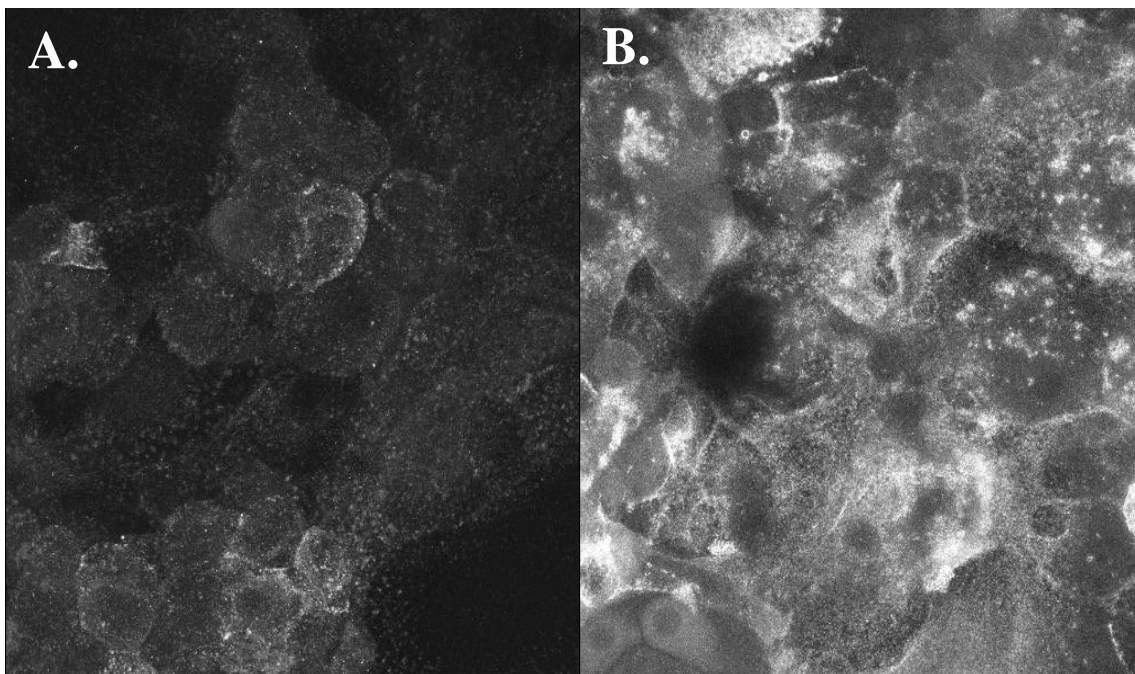
Figure 3-3 Confocal microscopy of the A) MDCKII cell line (passage number 10) and B) the MDCKII-BCRP cell line (passage number 14).

3.3.2 MDCKII, MDCKII-BCRP, and Caco2 Bidirectional Studies

Figures 3-4 and 3-5 show the effects of BCRP efflux transport inhibitors on ^{3}H-mitoxantrone (MXR) transport across the MDCKII cell line in the presence of 0.5μM Ko143 or 30μM efavirenz (Efv) compared to vehicle control (0.1% DMSO and 1% methanol) over a 90 min or 180 min timecourse at pH 7.4. The Ko143 treated group was supplemented with 1% methanol (MeOH), the Efv treated group was supplemented with 0.1% DMSO, and the control group was supplemented with 0.1% DMSO and 1% MeOH to insure all treatment groups had the same percentage of vehicle solvent (this same vehicle control scheme was used for all cell and Ussing chamber studies). Samples were taken at 30, 60, and 90 min or at 60, 120, and 180 min. Figure 3-6 and 3-7 show the effects of BCRP inhibitors on the MDCKII-BCRP cell line.
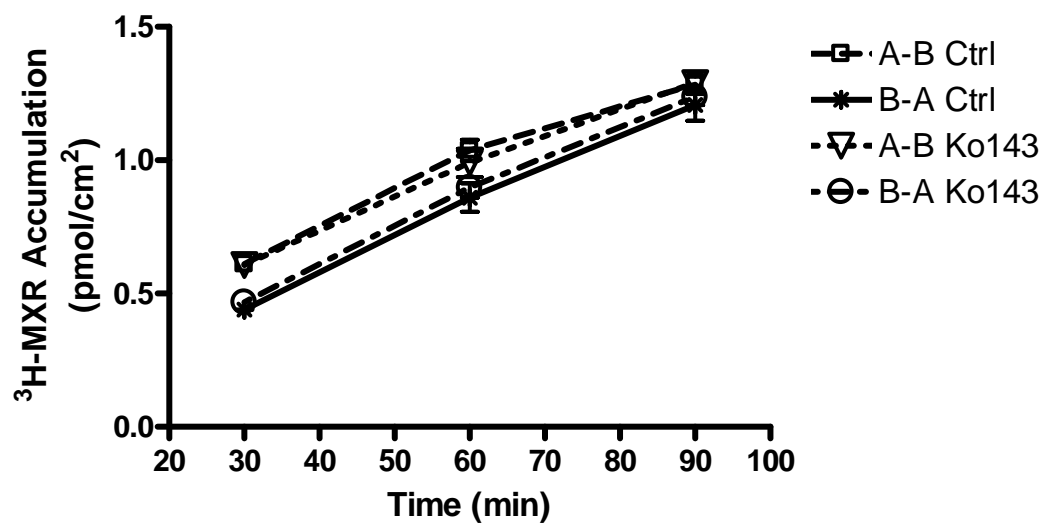
Figure 3-4 Effect of vehicle control (Ctrl, 0.1% DMSO and 1% MeOH) or 0.5μM Ko143

on transport of ^{3}H-MXR (62.5nM incubation) across MDCKII cells over 90 min at pH

7.4. Values are mean±SD, n=3 per group.
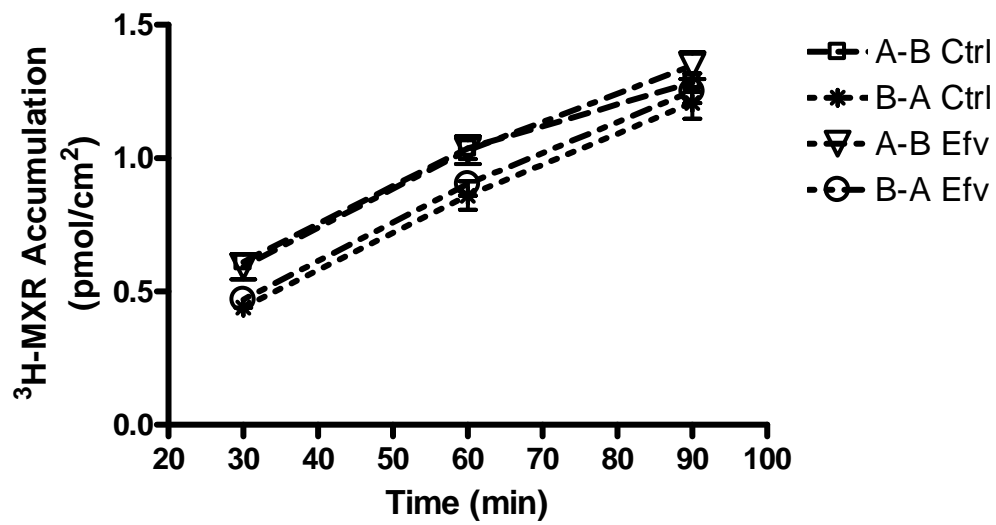
Figure 3-5 Effect of vehicle control (Ctrl, 0.1% DMSO and 1% MeOH) or 30μM Efv on

transport of ^{3}H-MXR (62.5nM incubation) across MDCKII cells over 90 min at pH 7.4.

Values are mean±SD, n=3 per group.
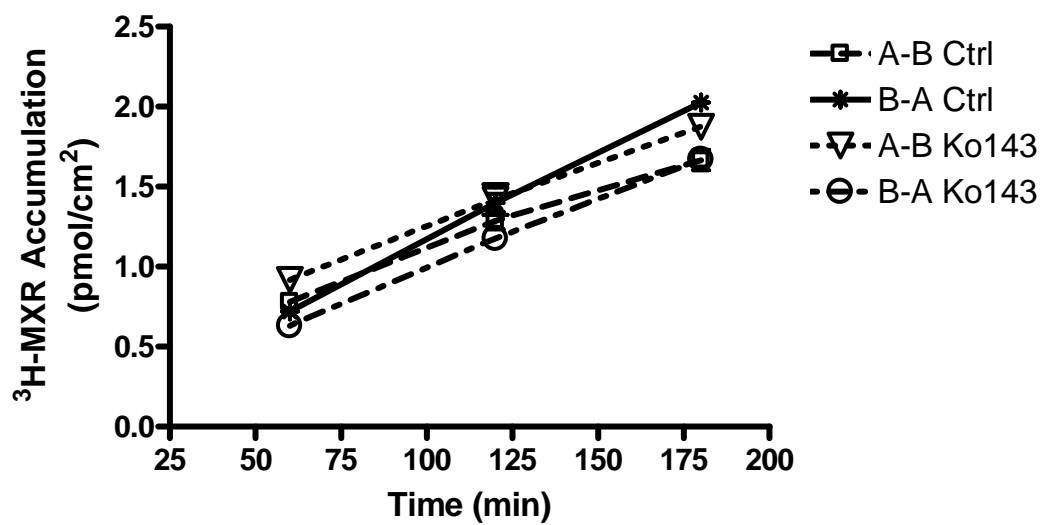
Figure 3-6 Effect of vehicle control (Ctrl, 0.1% DMSO and 1% MeOH) or 0.5μM Ko143 on transport of ^{3}H-MXR (62.5nM incubation) across MDCKII-BCRP cells over 180 min at pH 7.4. Values are mean±SD, n=3 per group.
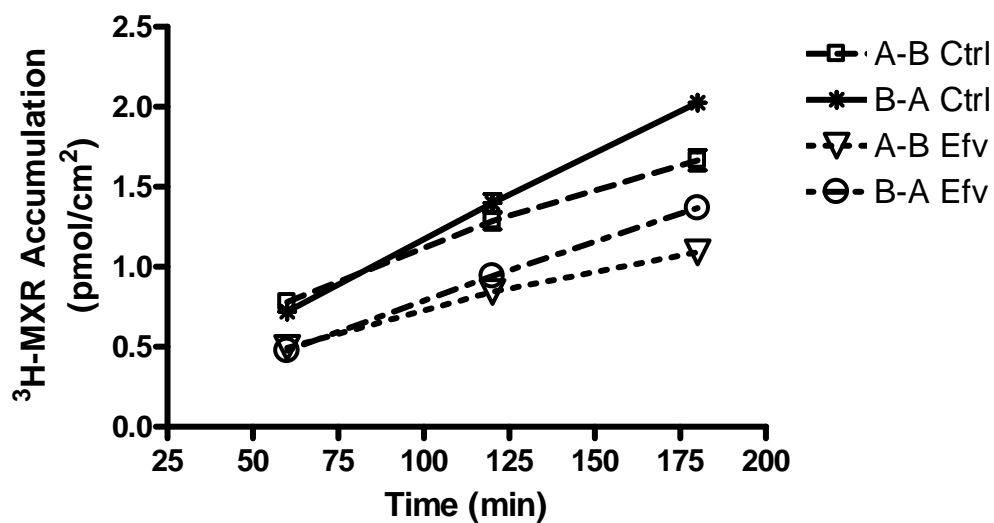
Figure 3-7 Effect of vehicle control (Ctrl, 0.1% DMSO and 1% MeOH) or 30μM Efv on

transport of ^{3}H-MXR (62.5nM incubation) across MDCKII-BCRP cells over 180 min at

pH 7.4. Values are mean±SD, n=3 per group.

Figures 3-8 and 3-9 show the effects of BCRP efflux transport inhibitors on

^{3}H-mitoxantrone (MXR) across the MDCKII cell line in the presence of 0.5μM Ko143 or

30μM efavirenz (Efv) compared to vehicle control (0.1% DMSO and 1% MeOH) over a

180 min timecourse at pH 6.5. Figure 3-10 and 3-11 show the effects of BCRP inhibitors

in the MDCKII-BCRP cell line.
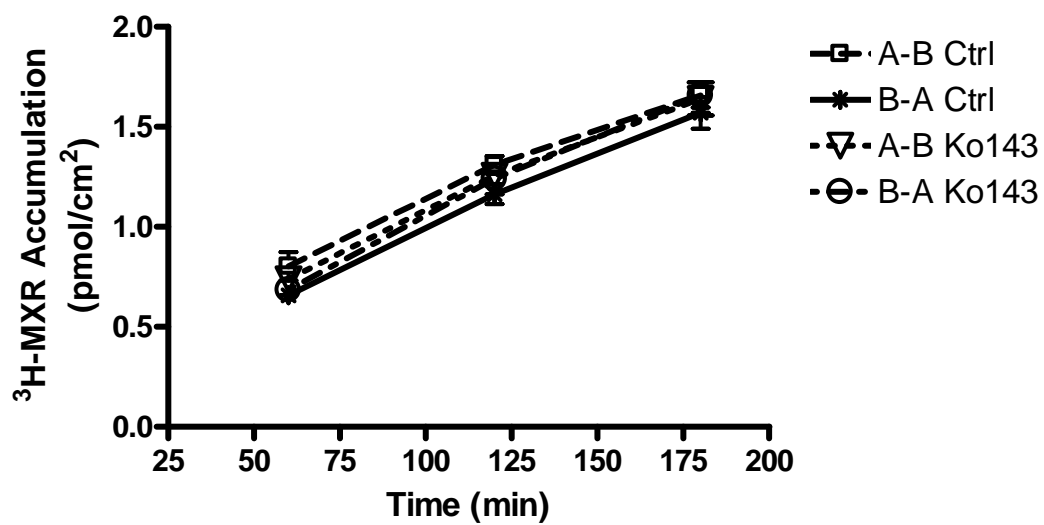
Figure 3-8 Effect of vehicle control (Ctrl, 0.1% DMSO and 1% MeOH) or 0.5µM Ko143 on transport of ^{3}H-MXR (62.5nM incubation) across MDCKII cells over 180 min at pH 6.5. Values are mean±SD, n=3 per group.
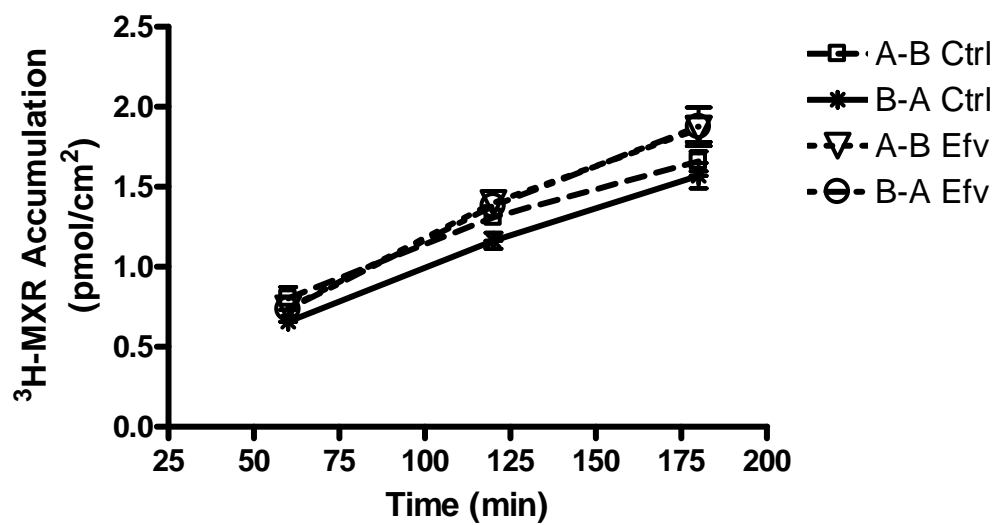
Figure 3-9 Effect of vehicle control (Ctrl, 0.1% DMSO and 1% MeOH) or 30μM Efv on

transport of ^{3}H-MXR (62.5nM incubation) across MDCKII cells over 180 min at pH 6.5.

Values are mean±SD, n=3 per group.
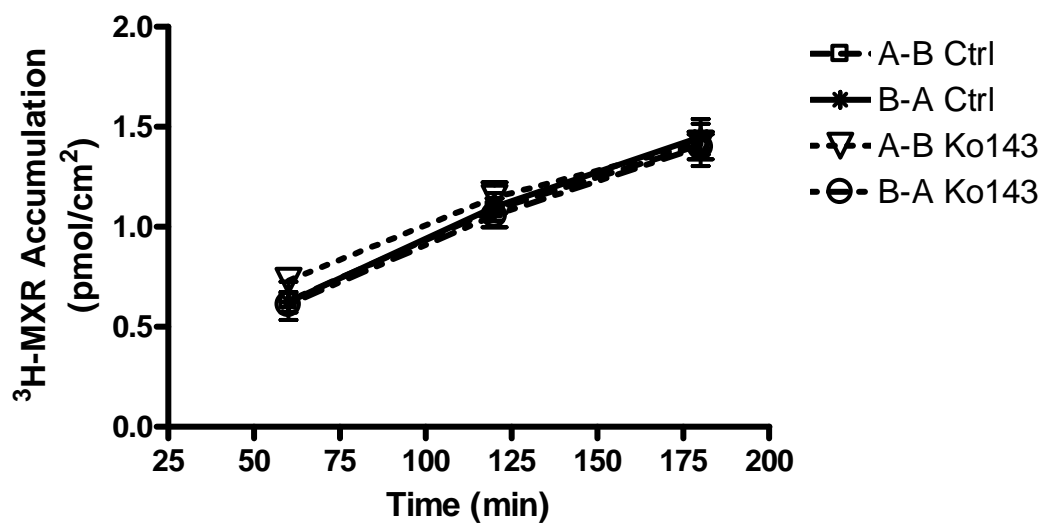
Figure 3-10 Effect of vehicle control (Ctrl, 0.1% DMSO and 1% MeOH) or 0.5µM

Ko143 on transport of ^{3}H-MXR (62.5nM incubation) across MDCKII-BCRP cells over

180 min at pH 6.5. Values are mean±SD, n=3 per group.
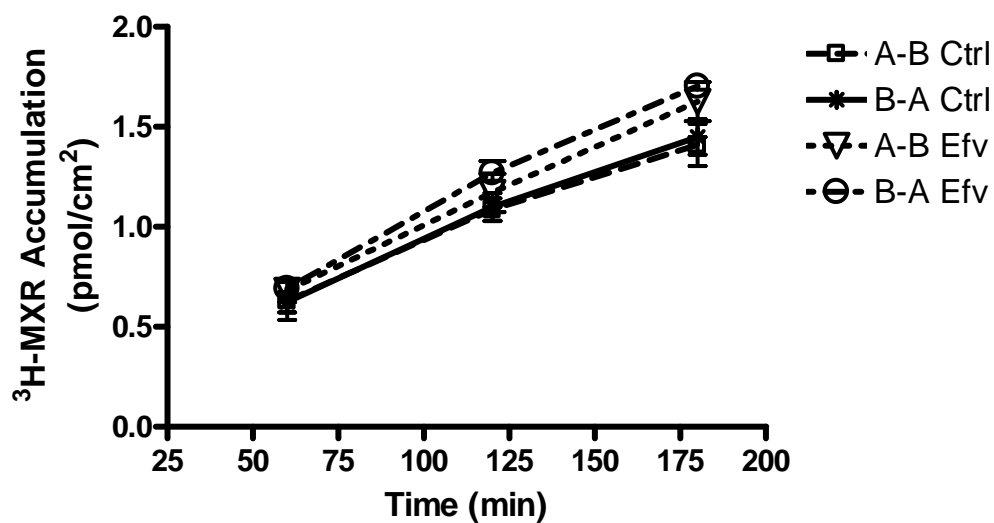
Figure 3-11 Effect of vehicle control (Ctrl, 0.1% DMSO and 1% MeOH) or 30μM Efv

on transport of ^{3}H-MXR (62.5nM incubation) across MDCKII-BCRP cells over 180 min

at pH 6.5. Values are mean±SD, n=3 per group.

Table 3-2 shows the apparent permeability (P_{app}) values in the Apical (A) to Basal

(B) direction and in the B to A direction, as well as the net flux ratios

($P_{app\ B-A}/P_{app\ A-B}$) for 62.5nM ^{3}H-mitoxantrone across MDCKII and MDCKII-BCRP cells

at both pH 7.4 and 6.5.

Cell Line and pH	Treatment	$P_{app\ A-B}$ (pmole/cm^2)	$P_{app\ B-A}$ (pmole/cm^2)	Net Flux Ratio
MDCKII pH 7.4	Control	3.01±0.19	3.39±0.32	1.13
	Ko143	3.03±0.085	3.42±0.13	1.13
	Efv	3.34±0.16	3.47±0.10	1.04
MDCKII-BCRP pH 7.4	Control	1.97±0.08	2.90±0.18	1.47
	Ko143	2.12±0.09	2.31±0.05	1.09
	Efv	2.64±0.24	3.97±0.36	1.50
MDCKII pH 6.5	Control	1.90±0.14	2.03±0.13	1.07
	Ko143	2.00±0.07	2.15±0.12	1.07
	Efv	2.49±0.12	2.54±0.14	1.02
MDCKII-BCRP pH 6.5	Control	1.73±0.14	1.83±0.08	1.06
	Ko143	1.53±0.24	1.75±0.12	1.14
	Efv	2.11±0.12	2.25±0.03	1.06

Table 3-2 Apparent permeabilities of ^{3}H-mitoxantrone (62.5nM) across MDCKII and MDCKII-BCRP cells at pH 6.5 and 7.4 in the presence of control (0.1% DMSO and 1% MeOH), 0.5μM Ko143, or 30μM Efv. Values are mean±SD, n=3 per group.

Figures 3-12 through 3-15 show the effects of BCRP efflux transport inhibitors on 10μM omeprazole transport across the MDCKII and the MDCKII-BCRP cell lines in the presence of 0.5μM Ko143 or 30μM efavirenz (Efv) compared to vehicle control (0.1% DMSO or 1% methanol) over a 180 min timecourse at pH 7.4.
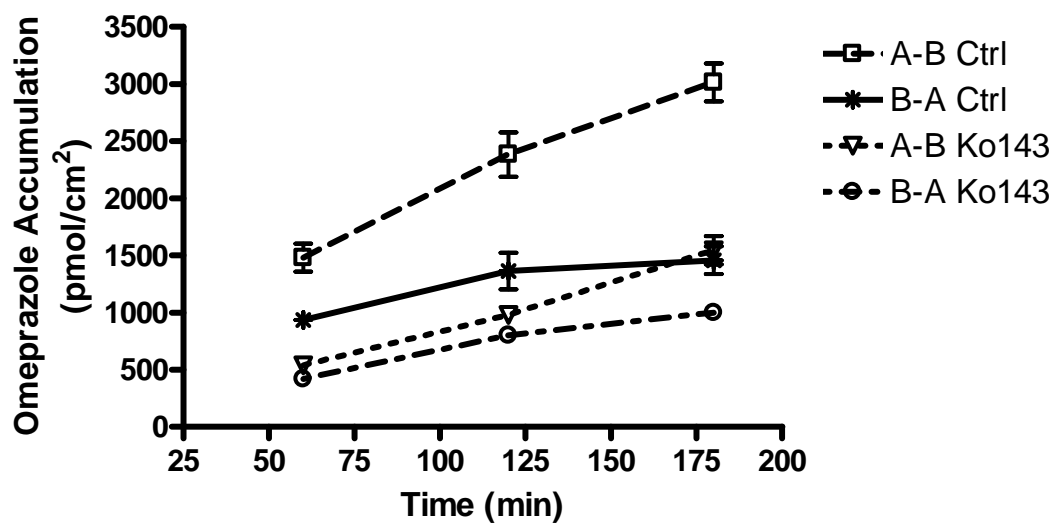
Figure 3-12 Effect of vehicle control (Ctrl, 0.1% DMSO and 1% MeOH) or 0.5μM

Ko143 on transport of omeprazole (10μM incubation) across MDCKII cells over 180 min

at pH 7.4. Values are mean±SD, n=3 per group.
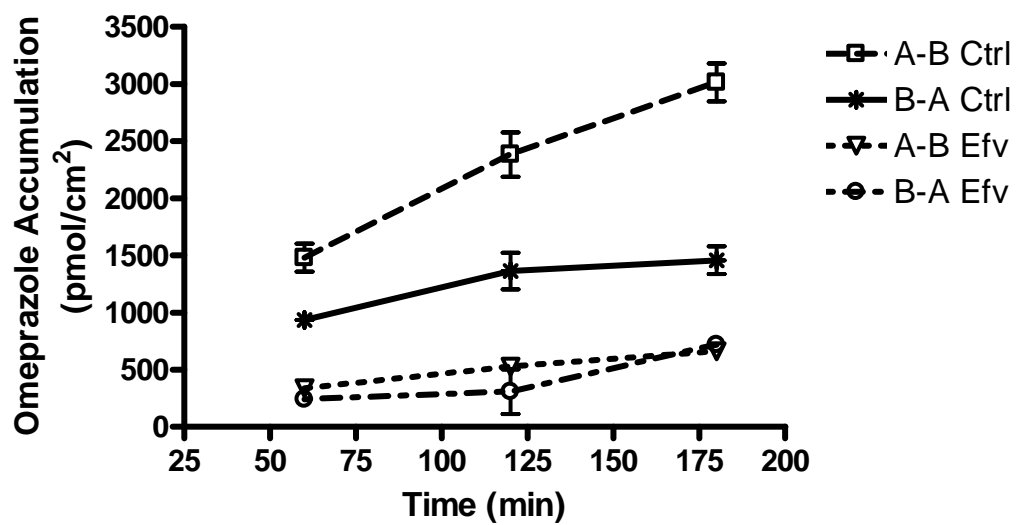
Figure 3-13 Effect of vehicle control (Ctrl, 0.1% DMSO and 1% MeOH) or 30μM Efv

on transport of omeprazole (10μM) across MDCKII cells over 180 min at pH 7.4. Values

are mean±SD, n=3 per group.
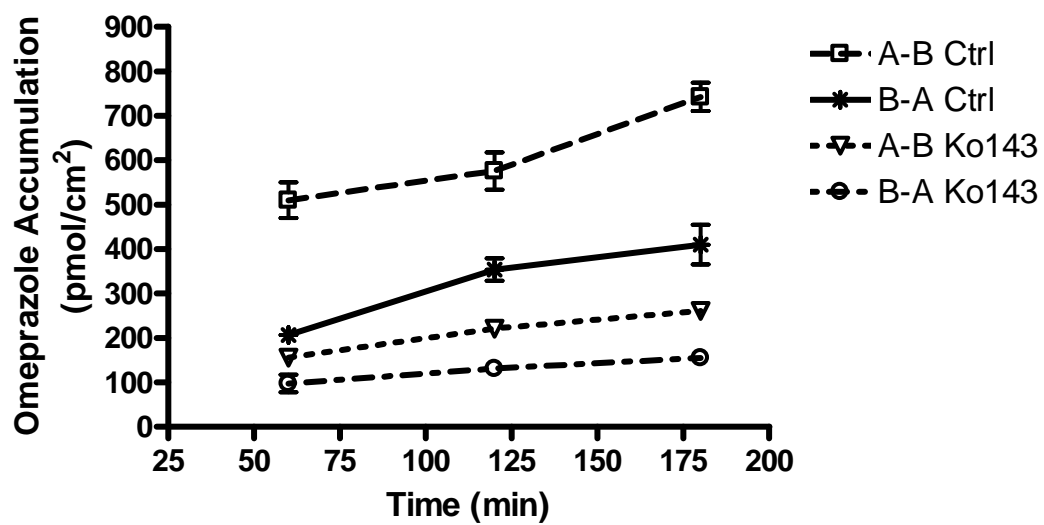
Figure 3-14 Effect of vehicle control (Ctrl, 0.1% DMSO and 1% MeOH) or 0.5μM

Ko143 on transport of omeprazole (10μM incubation) across MDCKII-BCRP cells over

180 min at pH 7.4. Values are mean±SD, n=3 per group.
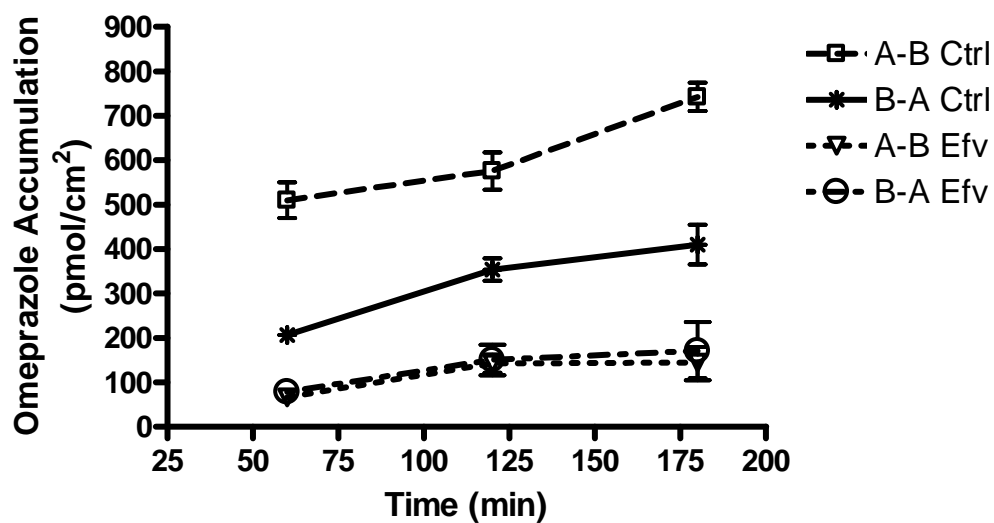
Figure 3-15 Effect of vehicle control (Ctrl, 0.1% DMSO and 1% MeOH) or 30μM Efv

on transport of omeprazole (10μM) across MDCKII-BCRP cells over 180 min at pH 7.4.

Values are mean±SD, n=3 per group.

Table 3-3 shows the P_{app} values in the A to B direction and in the B to A

direction, as well as the net flux ratios ($P_{app\ B-A}/P_{app\ A-B}$) for 10μM omeprazole across

MDCKII and MDCKII-BCRP cells at pH 7.4.

Cell Line and pH	Treatment	$P_{app\ A\text{-}B}$ (nmole/cm^2)	$P_{app\ B\text{-}A}$ (nmole/cm^2)	Net Flux Ratio
MDCKII pH 7.4	Control	21.3±1.0	7.25±0.98	0.34
	Ko143	14.0±1.4	8.07±1.4	0.58
	Efv	4.48±0.19	6.64±0.66	1.48
MDCKII-BCRP pH 7.4	Control	3.22±0.68	2.83±0.59	0.88
	Ko143	1.45±0.16	0.799±0.39	0.55
	Efv	1.08±0.59	2.00±0.19	1.85

Table 3-3 Apparent permeabilities of omeprazole (10μM) across MDCKII and MDCKII-BCRP cells at pH 7.4 in the presence of control (0.1% DMSO and 1% MeOH), 0.5μM Ko143, or 30μM Efv. Values are mean±SD, n=3 per group.

Figures 3-16 and 3-17 show the effects of BCRP efflux transport inhibitors on ^{3}H-mitoxantrone (MXR) across the Caco2 cell line in the presence of 0.5μM Ko143 or 30μM efavirenz (Efv) compared to vehicle control (0.1% DMSO and 1% MeOH) over a 90 min timecourse at pH 6.5.
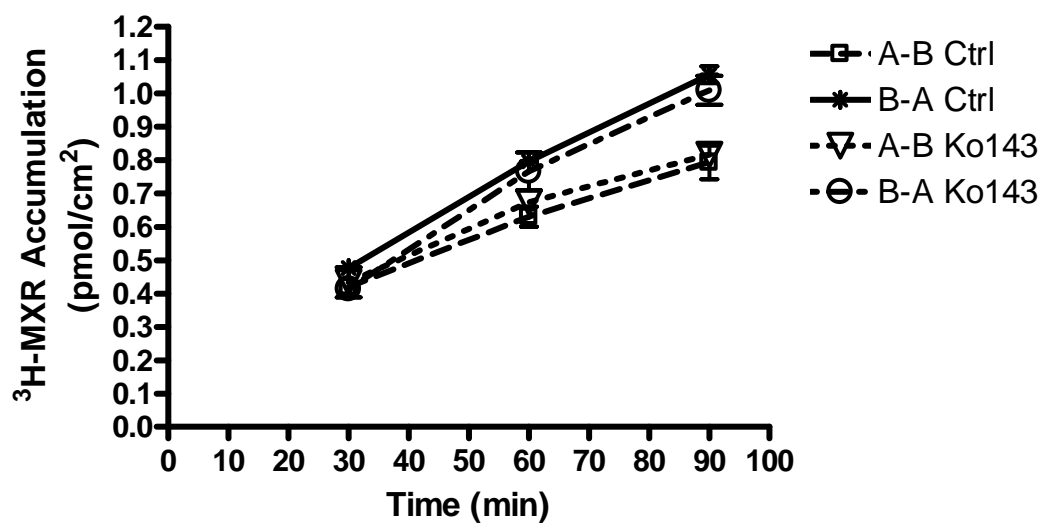
Figure 3-16 Effect of vehicle control (Ctrl, 0.1% DMSO and 1% MeOH) or 0.5μM

Ko143 on transport of ^{3}H-mitoxantrone (62.5nM) across Caco2 cells over 90 min at pH

7.4. Values are mean±SD, n=3 per group.
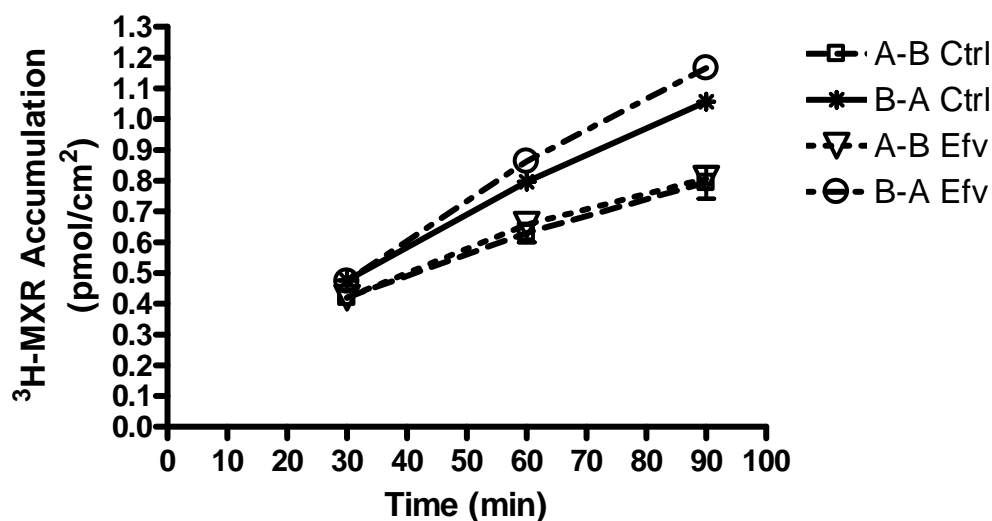
Figure 3-17 Effect of vehicle control (Ctrl, 0.1% DMSO and 1% MeOH) or 30μM Efv on transport of ^{3}H-mitoxantrone (62.5nM) across Caco2 cells over 90 min at pH 7.4. Values are mean±SD, n=3 per group.

Cell Line and pH	Treatment	$P_{app\ A-B}$ (pmole/cm^2)	$P_{app\ B-A}$ (pmole/cm^2)	Net Flux Ratio
Caco2 pH 7.4	Control	2.48±0.18	3.88±0.17	1.56
	Ko143	2.15±0.22	3.96±0.11	1.58
	Efv	2.57±0.05	4.60±0.15	1.79

Table 3-4 Apparent permeabilities of ^{3}H-mitoxantrone (62.5nM) across Caco2 cells at pH 7.4 in the presence of control (0.1% DMSO and 1% MeOH), 0.5μM Ko143, or 30μM Efv. Values are mean±SD, n=3 per group.

3.3.3 Rat Jejunum Segment Bidirectional Studies

Figures 3-18 and 3-19 show effects of Bcrp transport inhibitors, 0.5µM Ko143 or

10µM lopinavir, on bidirectional transport of ^{3}H-mitoxantrone (62.5nM) across rat

jejunum segments compared to vehicle control (0.1% DMSO and 1% MeOH).
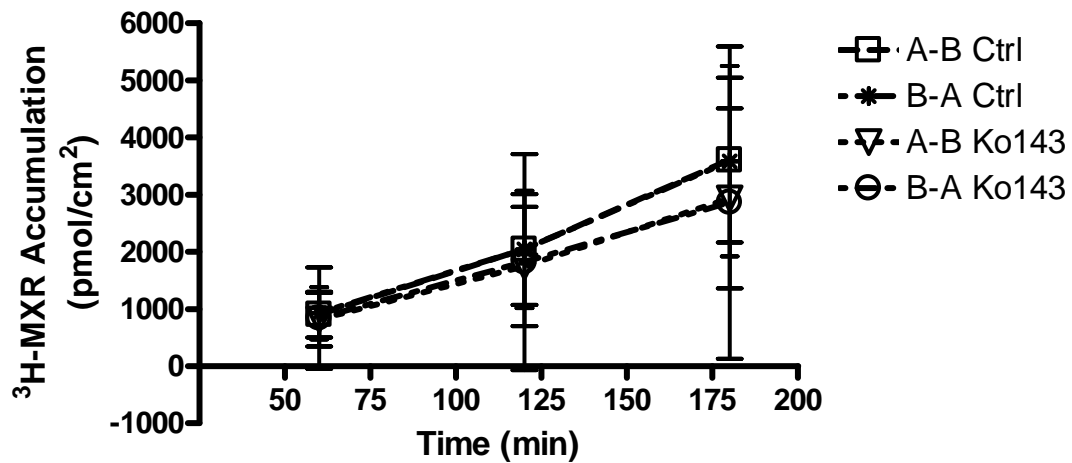
Figure 3-18 Effect of vehicle control (Ctrl, 0.1% DMSO and 1% MeOH) or 0.5µM

Ko143 on transport of ^{3}H-MXR (62.5nM incubation) across rat jejunum segments over

180 min. Values are mean±SD, n=3 per group.
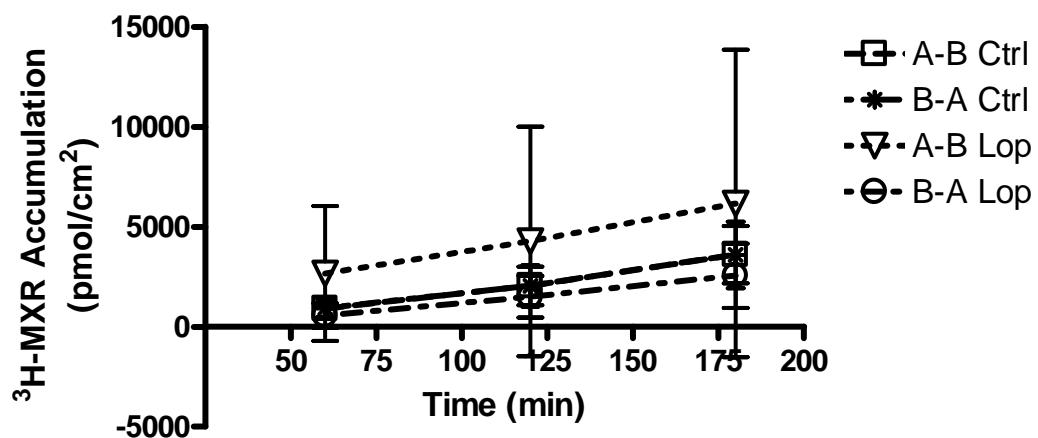
Figure 3-19 Effect of vehicle control (Ctrl, 0.1% DMSO and 1% MeOH) or 10μM lopinavir (Lop) on transport of ^{3}H-MXR (62.5nM incubation) across rat jejunum segments over 180 min. Values are mean±SD, n=3 per group.

Table 3-5 shows the P_{app} values in the A to B direction and in the B to A direction, as well as the net flux ratios ($P_{app\ B-A}/P_{app\ A-B}$) for ^{3}H-mitoxantrone (62.5nM) across rat jejunum segments.

	Treatment	$P_{app\ A\text{-}B}$ (nmole/cm^2)	$P_{app\ B\text{-}A}$ (nmole/cm^2)	Net Flux Ratio
Rat Jejunum	Control	17.2±26	19.0±29	1.10
	Ko143	10.3±15	4.82±4.9	0.47
	Lop	7.03±5.9	13.5±15	1.92

Table 3-5 Apparent permeabilities of ^{3}H-mitoxantrone (62.5nM) across rat jejunum segments in the presence of control (0.1% DMSO and 1% MeOH), 0.5μM Ko143, or 10μM Lop. Values are mean±SD, n=3 per group.

Figures 3-20 and 3-21 show effects of Bcrp transport inhibitors, 5μM FTC or 100μM pantoprazole (Pan), on dantrolene (10μM) bidirectional transport across rat jejunum segments compared to vehicle control (0.1% DMSO and 1% MeOH).
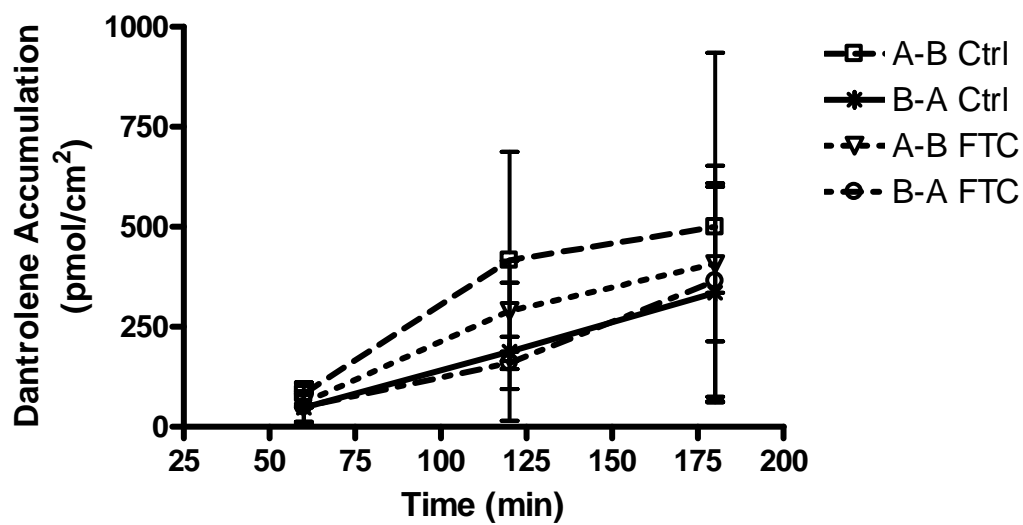
Figure 3-20 Effect of vehicle control (Ctrl, 0.1% DMSO and 1% MeOH) or 5μM FTC

on transport of dantrolene (10μM) across rat jejunum segments over 180 min. Values are
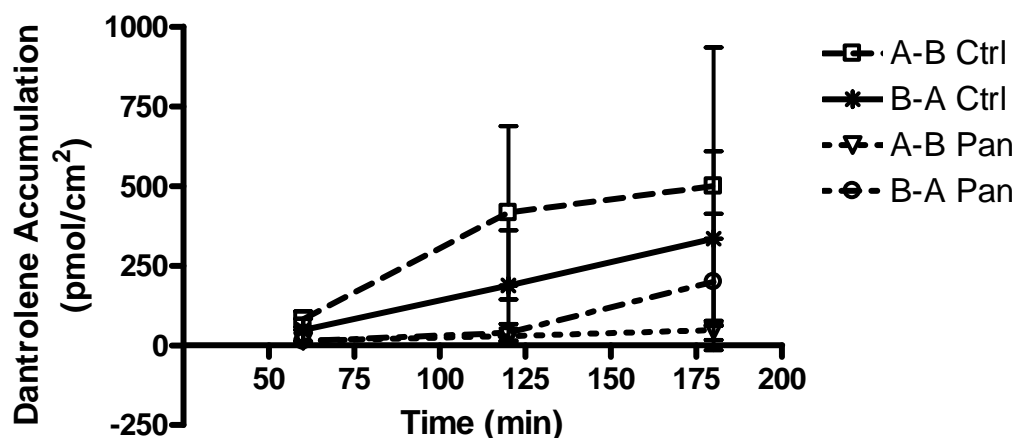
mean±SD, n=3 per group.

Figure 3-21 Effect of vehicle control (Ctrl, 0.1% DMSO and 1% MeOH) or $100\mu M$ pantoprazole (Pan) on transport of dantrolene ($10\mu M$ incubation) across rat jejunum segments over 180 min. Values are mean±SD, n=3 per group.

Table 3-6 shows the P_{app} values in the A to B direction and in the B to A direction, as well as the net flux ratios ($P_{app\ B-A}/P_{app\ A-B}$) for $10\mu M$ dantrolene across rat jejunum segments.

	Treatment	$P_{app\ A-B}$ (nmole/cm^2)	$P_{app\ B-A}$ (nmole/cm^2)	Net Flux Ratio
Rat Jejunum	Control	5.80±5.8	3.98±3.5	0.69
	FTC	4.82±2.0	4.37±3.9	0.90
	Pan	0.456±0.33	0.873±0.64	1.91

Table 3-6 Apparent permeabilities of 10μM dantrolene across rat jejunum segments in the presence of control (0.1% DMSO and 1% MeOH), 5μM FTC, or 100μM pantoprazole (Pan). Values are mean±SD, n=3 per group.

3.4 Discussion

The MDCKII-BCRP cell line showed no significant efflux for either known BCRP substrate (mitoxantrone [Solazzo et al., 2009]) or the test substrate (omeprazole). Likewise, no effects on transport by the known potent BCRP inhibitor Ko143 were seen in any of the bidirectional transport experiments. This could indicate that the cell line was not functioning properly. The confocal microscopy results indicated that BCRP was still being expressed by the cells, but its localization could not be absolutely determined, therefore it is possible that the BCRP expressed by the cell line was internalized or not properly expressed on the cell surface for transport to occur. The culturing conditions and bidirectional transport assay conditions used were as described in papers from the laboratory that provided the cells. Independent transport experiments were carried out by two other members of the laboratory to insure that the problem was not researcher-specific (data not shown). All three researchers' results agreed in that net flux ratio values (i.e. <2) did not indicate appreciable efflux of BCRP substrates. Transport of the

known substrate ^{3}H-mitoxantrone was also measured in Caco2 cells, since these cells have been shown to express BCRP (Xia et al., 2005). However, the experiment performed with the Caco2 cells did not show appreciable transport of ^{3}H-mitoxantrone either as evidenced by a low net flux ratio (<2) and no effect by Ko143. Since the Caco2 cell line is heterogeneous and transporter expression can be influenced by culture conditions, it is possible that BCRP expression was not very high in our Caco2 cell line, although this is conjecture since BCRP expression was not tested in these cells.

It is possible that the radiolabeled mitoxantrone was the issue rather than the BCRP-expressing MDCKII cell line or the Caco2 cell line. It is possible that the ^{3}H-mitoxantrone degraded, resulting in a ^{3}H-labeled entity that was not transported. Also possible is that ^{3}H-exchange occurred, resulting in the mitoxantrone losing its radiolabel. Using non-labeled compound or testing the purity of the ^{3}H-mitoxantrone by HPLC coupled to a radiometric detection method could help solve this potential problem.

Worth noting is the apparent effect efavirenz had on both ^{3}H-mitoxantrone and omeprazole transport. Efavirenz appeared to decrease both P_{appA-B} and P_{appB-A} of ^{3}H-mitoxantrone in the MDCKII-BCRP cell line at pH 7.4, but not in the control cell line or at pH 6.5, indicating that there may be differential expression of other endogenous transporters between the two cell lines. No effect of either inhibitor was seen at pH 6.5 in either the control or the BCRP-expressing cell line. Omeprazole showed very high permeability values (1000× greater than those seen for ^{3}H-mitoxantrone). P_{appA-B} was higher than P_{appB-A} in both the MDCKII and MDCKII-BCRP cell lines, which may indicate the presence of an endogenous apical uptake transporter or basal efflux transporter. In all cell lines both Ko143 and efavirenz were able to decrease the A-B and

B-A transport of omeprazole, leading to speculation that perhaps these compounds could inhibit an endogenous transporter.

Ussing chamber experiments testing known BCRP/Bcrp substrates ^{3}H-mitoxantrone and dantrolene (Enokizono et al., 2008) with rat jejunum segments were run as an alternative to the MDCKII-BCRP and the Caco2 cell lines. Rat small intestine expresses Bcrp (MacLean et al., 2008), and the Ussing chamber apparatus allowed bidirectional studies to be carried out with intestinal tissue segments. The results from all of the Ussing chamber experiments were extremely variable, which could be due to experimental technique or to other transporters either masking the effect of Bcrp inhibition or compensating for decreased Bcrp-mediated transport. Differential expression of Bcrp is seen along the rat intestinal tract and MacLean and colleagues (2008) determined high intra- and inter-variability in efflux transporter expression, even in adjacent 3cm segments (2008). The experiments described above used 3cm segments from the proximal jejunum, but MacLean et al. (2008) showed higher Bcrp expression levels in the distal jejunum and the ileum. Also, how much the segments are handled in their isolation and mounting in the chamber could affect membrane integrity or function. While care was taken to handle the segments as little as possible and mount them as quickly as possible, the effects of handling and of time exposed to open air could possibly have led to variation. One experiment was carried out with ^{14}C-mannitol used as a marker of membrane integrity to insure that the intestinal segments were viable over the entire timecourse of the transport experiments (integrity from hour 3 to hour 4 was tested after a 3 hour transport experiment), but these were not done at the end of every experiment, so breakdown of the segments over time cannot be entirely ruled out.

3.5 Conclusions

Little can be drawn from the results of these experiments, other than reiteration of the importance of testing an experimental system thoroughly when results are not what was expected and of having alternative systems in which to investigate hypotheses. Other laboratories have had more success with transfected cell lines and with knock-out mouse models to investigate the importance of BCRP/Bcrp in drug absorption and disposition.

3.6 References

Aungst, B.J. (1999). "P-glycoprotein, secretory transport, and other barriers to the oral delivery of anti-HIV drugs." Adv. Drug Deliv. Rev. **39:** 105–116.

Benet, L.Z., Cummins, C.L., and Wu, C.Y. (2004). "Unmasking the dynamic interplay between efflux transporters and metabolic enzymes." Int. J. Pharm. **277**: 3–9.

Busti, A.J., Bain, A.M., Hall II, R.G., Bedimo, R.G., Leff, R.D., Meek, C., and Mehvar, R. (2008). "Effects of atazanavir/ritonavir or fosamprenavir/ritonavir on the pharmacokinetics of rosuvastatin." J. Cardiovasc. Pharmacol. **51**(6): 605-610.

Enokizono, J., Kusuhara, H., Ose, A., Schinkel, A.H., and Sugiyama, Y. (2008). "Quantitative investigation of the role of breast cancer resistance protein (Bcrp/*Abcg2*) in limiting brain and testis penetration of xenobiotic compounds." Drug Metab. Dispos. **36**:995-1002.

Feinshtein, V., Holcberg, G., Amash, A., Erez, N., Rubin, M., Sheiner, E., Polachek, H., and Ben-Zvi, Z. (2009). "Nitrofurantoin transport by placental choriocarcinoma JAr cells: involvement of BCRP, OATP2B1 and other MDR transporters." Arch. Gynecol. Obstet. [Epub ahead of print].

MacLean, C., Moenning, U., Reichel, A., and Fricker, G. (2008). "Closing the gaps: full scan of the intestinal expression of p-glycoprotein, breast cancer resistance protein, and multidrug resistance-associated protein 2 in male and female rats." Drug Metab. Dispos. **36**:1249–1254.

Merino, G., Jonker, J.W., Wagenaar, E., van Herwaarden, A.E., and Schinkel, A.H. (2005). "The breast cancer resistance protein (BCRP/ABCG2) affects pharmacokinetics, hepatobiliary excretion, and milk secretion of the antibiotic nitrofurantoin." Mol. Pharmacol. **67**(5): 1758-1764.

Polli, J.W., Baughman, T.M., Humphreys, J.E., Jordan, H.H., Mote, A.L., Webster, L.O., Barnaby, R.J., Vitulli, G., Bertolotti, L., Read, K.D., and Serabjit-Singh, C.J. (2004). "The systemic exposure of an *n*-methyl-d-aspartate receptor antagonist is limited in mice by the p-glycoprotein and breast cancer resistance protein efflux transporters." Drug Metab. Dispos. **32**(7): 722-726.

Solazzo, M., Fantappie`, O., D'Amico, M., Sassoli, C., Tani, A., Cipriani,G., Bogani, C., Formigli, L., and Mazzanti, R. (2009). "Mitochondrial expression and functional activity of breast cancer resistance protein in different multiple drug-resistant cell lines." Cancer Res. **69**(18): 7235-7242.

Storch, C.H., Theile, D., Lindenmaier, H., Haefeli, W.E., and Weiss, J. (2007). "Comparison of the inhibitory activity of anti-HIV drugs on P-glycoprotein." Biochem. Pharmacol. **73**: 1573–1581.

Weiss, J., Rose, J., Storch, C.H., Ketabi-Kiyanvash, N., Sauer, A., Haefeli, W.E. and
    Efferth, T. (2007). "Modulation of human BCRP (ABCG2) activity by anti-HIV
    drugs." J. Antimicrob. Chemother. **59**: 238–245.

Xia, C.Q., Liu, N., Yang, D., Miwa, G., and Gan, L.S. (2005). "Expression,
    localization, and functional characteristics of breast cancer resistance protein in
    Caco-2 cells." Drug Metab. Dispos. **33**:637–643.

CHAPTER 4

Examining Hepatic Uptake of Wafarin and Phenytoin *in vitro*

4.1 Introduction

Narrow therapeutic index drugs can be particularly susceptible to drug-drug interactions through inhibition or induction of drug metabolizing enzymes or transporters. Overshooting the therapeutic range can lead to toxicity due to high plasma concentrations, while failing to reach therapeutic plasma levels can lead to treatment failure. Warfarin and phenytoin are both narrow therapeutic index drugs, with warfarin's therapeutic range typically reported as 2-3.5 international normalized ratio (INR) of prothrombin time (Kuruvilla and Gurk-Turner, 2001) and phenytoin's therapeutic range considered to be 10-20 mg/L total (free plus protein bound) phenytoin in serum (Banh et al., 2002). Warfarin is one of the most extensively prescribed anti-coagulants despite its narrow therapeutic index. It works through inhibition of the vitamin K_1 2,3-epoxide reductase (VKORC1) enzyme complex that prevents the activation of clotting factors II, V, IX and X and proteins C, S, and Z (Bristol-Myers Squibb Co. package insert). Subtherapeutic levels of warfarin can lead to continuing risk of thrombosis, while supratherapeutic levels increase the risk of hemorrhage. Phenytoin is an older generation anti-epileptic drug still in common use today that is postulated to work by promoting neuronal sodium efflux (Pfizer package insert). Low levels of phenytoin can lead to incomplete control of seizures, while some of the more serious side effects for plasma levels above the therapeutic range include respiratory and circulatory depression and coma (Pfizer package insert).

Warfarin and phenytoin both display high interpatient variability, some of which can be accounted for by covariates including age, gender, body size, diet, ethnicity (Wu et al., 2008) and for phenytoin, protein binding (Banh, 2002). Recent studies have also shown the importance of polymorphic enzymes in explaining high patient variability. Cytochrome P450 2C9 (CYP2C9) is the major enzyme responsible for metabolizing the more potent S-warfarin isomer and phenytoin, making it an important determining factor for the pharmacokinetics and pharmacodynamics of both drugs. CYP2C9 metabolizes S-warfarin to the 6- and 7-hydroxywarfarin forms while the less potent R-warfarin is metabolized by CYP1A1, 1A2, and 3A4 to the 6-, 8-, and 10-hydroxywarfarin metabolites (Zhou et al., 2009). The major metabolic conversion of phenytoin is to S-5-(4p-hydroxyphenyl)-5-phenylhydantoin by CYP2C9 (Zhou, et al, 2009). CYP2C9 is highly polymorphic, having 33 known variants, some showing decreased activity (Zhou et al., 2009) that have been clinically shown to affect warfarin and phenytoin pharmacokinetics. For example, Gage et al. (2008) observed that CYP2C9*2 and *3 alleles were associated with lower warfarin loading and maintenance doses in addition to higher incidence of bleeding complications, while Takahashi and Echizen (2001) showed that CYP2C9*3 homozygous subjects had 90% lower S-warfarin elimination than wildtype homozygous subjects. Phenytoin area under the curve (AUC) values were higher in healthy subjects having CYP2C9*2 or *3 variants than in subjects homozygous for CYP2C9*1 wildtype (Caraco et al., 2001). In addition to CYP2C9, polymorphisms in VKORC1, such as the promoter variant 3673 G>A, have been shown to be associated with warfarin resistance and an increase in warfarin dose requirements as summarized by Wadelius et al. (2007). Although these two genes have helped account for considerable

variability in warfarin and phenytoin dosing and response, variability is still not entirely explained. Nearly 33% of the interindividual variability for warfarin dosing remains to be explained even after these genetic factors are combined with other covariates (Zhou et al., 2009). In addition to CYP2C9, studies into the effect of MDR1 and CYP2C19 genotypes on phenytoin variability have indicated that while these may help explain an appreciable amount, there remain other factor as yet unknown (Kerb et al., 2001). Therefore, continuing to examine other pathways that could affect warfarin and phenytoin exposure is a worthwhile pursuit in order to improve the safety and efficacy of these drugs in a patient population.

Warfarin and phenytoin are both Biopharmaceutics Drug Disposition Classification System (BDDCS) Class 2 compounds, meaning that they have low solubility and high permeability. Based on these properties, we predict that uptake transporters in the intestinal lumen will have little influence on their pharmacokinetic behavior, but as yet do not know if hepatic uptake transporters will have any influence (Wu and Benet, 2005). Based upon the results seen by Lau et al. for atorvastatin (2007) and by Zheng et al. for glyburide (2009), both of which are also BDDCS Class 2 compounds, it is conceivable that warfarin and phenytoin may also be substrates for hepatic uptake transporters. The results of Lau et al. (2007) demonstrated the substantial effect that hepatic uptake can have on the pharmacokinetics of a BDDCS Class 2 compound. The uptake of atorvastatin by OATP1B1 became the rate limiting step in its metabolism and elimination, as evidenced by the decreased clearance in the presence of the OATP inhibitor rifampin. The results of Zheng et al. (2009) clearly demonstrated the influence of hepatic uptake on the pharmacodynamics of the BDDCS Class 2 compound

glyburide. Glucose levels were significantly decreased in response to inhibition of glyburide hepatic uptake by rifampin treatment, which increased plasma glyburide levels and hence exposure of pancreatic islet cells to glyburide. Several studies also exist showing the effect of hepatic uptake transporter polymorphisms on drug response. Couvert et al. (2008) showed that the OATP1B1 variant 463C>A, possibly an increased function variant, was significantly associated with increased lowering of LDL and total cholesterol upon fluvastatin treatment in a Caucasian patient population. Genetic variants in the organic cation transporter 1 (OCT1), a hepatic uptake transporter, were shown to alter metformin efficacy, with healthy subjects carrying variant alleles showing higher glucose levels than subjects with wildtype OCT1 (Shu et al., 2007). If warfarin or phenytoin is a substrate for hepatic uptake transporters that have altered function polymorphisms, this could help to explain interindividual variability and could be incorporated into dosing algorithms to improve initial dosing regimens.

In the present study, we sought to determine if warfarin or phenytoin utilize hepatic uptake transporters *in vitro*. Identification of such transporters may help guide future pharmacogenomic studies to investigate interindividual variability.

4.2 Materials and Methods

4.2.1 Chemicals and Materials

^{3}H-estrone sulfate was purchased from Perkin Elmer (Waltham, MA). Racemic warfarin, rifampin, cimetidine, phenytoin, and nimodipine were purchased from Sigma-Aldrich (St. Louis, MO). Cryopreserved human hepatocytes were purchased from CellzDirect™ (Durham, NC). Human embryonic kidney cells (HEK293) overexpressing

OATP1 B1 or OATP2B1 along with the empty vector HEK293-pCI-NEO cell line were kind gifts from Dr. Hideaki Okochi (University of California at San Francisco, CA). All cell culture media were obtained from the UCSF Cell Culture Facility (San Francisco, CA). Non-coated 6-well cell culture plates were purchased from Corning Life Sciences (Acton, MA). Poly-D-lysine coated 6-well and 12-well cell culture plates, as well as 0.4um low density polyethylene terephthalate (PET) transwell inserts were purchased from BD Bioscience (Bedford, MA).

4.2.2. Isolation of Rat Hepatocytes and Use of Cryopreserved Human Hepatocytes

Male Sprague-Dawley rats (250-300g, Charles River Laboratories, Wilmington, MA) were anesthetized via peritoneal injection of 1mL/kg ketamine:xylazine (80mg/mL: 12mg/mL) prior to portal vein cannulation. The liver was perfused with oxygenated liver perfusion buffer (Krebs-Henesleit [KH] buffer containing 10mM D-glucose, 2mM L-glutamine, and 1% bovine serum albumin) for 5 min at 30mL/min, followed by perfusion with hepatocyte wash buffer (KH buffer containing 10mM HEPES, 2mM L-glutamine) supplemented with 1.2 U/mL collagenase for 5 min at 20mL/min to digest the liver. The liver was excised and digestion completed. Hepatocytes were isolated by passing the liver digest through an 80μm nylon mesh. Hepatocytes were washed twice with ice-cold hepatocyte wash buffer not containing collagenase. The trypan blue exclusion method was used to assess cell viability and cells with viability greater than 90% were used for uptake studies. Hepatocytes were suspended in oxygenated hepatocyte wash buffer with 1% bovine serum albumin in place of collagenase buffer to yield a concentration of 1 million cells/mL.

Cryopreserved human hepatocytes pooled from 5 female and 5 male donors from CellzDirect™ were used according to the provider's instructions. In brief, hepatocytes were thawed quickly in a 37°C water bath and washed twice with ice-cold hepatocyte wash buffer to remove cryopreservation solution. Cells were suspended in oxygenated hepatocyte wash buffer to yield a concentration of 0.5 million cells/mL.

4.2.3 Hepatocyte Uptake Studies

Prior to incubation with substrate, hepatocytes suspended in hepatocyte wash buffer, pH 7.4, were pre-warmed in a 37°C water bath for 5 min. During this 5 min pre-incubation period, DMSO vehicle control, 100μM rifampin, or 100μM probenecid was added to the hepatocytes. After hepatocytes were warmed, uptake was initiated by addition of 1μM warfarin, 1μM phenytoin, or 4.3nM ^{3}H-estrone sulfate, which was used as a positive control. After 2 min of uptake, the reaction was terminated by removing a 0.5mL aliquot and transferring to a tube containing 700μL of silicone:mineral (83.3:16.7 v/v) oil mixture for warfarin and phenytoin or to a tube containing 150μL of 2N sodium hydroxide under a 500μL layer of the oil mixture in the case of ^{3}H-estrone sulfate. The hepatocytes were centrifuged for 10 sec at 13,000g to isolate the hepatocyte pellets. The oil mixture was removed and the pellets were lysed by sonication in the presence of 200μL H_2O in the case of warfarin and phenytoin or by overnight incubation at 65°C in 2N NaOH in the case of ^{3}H-estrone sulfate.

4.2.4 HEK293 Cell Culture and Uptake Studies

HEK293-OATP1B1, HEK293-OATP2B1, and HEK293-pCI-NEO cells were cultured in Dulbelcco's Modified Eagle Medium with 100 U/mL penicillin/streptomycin

and 0.5 mg/mL Geneticin® at 37˚C in 5% CO_2 atmosphere with 95% humidity. Cells were cultured in T-75 flasks and when ~90% confluent were trypsinized and plated in 6-well or 12-well poly-D-lysine coated plates. Cells were allowed to grow to confluence for ~48 to 72 hours. Prior to uptake studies, cells were washed for 5 min at 37˚C with Hanks Buffered Salt Solution (HBSS) at pH 7.4. Uptake studies were initiated by replacing wash buffer with HBSS containing 1μM warfarin, 1μM phenytoin, or 4.3nM ^{3}H-estrone sulfate with and without 100μM rifampin. After 2 min, the reaction was terminated by removing the incubation buffer and washing the cells three times with ice cold phosphate buffered saline (PBS). Cells were allowed to dry and then were collected by manually scraping the cells from the plate and suspending in 200μL or 400μL of H_2O for 12-well and 6-well plates, respectively. In the case of warfarin and phenytoin, samples were spun down at 13,000g for 10 min to isolate the cell pellet, then sonicated to lyse the cells prior to preparation for LC-MS/MS analysis. For ^{3}H-estrone sulfate, the entire 400μL aliquot was transferred to a scintillation vial for analysis by scintillation counting after the NaOH was neutralized with 1N hydrochloric acid.

4.2.5 Sample Preparation

The calibration curve and samples were prepared for HPLC-MS/MS analysis by liquid-liquid extraction. The curve range for warfarin and for phenytoin was 5nM-1000nM. A 500μL aliquot of methyl-t-butyl ether containing either 0.5μM cimetidine (warfarin internal standard) or 0.5μM nimodipine (phenytoin internal standard) was added to each sample. Samples were vortexed for 1 min then centrifuged at 13,000g for 10 min to separate the aqueous and organic layers. After centrifuging, the lower aqueous

layer was frozen in a methanol-dry ice bath and the top organic layer was transferred to a clean tube. The organic layer was dried down under N_2 and drugs were reconstituted in 200μL of the appropriate mobile phase.

4.2.6 Measurement of Racemic Warfarin

Samples were analyzed on an HPLC-MS/MS system consisting of a Shimadzu (Shimadzu Scientific Instruments, Columbia, MD) CBM-20A BUS module, two Shimadzu LC-20AD Prominence liquid chromatography pumps, a Shimadzu SIL-20AC HT Prominence autosampler, and an Applied Biosystems (Foster City, CA) MDS Sciex API4000 triple quadrupole mass spectrometer. All system components were controlled by Applied Biosystems Analyst software version 1.4.2. A Waters (Waters Corp., Milford, MA) Symmetry C18 analytical column with dimensions 50 x 2.1 mm and 5μm particle size was used at ambient temperature with an isocratic mobile phase consisting of 10mM ammonium acetate at pH 4.6:acetonitrile (10:90; v:v) at a flow rate of 0.3mL/min. The injection volume was 10μL and the run time was 3 min. The mass spectrometer was run in multiple reaction monitoring mode with the turbospray ion source in positive ionization mode. Conditions were as follows: collision gas 6 units, ionspray voltage 4500 volts, temperature 350°C, ion source gas 1 30 psi, ion source gas 2 20 psi, curtain gas 10 psi, declustering potential 50 volts, entrance potential 10 volts, collision energy 30 electron volts, and exit potential 8 volts. The mass transitions of 309.2→251.10 for warfarin and 253.1→95.1 for cimetidine were monitored.

4.2.7 Measurement of Phenytoin

The same HPLC-MS/MS system and analytical column described above was used for the warfarin analysis. The isocratic mobile phase consisted of methanol:1% acetic acid (80:20; v:v) pumped at a flow rate of 0.3mL/min. The injection volume was 25µL and the run time was 3.0 min. The mass spectrometer conditions were as follows: collision gas 12 units, ionspray voltage 5000 volts, temperature 500˚C, ion source gas 1 20 psi, ion source gas 2 40 psi, curtain gas 20 psi, declustering potential 16 volts, entrance potential 7 volts, collision energy 37 electron volts, and exit potential 15 volts. The mass transitions of 253.0→182.0 for phenytoin and 419.5→343.1 for nimodipine were monitored.

4.2.8 Measurement of ^{3}H-Estrone Sulfate

Once cell samples were transferred to scintillation vials, 5mL of Econo-Safe counting cocktail (Research Products International Corp., Mount Prospect, IL) were added and each sample was vortexed briefly before being analyzed in a Beckman LS6000 liquid scintillation counter (Beckman Coulter, Inc. Fullerton, CA). Tritium DPM were measured.

4.2.9 Data Analysis

The DPM or the concentration of drug per million hepatocytes or per mg of protein for HEK293 cell samples was calculated. One-way ANOVA followed by Bonferroni's test for multiple comparisons or the student's t-test were used to assess statistical significance with a p-value <0.05 considered significant.

4.3 Results

4.3.1 Warfarin Hepatic Uptake

Figure 4-1 displays that rat hepatocytes treated with 10μM warfarin showed significant 23% inhibition of warfarin uptake by 100μM rifampin ($p < 0.05$) but not by 100μM probenecid compared to control (0.1% DMSO and 1% methanol [MeOH]).
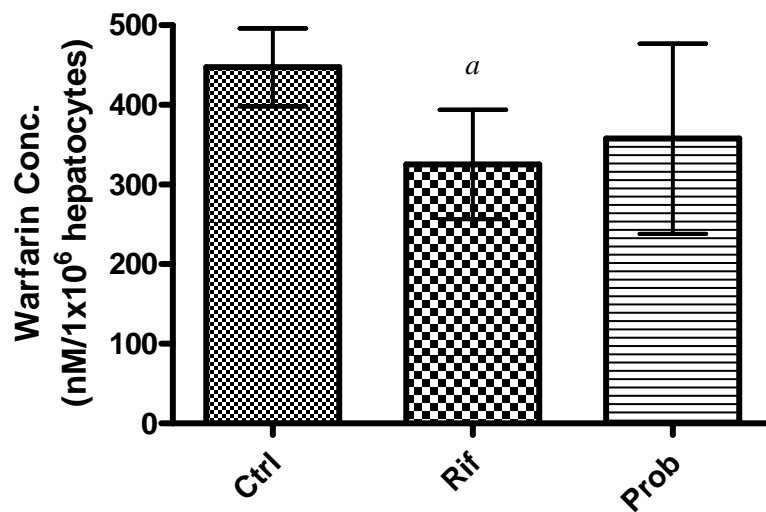
Figure 4-1 Warfarin 2 min uptake in rat hepatocytes with control (0.1% DMSO and 1% MeOH), 100μM rifampin, or 100μM probenecid treatment (5 min pre-incubation).

[a] $p < 0.05$ compared to control. Values are mean±SD, n=9 per group.

Figure 4-2 shows that in human hepatocytes, both 100μM rifampin and 100μM probenecid significantly inhibited the uptake of 1μM warfarin by 34% and 22%, respectively, compared to control (0.1% DMSO and 1% MeOH).
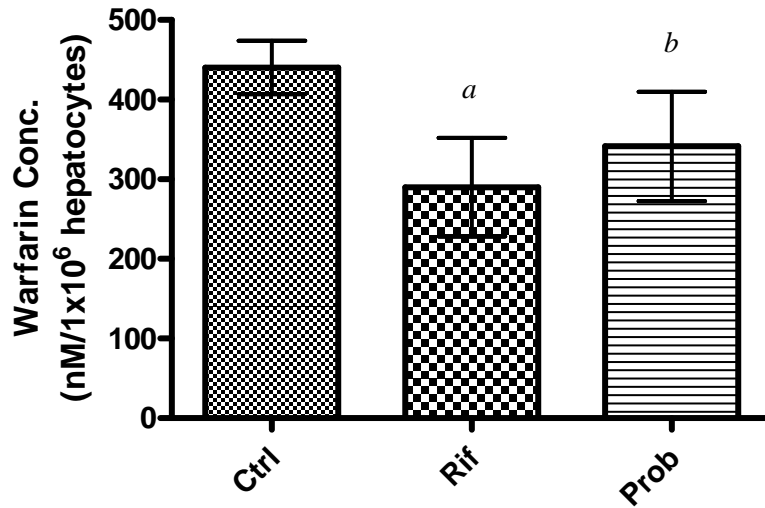
Figure 4-2 Warfarin 2 min uptake in human hepatocytes with control (0.1% DMSO and 1% MeOH), 100μM rifampin, or 100μM probenecid treatment (5 min pre-incubation). ^{a} p<0.001, ^{b} p<0.05 compared to DMSO control. Values are mean±SD, n=6 per group.

4.3.2 Warfarin HEK293 Cellular Uptake

Figures 4-3 and 4-4 show that 100μM rifampin had no inhibitory effect on 1μM warfarin uptake in HEK293 cells overexpressing OATP1B1 or OATP2B1 compared to vehicle control (0.1% DMSO).
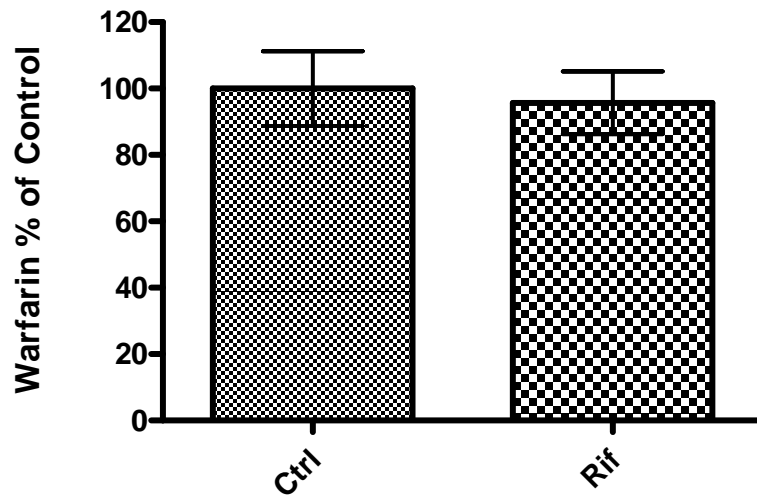
Figure 4-3 Warfarin 2 min uptake in HEK293-OATP1B1cells with 0.1% DMSO control (61.7nM±33) or 100μM rifampin treatment. Values are mean±SD, n=8 per group.
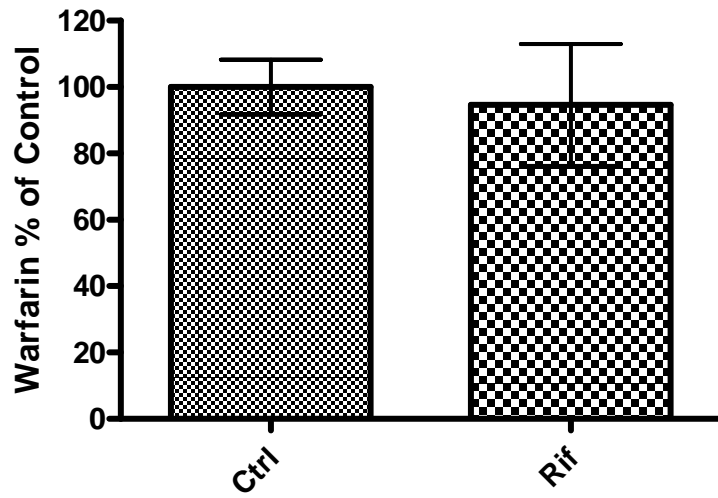
Figure 4-4 Warfarin 2 min uptake in HEK293-OATP2B1 cells with 0.1% DMSO control

(60.0±41nM) or 100μM rifampin treatment. Values are mean±SD, n=8 per group.

Figure 4-5 shows warfarin uptake in the vector control cell line, HEK293-pCI-NEO. The 100μM rifampin treated group showed a slight, but significant decrease in uptake compared to the 0.1% DMSO vehicle control group (26%, p<0.01).
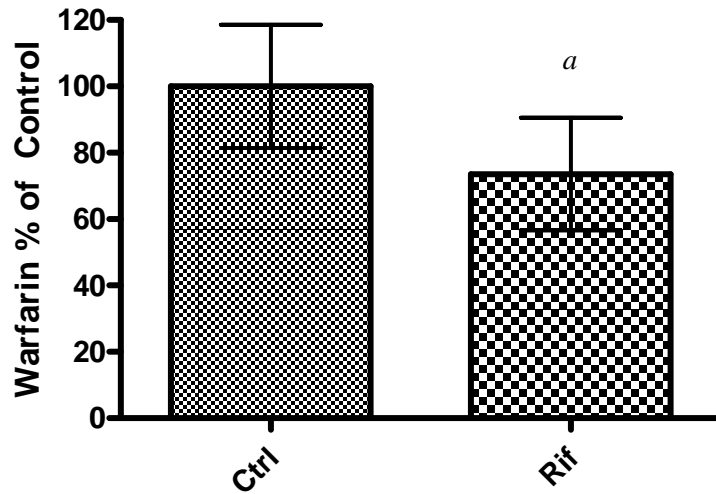
Figure 4-5 Warfarin 2 min uptake in HEK293-pCI-NEO empty vector cells with 0.1% DMSO control (0.66nM/μg protein±0.1) or 100μM rifampin treatment. [a] p<0.01 compared to control. Values are mean±SD, n=8.

4.3.3 Phenytoin Hepatic Uptake

Figures 4-6 and 4-7 show no inhibition of phenytoin uptake by either 100μM rifampin or 100μM probenecid in rat or human hepatocytes compared to vehicle control (0.1% DMSO and 1% MeOH). Rat hepatocytes were treated with 10μM phenytoin while human hepatocytes were treated with 1μM phenytoin.
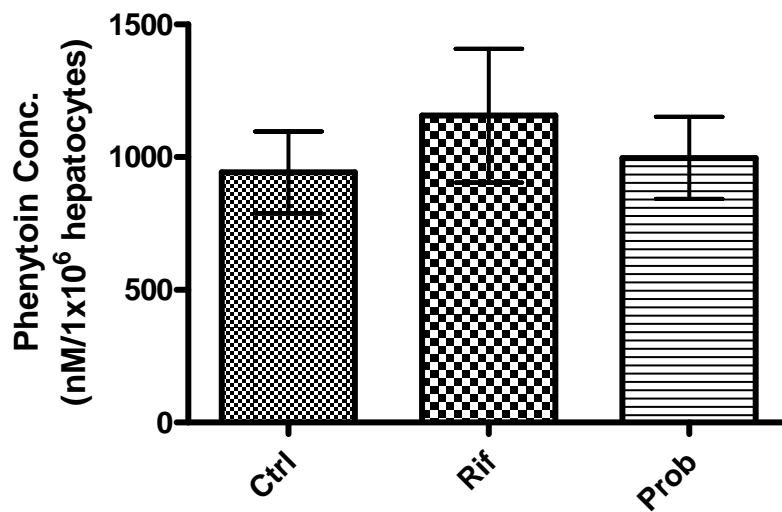
Figure 4-6 Phenytoin 2 min uptake in rat hepatocytes with control (0.1% DMSO and 1% MeOH), 100μM rifampin, or 100μM probenecid treatment (5 min pre-incubation). Values are mean±SD, n=6 per group.
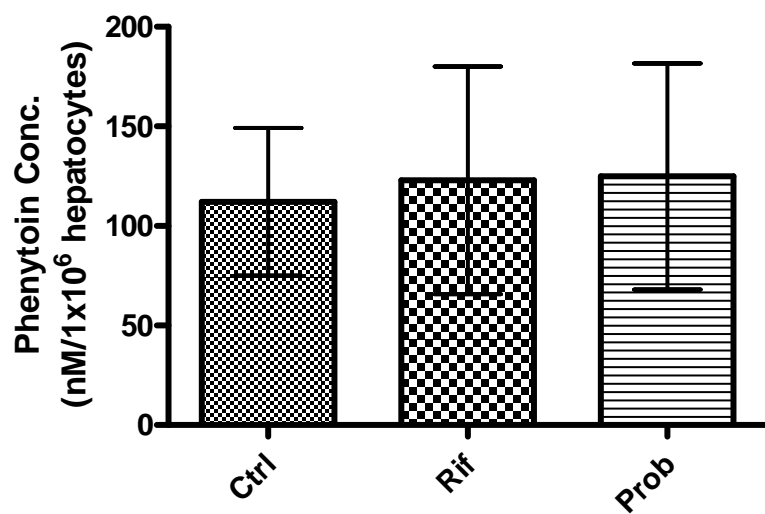
Figure 4-7 Phenytoin 2 min uptake in human hepatocytes with control (0.1% DMSO and

1% MeOH), 100μM rifampin, or 100μM probenecid treatment (5 min pre-incubation).

Values are mean±SD, n=9 per group.

4.3.4 Phenytoin HEK293 Cellular Uptake

Figures 4-8 through 4-10 show no significant inhibition of 1μM phenytoin uptake in HEK293-OATP1B1, HEK293-OATP2B1, or HEK293-pCI-NEO cells by 100μM rifampin compared to vehicle control (0.1% DMSO).
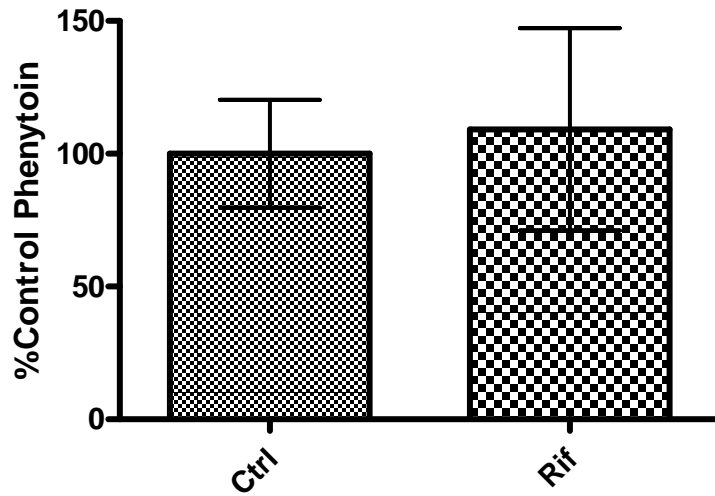
Figure 4-8 Phenytoin 2 min uptake in HEK293-OATP1B1 with 0.1% DMSO control (15.6 nM±21) or 100μM rifampin treatment. Values are mean±SD, n=12 per group.
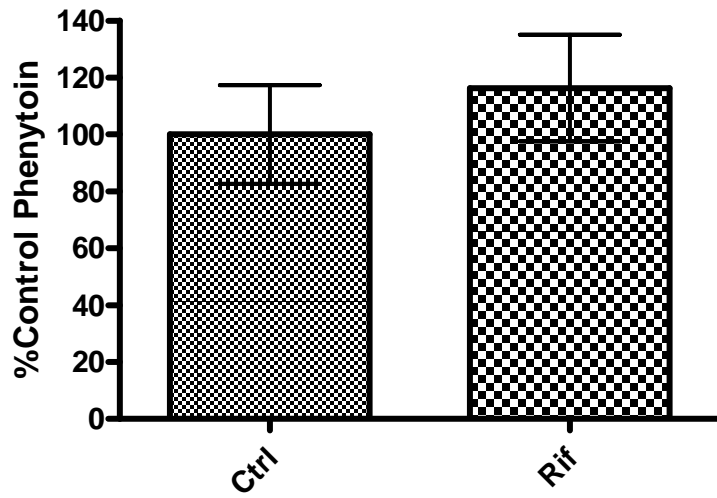
Figure 4-9 Phenytoin 2 min uptake in HEK293-OATP2B1 cells with 0.1% DMSO control (15.6nM±6) or 100μM rifampin treatment. Values are mean±SD, n = 6 per group.
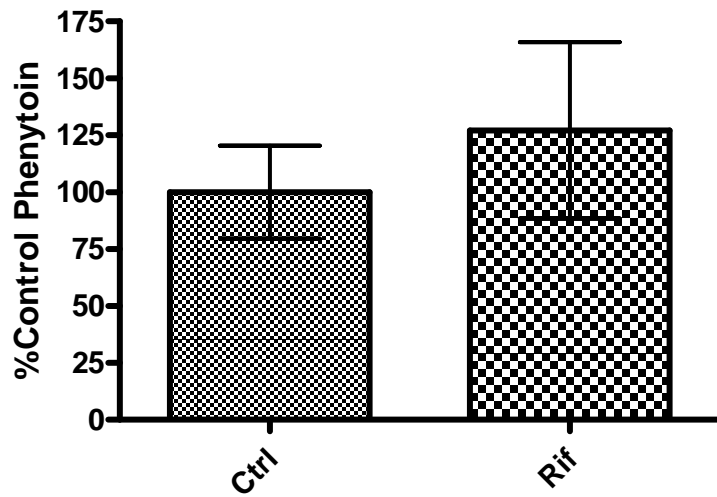
Figure 4-10 Phenytoin 2 min uptake in HEK293-pCI-NEO cells with 0.1% DMSO control (6.23nM±5.6) or 100μM rifampin treatment. Values are mean±SD, n=9 per group.

4.4 Discussion

The results from the rat and human hepatocyte uptake experiments indicate that warfarin may be a substrate for an Oatp/OATP transporter. Warfarin uptake in rat hepatocytes was reduced by 23% and in human hepatocytes by 34%. Since warfarin is a narrow therapeutic index drug and its site of action is in the liver, the degree of inhibition seen with100μM rifampin could cause a clinically relevant interaction by reducing the amount of warfarin that is able to get into hepatocytes and inhibit the VKORC1 enzyme. Investigation into which specific OATP isoform is responsible for warfarin uptake revealed that the liver-specific OATP1B1 does not mediate warfarin transport as indicated by the inability of rifampin to reduce HEK293-OATP1B1 intracellular levels compared to control. The same results were seen for OATP2B1, an isoform expressed in both the liver and the intestine. The levels of warfarin uptake in HEK293-OATP1B1, HEK293-OATP2B1, and HEK293-pCI-NEO were all very similar, providing further evidence that the OATP transporters overexpressed in the cell system were not mediating drug uptake. Unexpectedly, there was a significant difference in warfarin uptake in the HEK-293-pCI-NEO cell line in the presence of rifampin. It is possible that an endogenous transporter in the HEK293 cell line can transport warfarin. While one would expect to see the same thing in the overexpressing cell lines, it is possible that rifampin preferentially interacts with the overexpressed rather than the endogenous protein, preventing rifampin from inhibiting warfarin transport by the endogenous protein. Other OATP isoforms that could be responsible for warfarin transport are the liver-specific OATP1B3, as well as OATP1A2 which is expressed in the liver in addition to multiple other tissues.

Warfarin alternatively may be transported in humans by the organic anion transporter 2 (OAT2) which is also expressed on the hepatic basolateral membrane. In human hepatocytes, probenecid caused a 22% reduction in hepatocyte warfarin levels ($p<0.05$). In rat hepatocytes, no significant inhibition was seen in warfarin uptake in response to probenecid treatment, indicating a possible species difference in OAT2/Oat2 substrate specificity.

Rat and human hepatocyte data in addition to the cellular data indicate that phenytoin is not a substrate for hepatically expressed Oatp/OATP or Oat/OAT transporters. This indicates that phenytoin is unlikely to fall victim to drug-drug interactions through inhibition of hepatic uptake.

4.5 Conclusions

Inhibition of OATP and OAT separately led to moderate changes in hepatocyte warfarin levels, indicating that if one of these transporters is inhibited, the other may compensate. If both transporters were inhibited simultaneously, which is not unlikely in an elderly population on multiple medications, a larger reduction in uptake would be expected that would likely lead to a clinically relevant change in warfarin pharmacokinetics and pharmacodynamics.

In contrast to wafarin, inhibition of OATP and OAT had no effect on phenytoin uptake, making inhibition of hepatic uptake by an OATP or OAT transporter an unlikely route of drug-drug interactions for this compound.

4.6 References

Banh, H.L., Burton, M.E., and Sperling, M.R. (2002). "Interpatient and intrapatient variability in phenytoin protein binding." Ther. Drug Monit. **24:**379–385.

Caracoa, Y., Muszkata, M., and Wood, A.J.J. (2001). "Phenytoin metabolic ratio: a putative marker of CYP2C9 activity in vivo." Pharmacogenetics. **11**:587-596.

Couvert, P., Giral, P., Dejager, S., Gu, J., Huby, T., Chapman, M.J., Bruckert, E., and Carrie, A. (2008). "Association between a frequent allele of the gene encoding OATP1B1 and enhanced LDL-lowering response to fluvastatin therapy." Pharmacogenomics. **9**(9): 1217-1227.

Gage, B.F., Eby, C., Johnson, J.A., Deych, E., Rieder, M.J., Ridker, P.M., Milligan, P.E., Grice, G., Lenzini, P., Rettie, A.E., Aquilante, C.L., Gross, L., Marsh, S., Langaee, T., Farnett, L.E., Voora, D., Veenstra, D.L., Glynn, R.J., Barrett, A., and McLeod, H.L. (2008). "Use of pharmacogenetic and clinical factors to predict the therapeutic dose of warfarin." Clin. Pharmacol. Ther. **84**(3): 326–331.

Kerb, R., Aynacioglu, A.S., Brockmoeller, J., Schlagenhaufer, R., Bauer, S., Szekeres, T., Hamwi, A., Fritzer-Szekeres, M., Baumgartner, C., Oengen, H.Z., Guezelbey, P., Roots, I., and Brinkmann, U. (2001). " The predictive value of MDR1, CYP2C9, and CYP2C19 polymorphisms for phenytoin plasma levels." Pharmacogenomics J. **1**: 204–210.

Kuruvilla, M. and Gurk-Turner, C. (2001). "A review of warfarin dosing and monitoring." Baylor University Medical Center Proceedings. **14**:305–306.

Lau, Y.Y., Huang, Y., Frassetto, L. and Benet, L.Z. (2007). "Effect of OATP1B transporter inhibition on the pharmacokinetics of atorvastatin in healthy volunteers." Clin. Pharmacol. Ther. **81**(2): 194-204.

Shu, Y., Sheardown, S.A., Brown, C., Owen, R.P., Zhang, S., Castro, R.A., Ianculescu, A.G., Yue, L., Lo., J.C., Burchard, E.G., Brett, C.M., Giacomini, K.M. (2007). "Effect of genetic variation in the organic cation transporter 1 (OCT1) on metformin action." J. Clin. Invest. **117**(5): 1422-1431.

Takahashi, H. and Echizen, H. (2001). "Pharmacogenetics of warfarin elimination and its clinical implications." Clin. Pharmacokinet. **40** (8): 587-603.

Wadelius, M. and Pirmohamed, M. (2007). "Pharmacogenetics of warfarin: current status and future challenges." Pharmacogenomics J. **7**: 99–111.

Wu, A.H.B., Wang, P., Smith, A., Haller, C., Drake, K., Linder, M., and Valdes Jr., R. (2008). "Dosing algorithm for warfarin using CYP2C9 and VKORC1 genotyping from a multi-ethnic population: comparison with other equations." Pharmacogenomics. **9**(2): 169-178.

Zheng, H.X., Huang, Y., Frassetto, L. and Benet, L.Z. (2009). "Elucidating rifampin's inducing and inhibiting effects on glyburide pharmacokinetics and blood glucose in healthy volunteers: unmasking the differential effects of enzyme induction and transporter inhibition for a drug and its primary metabolite." Clin. Pharmacol. Ther. **85**(1): 78-85.

Zhou, S.F., Zhou, Z.W., and Huang, M. (2009). "Polymorphisms of human cytochrome P450 2C9 and the functional relevance." Toxicology. [Epub ahead of print].

CHAPTER 5

The Effect of Hepatic Organic Anion Transporting Polypeptides (OATPs) on the Disposition of Warfarin in Healthy Volunteers

5.1 Introduction

Warfarin is a commonly prescribed anticoagulant for the prevention of a variety of thromboembolic events. Successful use of warfarin has been difficult though, due to large inter-individual variation in required warfarin dose and its narrow therapeutic index (Ansell et al., 2004). Doses needed to achieve similar levels of anticoagulation can differ over 10-fold among patients. In attempts to explain the variability in warfarin dose, formal pharmacogenetic techniques have been applied to try to identify potential common genetic polymorphisms in genes that may be important. It is now well-recognized that Single Nucleotide Polymorphisms (SNPs) in warfarin's major metabolizing enzyme (cytochrome P-450; CYP2C9) and its pharmacodynamic target (vitamin K epoxide reductase; VKORC1) have a significant impact on warfarin dose requirement (Wadelius et al., 2007; Caldwell et al., 2008; Cooper et al., 2008; Takeuchi et al., 2009). Multiple investigators have incorporated patients' genetic status within these genes along with demographic factors (i.e. age, weight, gender, ethnicity, interacting drugs, etc.) into dosing algorithms for improved dose prediction (Gage et al., 2008; Wu et al., 2008; Wadelius et al., 2009). However, these regression models only account for at most 55-60% of the variability in warfarin dose requirement.

The Biopharmaceutics Drug Disposition Classification System (BDDCS), which classifies drugs based on the characteristics of solubility and extent of metabolism, allows investigators to predict the potential importance of intestinal and hepatic transporters in

the disposition of a drug (Wu and Benet, 2005). Specifically, BDDCS predicts that following oral dosing of poorly soluble, extensively metabolized drugs (Class 2 drugs), efflux transporter effects will predominate in the intestine, but both uptake and efflux transporter effects may be important in the liver. In those organs where the relevant metabolizing enzymes are located, extensive transporter-enzyme interplay may also occur. Recent human pharmacokinetic studies from our laboratory have demonstrated *in vivo* the importance of hepatic uptake via organic anion transporting polypeptides (OATPs) in the disposition of two BDDCS Class 2 drugs: atorvastatin and glyburide (Lau et al., 2007; Zheng et al., 2009). Using concomitant administration of single dose intravenous (IV) rifampin as a non-specific OATP inhibitor, hepatic uptake inhibition resulted in a 1.3- and 6.8-fold increase in glyburide and atorvastin exposure, respectively, as measured by the total area under the concentration-time curve (AUC).

Warfarin is a racemic mixture of S- and R-enatiomers with S-warfarin being 2-5 times more potent and conferring the majority of the anticoagulant activity (Coumadin package insert, 2007). The metabolism of warfarin is complex, involving regio- and stereo-specific hydroxylation at various sites mediated by multiple CYP isoforms. CYP2C9 is the primary enzyme responsible for metabolizing S-warfarin to 7-hydroxywarfarin, the major metabolite seen in humans. Other CYPs hydroxylate S-warfarin at positions 6, 8, 10, and 4´. R-warfarin is mainly metabolized by CYP2C19 to 6-hydroxywarfarin and 8-hydroxywarfarin (Jones et al., 2009). Figures 5-1 and 5-2 show the metabolic fates of S-warfarin and R-warfarin, respectively, in more detail.
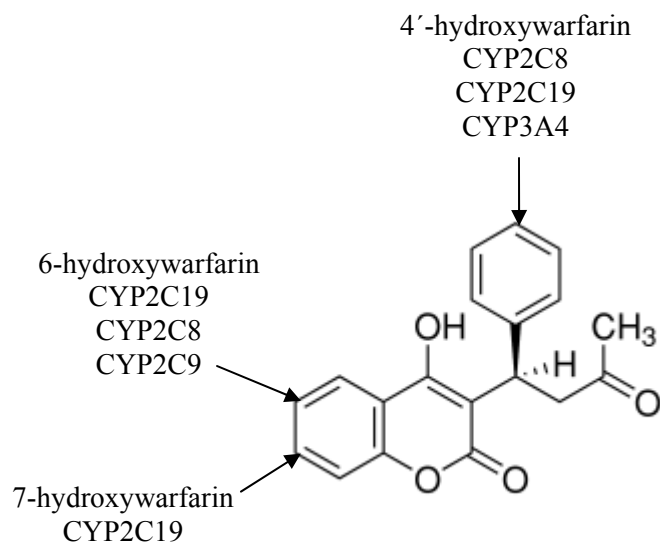
Figure 5-1 S-Warfarin sites of hydroxylation by CYPs. Adapted from Jones et al., 2009.
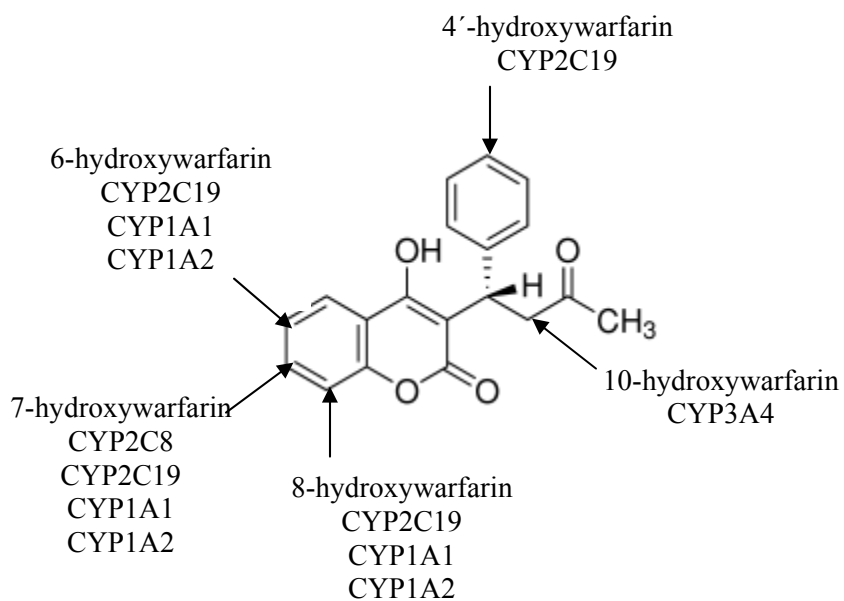
Figure 5-2 R-Warfarin sites of hydroxylation by CYPs. Adapted from Jones et.al., 2009.

Based on warfarin's extensive metabolism and poor solubility, it is classified as a BDDCS Class 2 drug. Therefore, the potential for hepatic uptake transporters to play a role in its pharmacokinetics should be considered. To date, no studies have been reported that examine whether warfarin is a substrate for hepatic uptake transporters *in vitro* or *in*

vivo. We carried out a set of experiments to investigate the hypothesis that uptake via hepatic OATP is important in the disposition of warfarin. By inhibiting the uptake of warfarin into the liver, warfarin would have decreased access to its major metabolizing CYP enzymes and to its therapeutic target, VKORC1, resulting in increased plasma exposure as measured by area under the plasma concentration-time curve (AUC) and decreased efficacy. Based on initial *in vitro* rat and human hepatocyte data (Chapter 4) showing decreased uptake of warfarin in the presence of rifampin (an Oatp/OATP inhibitor), a clinical trial in healthy volunteers was conducted to examine the clinical relevance of hepatic uptake inhibition using single dose IV rifampin on the pharmacokinetics of warfarin.

5.2 Methods

5.2.1 Clinical Study Subjects and Study Design

A randomized, open-label, two-period, crossover clinical pharmacokinetics study was conducted at the General Clinical Research Center at the University of California, San Francisco. The study protocol was approved by the Committee on Human Research of the University of California, San Francisco and the Clinical Research Center at the University of California, San Francisco. Written informed consent was obtained from 10 paid volunteers before enrollment.

Four women and six men were enrolled and all subjects completed the study. Participants' ethnicities were broken down as follows: 4 Caucasian (40%), 4 Asian/Pacific Islander (40%), and 2 Hispanic (20%). Subject demographics are given in Table 5-1. Participants' mean (±standard deviation) age and BMI were 30 (±10) years and 25.6 (±3.5) kg/m^2 respectively. All subjects underwent a screening visit consisting of

medical history, physical exam, and standard clinical laboratory tests (general

hematology, blood chemistry, coagulation studies, urinalysis, and urine pregnancy) to

insure eligibility. Genotyping of CYP2C9 was performed by our collaborator's

laboratory using the INFINITI™ CYP450-VKORC1 Assay kit (AutoGenomics,

Carlsbad, CA) and only those subjects homozygous for CYP2C9*1 (wildtype) were

allowed to participate in the study. In addition to CYP2C9, VKORC1 was also

genotyped although these results were not used for exclusion purposes. One subject was

homozygous for VKORC1 wildtype, 6 subjects were heterozygous for wildtype and the -

1639G>A polymorphism, and 3 subjects were homozygous for the -1639G>A

polymorphism. At the end of the study, the physical exam and clinical laboratory tests

were repeated except for the pregnancy test.

Demographic	
Age[a], years	30 ± 10
BMI[a], kg/m^2	25.6 ± 3.5
Sex	
Female, N (%)	4 (40%)
Race, N (%)	4 (40%)
Caucasian	4 (40%)
Asian/Pacific Islander	2 (20%)
Hispanic	
VKORC1 genotype, N (%)	
G/G (wild type)	1 (10%)
AG	6 (60%)
AA	3 (30%)

Table 5-1 Healthy volunteer demographics. [a] Values are mean ± SD.

Subjects were enrolled for two study periods to receive either (A) 7.5mg warfarin

(one 7.5mg warfarin tablet; Bristol-Myers Squibb, Princeton, NJ) on Day 1 or (B) 7.5mg

warfarin immediately following a 30-minute intravenous infusion of 600mg rifampin

(600mg rifampin powder for injection reconstituted in 10mL sterile water; Bedford

Laboratories, Bedford, OH). Treatments were separated by a minimum 14 day washout

period. To minimize potential interactions and inter-occasion variability, subjects fasted

starting the night before until 3 hours after the warfarin dose. In addition, subjects

abstained from caffeinated beverages, alcoholic beverages and orange juice starting the

night before until 24 hours after the warfarin dose. Grapefruit and grapefruit juice were

not allowed to be consumed from 7 days before the first study day until completion of the entire study.

Venous blood samples (8ml) were collected for drug level measurement at the following times relative to warfarin dosing: predose, 1, 2, 3, 4, 6, 8, 12, 24, 48, 72, 96, and 120 hours postdose. The blood samples were centrifuged within 30 minutes, and plasma was separated and stored at $-80^{o}C$ until analysis. In addition, venous blood samples (5ml) were collected for INR determination at predose, 12, 24, 48, 72 and 96 hours post warfarin dosing.

5.3 Measurement of R-Warfarin and S-Warfarin Plasma Levels

5.3.1 Plasma Sample Preparation

The samples and standards were prepared by liquid-liquid extraction of 0.5mL plasma with 2.5mL methyl t-butyl ether (MTBE) containing $1\mu M$ d_5-warfarin as internal standard. After addition of MTBE, samples were vortexed for 1 min, then centrifuged at 3000 rpm for 10 min to separate organic and aqueous layers. The bottom aqueous layer was frozen in a dry-ice:methanol bath and the top organic layer was transferred to a clean tube. The organic layer was dried down under nitrogen and samples were reconstituted in acetonitrile and transferred to HPLC vials for analysis. The calibration curve was validated and linear over the range of 5nM to 1000nM with $1/x^2$ weighting.

5.3.2 HPLC-MS/MS Analysis of R- and S-Warfarin

Samples were analyzed on an HPLC-MS/MS system consisting of a Shimadzu (Shimadzu Scientific Instruments, Columbia, MD) CBM-20A BUS module, two

Shimadzu LC-20AD Prominence liquid chromatography pumps, a Shimadzu SIL-20AC

HT Prominence autosampler, and an Applied Biosystems (Foster City, CA) MDS Sciex

API4000 triple quadrupole mass spectrometer. All system components were controlled

by Applied Biosystems Analyst software version 1.4.2.

Chromatographic conditions were as described by Naidong and colleagues

(2001). In brief, R-warfarin and S-warfarin (Sigma-Aldrich, St. Louis, MO) were

separated isocratically on a Cyclobond™ I 2000 β-cyclodextrin 250 x 4.6mm, 5μm

column with a Cyclobond™ I 2000 50 x 4.6, 5μm guard column (Sigma-Aldrich, St.

Louis, MO). R-d_5-warfarin and S-d_5-warfarin (racemic d_5-warfarin from Toronto

Research Chemicals, Inc., Ontario, Canada) enantiomers were also separated by the β-

cyclodextrin column and co-eluted with R-warfarin and S-warfarin, respectively. The

mobile phase consisted of acetonitrile:acetic acid:triethylamine (1000:3:2.5 v:v:v) and the

flow rate was 1mL/min. The injection volume was 100μL. Retention times were 7.5 min

for S-warfarin and 8.3 min for R-warfarin.

The mass spectrometer was run in multiple reaction monitoring mode with the

turbospray ion source in negative ionization mode. Conditions were as follows: collision

gas 8 units, ionspray voltage -4500 volts, temperature 400˚C, ion source gas 1 12 psi, ion

source gas 2 0 psi, curtain gas 10 psi, declustering potential -56 volts, entrance potential

-10 volts, collision energy -26 electron volts, and exit potential -5 volts. The mass

transitions 307→161 for R- and S-warfarin and 312→166 d_5-warfarin (internal standard)

were monitored.

5.3.3 Pharmacokinetic and Pharmacodynamic Analysis

Pharmacokinetic parameters for R- and S-warfarin were estimated from plasma concentration data via non-compartmental analysis using WinNonlin Professional software (version 5.2.1; Pharsight Corporation, Mountain View, CA). The C_{max} and corresponding t_{max} were obtained directly from the observed data. The terminal rate constant (λ_z) was determined by linear regression analysis of the terminal portion of the log plasma concentration–time profile. AUC_{0-12h} and AUC_{0-120h} were found using the linear/logarithmic trapezoidal method. Summation of AUC_{0-120h} and the concentration at the last measured point divided by λ_z yielded $AUC_{0-\infty}$. The terminal half-life ($t_{1/2}$) was calculated as $\ln2/\lambda_z$. CL/F was calculated as dose/$AUC_{0-\infty}$. The mean residence time (MRT) was calculated as the ratio of the area under the first moment curve ($AUMC_{0-\infty}$) divided by $AUC_{0-\infty}$ minus the estimated mean absorption time (MAT) (i.e., MRT=($AUMC_{0-\infty}$ / $AUC_{0-\infty}$) - MAT). MAT was the reciprocal of the first-order absorption rate constant (k_a) estimated by fitting the warfarin data to a two-compartment model with first-order absorption. V_{ss}/F was calculated as MRT x CL/F. The values of CL/F and Vss/F were normalized by body weight.

Pharmacodynamic parameters were estimated from the INR data on each treatment day by non-compartmental methods using WinNonlin Professional software. Baseline INR ($INR_{baseline}$) and maximum INR (INR_{max}) were obtained directly from the observed data. Area under the INR-time curve from 0 to 96 hours ($AUC_{0-96h, INR}$) was calculated using the linear/logarithmic trapezoidal method.

5.3.4 Statistical Analysis

Using previously reported warfarin pharmacokinetic data in healthy volunteers (Washington et al., 2007), a sample size of 10 subjects would provide > 80% power to detect a 30% difference in S-warfarin $AUC_{0-\infty}$ between the two treatments. Logarithmic transformation of C_{max}, $t_{1/2}$, V_{ss}/F, CL/F, AUC_{0-12h}, $AUC_{0-\infty}$ was performed prior to statistical analysis. Pharmacokinetic and pharmacodynamic parameters were compared between the two treatments by use of the paired t-test, except t_{max} for which the Wilcoxon's signed rank test was used. Data are presented as mean ± standard deviation. In addition, the geometric mean ratios of the rifampin treatment values relative to control values (warfarin alone) and their 95% confidence intervals were calculated for all parameters. The data were analyzed using STATA 10 (StataCorp LP, College Station, TX). Differences were considered statistically significant at $p < 0.05$.

5.4 Results

Figure 5-3 shows that there was no significant effect of a single dose of IV rifampin on the mean plasma concentrations of (a) S-warfarin and (b) R-warfarin in healthy volunteers after a single oral dose of 7.5 mg racemic warfarin.
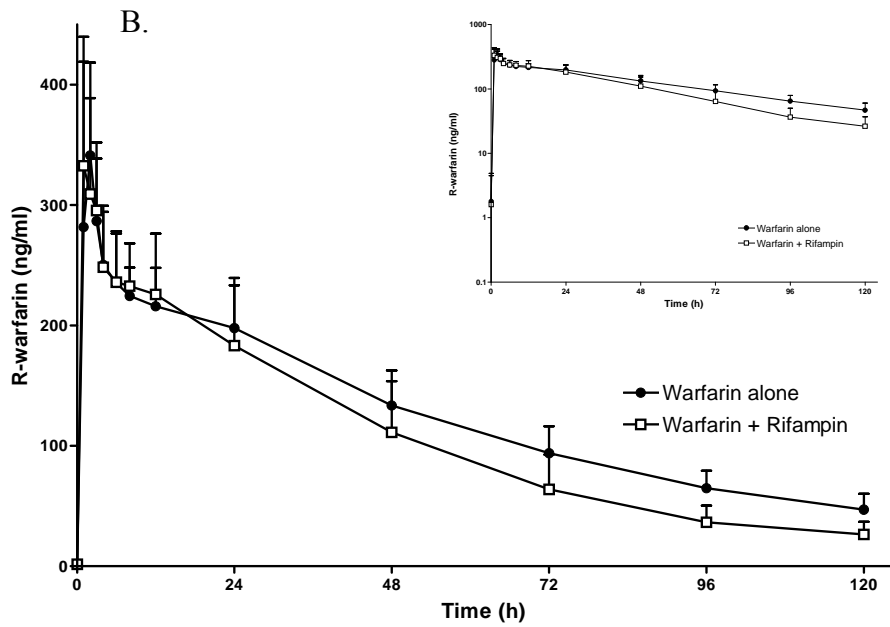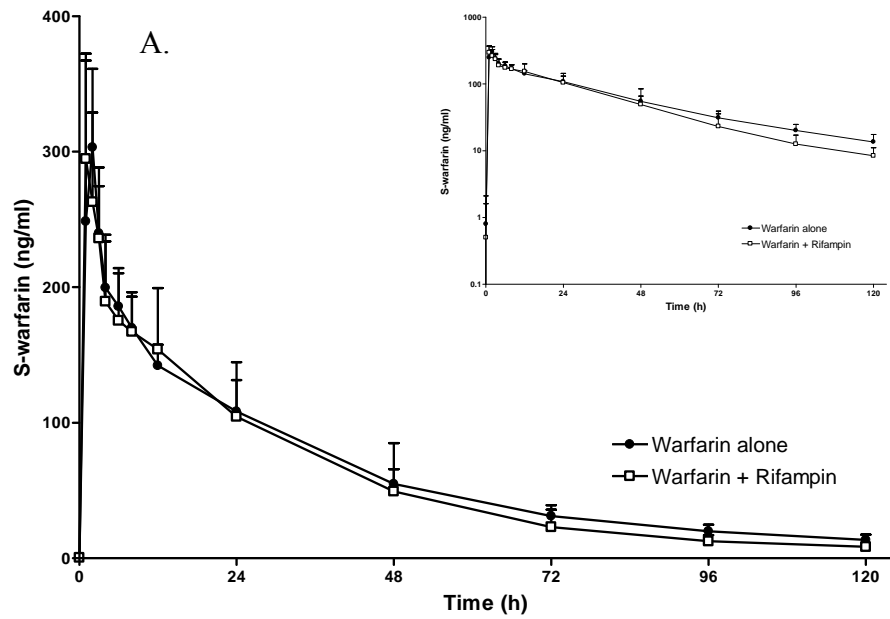
Figure 5-3 Concentration-time profiles of (A) S-warfarin and (B) R-warfarin after a

single oral dose of 7.5mg racemic warfarin in the presence and absence of a single 600mg

IV dose of rifampin. *Inset:* depicts the same data on a semilogarithmic scale. Data are mean±SD.

Figure 5-4 shows the mean INR profiles in healthy volunteers following a single oral dose of 7.5 mg racemic warfarin with and without a single dose of IV rifampin. No significant effect is seen in the presence versus absence of rifampin.
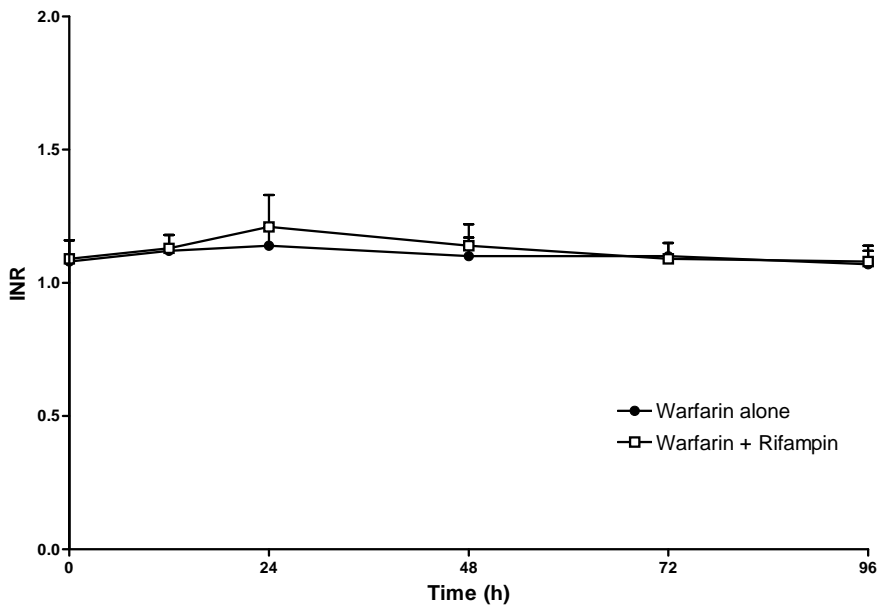
Figure 5-4 INR values after a single oral dose of 7.5mg racemic warfarin in the presence and absence of a single 600mg IV dose of rifampin. Data are mean±SD.

Table 5-2 lists the pharmacokinetic parameters of R- and S-warfarin in healthy volunteers following a single oral dose of 7.5 mg warfarin alone or in combination with a single dose of intravenous rifampin.

Parameter	Warfarin alone[a]	Rifampin phase[a]	Geometric Mean Ratio (rifampin to control)	
			Mean	95% C.I.
S-warfarin				
C_{max} (ng/ml)	329 ± 70	303 ± 82	0.91	$0.78 - 1.05$
t_{max}[b] (hr)	1.5 (1-2)	1 (1-2)	--	--
$t_{1/2}$ (hr)	39.4 ± 6.1	34.6 ± 7.4	0.87	$0.72 - 1.05$
$AUC_{0-12\,h}$ (ng/ml · hr)	2248 ± 337	2233 ± 459	0.98	$0.89 - 1.08$
$AUC_{0-120\,h}$ (ng/ml · hr)	7596 ± 949	6987 ± 2486	0.89	$0.77 - 1.02$
$AUC_{0-\infty}$ (ng/ml · hr)	8416 ± 1088	7407 ± 2501*	0.85	$0.74 - 0.99$
CL/F (mL/hr/kg)	11.8 ± 2.2	13.8 ± 2.4*	1.17	$1.01 - 1.36$
V_{ss}/F (mL/kg)	527 ± 61	514 ± 133	0.95	$0.80 - 1.13$
R-warfarin				
C_{max} (ng/ml)	375 ± 116	351 ± 85	0.95	$0.82 - 1.12$
T_{max}[b] (hr)	2 (1-2)	2 (1-3)	--	--
$t_{1/2}$ (hr)	49.0 ± 8.7	36.8 ± 7.2†	0.75	$0.66 - 0.85$
$AUC_{0-12\,hr}$ (ng/ml· hr)	2853 ± 461	2925 ± 508	1.02	$0.96 - 1.09$
$AUC_{0-120\,h}$ (ng/ml · hr)	15164 ± 2511	12726 ± 3712	0.82	$0.75 - 0.90$†
$AUC_{0-\infty}$ (ng/ml · hr)	18589 ± 3351	14130 ± 4063†	0.75	$0.68 - 0.82$
CL/F (mL/hr/kg)	5.4 ± 1.1	7.2 ± 1.5†	1.34	$1.22 - 1.47$
V_{ss}/F (mL/kg)	366 ± 55	351 ± 66	0.95	$0.87 - 1.04$

Table 5-2 Pharmacokinetic parameters for R- and S-warfarin in the presence and absence of rifampin. AUC, area under the plasma concentration-time curve; CI, confidence interval; Cl/F, oral clearance; $t_{1/2}$, terminal half-life; t_{max}, time of observed maximal concentration; V_{ss}/F, oral steady-state volume of distribution. [a] Values are shown as mean $\pm$ SD unless otherwise stated. [b] t_{max} data are given as median and range. * $p < 0.05$; † $p < 0.001$ significantly different from warfarin alone control phase as determined by the paired t-test or the Wilcoxon's signed rank test.

Table 5-3 shows the pharmacodynamic parameters in healthy volunteers after a single oral dose of 7.5mg warfarin alone of with a single IV dose of rifampin.

Parameter	Warfarin alone[a]	Rifampin phase[a]
$INR_{baseline}$	1.1 ± 0.1	1.1 ± 0.1
INR_{max}	1.2 ± 0.1	1.2 ± 0.1
$AUC_{0-96h,\ INR}$ (INR · h)	106.1 ± 2.8	108.2 ± 7.2

Table 5-3 INR, International Normalized Ratio, from baseline; INR_{max}, maximum INR; $t_{max,\ INR}$, time of observed maximum INR; $AUC_{0-96h,\ INR}$, area under the INR versus time curve from 0 to 96 hours. Values are shown as mean $\pm$ SD unless otherwise stated.

5.5 Discussion

We were most interested in the effect of hepatic OATP inhibition and the anticipated changes in R- and S-warfarin pharmacokinetics (i.e. AUC). Rifampin was chosen as a model OATP inhibitor to block the *in vivo* OATP-mediated hepatic uptake of warfarin (Vavricka et al., 2002; Baldes et al., 2006; Lau et al., 2007). Because of rifampin's shorter $t_{1/2}$ (~3h [Loos et al., 1985]) relative to that for S- and R- warfarin (39h and 49h, respectively, as determined in our clinical study), and because we did not want to create the potential for metabolic induction, therefore giving only a single rifampin dose, rifampin was only present in plasma for the early portion of warfarin's concentration-time profile. Since OATP inhibition and any potential effect on warfarin pharmacokinetics occurred at most during the time of rifampin presence, outcome measures for our study needed to be suitably selected to capture this period of OATP inhibition. Previous reports have shown that after a single 600mg IV dose of rifampin to healthy volunteers, rifampin was present for up to 12-24 hours in plasma (Rifampin package insert, 2004; Lau et al., 2007). Assuming a similar time of exposure for rifampin in our clinical study, the best parameters to capture the potential effects of OATP inhibition on warfarin pharmacokinetics were the AUC_{0-12h} and C_{max}. As mentioned above, rifampin could not be given as multiple doses due to its secondary CYP enzyme induction effect (Finch et al., 2002; Niemi et al., 2003; Rifampin package insert, 2004).

Two previous clinical studies by our laboratory using a similar study design as in the present study demonstrated significant changes in the pharmacokinetics of atorvastatin and glyburide with hepatic OATP inhibition by rifampin (Lau et al., 2007; Zheng et al., 2009). The AUC of atorvastatin increased 6.8-fold and the AUC of

glyburide increased 1.3-fold in the presence of a single dose of IV rifampin. By

inhibiting the uptake of parent drug into the liver, access to its major metabolizing

enzymes was decreased resulting in the increased plasma exposure of each drug.

Interestingly, in these clinical studies rifampin also produced a large decrease in the V_{ss}/F

for both drugs (atorvastatin, 93% decrease; glyburide, 60% decrease). This decrease in

V_{ss}/F likely demonstrates inhibition of uptake transport important for drug distribution in

tissues. In the current study we did not see a change in V_{ss}/F for either S- or R-warfarin

on rifampin days (Table 5-2), which we would have predicted if OATP-mediated

transport was important for warfarin distribution.

In contrast to our clinical study, our *in vitro* data showed that warfarin uptake into

hepatocytes was inhibited by rifampin in both rats (23%, $p<0.05$) and humans (34%,

$p<0.001$) (Chapter 4), presumably due to Oatp/OATP uptake transporter inhibition. The

magnitude of warfarin uptake inhibition was modest at the concentration of rifampin (100

µM) used for the hepatocyte uptake studies. This concentration of rifampin is

significantly higher than peak plasma concentrations that were likely achieved (17-

20µM) in our healthy volunteers after a single IV dose of 600mg rifampin and could

partially explain the disagreement between the *in vitro* and *in vivo* results. The

discordance between *in vitro* and *in vivo* data highlights the importance of translational

research in drug transporter research and the need to verify the clinical relevance of all

preclinical findings using appropriately designed clinical trials. Although we cannot rule

out that higher plasma concentrations of rifampin would have resulted in additional

OATP inhibition and therefore altered warfarin pharmcokinetics, the clinical relevance

would be arguable given that rifampin plasma concentrations this high would not be seen in patients.

The healthy volunteer clinical data described herein are in line with the numerous genome-wide association studies (GWAS) undertaken to identify polymorphisms in the human genome that may be important in warfarin dose selection. In these GWAS studies, no common variants in hepatic uptake transporters or any other drug transporters were found to be significant in determining the warfarin dose requirements of patients (Wadelius et al., 2007; Caldwell et al., 2008; Cooper et al., 2008; Takeuchi et al., 2009). Genetic variants of a transporter will not produce a significant signal in a GWAS if the drug is not a substrate for the transporter of interest since changes in transporter function will not alter the drug's pharmacokinetics and thus dose requirements. This negative predictive value was demonstrated for warfarin and OATP uptake transporters through the results of our clinical study and the above mentioned GWAS studies. In contrast, for drugs that are known substrates of uptake transporters including OATP1B1 and OATP1B3, established polymorphisms in the corresponding transporter have been shown to alter drug pharmacokinetics in human clinical studies (Niemi 2007; Zair et al., 2008; Shugarts and Benet, 2009).

Intravenous administration of rifampin conceivably minimized any potential confounding interactions in the intestine at either the enzyme or transporter level, although the lack of an interaction cannot be fully confirmed. By giving rifampin as a single dose, we attempted to avoid the well-described and clinically relevant CYP induction effect seen with multiple dosing (Finch et al., 2002; Niemi et al., 2003; Rifampin package insert, 2004). Induction of both CYP2C9 (Heimark et al., 1987;

Kanebratt et al., 2008) and CYP3A4 (Backman et al., 1998; Bidstrup et al., 2004; Kyrklund et al., 2004; Kanebratt et al., 2008), the major metabolizing enzymes for S- and R-warfarin respectively, has been described after multiple doses of rifampin. The effect of multiple doses of rifampin on warfarin pharmacokinetics was highlighted in a clinical trial of four healthy men. After 3 days of pretreatment with 300mg oral rifampin twice per day, a three-fold increase in R-warfarin clearance and a two-fold increase in S-warfarin clearance were seen (Heimark et al., 1987). In contrast, our clinical study using single dose rifampin given as 600mg IV did not demonstrate this large inductive effect on warfarin metabolism. But, our data may demonstrate a mild enzyme inductive effect indicated by the significantly decreased $AUC_{0-\infty}$ and significantly increased CL/F of S- and R-warfarin, in addition to the decreased $t_{1/2}$ for R-warfarin with rifampin treatment (Table 5-2). The effect appeared to be delayed, since early in the time course S- and R-warfarin concentration-time curves and AUC_{0-12} were not significantly different between control and rifampin-treated groups. CYP induction after single dose rifampin has been shown previously using a larger dose (1200mg) of oral rifampin given 12 hours before nifedipine, resulting in a 64% decrease in the $AUC_{0-\infty}$ of nifedipine (Ndanusa et al., 1997). Even if a delayed and mild enzyme induction by rifampin was present in our study at the later time points, the effect was small and does not alter the interpretation of the primary objective of this study. It should be noted that for R-warfarin 18% of the $AUC_{0-\infty}$ was extrapolated. The study was designed in order to make sure 90% of S-warfarin $AUC_{0-\infty}$ was included in the sampling time since S-warfarin is the more potent enantiomer. While the high percentage of $AUC_{0-\infty}$ extrapolated for R-warfarin is not ideal, it does not cast doubt on the overall interpretation of the results.

We purposely selected a warfarin dose for this study (7.5mg) that would provide adequate drug levels for pharmacokinetic analysis, yet in favor of subject safety produce minimal anticoagulation. Population PK-PD modeling of warfarin in patients requiring long-term anticoagulation predicted an EC_{50} for S-warfarin to range between 2.2 to 4.6 µg/ml depending on VKORC1 genotype (Hamberg et al., 2007). R-warfarin concentrations were not found to influence the PD response. The concentrations of S-warfarin in our healthy subjects were well below the EC_{50} (C_{max} 0.329 µg/ml; Table 5-2), yet warfarin still produced a small but temporary elevation in INR (Figure 5-4). This response was similar to a previous healthy volunteer study that also used a single 7.5mg dose of oral warfarin (Washington et al., 2007). The addition of rifampin had no effect on the warfarin pharmacodynamic response as measured by INR_{max} and $AUC_{0-96h, INR}$ (Table 5-3). The lack of a PD effect with rifampin paralleled the pharmacokinetic data from 0-24 hours during which time warfarin plasma concentrations were similar between treatment groups. Although decreased drug exposure after 24-48 hours was seen for both S- and R-warfarin on rifampin days (Figure 5-3), this decrease was small for the more biologically active S-warfarin. In addition, the drug concentrations of warfarin during the later time period were >20-fold lower than the EC_{50}, therefore no pharmacological response was likely indicating that the PK difference did not translate into a difference in PD response. Lastly, it is important to note, the study was neither designed nor powered to detect a difference in warfarin pharmacodynamics and thus was biased to show no treatment effect.

5.6 Conclusions

In this study, we attempted to determine the importance of hepatic uptake transporters for the disposition of the widely-used, narrow therapeutic index anticoagulant warfarin. The results of our clinical study demonstrated that co-administration of the potent OATP inhibitor rifampin, given as a single intravenous dose, had no effect on the AUC_{0-12h} and C_{max} values of S- and R-warfarin. Therefore, OATP uptake transport is not clinically significant for the disposition of warfarin and will provide no further insight into mechanisms of warfarin drug-drug interactions or genetic variation important in warfarin dose selection.

5.7 References

Ansell, J., Hirsh, J., Poller, L., Bussey, H., Jacobsen, A., and Hylek, E. (2004). "The pharmacology and management of the vitamin K antagonists: the Seventh ACCP Conference on Antithrombotic and Thrombolytic Therapy." Chest. **126**(3 Suppl): 204S-233S.

Backman, J. T., Kivisto, K.T., Olkkola, K.T., and Neuvonen, P.J. (1998). "The area under the plasma concentration-time curve for oral midazolam is 400-fold larger during treatment with itraconazole than with rifampicin." Eur. J. Clin. Pharmacol. **54**(1): 53-8.

Baldes, C., Koenig, P., Neumann, D., Lenhof, H.P., Kohlbacher, O., and Lehr, C.M. (2006). "Development of a fluorescence-based assay for screening of modulators of human organic anion transporter 1B3 (OATP1B3)." Eur. J. Pharm. Biopharm. **62**(1): 39-43.

Bidstrup, T. B., Stilling, N., Damkier, P., Scharling, B., Thomsen, M.S., and Brosen, K. (2004). "Rifampicin seems to act as both an inducer and an inhibitor of the metabolism of repaglinide." Eur. J. Clin. Pharmacol. **60**(2): 109-14.

Caldwell, M.D., Awad, T., Johnson, J.A., Gage, B.F., Falkowski, M., Gardina, P., Hubbard, J., Turpaz, Y., Langaee, T.Y., Eby, C., King, C.R., Brower, A., Schmelzer, J.R., Glurich, I., Vidaillet, H.J., Yale, S.H., Qi Zhang, K., Berg, R.L., and Burmester, J.K. (2008). "CYP4F2 genetic variant alters required warfarin dose." Blood. **111**(8): 4106-12.

Cooper, G.M., Johnson, J.A., Langaee, T.Y., Feng, H., Stanaway, I.B., Schwarz, U.I., Ritchie, M.D., Stein, C.M., Roden, D.M., Smith, J.D., Veenstra, D.L., Rettie, A.E., and Rieder, M.J. (2008). "A genome-wide scan for common genetic variants with a large influence on warfarin maintenance dose." Blood. **112**(4): 1022-7.

Coumadin(R) Tablets [package insert]. (2007). Princeton, NJ, Bristol-Meyers Squibb Company.

Finch, C.K., Chrisman, C.R., Baciewicz, A.M., and Self, T.H. (2002). "Rifampin and rifabutin drug interactions: an update." Arch. Intern. Med. **162**(9): 985-92.

Gage, B.F., Eby, C., Johnson, J.A., Deych, E., Rieder, M.J., Ridker, P.M., Milligan, P.E., Grice, G., Lenzini, P., Rettie, A.E., Aquilante, C.L., Grosso, L., Marsh, S., Langaee, T., Farnett, L.E., Voora, D., Veenstra, D.L., Glynn, R.J., Barrett, A., and McLeod, H.L. (2008). "Use of pharmacogenetic and clinical factors to predict the therapeutic dose of warfarin." Clin. Pharmacol. Ther. **84**(3): 326-31.

Hamberg, A.K., Dahl, M.L., Barban, M., Scordo, M.G., Wadelius, M., Pengo, V., Padrini, R., and Jonsson, E.N. (2007). "A PK-PD model for predicting the impact of age, CYP2C9, and VKORC1 genotype on individualization of warfarin therapy." Clin. Pharmacol. Ther. **81**(4): 529-38.

Heimark, L. D., Gibaldi, M., Trager, W.F., O'Reilly, R.A., and Goulart, D.A. (1987). "The mechanism of the warfarin-rifampin drug interaction in humans." Clin. Pharmacol. Ther. **42**(4): 388-94.

Jiang, X., Williams, K.M., Liauw, W.S., Ammit, A.J., Roufogalis, B.D., Duke, C.C., Day, R.O., and McLachlan, A.J. (2004). "Effect of St John's wort and ginseng on the pharmacokinetics and pharmacodynamics of warfarin in healthy subjects." Br. J. Clin. Pharmacol. **57**(5): 592-9.

Jiang, X., Williams, K.M., Liauw, W.S., Ammit, A.J., Roufogalis, B.D., Duke, C.C., Day, R.O., and McLachlan, A.J. (2005). "Effect of ginkgo and ginger on the pharmacokinetics and pharmacodynamics of warfarin in healthy subjects." Br. J. Clin. Pharmacol. **59**(4): 425-32.

Jones, D.R., Moran, J.H., and Miller, G.P. (2009). "Warfarin and UDP-glucuronosyltransferases: writing a new chapter of metabolism." Drug Metab. Rev. [Epub ahead of print].

Kaminsky, L. S. and Zhang, Z.Y. (1997). "Human P450 metabolism of warfarin." Pharmacol. Ther. **73**(1): 67-74.

Kanebratt, K.P., Diczfalusy, U., Bäckström, T., Sparve, E., Bredberg, E., Böttiger, Y., Andersson, T.B., and Bertilsson, L. (2008). "Cytochrome P450 induction by rifampicin in healthy subjects: determination using the Karolinska cocktail and the endogenous CYP3A4 marker 4beta-hydroxycholesterol." Clin. Pharmacol. Ther. **84**(5): 589-94.

Kim, J.S., Nafziger, A.N., Gaedigk, A., Dickmann, L.J., Rettie, A.E., Bertino, J.S. Jr. (2001). "Effects of oral vitamin K on S- and R-warfarin pharmacokinetics and pharmacodynamics: enhanced safety of warfarin as a CYP2C9 probe." J. Clin. Pharmacol. **41**(7): 715-22.

Kong, A.N., Tomasko, L., Waldman, S.A., Osborne, B., Deutsch, P.J., Goldberg, M.R., and Bjornsson, T.D. (1995). "Losartan does not affect the pharmacokinetics and pharmacodynamics of warfarin." J. Clin. Pharmacol. **35**(10): 1008-15.

Kyrklund, C., Backman, J.T., Neuvonen, M., and Neuvonen, P.J. (2004). "Effect of rifampicin on pravastatin pharmacokinetics in healthy subjects." Br. J. Clin. Pharmacol. **57**(2): 181-7.

Lau, Y.Y., Huang, Y., Frassetto, L., and Benet, L.Z. (2007). "effect of OATP1B transporter inhibition on the pharmacokinetics of atorvastatin in healthy volunteers." Clin. Pharmacol. Ther. **81**(2): 194-204.

Lilja, J. J., Backman, J.T., and Neuvonen, P.J. (2007). "Effects of daily ingestion of cranberry juice on the pharmacokinetics of warfarin, tizanidine, and midazolam--probes of CYP2C9, CYP1A2, and CYP3A4." Clin. Pharmacol. Ther. **81**(6): 833-9.

Loos, U., Musch, E., Jensen, J.C., Mikus, G., Schwabe, H.K., and Eichelbaum, M. (1985). "Pharmacokinetics of oral and intravenous rifampicin during chronic administration." Klin. Wochenschr. **63**(23): 1205-11.

Mohammed Abdul, M.I., Jiang, X., Williams, K.M., Day, R.O., Roufogalis, B.D., Liauw, W.S., Xu, H., and McLachlan, A.J. (2008). "Pharmacodynamic interaction of warfarin with cranberry but not with garlic in healthy subjects." Br. J. Pharmacol. **154**(8): 1691-700.

Naidong, W., Ring, P.R., Midtlien, C., and Jiang, X. (2001). "Development and validation of a sensitive and robust LC-tandem MS method for the analysis of warfarin enantiomers in human plasma." Pharm. Biomed. Anal. 25(2):219-26.

Ndanusa, B.U., Mustapha, A., and Abdu-Aguye, I. (1997). "The effect of single dose rifampicin on the pharmacokinetics of oral nifedipine." J. Pharm. Biomed. Anal. 15(9-10): 1571-5.

Niemi, M. (2007). "Role of OATP transporters in the disposition of drugs." Pharmacogenomics. **8**(7): 787-802.

Niemi, M., Backman, J.T., Fromm, M.F., Neuvonen, P.J., and Kivistö, K.T. (2003). "Pharmacokinetic interactions with rifampicin : clinical relevance." Clin. Pharmacokinet. **42**(9): 819-50.

(2004). Rifampin for injection USP [package insert]. Bedford, OH, Bedford Laboratories.

Shugarts, S. and Benet, L.Z. (2009). "The role of transporters in the pharmacokinetics of orally administered drugs." Pharm. Res. **26**(9): 2039-54.

Soon, D., Kothare, P.A., Linnebjerg, H., Park, S., Yuen, E., Mace, K.F., and Wise, S.D. (2006). "Effect of exenatide on the pharmacokinetics and pharmacodynamics of warfarin in healthy Asian men." J. Clin. Pharmacol. **46**(10): 1179-87.

Takeuchi, F., McGinnis, R., Bourgeois, S., Barnes, C., Eriksson, N., Soranzo, N., Whittaker, P., Ranganath, V., Kumanduri, V., McLaren, W., Holm, L., Lindh, J., Rane, A., Wadelius, M., and Deloukas, P. (2009). "A genome-wide association study confirms VKORC1, CYP2C9, and CYP4F2 as principal genetic determinants of warfarin dose." PLoS Genet. **5**(3): e1000433.

Uno, T., Sugimoto, K., Sugawara, K., and Tateishi, T. (2008). "The effect of CYP2C19 genotypes on the pharmacokinetics of warfarin enantiomers." J. Clin. Pharm. Ther. **33**(1): 67-73.

Vavricka, S.R., Van Montfoort, J., Ha, H.R., Meier, P.J., and Fattinger, K. (2002). "Interactions of rifamycin SV and rifampicin with organic anion uptake systems of human liver." Hepatology. **36**(1): 164-72.

Wadelius, M., Chen, L.Y., Eriksson, N., Bumpstead, S., Ghori, J., Wadelius, C., Bentley, D., McGinnis, R., and Deloukas, P. (2007). "Association of warfarin dose with genes involved in its action and metabolism." Hum. Genet. **121**(1): 23-34.

Wadelius, M., Chen, L.Y., Lindh, J.D., Eriksson, N., Ghori, M.J., Bumpstead, S., Holm, L., McGinnis, R., Rane, A., and Deloukas, P. (2009). "The largest prospective warfarin-treated cohort supports genetic forecasting." Blood. **113**(4): 784-92.

Washington, C., Hou, S.Y., Hughes, N.C., Campanella, C., and Berner, B. (2007). "Ciprofloxacin prolonged-release tablets do not affect warfarin pharmacokinetics and pharmacodynamics." J. Clin. Pharmacol. **47**(10): 1320-6.

Wu, A.H., Wang, P., Smith, A., Haller, C., Drake, K., Linder, M., and Valdes, R. Jr. (2008). "Dosing algorithm for warfarin using CYP2C9 and VKORC1 genotyping from a multi-ethnic population: comparison with other equations." Pharmacogenomics. **9**(2): 169-78.

Zaïr, Z.M., Eloranta, J.J., Stieger, B., and Kullak-Ublick, G.A. (2008). "Pharmacogenetics of OATP (SLC21/SLCO), OAT and OCT (SLC22) and PEPT (SLC15) transporters in the intestine, liver and kidney." Pharmacogenomics. **9**(5): 597-624.

Zheng, H. X., Huang, Y., Frassetto, L.A., and Benet, L.Z. (2009). "Elucidating rifampin's inducing and inhibiting effects on glyburide pharmacokinetics and blood glucose in healthy volunteers: unmasking the differential effects of enzyme induction and transporter inhibition for a drug and its primary metabolite." Clin. Pharmacol. Ther. **85**(1): 78-85.

CHAPTER 6

Investigation of Potential Drug-Drug Interactions Between Immunosuppressants, Tacrolimus and Cyclosporine, and the HIV Integrase Inhibitor Raltegravir

6.1 Introduction

With the introduction of highly active antiretroviral therapy (HAART) in 1996 (Ciuffreda et al., 2007), survival of HIV+ patients has improved dramatically. In developed nations, major causes of death in HIV+ populations are end-stage renal failure, due in some cases to HIV-associated nephropathy (HIVAN) or HAART nephrotoxicity, and liver disease, potentially exacerbated by HAART hepatotoxicity or co-infection with hepatitis B or C (Ciuffreda et al., 2007). In light of improved HIV treatment and survival, use of solid organ transplants to treat co-morbidities is on the rise. This means clinicians must be aware of the drug-drug interactions between HIV therapies and immunosuppressants in order to maintain viral suppression while avoiding organ rejection. Two commonly used immunosuppressants are tacrolimus (FK-506) and cyclosporine (CsA), both calcineurin inhibitors that suppress T-cell activation (Izzedine et al., 2004). Tacrolimus is a dual substrate of P-glycoprotein (Pgp) (Goto et al., 2002) and cytochrome P450 3A4 (CYP3A4) (Iwasaki, 2007) while cyclosporine is transported by both Pgp and the multidrug resistance protein 2 (MRP2) and is also a CYP3A4 substrate (Izzedine et al., 2004). Many drugs in the HAART regimen also interact with CYP enzymes and drug transporters, including Pgp and MRP1 and 2. See Table 6-1.

HAART Drug	Class	CYP Enzyme	Efflux Transporter	Uptake Transporter
Lamivudine	NRTI[a]			OCT[f] 1, 2, 3
Stavudine	NRTI			CNT[g] 1
Zalcitabine	NRTI			OCT1,2, ENT[h] 2, CNT3
Didanosine	NRTI			ENT2, CNT1, 3
Zidovudine	NRTI		Pgp, MRP4, 5, BCRP[e]	ENT2, CNT1, 3
Abacavir	NRTI		Pgp, BCRP	
Delavirdine	NNRTI[b]	3A4, 2D6	Pgp	
Efavirenz	NNRTI	3A4, 2D6	Pgp	
Nevirapine	NNRTI	3A4	Pgp	
Tenofovir	NtRTI[c]		MRP4	OAT[i] 1, 3
Amprenavir	PI[d]	3A4	Pgp	
Indinavir	PI	3A4	Pgp, MRP2	
Lopinavir	PI	3A4	Pgp, MRP1, 2	
Nelfinavir	PI	3A4	Pgp	
Ritonavir	PI	3A4, 2D6	Pgp, MRP1, 2	
Saquinavir	PI	3A4	Pgp, MRP1, 2	

Table 6-1 Enzymes and transporters for common HAART drugs. [a] nucleoside reverse transcriptase inhibitor, [b] non-nucleoside reverse transcriptase inhibitor, [c] nucleotide reverse transcriptase inhibitor, [d] protease inhibitor, [e] breast cancer resistance protein, [f] organic cation transporter, [g] concentrative nucleoside transporter, [h] equilibrative nucleoside transporter, [i] organic anion transporter. Adapted from Izzedine et al. (2004), Varatharajan et al. (2009), Cihlar et al., (2007), Huisman et al. (2002), and Minuesa et al. (2009).

Interactions of antiretroviral drugs with Pgp or MRP and CYP3A4 may alter the pharmacokinetics of immunosuppressants with serious consequences. For example, inhibition of CYP3A4 metabolism or of efflux of immunosuppressants would lead to increased, and potentially toxic, plasma levels, while induction of CYP3A4 metabolism

or of efflux via Pgp or MRP would lead to decreased drug exposure and potentially therapeutic failure. Frassetto and colleagues (2007) conducted pharmacokinetic studies in HIV+ patients receiving kidney, liver, or dual kidney and liver transplants to observe the effects of HAART on tacrolimus and cyclosporine dose requirements. It was observed that cyclosporine dosage had to be lowered for NNRTI, PI, and NNRTI + PI regimens and the dosing intervals were longer for regimens that included PIs. For tacrolimus, lower doses were needed for all HAART regimens as was the case with cyclosporine, however the dosing interval was increased for the PI-only regimen, but not the NNRTI or NNRTI + PI regimens. These adjustments fit the scenario for drug-drug interaction through inhibition of CYP3A4 and Pgp that would lead to increased immunosuppressant levels.

The development of raltegravir (Issentress™), Merck and Co.'s first-in-class integrase inhibitor that prevents the covalent insertion of linear HIV-1 DNA into the host cell genome, circumvents these issues as it does not interact with Pgp or CYP3A4 (Merck product information sheet).
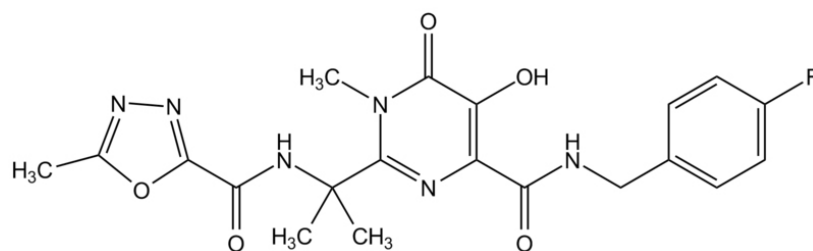
Figure 6-1 Structure of raltegravir (Issentress™)

However, preliminary data from a UCSF-led multicenter study on liver and kidney transplant safety and efficacy in HIV+ patients suggest that raltegravir (RAL) may

be involved in drug-drug interactions with tacrolimus and cyclosporine through alternative mechanisms. Patients already receiving ritonavir-boosted protease inhibitor therapy and immunosuppressant therapy (two receiving tacrolimus and two receiving cyclosporine) had raltegravir added as part of the antiretroviral regimen. Instead of seeing no change in immunosuppressant levels as expected, addition of raltegravir was followed by an increase in tacrolimus trough levels to more than twice those seen prior to raltegravir initiation. For the two patients on cyclosporine therapy, trough levels decreased markedly, though to widely differing degrees (one patient showed a 32% decrease with a 16-fold dosing rate increase while the other patient showed a 22% decrease with no change in dosing rate.) See Table 6.2.

Patient	Prior ARVs	IS	IS dose (mg)	IS trough (ng/mL)	+RAL (mg)	New IS dose (mg)	New IS trough (ng/mL)
1	ATV[a] 300 qd KAL[b] 2 bid	FK506	0.5 q 10d	5.4	RAL[e] 400 bid	No change	⇑(13.3)
2	DRV[c] 600 bid RTV[d] 100 bid	FK506	1.0 qd	3.0	RAL 400 bid	No change	⇑(6.7)
3	DRV 600 bid RTV100 bid	CsA	25 bid/25 qd	160	RAL 400 bid	No change	⇓(115)
4	KAL 2 bid	CsA	25 qod	220	RAL 400 bid	100 bid	⇓(150)

Table 6-2 Effect of addition of raltegravir to antiretroviral (ARV) regimen on

immunosuppressant (IS) levels. [a] atanazavir, [b] kaletra, [c] darunavir, [d] ritonavir, [e] raltegravir.

We hypothesize that raltegravir may be interacting with the immunosuppressants through a transporter by a previously unrecognized mechanism. While both tacrolimus and cyclosporine are recognized as Pgp substrates, it remains to be determined whether they are substrates for hepatic uptake transporters. Also, cyclosporine is a known MRP2 substrate, but the inhibitory potential of raltegravir on MRP2 transport is unknown. Previous data from our lab (Lau et al., 2007; Zheng et al., 2009) has shown that Biopharmaceutics Drug Disposition and Classification System (BDDCS) Class 2 drugs, which both tacrolimus and cyclosporine are, may fall victim to interactions at the hepatic transporter level. Data from a human clinical study showed a significant interaction of the BDDCS Class 2 drug atorvastatin with the OATP inhibitor rifampin, leading to increased plasma levels due to inhibition of hepatic uptake of atorvastatin by OATP1B1 (Lau et al., 2007). The result of increased tacrolimus plasma levels seen upon addition of raltegravir may indicate a similar interaction as that seen between atorvastatin and rifampin. The decrease in cyclosporine plasma levels seen would make it unlikely that it is falling victim to the same kind of interaction as tacrolimus. It is possible that instead its hepatic efflux via MRP2 may be inhibited or that raltegravir stimulates hepatic uptake, both of which could lead to decreased plasma levels via increased hepatic metabolism. The aims of this study were to determine if tacrolimus or cyclosporine are substrates for transporters other than Pgp or MRP2 and if raltegravir can inhibit transport of tacrolimus or cyclosporine.

6.2 Materials and Methods

6.2.1 Chemicals and Materials

Raltegravir was purchased from Toronto Research Chemicals, Inc. (Ontario, Canada) and ^{3}H-estrone sulfate (^{3}H-ES) was purchased from Perkin Elmer (Waltham, MA). Rifampin, tacrolimus, cyclosporine, and atorvastatin were purchased from Sigma-Aldrich (St. Louis, MO). Cryopreserved human hepatocytes were purchased from CellzDirect™ (Durham, NC). Human embryonic kidney cells (HEK293) overexpressing OATP1B1 or OATP2B1 along with the empty vector HEK293-pCI-NEO cell line were kind gifts from Dr. Hideaki Okochi (University of California at San Francisco, CA). The MRP2 overexpressing cell line (MDCKII-cMOAT) along with the MDCKII wildtype (MII) cell line were a generous gift from Professor Piet Borst and Dr. Raymond Evers (The Netherland Cancer Institute, Netherlands). All cell culture media were obtained from the UCSF Cell Culture Facility (San Francisco, CA). Non-coated 6-well cell culture plates were purchased from Corning Life Sciences (Acton, MA). Poly-D-lysine coated 6-well and 12-well cell culture plates, as well as 0.4μm low density polyethylene terephthalate (PET) transwell inserts were purchased from BD Bioscience (Bedford, MA).

6.2.2. Isolation of Rat Hepatocytes and Use of Cryopreserved Human Hepatocytes

Male Sprague-Dawley rats (250-300g, Charles River Laboratories, Wilmington, MA) were anesthetized via peritoneal injection of 1mL/kg ketamine/xylazine (80mg/mL; 12mg/mL) prior to portal vein cannulation. The liver was perfused with oxygenated liver perfusion buffer (Krebs-Henesleit [KH] buffer containing 10mM D-glucose, 2mM L-

glutamine, and 1% bovine serum albumin) for 5 min at 30mL/min, followed by

perfusion with hepatocyte wash buffer (KH buffer containing 10mM HEPES, 2mM L-

glutamine) supplemented with 1.2 U/mL collagenase for 5 min at 20mL/min to digest

the liver. The liver was excised and digestion completed. Hepatocytes were isolated by

passing the liver digest through an 80μm nylon mesh. Hepatocytes were washed twice

with ice-cold hepatocyte wash buffer not containing collagenase. The trypan blue

exclusion method was used to assess cell viability and cells with viability greater than

90% were used for uptake studies. Hepatocytes were suspended in oxygenated

hepatocyte wash buffer with 1% bovine serum albumin in place of collagenase buffer to

yield a concentration of 1 million cells/mL.

Cryopreserved human hepatocytes pooled from 5 female and 5 male donors from

CellzDirect™ were used according to the provider's instructions. In brief, hepatocytes

were thawed quickly in a 37˚C water bath and washed twice with ice-cold hepatocyte

wash buffer to remove cryopreservation solution. Cells were suspended in oxygenated

hepatocyte wash buffer to yield a concentration of 0.5 million cells/mL.

6.2.3 Hepatocyte Uptake Studies

Prior to incubation with substrate, hepatocytes suspended in hepatocyte wash

buffer, pH 7.4, were pre-warmed in a 37˚C water bath for 5 min. During this 5 min pre-

incubation period, DMSO vehicle control, 100μM rifampin, or 100μM raltegravir was

added to the hepatocytes. After hepatocytes were warmed, uptake was initiated by

addition of 1μM tacrolimus or cyclosporine, or 4.3nM ^{3}H-estrone sulfate, which was used

as a positive control. After 2 min, the reaction was terminated by removing a 0.5mL

aliquot and transferring to a tube containing 700μL of a silicone:mineral oil (83.3:16.7; v/v) mixture for tacrolimus and cyclosporine or to a tube containing 150μL of 2N sodium hydroxide under a 500μL layer of the oil mixture in the case of ^{3}H-estrone sulfate. The hepatocytes were centrifuged for 10 sec at 13,000g to isolate the hepatocyte pellets. The oil mixture was removed and the pellets were lysed by sonication in the presence of 200μL H_2O in the case of tacrolimus and cyclosporine or by overnight incubation at 65˚C in the 2N NaOH in the case of ^{3}H-estrone sulfate.

6.2.4 HEK293 Cell Culture and Uptake Studies

HEK293-OATP1B1, HEK293-OATP2B1, and HEK293-pCI-NEO cells were cultured in Dulbelcco's Modified Eagle Medium with 100 U/mL penicillin/streptomycin and 0.5 mg/mL geneticin at 37˚C in 5% CO_2 atmosphere with 95% humidity. Cells were cultured in T-75 flasks and when ~90% confluent were trypsinized and plated in 6-well or 12-well poly-D-lysine coated plates. Cells were allowed to grow to confluence for ~48-72 hours. Prior to uptake studies, cells were washed for 5 min at 37˚C with Hanks Buffered Salt Solution (HBSS) at pH 7.4. Uptake studies were initiated by replacing wash buffer with HBSS containing 1μM tacrolimus, 1μM cyclosporine, 1μM atorvastatin, or 4.3nM ^{3}H-estrone sulfate with DMSO vehicle control, 100μM rifampin, or 100μM raltegravir. After 2 min, the reaction was terminated by removing the incubation buffer and washing the cells three times with ice cold phosphate buffered saline (PBS). Cells were allowed to dry and then were collected by manually scraping the cells from the plate and suspending in 200μL or 400μL of H_2O for 12-well and 6-well plates, respectively. In the case of tacrolimus, cyclosporine, and atorvastatin, samples

were spun down at 13,000g for 10 min to isolate the cell pellet, then sonicated to lyse the cells prior to preparation for HPLC-MS/MS and protein analysis. For ^{3}H-estrone sulfate, the entire aliquot was transferred to a scintillation vial for analysis by scintillation counting.

6.2.5 MDCKII and MDCKII-MRP2 Cell Culture and Bidirectional Transport

MDCKII and MDCKII-MRP2 cells were cultured in Dulbelcco's Modified Eagle Medium with 100 U/mL penicillin/streptomycin at 37°C in 5% CO_2 atmosphere with 95% humidity. Cells were cultured in T-75 flasks and when ~90% confluent were trypsinized and plated on PET inserts in Corning 6-well cell culture plates. Cells were allowed to grow to confluence for 6 days. Prior to bidirectional studies, cells were washed for 5 min at 37°C with Hanks Buffered Salt Solution (HBSS) at pH 7.4. The experiment was initiated by replacing wash buffer with HBSS containing test substrate in either the apical (A) chamber or in the basal (B) chamber with MRP inhibitor or vehicle control in both A and B chambers. At selected timepoints, 200µL aliquots of buffer were removed from the receiver chamber and replaced with fresh buffer. At the end of the timecourse, buffer was removed, inserts were washed 3x in ice-cold phosphate buffered saline and allowed to dry at room temperature before cells were scraped manually with 200µL of H_2O and stored in Eppendorf tubes. Both buffer and cell samples were stored at -80°C until analysis.

6.2.6. Non-Specific Binding to Cell Cultureware

Poly-D-lysine coated 6-well plates with no cells present were incubated for 2 min at 37°C with HBSS at pH 7.4 containing 1µM tacrolimus with DMSO, 100µM rifampin,

100µM raltegravir, or 200µM raltegravir. After 2 min, a 200µL aliquot of buffer was removed from each well and, along with 200µL aliquots of the original incubation solutions, was analyzed by HPLC-MS/MS.

6.2.7 Sample Preparation

The calibration curve and samples were prepared for HPLC-MS/MS analysis by liquid-liquid extraction. The calibration curve range for tacrolimus, cyclosporine, and atorvastatin was 5nM-1000nM. A 500µL aliquot of methyl-t-butyl ether containing either 0.5µM ritonavir (tacrolimus internal standard), 0.5µM cimetidine (cyclosporine internal standard), or 0.5µM fluvastatin (atorvastatin internal standard) was added to each sample. Samples were vortexed for 1 min then centrifuged at 13,000g for 10 min to separate the aqueous and organic layers. After centrifuging, the lower aqueous layer was frozen in a methanol-dry ice bath and the top organic layer was transferred to a clean tube. The organic layer was dried down under N_2 and drugs were reconstituted in 200µL of the appropriate mobile phase.

6.2.8 Measurement of Tacrolimus

Samples were analyzed on an HPLC-MS/MS system consisting of a Shimadzu (Shimadzu Scientific Instruments, Columbia, MD) CBM-20A BUS module, two Shimadzu LC-20AD Prominence liquid chromatography pumps, a Shimadzu SIL-20AC HT Prominence autosampler, and an Applied Biosystems (Foster City, CA) MDS Sciex API4000 triple quadrupole mass spectrometer. All system components were controlled by Applied Biosystems Analyst software version 1.4.2. A Waters (Waters Corp., Milford, MA) Symmetry C18 analytical column with dimensions 50 x 2.1mm and 5µm

particle size was used at ambient temperature with an isocratic mobile phase consisting of 0.1% formic acid:methanol:acetronitrile (5:85:10; v/v/v) at a flow rate of 0.3mL/min. The injection volume was 25μL and the run time was 3 min. The mass spectrometer was run in multiple reaction monitoring mode with the turbospray ion source in positive ionization mode. Conditions were as follows: collision gas 10 units, ionspray voltage 5500 volts, temperature 500˚C, ion source gas 1 30 psi, ion source gas 2 40 psi, curtain gas 20 psi, declustering potential 120 volts, entrance potential 10 volts, collision energy 52 electron volts, and exit potential 8 volts. The mass transitions of 826.4→616.3 for tacrolimus and 743.4→573.2 for ritonavir were monitored.

6.2.9 Measurement of Cyclosporine

The same HPLC-MS/MS system and analytical column described above were used for the cyclosporine analysis. The isocratic mobile phase consisted of methanol:30mM ammonium acetate (95:5; v/v) pumped at a flow rate of 0.3mL/min. The injection volume was 20μL and the run time was 3.0 min. The mass spectrometer conditions were as follows: collision gas 5 units, ionspray voltage 4500 volts, temperature 350˚C, ion source gas 1 30 psi, ion source gas 2 20 psi, curtain gas 10 psi, declustering potential 71 volts, entrance potential 10 volts, collision energy 29 electron volts, and exit potential 30 volts. The mass transitions of 1220.1→1202.9 for cyclosporine and 253.1→95.1 for cimetidine were monitored.

6.2.10 Measurement of Atorvastatin

The same HPLC-MS/MS system and analytical column described above were used for the atorvastatin analysis. The isocratic mobile phase consisted of

acetonitrile:1mM ammonium acetate (70:30; v/v) pumped at a flow rate of 0.3mL/min. The injection volume was 20μL and the run time was 3.0 min. The mass spectrometer conditions were as follows: collision gas 7 units, ionspray voltage 5000 volts, temperature 400˚C, ion source gas 1 30 psi, ion source gas 2 30 psi, curtain gas 10 psi, declustering potential 100 volts, entrance potential 10 volts, collision energy 43 electron volts for atorvastatin and 20 for the internal standard, fluvastatin, and exit potential 24 volts. The mass transitions of 559.4→440.5 for atorvastatin and 434.4→354.1 for fluvastatin were monitored.

6.2.11 Measurement of ^{3}H-Estrone Sulfate (^{3}H-ES)

Prior to transfer of samples to scintillation vials, 150mL of 1N hydrochloric acid were added to neutralize the sodium hydroxide. Once cell samples were transferred to scintillation vials, 5mL of Econo-Safe counting cocktail (Research Products International Corp., Mount Prospect, IL) were added and each sample was vortexed briefly before being analyzed in a Beckman LS6000 liquid scintillation counter (Beckman Coulter, Inc. Fullerton, CA). Tritium DPM were measured.

6.2.12 Data Analysis

The DPM or the concentration of drug per million hepatocytes or per mg of protein for HEK293 cell samples was calculated. One-way ANOVA followed by Bonferroni's test for multiple comparisons were used to assess statistical significance with a p-value <0.05 considered significant.

6.3 Results

6.3.1 Tacrolimus Hepatic Uptake

The human cryopreserved hepatocyte system described previously (Methods 6.2.2) was used to test the uptake of $1\mu M$ tacrolimus. Figure 6-2 shows that the uptake of tacrolimus was unaffected by treatment with $100\mu M$ rifampin or with $100\mu M$ raltegravir.
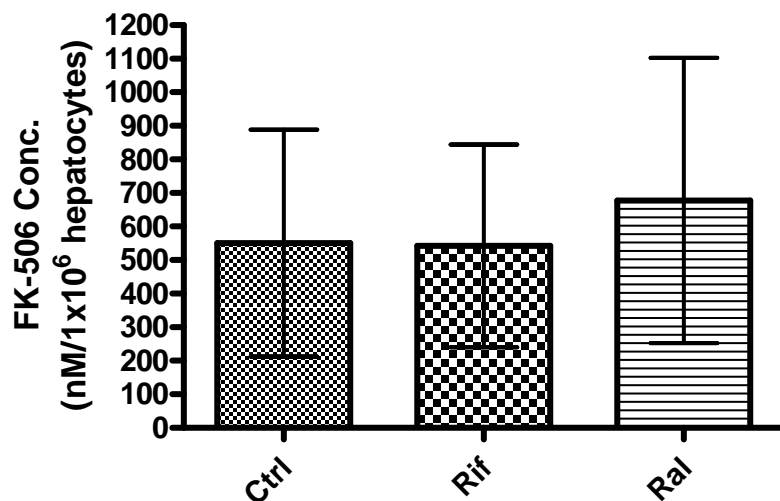
Figure 6-2 Tacrolimus (FK-506) 2 min uptake in human hepatocytes with control (1% DMSO), $100\mu M$ rifampin (Rif), or $100\mu M$ raltegravir (Ral) treatment. Values are mean±SD, n=5 per group.

In order to make sure uptake transport was not being saturated by $1\mu M$ tacrolimus, a rising dose study was conducted in human hepatocytes testing the concentration range of 100nM to $1\mu M$ tacrolimus. Inhibition by $100\mu M$ rifampin or $100\mu M$ raltegravir was tested concurrently with the rising doses of tacrolimus. Figure

6-3 shows that intracellular levels increased linearly with rising tacrolimus dose and that

neither rifampin nor raltegravir inhibited tacrolimus uptake by human hepatocytes.
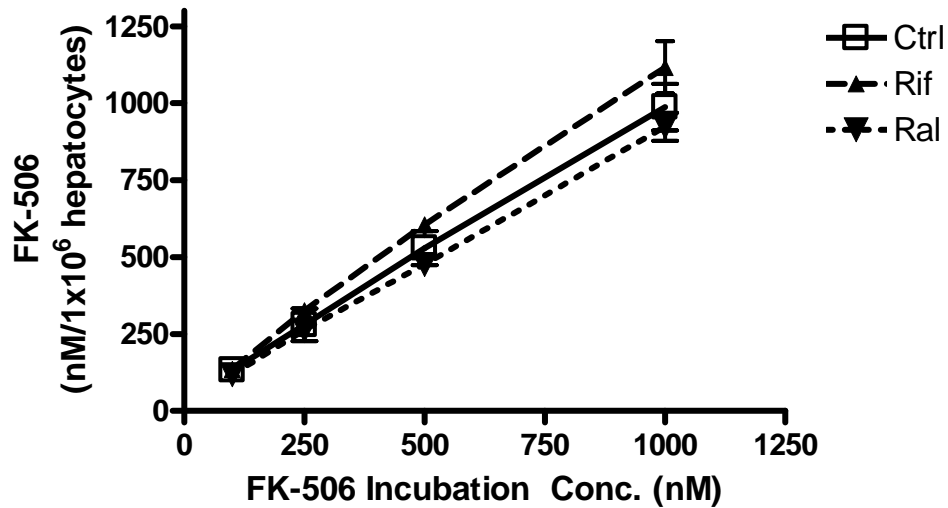
Figure 6-3 Rising tacrolimus (FK-506) dose in human hepatocytes with control (1%

DMSO), 100μM rifampin (Rif), or 100μM raltegravir (Ral) treatment. Values are

mean±SD, n=3 per group.

6.3.2 Tacrolimus HEK293 Cellular Uptake

HEK293 cells stably over-expressing OATP1B1 were tested for tacrolimus

transport to determine if there was any active transport component that may have been

masked by an overwhelming passive diffusion component in the hepatocytes. Figures

6-4 and 6-5 show that there was no difference between the control intracellular levels and

the rifampin- or raltegravir- treated cells in the control vector cell line, HEK293-pCI-

NEO, or in HEK293-OATP1B1 cells.
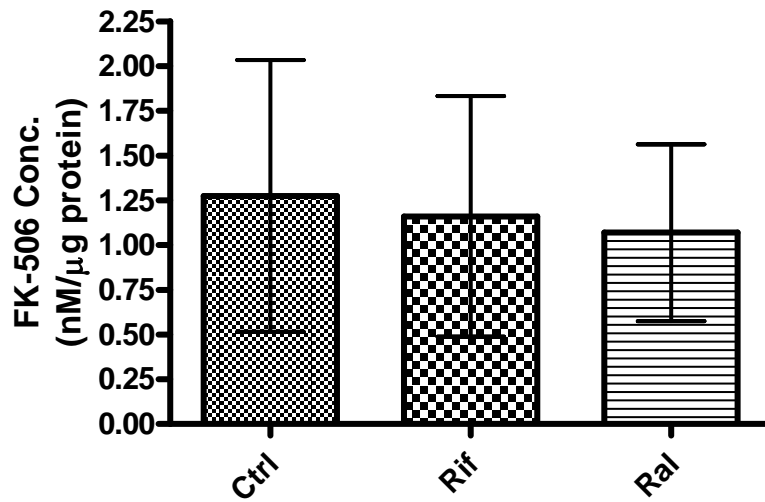
Figure 6-4 Tacrolimus (FK-506) 2 min uptake in HEK293-pCI-NEO cells with 100μM

rifampin (Rif) or 100μM raltegravir (Ral) treatment versus 1% DMSO control (Ctrl).

Values are mean±SD, n=6 per group.
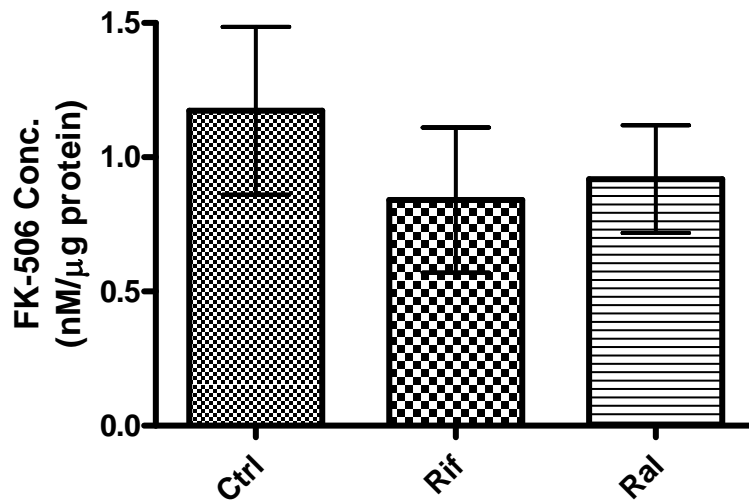
Figure 6-5 Tacrolimus (FK-506) 2 min uptake in HEK293-OATP1B1cells with 100μM

rifampin (Rif) or 100μM raltegravir (Ral) treatment versus 1% DMSO control (Ctrl).

Values are mean±SD, n=6 per group.

Figure 6-6 shows that there were minimal changes in free tacrolimus in the buffer in response to the presence of 100μM or 200μM raltegravir but none in response to rifampin treatment. The 500nM tacrolimus treatment with 100μM raltegravir was significantly higher (13%, $p < 0.05$) than the corresponding DMSO control.
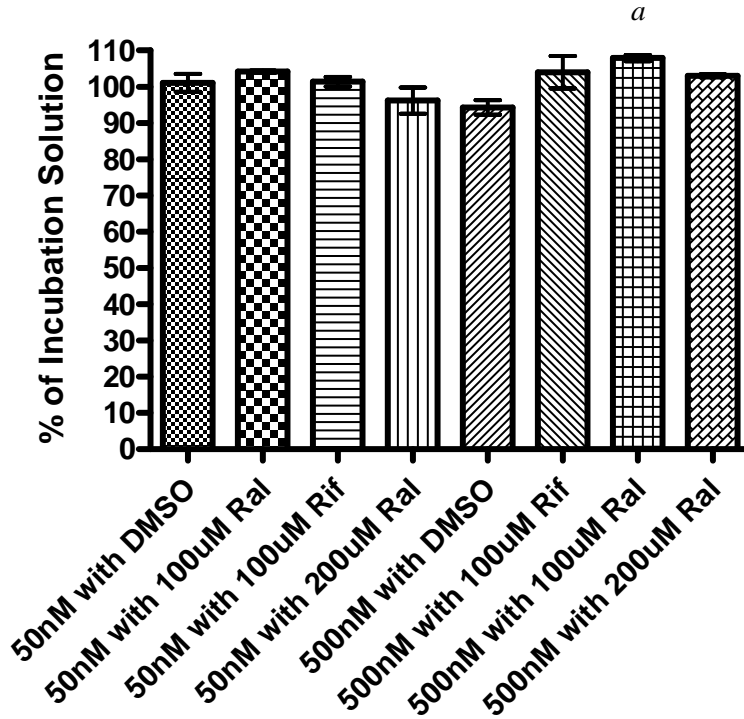
Figure 6-6 Non-specific binding of tacrolimus to cell culture plates in the presence of 1% DMSO control, 100μM rifampin, 100μM or 200μM raltegravir. [a] $p < 0.05$ compared to 500nM with DMSO. Values are mean±SD, n=3 per group.

6.3.3 Cyclosporine Hepatic Uptake

The human cryopreserved hepatocyte system described previously (Methods 6.2.2) was used to test the uptake of 1μM cyclosporine. Figure 6-7 shows that the uptake

of cyclosporine in human hepatocytes did not change in response to treatment with 100μM rifampin or 100μM raltegravir.
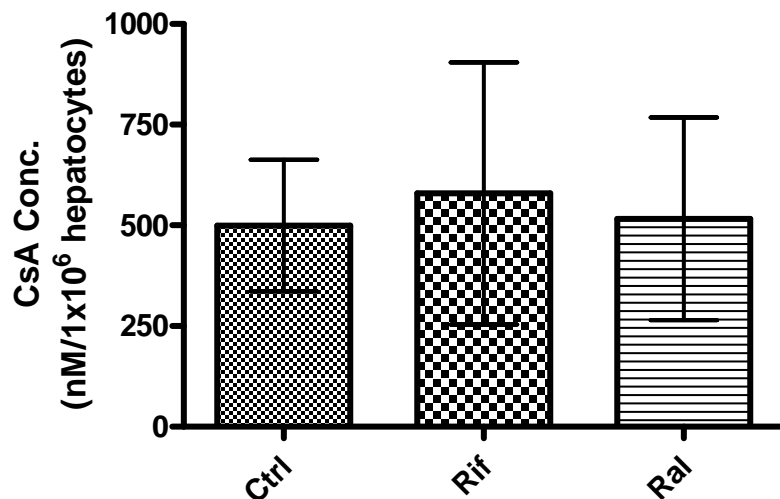
Figure 6-7 Cyclosporine (CsA) 2 min uptake in human hepatocytes with 100μM rifampin (Rif), or 100μM raltegravir (Ral) treatment versus 1% DMSO control (Ctrl). Values are mean±SD, n=6 per group.

6.3.4 Cyclosporine HEK293 Cellular Uptake

HEK293 cells stably overexpressing OATP2B1 were tested to rule out a possible gut effect on cyclosporine transport. Figures 6-8 through 6-11 show that cyclosporine uptake in HEK293-OATP2B1 cells was not inhibited by 100μM rifampin or 100μM raltegravir at either pH 6.5 or pH 7.4.
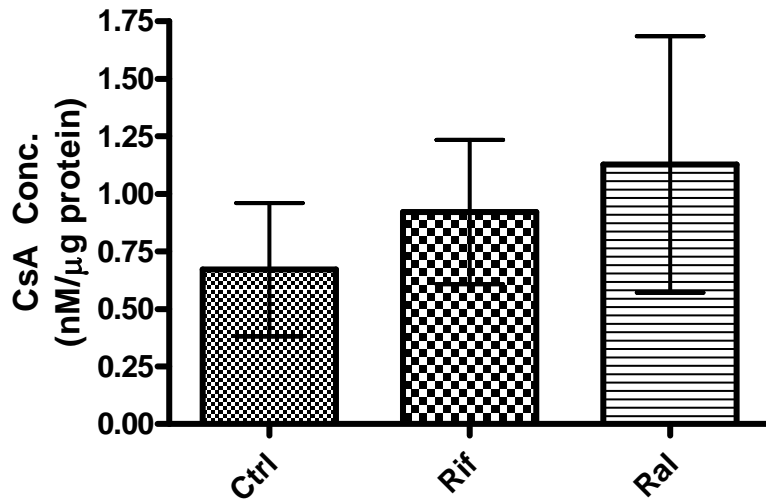
Figure 6-8 Cyclosporine (CsA) 2 min uptake in HEK293-OATP2B1 cells at pH 7.4 with

100µM rifampin (Rif) or 100µM raltegravir (Ral) treatment versus 1% DMSO control

(Ctrl). Values are mean±SD, n=6 per group.
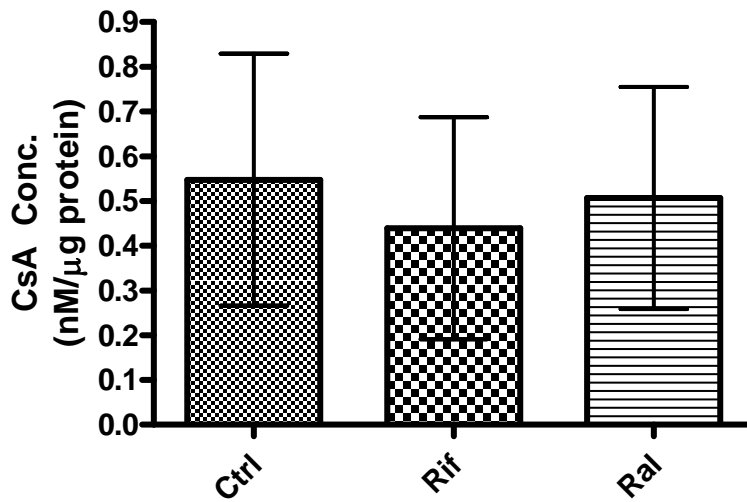
Figure 6-9 Cyclosporine (CsA) 2 min uptake in HEK293-OATP2B1 cells at pH 6.5 with

100µM rifampin (Rif) or 100µM raltegravir (Ral) treatment versus 1% DMSO control

(Ctrl). Values are mean±SD, n=9 per group.
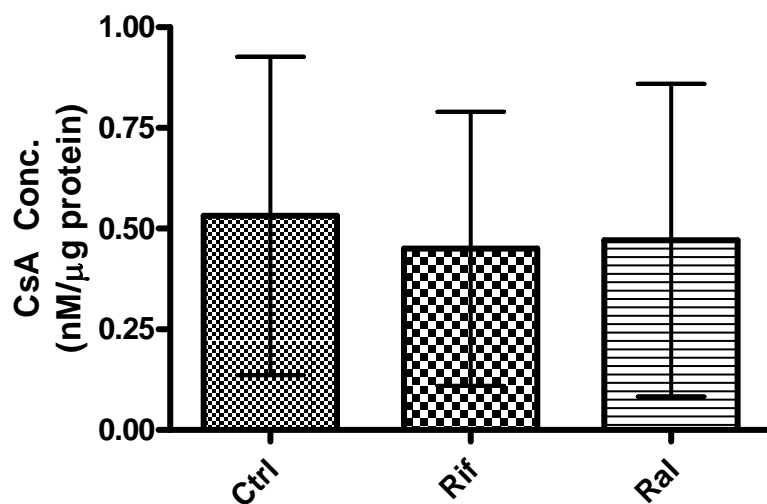
Figure 6-10 Cyclosporine (CsA) 2 min uptake in HEK293-pCI-NEO cells at pH 6.5 with

100μM rifampin (Rif) or 100μM raltegravir (Ral) treatment versus 1% DMSO control

(Ctrl). Values are mean±SD, n=6 per group.
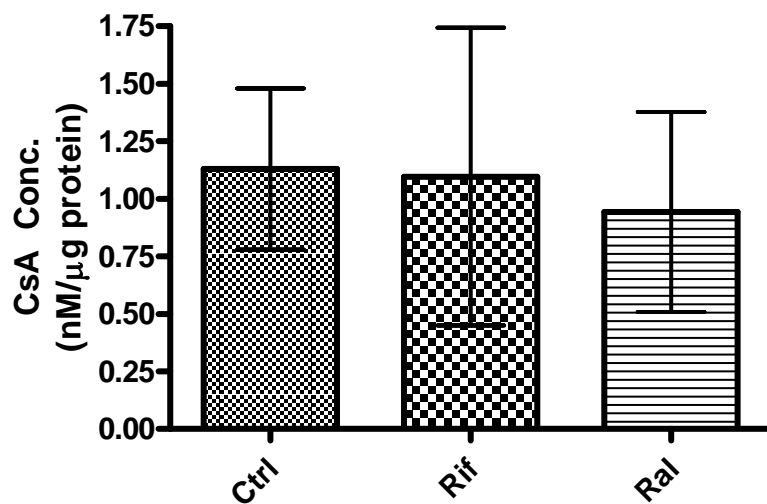
Figure 6-11 Cyclosporine (CsA) 2 min uptake in HEK293-pCI-NEO cells at pH 7.4 with

100μM rifampin (Rif) or 100μM raltegravir (Ral) treatment versus 1% DMSO control

(Ctrl). Value are mean±SD, n=6 per group.

6.3.5 Cyclosporine MDCKII and MDCKII-MRP2 Bidirectional Transport

The inhibitory potential of raltegravir against cyclosporine transport by MRP2 was also tested. Figure 6-12 shows the comparison of control and MK-571-inhibited cyclosporine bidirectional transport in MDCKII-MRP2 cells while Figure 6-13 shows the effect of raltegravir on cyclosporine bidirectional transport in the same cell system. Figures 6-14 and 6-15 show the same treatments in the MDCKII control cell line. Figure 6-16 shows the intracellular levels in both MDCKII-MRP2 and MDCKII cells for control, MK-571, and raltegravir treatments.
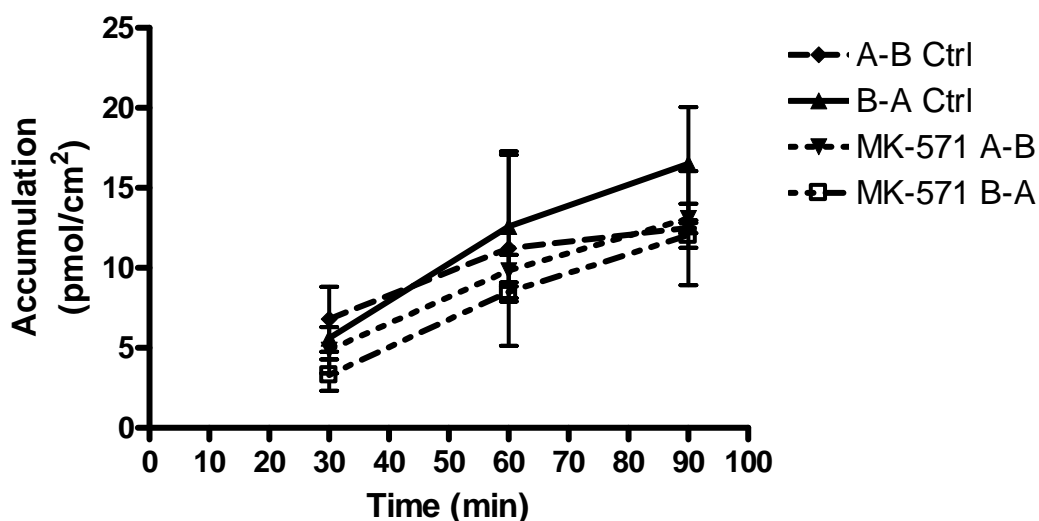
Figure 6-12 Comparison of bidirectional transport of cyclosporine across MDCKII-MRP2 cells in response to control (1% DMSO) and 9μM MK-571 treatment. Values are mean±SD, n=4 for control group and n=6 for MK-571 group.
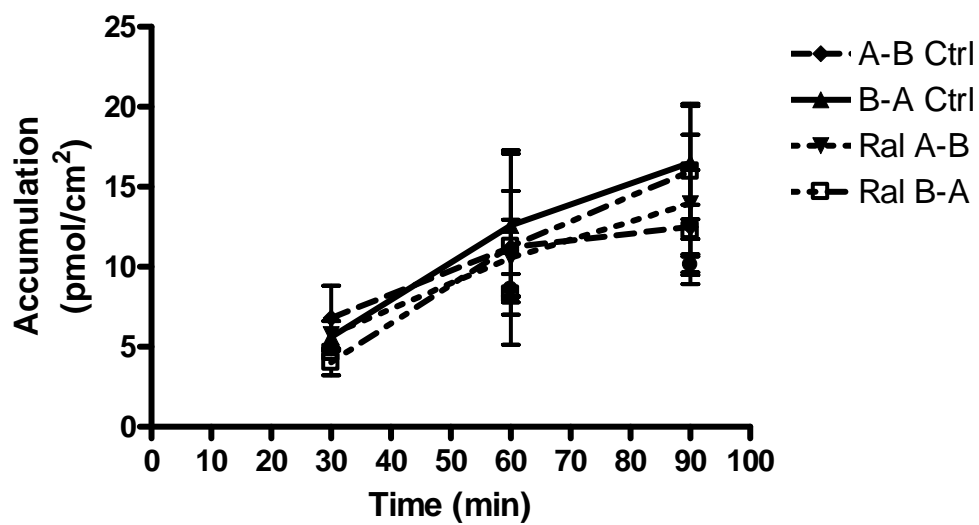
Figure 6-13 Comparison of bidirectional transport of cyclosporine across MDCKII-

MRP2 cells in response to 1% DMSO control (Ctrl) and 100μM raltegravir (Ral)

treatment. Values are mean±SD, n=6 per group.
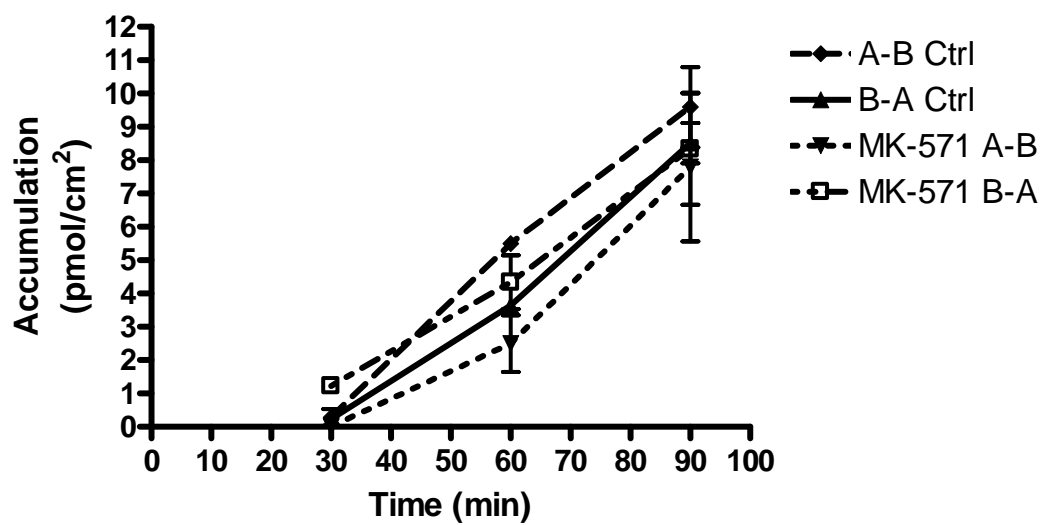
Figure 6-14 Comparison of bidirectional transport of cyclosporine across MDCKII cells

in response to 1% DMSO control (Ctrl) and 9μM MK-571 treatment. Values are
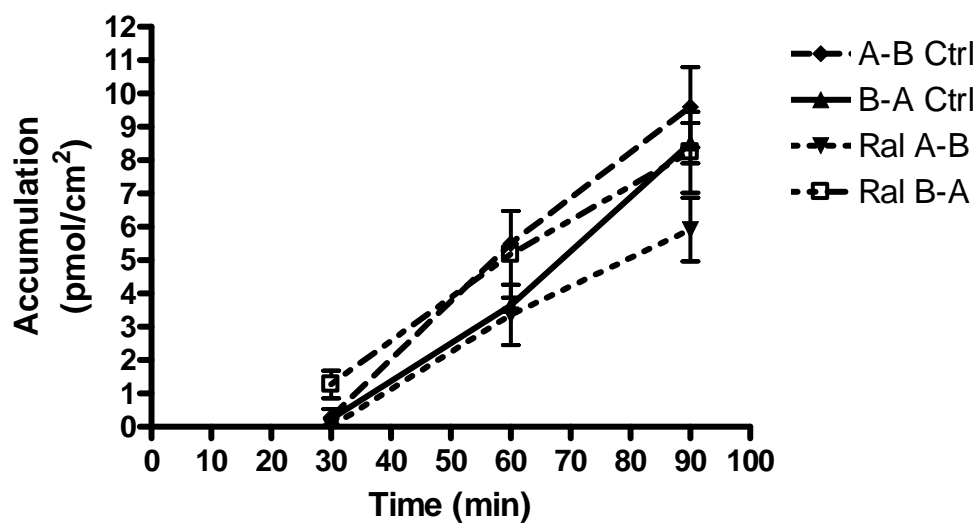
mean±SD, n=3 per group.

Figure 6-15 Comparison of bidirectional transport of cyclosporine across MDCKII cells in response to 1% DMSO control (Ctrl) and 100μM raltegravir (Ral) treatment. Values are mean±SD, n=3 per group.

Figures 6-16 and 6-17 show the intracellular cyclosporine levels in MDCKII-MRP2 and MDCKII cells, respectively, for each treatment group.
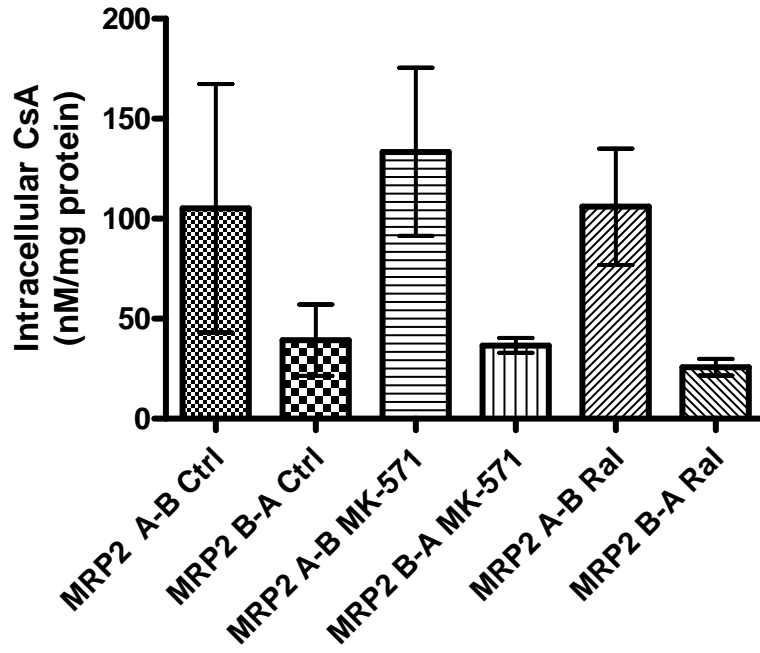
Figure 6-16 Intracellular cyclosporine (CsA, 1μM incubation) levels in MDCKII-MRP2 cells for control (1% DMSO), 9μM MK-571, and 100μM raltegravir treatment. Values are mean±SD, n=6 per group.
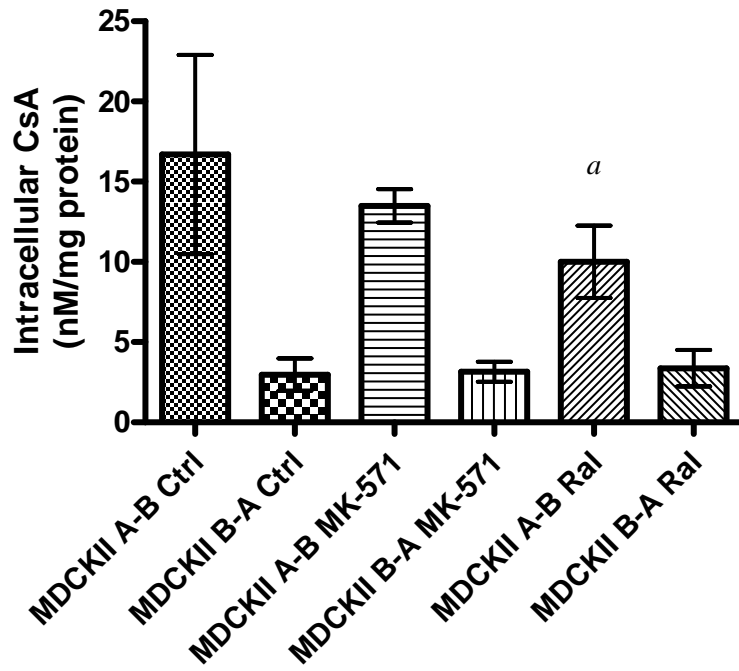
Figure 6-17 Intracellular cyclosporine (CsA, 1μM incubation) levels in MDCKII cells for control (1% DMSO), 9μM MK-571, and 100μM raltegravir treatment. [a] $p < 0.05$ compared to A-B control. Values are mean±SD, n=6 for control, MK-571, and the B-A raltegravir groups and n=3 for the A-B raltegravir group.

Table 6-3 shows the P_{app} values and ratios for control, MK-571 treatment, and raltegravir treatment while Figures 6-18 and 6-19 are bar graphs of the B-A/A-B ratios for each treatment in the MRP2-expressing and control cell lines, respectively.

MDCKII-MRP2		P_{app} A-B	P_{app} B-A	Ratio B-A/A-B
	DMSO	5.26 (±1.4)	10.0 (±3.4)	1.91 (±0.26)
	MK-571	7.63 (±1.2)	8.08 (±1.0)	1.08 (±0.18)
	Ral	7.58 (±3.6)	11.0 (±4.4)	1.52 (±0.24)
MDCKII				
	DMSO	8.61 (±1.3)	7.66 (±0.61)	0.907 (±0.18)
	MK-571	7.22 (±2.0)	6.59 (±1.4)	0.943 (±0.25)
	Ral	5.44 (±0.88)	6.45 (±0.89)	1.19 (±0.20)

Table 6-3 Apparent permeabilities of cyclosporine for A-B and B-A transport, and the ratios of B-A/A-B permeabilities for each treatment group in MDCKII-MRP2 and MDCKII cells. Values are mean±SD, n=4 for MDCKII-MRP2 DMSO, n=6 for MDCKII-MRP2 MK-571 and Ral, n=3 for all MDCKII groups.
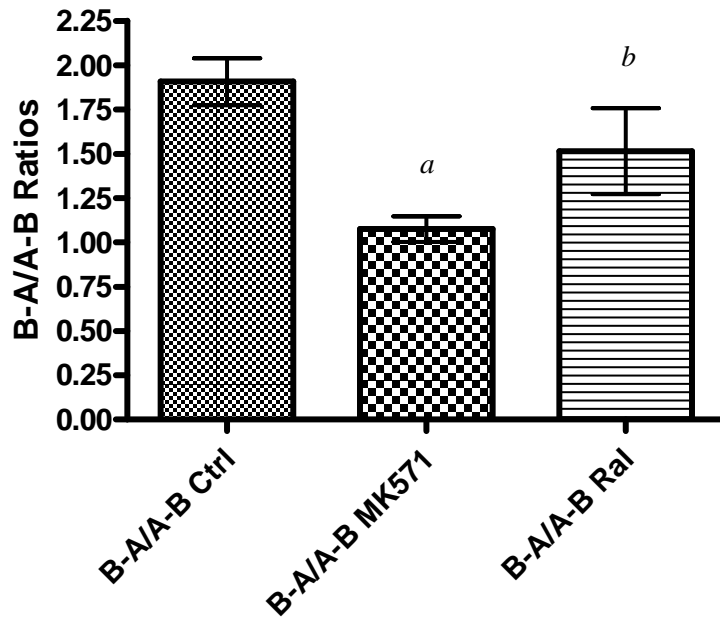
Figure 6-18 Cyclosporine apparent permeability ratios across MDCKII-MRP2 cells for

1% DMSO control, 9μM MK-571, or 100μM raltegravir treatment.

[a] $p < 0.001$, [b] $p < 0.05$ compared to control (Ctrl). Values are mean±SD, n=4 for control,

n=6 for MK-571 and raltegravir (Ral).
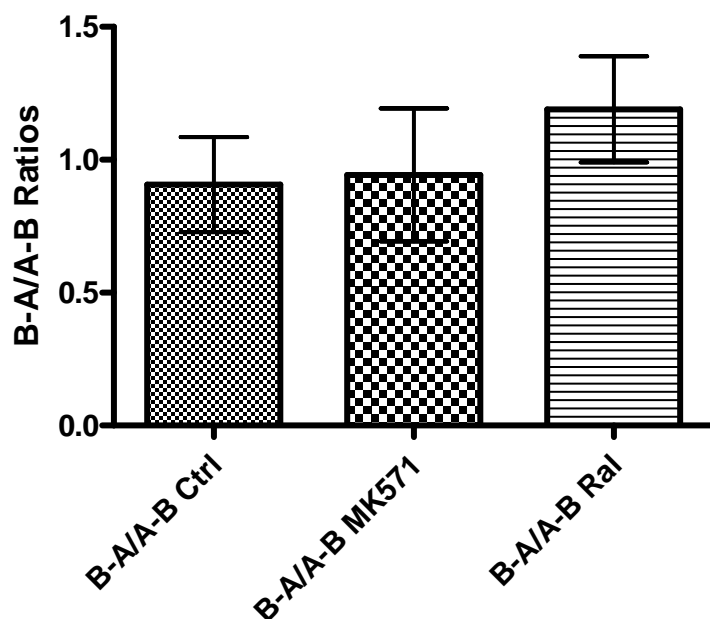
Figure 6-19 Cyclosporine apparent permeability ratios across MDCKII cells for 1% DMSO control, 9μM MK-571, and 100μM raltegravir. Values are mean±SD, n=3 per group.

6.3.6 Atorvastatin HEK293 Cellular Uptake

HEK293 cells stably overexpressing OATP1B1 were tested with 1μM atorvastatin in order to examine whether or not 100μM raltegravir had any inhibitory potential towards hepatic OATP isoforms. Figure 6-20 shows that atorvastatin transport was significantly inhibited 35% ($p<0.01$) by 100μM raltegravir. Figure 6-21 shows no significant inhibition of OATP1B1 transport of atorvastatin by 100μM rifampin or 100μM raltegravir in the vector control cell line.
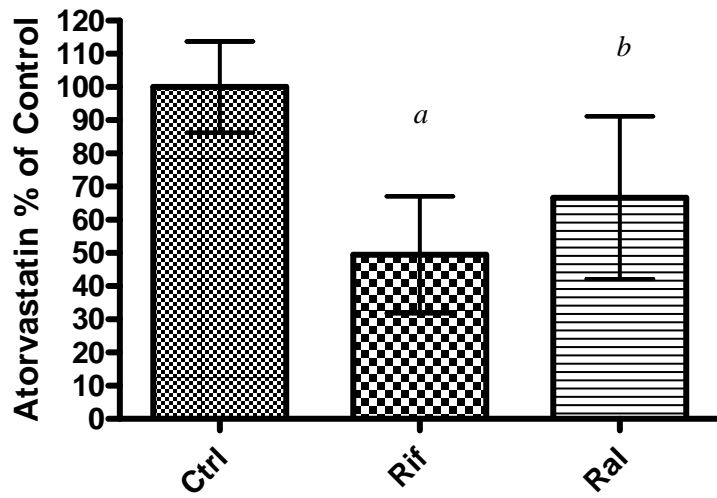
Figure 6-20 Atorvastatin 2 min uptake (1μM) in HEK293-OATP1B1 cells with 100μM rifampin (Rif) or 100μM raltegravir (Ral) treatment. [a] $p<0.001$, [b] $p<0.01$ compared to 1% DMSO control (Ctrl). Values are mean±SD, n=9 per group.
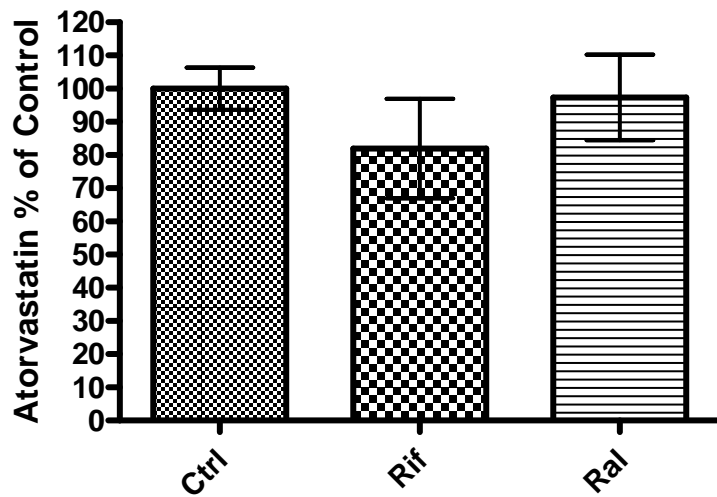
Figure 6-21 Atorvastatin 2 min uptake (1μM) in HEK293-pCI-NEO cells with100μM rifampin (Rif) or 100μM raltegravir (Ral) treatment versus 1% DMSO control (Ctrl). Values are mean±SD, n=9 per group.

6.3.7. ^{3}H-Estrone Sulfate Hepatocyte Uptake

The human cryopreserved hepatocyte system described previously (Methods 6.2.2) was used to test the uptake of 4.3nM ^{3}H-estrone sulfate, a commonly used known substrate of multiple OATP isoforms. Figure 6-22 shows that the transport of ^{3}H-estrone sulfate was inhibited significantly by 100μM raltegravir (27%, $p<0.01$), though not as strongly as by the known OATP inhibitor rifampin (66%, $p<0.001$).
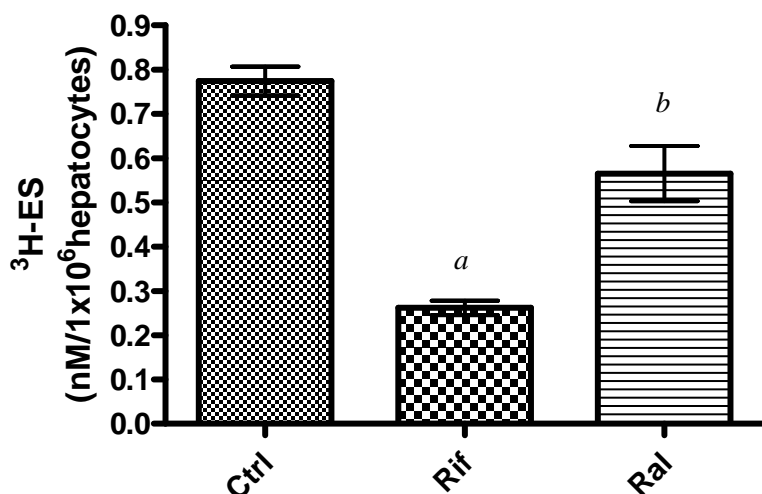
Figure 6-22 ^{3}H-Estrone sulfate (ES) 2 min uptake in human hepatocytes with 100μM rifampin (Rif) or 100μM raltegravir (Ral) treatment. [a] $p<0.01$ versus 1% DMSO, [b] $p<0.001$ compared to control (Ctrl). Values are mean±SD, n=3 per group.

6.3.8 ^{3}H-Estrone Sulfate HEK293 Cellular Uptake

To further investigate hepatic OATP inhibition by raltegravir, HEK293 cells stably expressing OATP1B1 were tested with 4.3nM ^{3}H-estrone sulfate in the presence

and absence of 100μM rifampin and 100μM raltegravir. Figure 6-23 shows a significant

35% inhibition of ^{3}H-estrone sulfate transport by raltegravir (p<0.001).
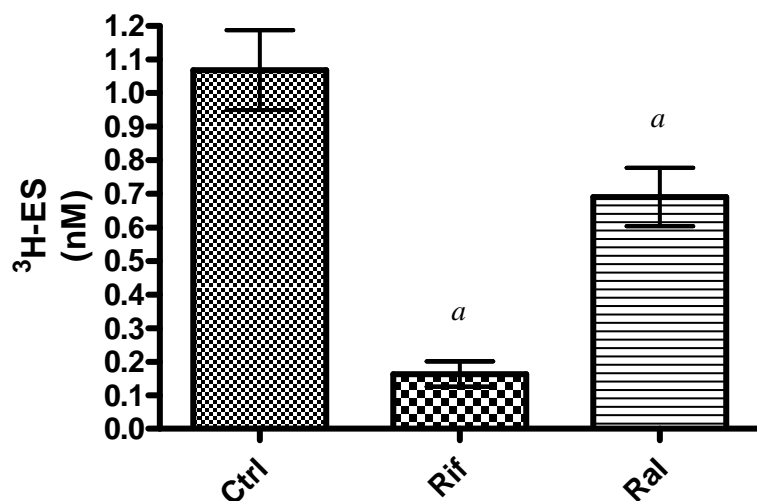
Figure 6-23 ^{3}H-Estrone sulfate (ES) 2 min uptake in HEK293-OATP1B1 cells with

100μM rifampin (Rif) or 100μM raltegravir (Ral) treatment compared to 1% DMSO

control (Ctrl). ^{a} p<0.001 compared to control. Values are mean±SD, n=9 per group

In order to determine at what concentration raltegravir began to show appreciable

inhibition of OATP1B1-mediated transport of ^{3}H-estrone sulfate, cells were treated with

4.3nM ^{3}H-estrone sulfate in the presence of increasing raltegravir doses. Figure 6-24

shows that significantly lower intracellular levels of ^{3}H-estrone sulfate were seen with

50μM raltegravir with increased inhibition seen with increased raltegravir dose.   For

50μM, 100μM, 150μM, and 200μM raltegravir the percent inhibition values were 13%,

(p<0.05) 23% (p<0.001), 40% (p<0.001), and 46% (p<0.001), respectively.
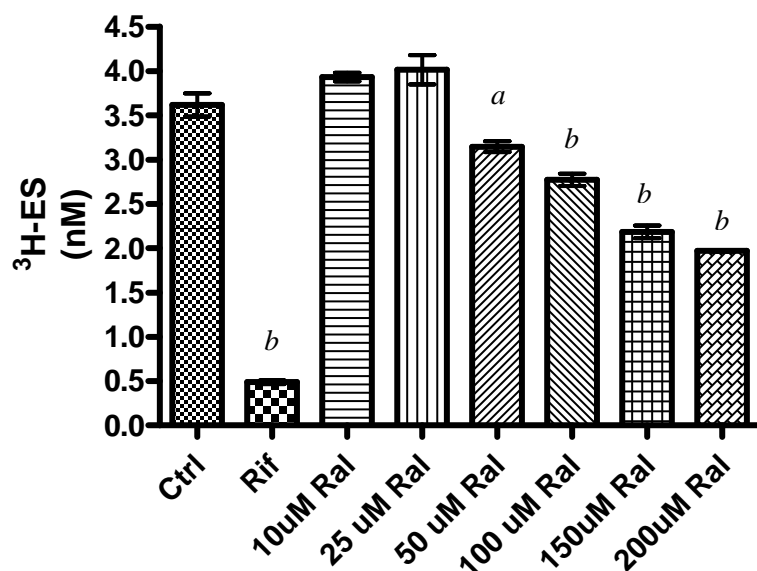
Figure 6-24 ^{3}H-Estrone sulfate (ES) 2 min uptake in HEK293-OATP1B1 cells with rising raltegravir (Ral) dose. ^{a} $p<0.05$, ^{b} $p<0.001$ compared to 1% DMSO control (Ctrl). Values are mean±SD, n=3 per group.

To examine raltegravir's inhibitory action against another OATP isoform, OATP2B1, HEK293 cells stably expressing OATP2B1 were tested with 4.3nM ^{3}H-estrone sulfate and Figures 6-25 and 6-26 show that raltegravir inhibited OATP2B1 ^{3}H-estrone sulfate transport by 34% ($p<0.01$) at pH 7.4 and by 25% ($p<0.01$) at pH 6.5. Figure 6-27 shows no effect on ^{3}H-estrone sulfate intracellular levels by rifampin or raltegravir in the control HEK293-pCI-NEO cell line.
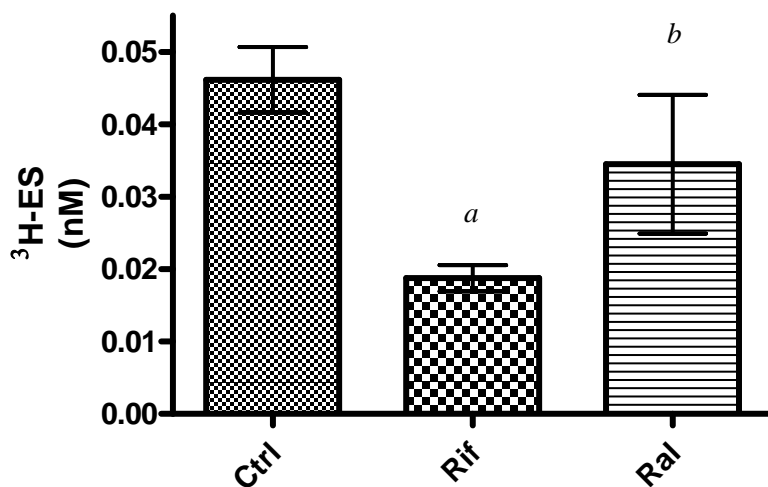
Figure 6-25 ^{3}H-Estrone sulfate (ES) 2 min uptake in HEK293-OATP2B1 cells at pH 6.5 with 100μM rifampin (Rif) or 100μM raltegravir (Ral) treatment. [a] $p < 0.001$, [b] $p < 0.01$ compared to 1% DMSO control (Ctrl). Values are mean±SD, n=9 per group.
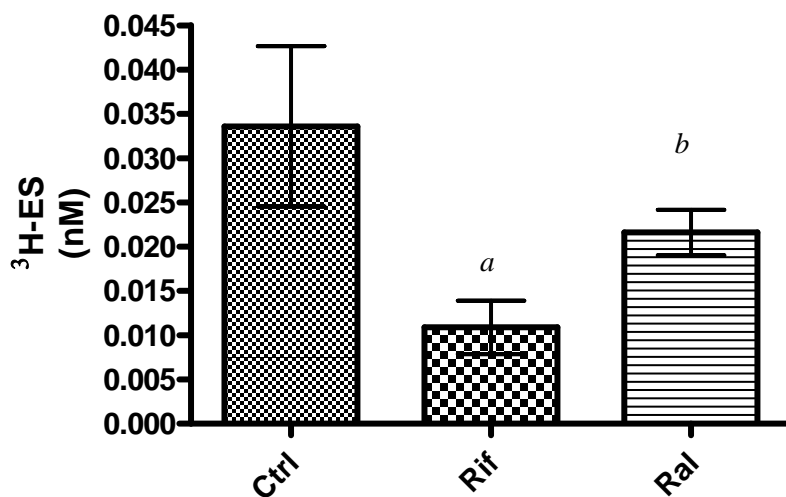
Figure 6-26 ^{3}H-Estrone sulfate (ES) 2 min uptake in HEK293-OATP2B1 cells at pH 7.4 with 100μM rifampin (Rif) or 100μM raltegravir (Ral) treatment. [a] $p < 0.001$, [b] $p < 0.01$ compared to 1% DMSO control (Ctrl). Value are mean±SD, n=6 per group.
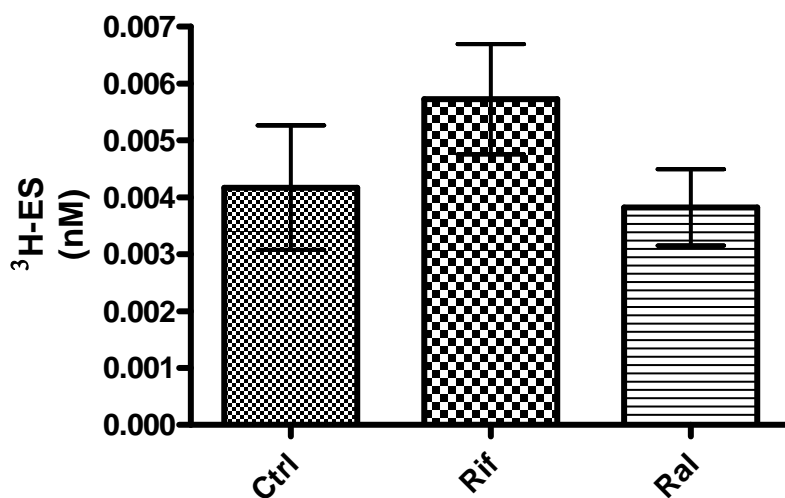
Figure 6-27 ^{3}H-Estrone sulfate (ES) 2 min uptake in HEK293-pCI-NEO cells at pH 7.4 with 100μM rifampin (Rif) or100μM raltegravir (Ral) treatment compared to 1% DMSO control (Ctrl). Values are mean±SD, n=3 per group.

6.4 Discussion

In the present study, we investigated the *in vitro* disposition of tacrolimus, cyclosporine, and ^{3}H-estrone sulfate in cryopreserved human hepatocytes and the aforementioned drugs in addition to atorvastatin in HEK293 cells stably over-expressing OATP isoforms 1B1 or 2B1 in the presence of the OATP inhibitor rifampin and the test inhibitor raltegravir. Although previous studies with the BDDCS Class 2 compounds atorvastatin (Lau et al., 2007) and glyburide (Zheng et al., 2009) showed the importance of hepatic uptake transporters in their disposition, neither of the BDDCS Class 2 compounds tacrolimus or cyclosporine showed dependence on active uptake processes to gain intrahepatocyte access. No significant differences were seen for tacrolimus levels in hepatocytes upon treatment with known or test inhibitor. Likewise, the inhibitors had no

influence on intracellular tacrolimus levels in the transporter over-expressing HEK293 cells systems. Since the preliminary human clinical results indicated an increase in tacrolimus area under the curve (AUC) upon co-administration of raltegravir yet no decrease in tacrolimus intracellular or intrahepatocyte levels were seen with inhibition of uptake transporters, it may be concluded that hepatic uptake transporters are not playing a role in this drug-drug interaction.

The preliminary human clinical results for cyclosporine showed a decrease in cyclosporine AUC, in contrast to the increase seen for tacrolimus. While inhibition of hepatic uptake would not cause this clinical result, induction of hepatic uptake could, therefore we examined whether or not cyclosporine was a substrate for hepatic uptake transporters. The human cryopreserved hepatocyte data indicate that cyclosporine uptake is not influenced by active processes and this was supported by the HEK293-OATP1B1 cellular studies. To examine whether an intestinal uptake transporter effect could play a role, cyclosporine uptake by HEK293-OATP2B1 cells was studied at pH 7.4 and pH 6.5 to determine if cyclosporine could be transported by OATP2B1 and if pH could influence this transport. The lack of inhibition by rifampin at both pH 7.4 and pH 6.5 indicate that this pathway is not causative of the clinical result seen.

Experiments examining raltegravir's effect on MRP2-mediated cyclosporine transport showed that there were significant differences between the B-A/A-B ratios in response to raltegravir compared to control. The B-A/A-B for raltegravir was 20% lower than the B-A/A-B for control ($p < 0.05$). While this moderate effect could possibly lead to a clinically relevant drug-drug interaction, it was not nearly as pronounced as the difference between B-A/A-B seen with the known MRP2 inhibitor MK-571 that was 43%

lower than control (p<0.001). No significant differences were seen in the B-A/A-B ratios in the control cell line. Although the B-A/A-B ratios did differ significantly in response to inhibitor treatment in the MDCKII-MRP2 cell line, no significant differences were seen in the A-B permeabilities or in the B-A permeabilities. Intracellular cyclosporine levels also did not differ significantly in the MDCKII-MRP2 cell line with either inhibitor, however there was a significant 40% (p<0.05) decrease in the intracellular cyclosporine levels when dosed in the apical compartment in response to raltegravir treatment, possibly indicating inhibition of some unidentified uptake transporter expressed on the MDCKII apical surface.

A recent paper by Tricot and colleagues (2009) may shed light on the interaction observed in the UCSF-led study. In the UCSF-led study, raltegravir was added to a HAART regimen that included a boosted protease inhibitor. In the study by Tricot et al. (2009), patients receiving tacrolimus or cyclosporine had the boosted protease inhibitor replaced by raltegravir. In one group that was switched to raltegravir immediately after transplantation, target trough levels of each immunosuppressant were reached with the standard tacrolimus or cyclosporine dosage. In another group that was switched to raltegravir 3-57 months post-transplant, both tacrolimus and cyclosporine doses had to be increased to maintain immunosuppressant therapeutic levels as would be expected since CYP3A4 and Pgp are no longer subject to inhibition by the boosted protease inhibitor. This would suggest that there is not a strong interaction directly between raltegravir and the immunosuppressants, but perhaps rather an interaction between raltegravir and the protease inhibitor that indirectly affects tacrolimus and cyclosporine. Since raltegravir has some inhibitory action against MRP2 and several of the protease inhibitors are

substrates for MRP2 (Huisman et al., 2002), perhaps inhibition of protease inhibitor transport by MRP2 leads to increased protease inhibitor levels and more effective inhibition of CYP3A4 and Pgp, which would decrease metabolism of tacrolimus leading to the observed higher plasma levels. Since cyclosporine is also a substrate for MRP2, decreased transport in the gut may be ameliorated by decreased transport in the liver, making the overall effect on cyclosporine plasma levels difficult to predict. Further study is required to determine if this is a possible avenue of drug-drug interactions.

6.5 Conclusions

The results obtained for tacrolimus and cyclosporine did not indicate that they rely on hepatic uptake transporters for uptake. This contrasts with the data obtained for atorvastatin and glyburide. A possible explanation for the discrepancy may be that hepatocytes can lose transporter expression compared to the whole liver (Ho et al., 2006). While uptake of the known OATP substrate ^{3}H-estrone sulfate was seen in hepatocytes, if tacrolimus or cyclosporine are not as good substrates, decreased expression may lead to loss of transport that perhaps could be seen in an intact *in vivo* system. All four drugs (tacrolimus, cyclosporine, atorvastatin, and glyburide) are considered BDDCS Class 2 compounds and would be expected to behave in similar ways. To date, no extensive comparisons have been made between BDDCS Class 2 compounds to determine which ones significantly rely on hepatic uptake transporters and which do not, therefore no correlations between physicochemical properties and reliance on hepatic uptake have been observed and predictions are not yet possible.

In order to assess the ability of raltegravir to inhibit hepatic uptake through OATP1B1, known substrates atorvastatin and ^{3}H-estrone sulfate were examined. Significant inhibition of uptake of both of these compounds was demonstrated, however the concentration of raltegravir needed to cause what would be considered clinically significant inhibition was well above physiologically relevant concentrations. The C_{max} after a standard 400mg dose is reported to be about 11μM (Iwamoto et al., 2008), while the concentration needed to cause appreciable *in vitro* inhibition of OATP1B1 is about 50μM. Therefore, inhibition of hepatic uptake of OATP1B1 substrates by raltegravir is unlikely to cause clinically relevant drug-drug interactions.

6.6 References

Cihlar, T., Ray, A.S., Laflamme, G., Vela, J.E.,, Tong, L., Fuller, M.D., Roy, A., and Rhodes, G.R. (2007). "Molecular assessment of the potential for renal drug interactions between tenofovir and HIV protease inhibitors." Antivir. Ther. **12**(2): 267-272.

Ciuffreda, D., Pantaleo, G., and Pascual, M. (2007). "Effects of immunosuppressive drugs on HIV infection: implications for solid-organ transplantation." Transpl. Int. **20**(8):649-58.

Frassetto, L.A., Browne, M., Cheng, A., Wolfe, A.R., Roland, M.E., Stock, P.G., Carlson, L., and Benet, L.Z. (2007). "Immunosuppressant pharmacokinetics and dosing modifications in HIV-1 infected liver and kidney transplant recipients." Am. J. Transplant. **7**: 2816–2820.

Goto, M., Masuda, S., Saito, H., Inui, K. (2003). "Decreased expression of P-glycoprotein during differentiation in the human intestinal cell line Caco-2." Biochem. Pharmacol. **66**(1):163-70.

Ho, R.H., Tirona, R.G., Leake, B.F., Glaeser, H., Lee, W., Lemke, C.J., Wang, Y., and Kim, R.B. (2006). "Drug and bile acid transporters in rosuvastatin hepatic uptake: function, expression, and pharmacogenetics." Gastroenterology. **130**:1793–1806.

Huisman, M.T., Smit, J.W., Crommentuyn, K.M.L., Zelcer, N., Wiltshire, H.R., Beijnen, J.H., and Schinkel, A.H. (2002). "Multidrug resistance protein 2 (MRP2) transports HIV protease inhibitors, and transport can be enhanced by other drugs." AIDS. **16**:2295–2301.

Isentress™ [package insert.] (2007). Merck & Co., Inc.

Iwamoto, M., Wenning, L.A., Petry, A.S., Laethem, M., De Smet, M., Kost, J.T., Merschman, S.A., Strohmaier, K.M., Rameal, S., Lasseter, K.C., Stone, J.A., Gottesdiener, K.M., and Wagner, J.A. (2008). "Safety, tolerability, and pharmacokinetics of raltegravir after single and multiple doses in healthy subjects." Clin. Pharmacol. Ther. **83**(2): 293-299.

Iwasaki, K. (2007). "Metabolism of tacrolimus (FK506) and recent topics in clinical pharmacokinetics." Drug Metab. Pharmacokinet. **22**(5): 328–335.

Izzedine, H., Launay-Vacher, V., Baumelou, A., and Deray, G. (2004). "Antiretroviral and immunosuppressive dru-drug interactions: an update." Kidney Int. **66**(2):532-41.

Lau, Y.Y., Huang, Y., Frassetto, L. and Benet, L.Z. (2007). "Effect of OATP1B transporter inhibition on the pharmacokinetics of atorvastatin in healthy volunteers." Clin. Pharmacol. Ther. **81**(2): 194-204.

Minuesa, G., Volk, C., Molina-Arcas, M., Gorboulev, V., Erkizia, I., Arndt, P., Clotet, B., al Pastor-Anglada, M., Koepsell, H., and Martinez-Picado, J. (2009). "Transport of lamivudine [(-)-β-L-2',3'-Dideoxy-3'-thiacytidine] and high-affinity interaction of nucleoside reverse transcriptase inhibitors with human organic cation transporters 1, 2, and 3." J. Pharmacol. Exp. Ther. **329**(1):252-61.

Tricot, L., Teicher, E., Peytavin, G., Zucman, D., Conti, F., Calmus, Y., Barrou, B., Duvivier, C., Fontaine, C., Welker, Y., Billy, C., de Truchis, P., Dealhousse, M., Vittecoq, D., and Salmon-Ceron, D. (2009). "Safety and efficacy of raltegravir in HIV-infected transplant patients cotreated with immunosuppressive drugs." Am. J. Transpl. **9**: 1946–1952.

Varatharajana, L. and Thomas, S.A. (2009). "The transport of anti-HIV drugs across blood-CNS interfaces: summary of current knowledge and recommendations for further research." Antiviral Res. **82**(2): A99–A109.

Zheng, H.X., Huang, Y., Frassetto, L. and Benet, L.Z. (2009). "Elucidating rifampin's inducing and inhibiting effects on glyburide pharmacokinetics and blood glucose in healthy volunteers: unmasking the differential effects of enzyme induction and transporter inhibition for a drug and its primary metabolite." Clin. Pharmacol. Ther. **85**(1): 78-85.

CHAPTER 7

Conclusions and Perspectives

7.1 Overview

While the experiments described in the preceding chapters of this thesis may seem disparate at first glance, all of them fall under the overarching theme of investigating how drug transporters fit into the grand scheme of determining the absorption, distribution, metabolism, and elimination (ADME) properties of xenobiotics. The role of Pgp in drug absorption and distribution is now well-recognized, to the point where the FDA offers guidance (Zhang et al., 2006) on testing new molecular entities for substrate status or inhibitory potential against the transporter. Uptake transporters are beginning to gain recognition as important players in dictating the rate and extent of some drugs' metabolism and elimination. Polymorphic forms of both uptake and efflux transporters are being investigated as possible reasons for the high inter-individual variability in drug response in patient populations. In addition to providing further explanation for inter-individual variability, drug transporters are also increasingly recognized as players in drug-drug interactions, while previously focus was on interactions through metabolizing enzymes only. While great strides have been made in all of these areas, work on the full range and the finer nuances of drug transporter influence on drug ADME properties remains to be done.

7.2 Hepatic Basolateral Efflux Mediated by the Organic Anion Transporting Polypeptides (OATP/Oatp) (Chapter 2)

Investigations into the influence of hepatic basolateral uptake have demonstrated a clear role for transporters in influencing drug pharmacokinetic properties, as demonstrated by Lau et al. (2007) in the case of atorvastatin and Zheng et al. (2009) in the case of glyburide. Based upon metabolite data seen in Lau and colleagues' work, namely increased metabolite levels in the plasma in addition to increased parent in the presence of OATP inhibitor rifampin, the hypothesis that hepatic basolateral transporters can efflux low permeability compounds out of hepatocytes and back into blood was deemed worthy of further investigation. How compounds traverse the hepatic basolateral membrane and move from the intracellular environment to the systemic blood was investigated by studying the ability of the hepatic OATPs to mediate bidirectional transport.

Biopharmaceutics Drug Disposition Classification System (BDDCS) Class 3 drugs (low permeability, high solubility, and little metabolism) that were known substrates of OATP/Oatp transporters were chosen for study to avoid confounding effects from hepatic enzymes. These compounds were loaded into cells expressing an OATP/Oatp transporter along with known OATP/Oatp inhibitors. The appearance of drug into buffer with or without inhibitor was measured to determine if there were any differences between the condition in which the OATP/Oatp was inhibited over the entire timecourse versus when it was not. A similar strategy was used in isolated perfused rat liver (IPRL) experiments, in which livers were loaded with drug and inhibitor and efflux of drug into perfusate with or without inhibitor was measured. Although we tried to design our experimental system carefully, no strong conclusions could be drawn from our

data. The phenomenon of OATP/Oatp mediated hepatic efflux is one that may warrant

further investigation in the future with a different experimental system. A better proof of

concept system may be to use inside-out membrane vesicles made from cells (such as

insect Sf9 cells) expressing OATPs/Oatps or to use *xenopus laevis* oocytes expressing

OATPs/Oatps. The loading step could be eliminated with inside-out vesicles, since the

opposite orientation would cause the OATP/Oatp to pump drug into the vesicle and

intracellular levels could be measured as an indicator of OATP/Oatp efflux ability.

Oocytes could be injected to load a known amount of drug. With both systems, the

problem of loading with inhibitor could be avoided since again, the potential intracellular

binding site would either be expressed on the outside of the inside-out vesicles or

inhibitor could be directly injected into oocytes. Moving from these systems to a more

physiologically relevant system however still presents interesting technical challenges.

7.3 Interplay Between Drug Metabolizing Enzymes and the Breast Cancer Resistance Protein (BCRP/Bcrp) (Chapter 3)

The interplay between CYP3A4 and Pgp in the intestine has been well-

characterized (Cummins et al, 2004) and is recognized as a major factor affecting oral

drug absorption and bioavailability. The Breast Cancer Resistance Protein (BCRP) co-

localizes on the apical enterocyte border, meaning it could also be a major factor in

determining drugs' bioavailability by influencing absorption and gut metabolism. We

sought to further investigate this role through *in vitro* cellular studies with a BCRP-

overexpressing MDCKII cell line and *ex situ* studies with isolated rat jejunum segments

in an Ussing chamber. We used known BCRP/Bcrp substrates and known potent

inhibitors in addition to anti-HIV drugs as investigational inhibitors to begin studying

possible mechanisms of drug-drug interactions in HIV+ populations. Unfortunately, we

were unable to demonstrate BCRP/Bcrp mediated transport of the model compounds in either system. Confocal microscopy showed that the cell line was expressing BCRP, but whether it was appropriately expressed on the apical border was not specifically determined. The Ussing chamber experiments showed very high variability that could have been due to experimental technique or to inter- and intra-variability in rat intestinal expression of Bcrp (MacLean et al., 2008). Although we were not successful in demonstrating the same interplay between BCRP/Bcrp and intestinal drug metabolizing enzymes or in showing the potential for drug-drug interactions with the important therapeutic class of anti-HIV drugs, we believe further work is necessary and important for advancing knowledge in this area.

7.4 Hepatic Uptake of Warfarin and Phenytoin (Chapter 4)

Previous work in the laboratory clearly showed the importance of hepatic uptake transporters on the pharmacokinetic and pharmacodynamic properties of the BDDCS Class 2 compounds atorvastatin (Lau et al., 2007) and glyburide (Zheng et al., 2009). These results led us to the conclusion that it is worthwhile to investigate the effect of hepatic uptake on other BDDCS Class 2 compounds. Warfarin and phenytoin are both BDDCS Class 2 compounds that have narrow therapeutic indexes and serious adverse events when plasma concentrations fall either above or below target therapeutic levels. We used freshly isolated rat hepatocytes, cryopreserved human hepatocytes, and HEK293 cells stably expressing hepatically expressed OATP isoforms to study the potential impact of hepatic uptake transporters on warfarin and phenytoin disposition.

Both rat and human hepatocytes showed significant inhibition of warfarin uptake by the OATP/Oatp inhibitor rifampin. In rat hepatocytes, uptake was inhibited by 23% while in human hepatocytes warfarin uptake was inhibited by 34%. The OAT2/Oat2 inhibitor probenecid did not have a significant inhibitory effect on warfarin uptake in rat hepatocytes, but did cause a significant 22% inhibition of uptake in human hepatocytes, indicating a possible species difference in warfarin transport. Stably transfected HEK293 cells expressing the liver-specific OATP1B1 or OATP2B1, which is expressed in both gut and liver, showed no uptake of warfarin due to the transporter as evidenced by the inability of rifampin to inhibit uptake and by similar intracellular levels seen in both the transfected cells and in control cells not over-expressing the transporters. Investigation into the ability of other OATPs or of OATs to transport warfarin remains to be done.

Neither human nor rat hepatocytes showed any evidence of phenytoin uptake mediated by OATP/Oatp or OAT/Oat as evidenced by the lack of effect of rifampin and probenecid on intra-hepatocyte phenytoin levels. Further investigation with OATP1B1- and OATP2B1-expressing HEK293 cells supported a lack of interaction.

7.5 Human Clinical Study of Effect of OATP Inhibition on Warfarin Pharmacokinetics (Chapter 5)

Based upon the human hepatocyte data showing significant inhibition of warfarin (Chapter 4), a human clinical study was run to examine the effects of inhibiting OATP-mediated hepatic uptake on warfarin pharmacokinetics. A randomized, two-period cross-over study was conducted in 10 healthy volunteers who received two 7.5mg oral warfarin doses, one in study period 1 and one in study period 2. One period had, in addition to the

oral warfarin dose, an intravenous infusion of 600mg rifampin administered as an infusion over 30min prior to warfarin dosing.

The clinical results showed no significant increase in warfarin plasma area under the concentration-time curve (AUC) over the 0-12 hour period when rifampin inhibition of OATP would be evident, indicating that inhibition of OATP did not affect warfarin uptake into the liver. The C_{max} and Vss/F were likewise not different between the two treatment groups, providing further evidence against any relevant effect of OATP inhibition on warfarin pharmacokinetics *in vivo*. Interestingly, data from the longer timeframe measurements indicated a significant effect of CYP induction by rifampin. The $AUC_{0-\infty}$ for both R- and S-warfarin were significantly reduced in the rifampin-treatment arm while CL/F for both enantiomers increased. In addition, the $t_{1/2}$ of R-warfarin was significantly shorter in the rifampin-treatment arm than in the warfarin-only arm. Since sampling was carried out to 5 days, this would allow enough time for induced CYP protein to be synthesized and expressed.

The lack of effect by OATP inhibition seen *in vivo* compared to the significant effect seen *in vitro* could be explained by the different concentrations of rifampin used between the two studies. It is also possible that there are transporters expressed *in vivo* whose expression is lost or decreased in cryopreserved human hepatocytes that can compensate when OATP transport is inhibited *in vivo*. The lack of interaction in our study indicates that hepatic OATPs are not going to be a significant factor in determining warfarin pharmacokinetic or pharmacodynamic behavior and that explanations for the high inter- and intra-individual variability still remain to be found.

7.6 Investigating Transporter-Based Mechanisms for Interactions Between Raltegravir and Tacrolimus and Raltegravir and Cyclosporine (Chapter 6)

In a UCSF-led multicenter study examining the safety and efficacy of liver and kidney transplants in HIV+ patients alterations in cyclosporine and tacrolimus pharmacokinetics were seen in four patients after addition of raltegravir to their anti-HIV treatment regimen. Since raltegravir does not interact with Pgp or CYP3A4, another mechanism must be responsible for the increase in tacrolimus trough levels and the decrease in cyclosporine trough levels. We investigated whether or not tacrolimus or cyclosporine were substrates for hepatic uptake transporters and whether raltegravir could inhibit hepatic uptake transporters or the hepatic and intestinal efflux transporter, Multidrug Resistance Protein 2 (MRP2), as possible mechanisms for the clinical results seen.

Neither tacrolimus nor cyclosporine appeared to be substrates for a hepatic uptake transporter that could be inhibited by rifampin or raltegravir as shown by the lack of effect on intra-hepatic levels by rifampin and raltegravir. Further studies in HEK293 cells stably expressing OATP1B1 or OATP2B1 confirmed the results seen in human hepatocytes.

Raltegravir did appear to have significant inhibitory potential against MRP2 (Chapter 6). By investigating cyclosporine transporter in the MDCKII-MRP2 cell line, a significant reduction in the net flux ratio in the presence of raltegravir was seen compared to control. Raltegravir also significantly inhibited OATP-mediated uptake of the known OATP substrates atorvastatin and 3H-estrone sulfate. Raltegravir inhibited atorvastatin uptake in HEK293-OATP1B1 cells by 35%. ^{3}H-Estrone sulfate uptake was inhibited by

27% in human hepatocytes, by 35% in HEK293-OATP1B1 cells, and by 34% in HEK293-OATP2B1 cells. A rising raltegravir dose study in HEK293-OATP1B1 cells was performed using ^{3}H-estrone sulfate as the test substrate and showed significant inhibition starting at a raltegravir concentration of 50μM.   Although the data show that raltegravir is able to inhibit both hepatic OATP mediate uptake and MRP2-mediated efflux, the concentrations needed to do so are well above those seen *in vivo*. Therefore, raltegravir inhibition of these hepatic transporters is not likely to cause clinically relevant drug-drug interactions.

7.7 Concluding Remarks

Drug transporters have been accepted as an important influence on the ADME properties of many drugs. Over the last 15 years, a large amount of work has been done to characterize substrates, specific inhibitors, regulatory elements, species differences, and genetic polymorphisms in transporter proteins. Their roles in drug disposition and elimination as well as drug-drug interactions continue to be exciting areas of translational research. The increasing acceptance and utilization of the BDDCS allows easier prediction of when transporter effects will be important.

As more research is done, discrepancies become evident as to what one may expect transporter effects to be versus what is seen in vitro and in vivo. For example, hepatic uptake transport is known to be an important determining factor in the pharmacokinetics of BDDCS Class 2 drugs atorvastatin and glyburide, however for the Class 2 drugs warfarin, phenytoin, tacrolimus, and cyclosporine, little effect of hepatic uptake was seen in vitro and in vivo, leading to the question of why some BDDCS Class

2 drugs fall victim to interactions at the hepatic uptake level but others do not. Examining the physicochemical properties of different BDDCS Class 2 drugs to determine if correlations could be drawn between some property or properties and the susceptibility to hepatic uptake could be useful for refining their classification, possibly leading to subclasses within the overall Class 2 group. Another area of interest is in characterizing differences between the intestinal membrane and the hepatic membrane and how these influence a drug's reliance on uptake transporters. Again referencing the BDDCS, Class 2 drugs are believed to have sufficient permeability that they do not require intestinal uptake transporters, but again, as the results with atorvastatin and glyburide have shown, some Class 2 drugs do utilize hepatic uptake transporters.

We have accrued a large body of knowledge regarding the effects of transporters expressed on the apical surface of enterocytes and on the influence of hepatic basolateral uptake and apical efflux. It is natural that we should seek to begin elucidating more fully the effects of transporters expressed on the basolateral surface of enterocytes (i.e. OATP1A4) and of hepatic basolateral efflux on the pharmacokinetics and pharmacodynamics of drugs. By fully understanding the role of more transporters expressed in the major eliminating organs we can improve our predictive abilities by incorporating them into modeling systems, improve our understanding of transporter-based drug-drug interactions, and possibly identify candidate genes leading to inter-individual variability seen so commonly in patient populations.

7.8 References

Benet, L.Z., Cummins, C.L., and Wu, C.Y. (2004). "Unmasking the dynamic interplay between efflux transporters and metabolic enzymes." Int. J. Pharm. **277**(1-2):3-9.

Lau, Y.Y., Huang, Y., Frassetto, L. and Benet, L.Z. (2007). "Effect of OATP1B transporter inhibition on the pharmacokinetics of atorvastatin in healthy volunteers." Clin. Pharmacol. Ther. **81**(2): 194-204.

MacLean, C., Moenning, U., Reichel, A., and Fricker, G. (2008). "Closing the gaps: full scan of the intestinal expression of p-glycoprotein, breast cancer resistance protein, and multidrug resistance-associated protein 2 in male and female rats." Drug Metab. Dispos. **36**:1249–1254.

Zhang, L., Strong, J.M., Qiu, W., Lesko, L.J., and Huang, S.M. (2006). "Scientific perspectives on drug transporters and their role in drug interactions." Mol. Pharmaceutics. **3**(1):62-69.

Zheng, H.X., Huang, Y., Frassetto, L. and Benet, L.Z. (2009). "Elucidating rifampin's inducing and inhibiting effects on glyburide pharmacokinetics and blood glucose in healthy volunteers: unmasking the differential effects of enzyme induction and transporter inhibition for a drug and its primary metabolite." Clin. Pharmacol. Ther. **85**(1): 78-85.

Publishing Agreement

It is the policy of the University to encourage the distribution of all theses and dissertations. Copies of all UCSF theses and dissertations will be routed to the library via the Graduate Division. The library will make all theses and dissertations accessible to the public and will preserve these to the best of their abilities, in perpetuity.

Please sign the following statement:

I hereby grant permission to the Graduate Division of the University of California, San Francisco to release copies of my thesis or dissertation to the Campus Library to provide access and preservation, in whole or in part, in perpetuity.

Sarah B. Shugart 08 Jan 2010

Author Signature Date